Applied Optics

January
1963

ASTRONOMICAL INSTRUMENTATION I

Effective Jan. 1, 1965. All back issues and single copies are sold at $3.00 per copy.

UNUSUAL CAREER OPPORTUNITIES

Interested In Working With A Dynamic New Group Where Your Creative Abilities Will Be Recognized?

Want To See Your Ideas Implemented By A Technically-Managed Group With Strong Engineering Support?

Are you qualified and interested in the following areas of Quantum Electronics—

LIQUID and PLASTIC LASER MATERIALS DEVELOPMENT—OPTICAL COMMUNICATIONS SYSTEMS—RANGING—OPTICAL and NON-OPTICAL PUMPING—ULTRA HIGH ENERGY SOLID-STATE LASERS—COHERENT RADIATION INDUCED CATALYSIS—PRECISION GUIDANCE—HIGH-POWER GASEOUS LASERS—QUANTUM ELECTRONICS IN INSTRUMENTATION and SYSTEMS.

Immediate openings exist for Physicists and Physical Chemists with significant experience in Quantum Electronics, Spectroscopy, Optical Physics, Communication Theory, Organic and Inorganic Non-Crystalline Solids.

You can make a significant contribution in the field of Quantum Electronics, become a part of a new team in a growing Company, and still live in the most choice spot in the United States.

Interested parties should call direct, or send a resume to:

Jack Pagen, Personnel Manager

RADIATION at Stanford

3180 Hanover Street
Palo Alto, California
Area Code 415, Tel: 326-1640

ALL REPLIES WILL BE KEPT CONFIDENTIAL

An Equal Opportunity Employer

Applied Optics

VOLUME 2
NUMBER 1
JANUARY
1963

A monthly publication of the Optical Society of America

John N. Howard, Editor

James G. Baker, Feature Editor

Patricia R. Wakeling, Managing Editor

COVER: For the most precise measurement of star positions, the limiting errors of telescope, photographic materials, and comparator are of nearly equal importance. With optimization of all stages the skilled astronomer can determine the relative positions of good star images to a precision of a micron or less in each coordinate representing an angular accuracy of about 0.01 second of arc. The cover shows a model of the new 60-in. (152-cm) astrometric reflector of the Naval Observatory in the inset (Official U.S. Naval Photograph) and a David W. Mann Comparator for X and Y measurements on an 8 × 10-inch plate. Both represent optimization of the measuring procedure according to current technology. The cover is reproduced through the generosity of the David W. Mann Company.

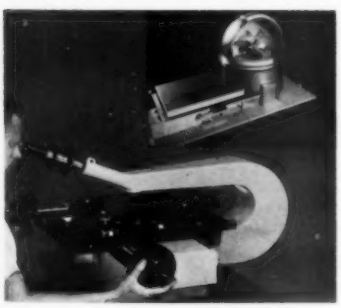

Published monthly by the Optical Society of America, Inc., in cooperation with the American Institute of Physics, at 20th and Northampton Streets, Easton, Pa. Editorial offices: 1155 16th St. N.W., Washington 6, D.C. Supported in part by a grant from the National Science Foundation. Advertising Office: 55 West 16th Street, New York 11, N.Y. A. P. Oppenheim—Chelsea 2-1311. Subscription rates: $6.00 to OSA members, $8.00 other AIP Societies' members; nonmembers and libraries: $10.00 per year. Single copies $2.00. Second class postage paid at Easton, Pa.
© Copyright 1962 by the Optical Society of America.

1 **The 60-in. (152-cm) Astrometric Reflector of the U.S. Naval Observatory**—K. Aa. Strand

9 **Problems of Long-Focus Photographic Astronomy**—Peter van de Kamp

17 **The Relationship Between Standard Coordinates of Stars and the Measured Coordinates of Their Images**—Heinrich Eichhorn

23 **Limitations à la Qualité des Images d'un Grand Télescope**—Jean Texereau

31 **A Direct Analyzer for Stellar Images**—Stanley H. Zisk and Robert A. Fish

41 **Optical Problems of Television Recording of the Moon and Planets from Approaching Spacecraft**—E. P. Martz, Jr.

51 **Temperature Effects in Photomultipliers and Astronomical Photometry**—Andrew T. Young

61 **The Effects of Telescopes on Astronomical Polarization Measurements**—R. H. Miller

67 **The Wavelength Dependence of Polarization**—Thomas Gehrels and Thomas M. Teska

79 **Spectromètre à Grilles**—A. Girard

89 **A Sensitive Visual Photometer for Solar Research**—Yngve Öhman

93 **A Solar Observatory on Long Island**—William A. Miller

105 **Simulating the Solar Spectrum with a Filtered High-Pressure Xenon Lamp**—E. A. Boettner and L. J. Miedler

109 **Selected Ordinates for Solar Absorptivity Calculations**—O. H. Olson

DEPARTMENTS

Meeting Reports

16 **Optical Activities in the Universities**

30 **From the Editor**

40 **The Optical Society of America**

66 **Letters to the Editor**

66 **High-Speed Calculation of Diffusion Coefficients from Rayleigh Interference Fringes**—Lee Hook, Warren W. Davis, and L. Kotin

77 **Angular Measurements by Means of a Ronchi Ruling**—Jurgen R. Meyer-Arendt and Ellis D. Miner, Jr.

78 **Shadowgraph of Self-Luminous Objects**—M. A. Levine and J. C. Hegarty

87 **Operation of a Nd^{3+} Glass Optical Maser at 9180 Å**—R. D. Maurer

91 **An Unusual Property of MgF_2 Films in the Infrared**—Milton Laikin

92 **Low Cost Noncontact Thickness Gauge**—L. C. Lynnworth

NOW!

10 LASER PULSES PER SECOND

Model 325 Power Supply available for:

- Up to 10 Laser pulses per second
- Higher average powers
- Greater average Laser output
- Fast cycling for tracking purposes and product research
- Up to 20,000 joules of energy storage
- Individual capacitor fusing, safety interlocks and automatic discharge

NOW!

A 100,000 JOULE POWER SUPPLY

Model 350 Power Supply available for: ■ 100,000 joules of energy storage ■ Choice of operating voltages: 5,000, 10,000 or 20,000 ■ Average powers to 5KW ■ Forced air circulation ■ Maximum safety: individually fused capacitors, safety interlocks and automatic discharge

NEW!

ARC QUENCH AT 50 MICROSECONDS

Model 3C-4000 Rotary Arc Quench Variable trigger makes it possible to shorten flash duration to as little as 50 microseconds yet retain maximum peak light. This provides:

- Reduced flash tube heat
- Higher repetition rates
- Faster re-cycling
- Greater Laser output with less average pump power

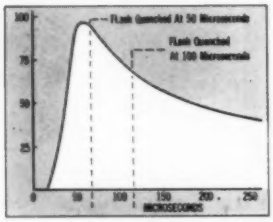

Other Accessories include: ■ Solid State Laser Mounts — air cooled or liquid nitrogen cooled — for rods of all sizes ■ Q Spoiling ■ Peak Power Meter ■ Optical Bench

Technical questions? Phone or write our engineering staff.

ELECTRO POWERPACS, INC.

Manufacturers of Power Supplies, Laser Mounts and Accessories

A SUBSIDIARY OF HYDRA-POWER CORPORATION

6 Hadley Street, Cambridge 40, Mass., Phone: 617-876-9220

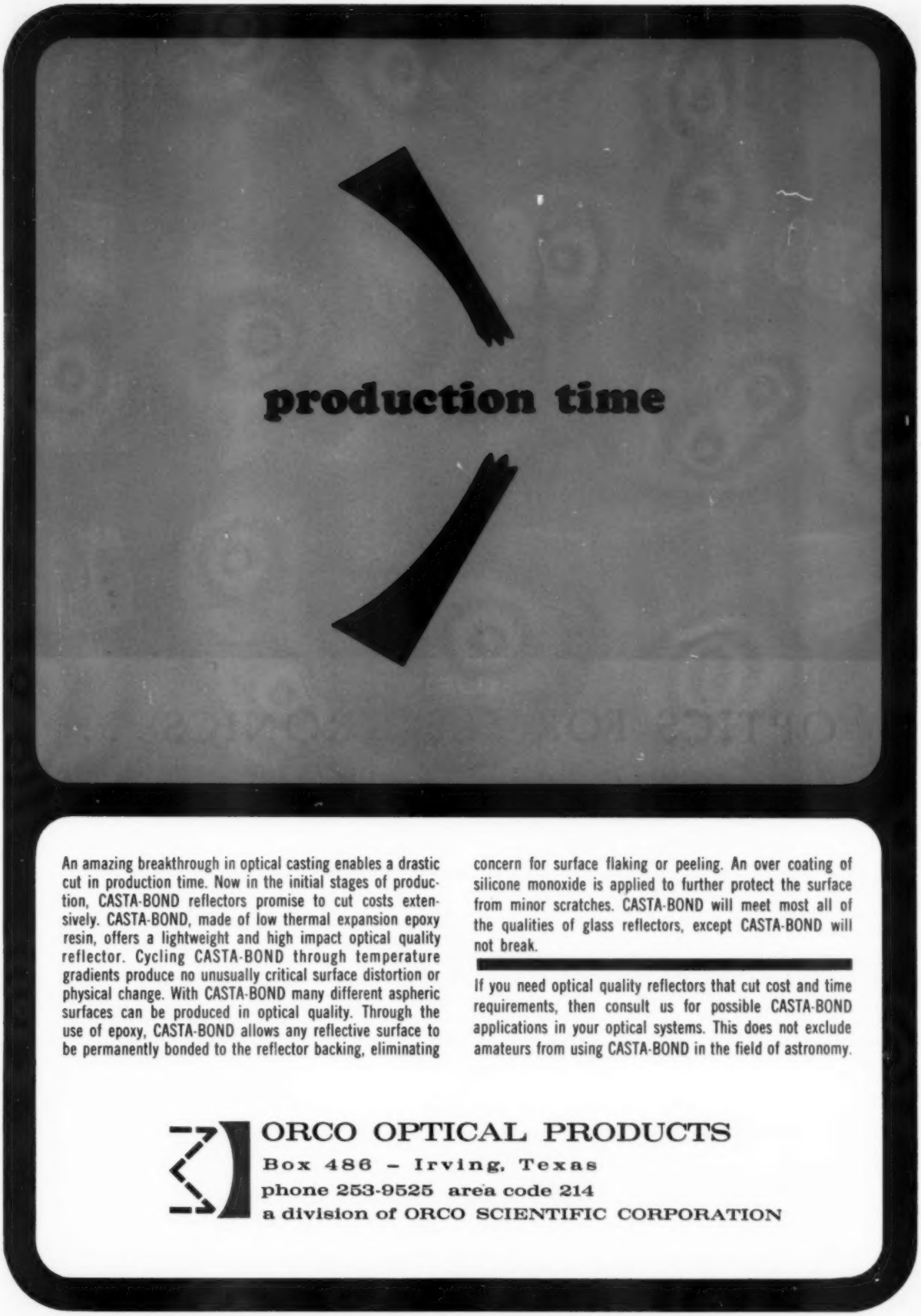

An amazing breakthrough in optical casting enables a drastic cut in production time. Now in the initial stages of production, CASTA-BOND reflectors promise to cut costs extensively. CASTA-BOND, made of low thermal expansion epoxy resin, offers a lightweight and high impact optical quality reflector. Cycling CASTA-BOND through temperature gradients produce no unusually critical surface distortion or physical change. With CASTA-BOND many different aspheric surfaces can be produced in optical quality. Through the use of epoxy, CASTA-BOND allows any reflective surface to be permanently bonded to the reflector backing, eliminating concern for surface flaking or peeling. An over coating of silicone monoxide is applied to further protect the surface from minor scratches. CASTA-BOND will meet most all of the qualities of glass reflectors, except CASTA-BOND will not break.

If you need optical quality reflectors that cut cost and time requirements, then consult us for possible CASTA-BOND applications in your optical systems. This does not exclude amateurs from using CASTA-BOND in the field of astronomy.

ORCO OPTICAL PRODUCTS
Box 486 – Irving, Texas
phone 253-9525 area code 214
a division of ORCO SCIENTIFIC CORPORATION

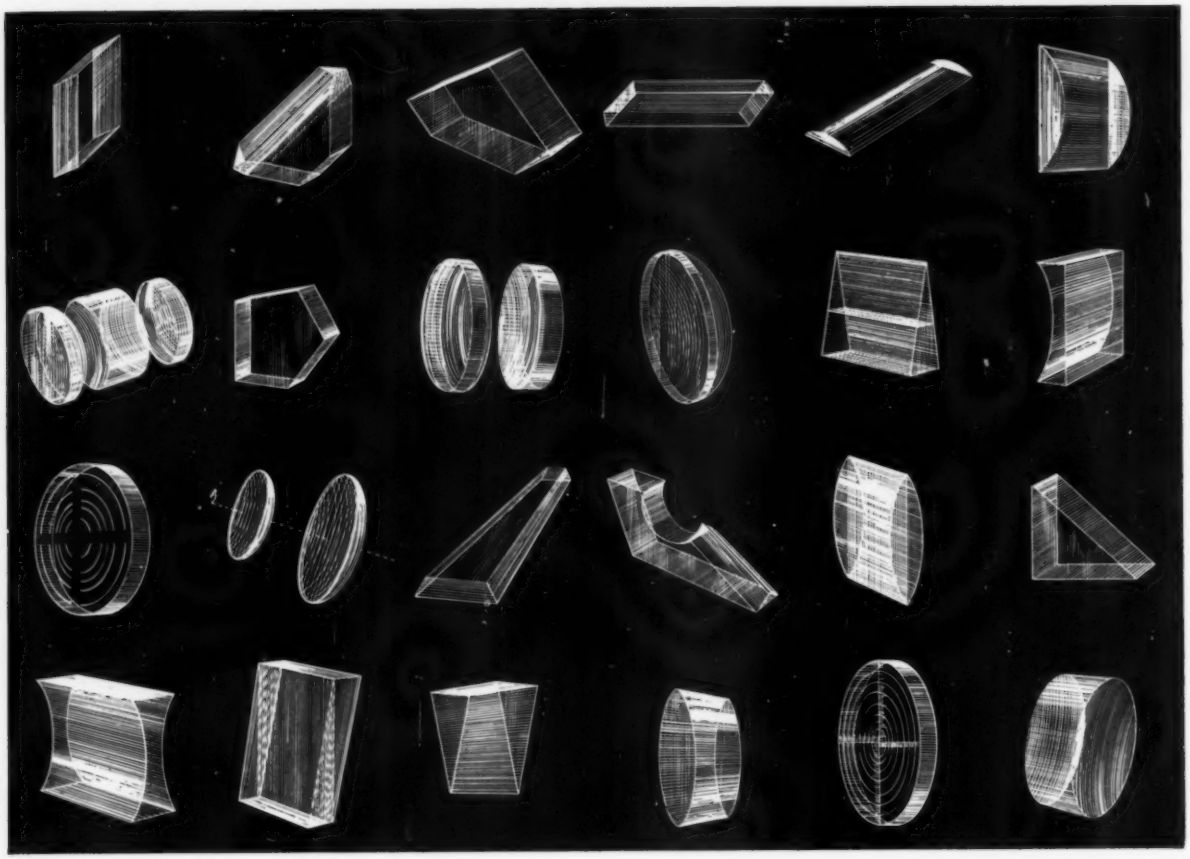

OPTICS FOR ELECTRONICS . . .

Components and systems for visible, ultraviolet, and infrared radiation. GEC's Astron-Optics Division specializes in design, development, and manufacturing of optical components and systems for the ultraviolet through infrared spectrum.

Here are a few of the optical components you can order from Astron-Optics: prisms, flats, spherical, aspherical and parabolic surfaces, reticles, information choppers, encoders, precision vacuum coating, and optically polished synthetic crystals.

Also available from Astron-Optics are infrared and optical-electronic systems.

For complete information regarding your precision optical requirements, write today to:

ASTRON OPTICS DIVISION

. . . precision optics at work

GENERAL ELECTRODYNAMICS CORPORATION

4430 FOREST LANE • GARLAND, TEXAS • BROADWAY 6-1161

HERE'S HELP

from Bausch & Lomb

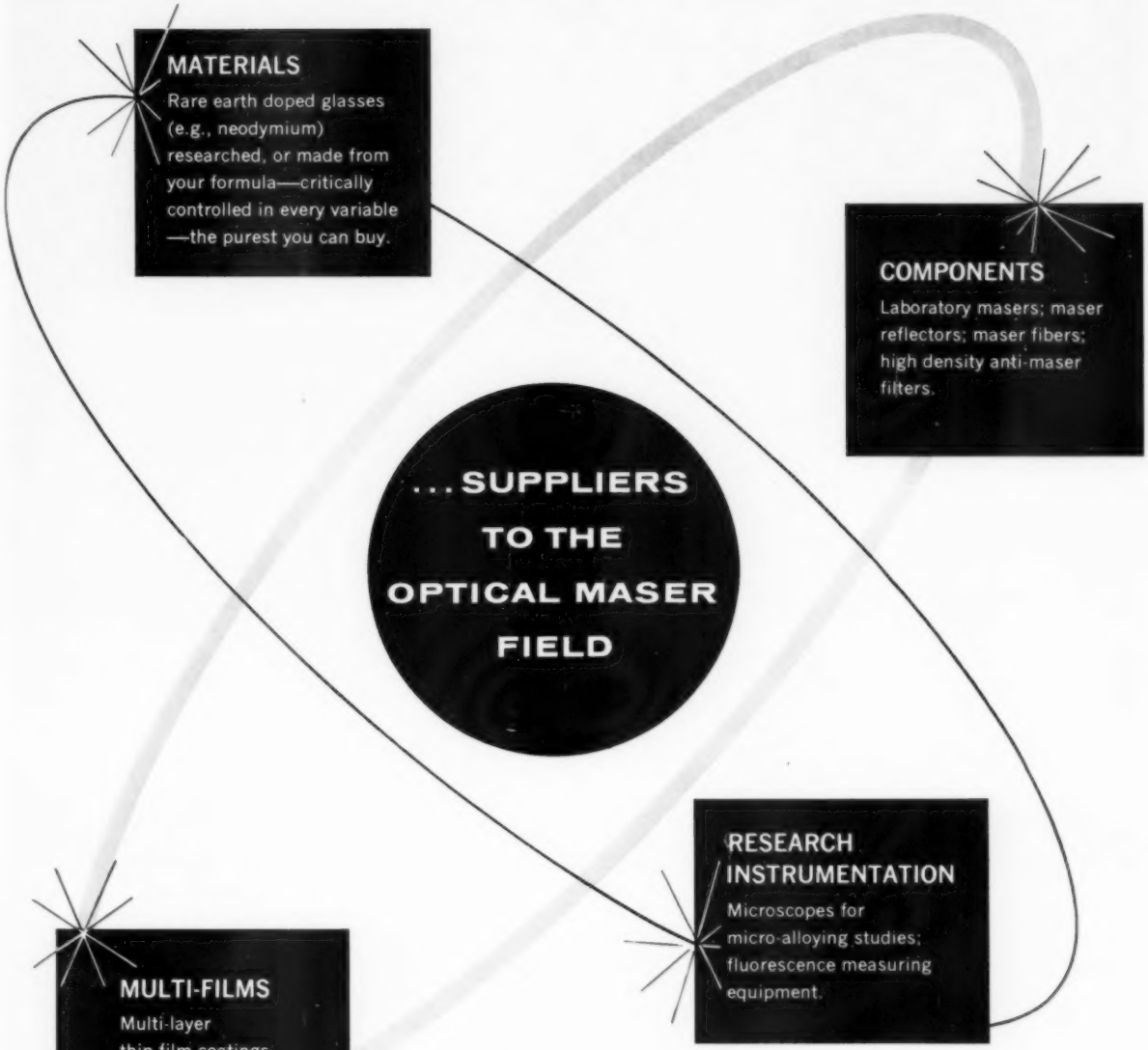
MATERIALS
Rare earth doped glasses (e.g., neodymium) researched, or made from your formula—critically controlled in every variable —the purest you can buy.
COMPONENTS
Laboratory masers; maser reflectors; maser fibers; high density anti-maser filters.
...SUPPLIERS TO THE OPTICAL MASER FIELD
RESEARCH INSTRUMENTATION
Microscopes for micro-alloying studies; fluorescence measuring equipment.
MULTI-FILMS
Multi-layer thin film coatings for all known lasers and masers.

Here's *real* help on your optical maser problems. B&L capabilities cover all the bases—materials, components, coatings, R&D—to fill your present needs and to help with your maser development programs. And you're sure of quality—it's written right into your contract.
For information on your specific problems, write: Commercial Contract Sales Dept., Bausch & Lomb Inc., 77137 Bausch Street, Rochester 2, N. Y.

BAUSCH & LOMB

Baird-Atomic's exclusive sidewing blocking techniques produce all-dielectric, multilayer interference filters with the highest total transmission and a transmission-rejection ratio of less than 0.1%. Only B/A Interference Filters have a block shape ⎍ band pass assuring the greatest degree of spectral purity.

B/A Interference Filters covering two ultraviolet ranges and the visible spectrum are stocked in 1″ x 1″ and 2″ x 2″ sizes. Half-band widths, additional blocking and special shapes and sizes are also available. Only 21 days maximum is required to fill special orders. Special quantity prices prevail.

Filter Classifications

Visible Spectrum	4000-8000 Å
Standard Ultraviolet	2100-3400 Å
Special Ultraviolet	3900-3999 Å
Half-band Widths	4.8-1600 Å
Maximum Transmission (Complete Curves Available $15 Extra)	25-70%
Rejection	0.1%
Blocking	Maximum blocking with reduced thickness for improved signal-to-noise ratio.

For full information, write Adv. Dept. for brochure X-44

BAIRD-ATOMIC, INC.
33 University Road · Cambridge 38, Mass.

Engineers and Scientists: *Investigate challenging opportunities with B/A. Write Industrial Relations Director. An equal opportunity employer.*

ADVANCED OPTICS AND ELECTRONICS...SERVING SCIENCE

For those on the East Coast, those on the West Coast, and those in between, we are thinking of your convenience in establishing a precision optical grinding laboratory in the Dallas area.

Our facilities will offer those in need of precision optics, in the micro and macro range, competitive prices and quality with short-time requirements in mind. We will also have available complete consulting services for those grinding problems in optics.

We invite your inquiries about our services and facilities and hope to be of service to you soon.

ORCO OPTICAL PRODUCTS
Box 486 – Irving, Texas
phone 253-9525 area code 214
a division of ORCO SCIENTIFIC CORPORATION

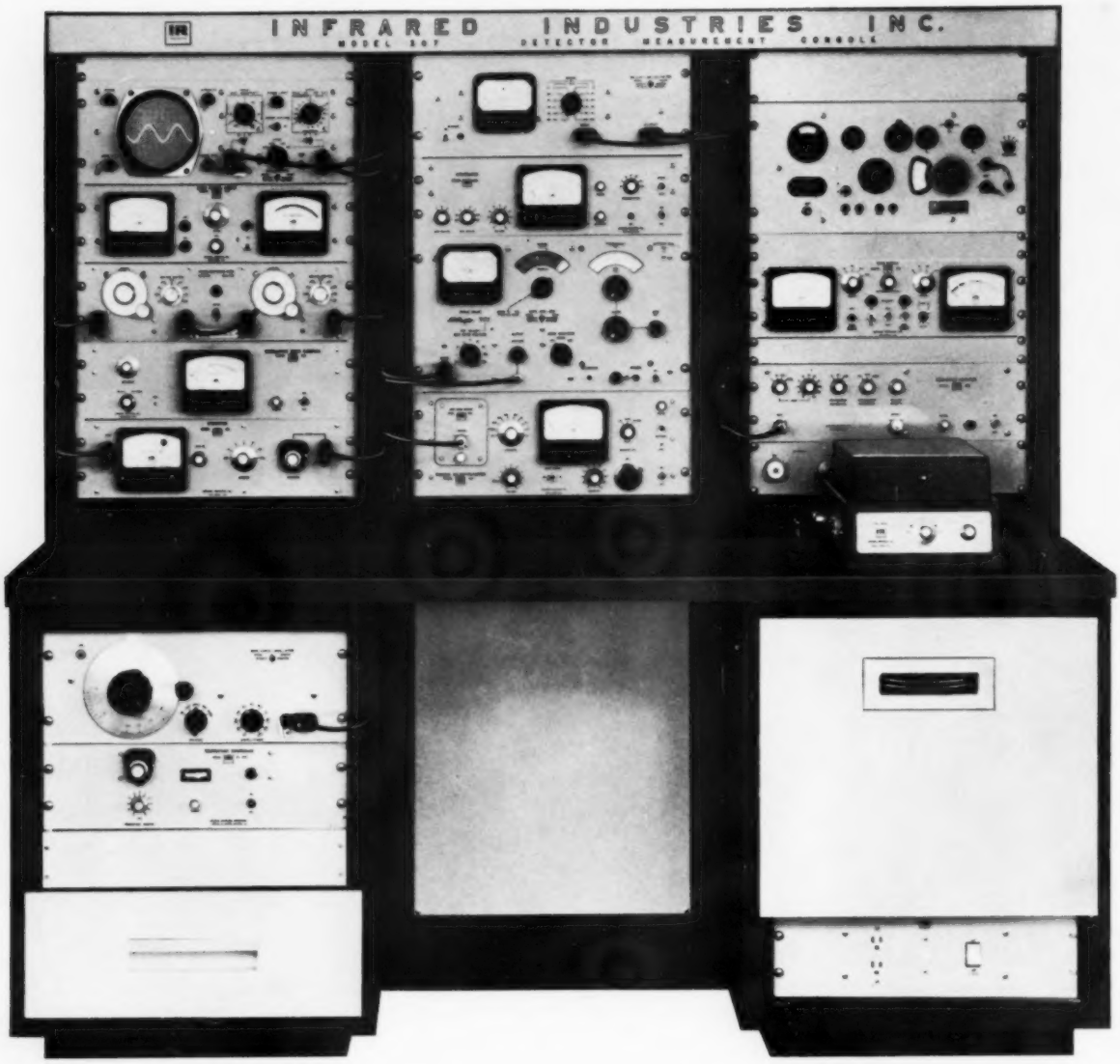

MODEL 307
Detector Measurement Console

A compact improved addition to a successful series of comprehensive detector measurement laboratories. ☐ Model 307 accurately measures all important operating parameters of infrared detectors. ☐ It is presently in use by the military, and within its selective wide range of capabilities may be the answer to your measurement needs. ☐ Decision making information is available to you from

IR INDUSTRIES, INC.

INFRARED INDUSTRIES, INC.

Box 989, Santa Barbara, California · Phone 684-4181 (Area Code 805)

BARNES leads in

SYSTEMS and INSTRUMENTS from ultraviolet through far infrared

BLACKBODY RADIATION STANDARDS
- Point Sources
- Extended-Area Sources
- Collimated Radiation Sources
- Selectable-Aperture Sources
- Chopped Radiation Sources

RADIOMETERS
- Research
- Contrast
- Meteorological
- Spectral
- Special Purpose

DETECTORS
- Thermistor Bolometers
- Photoconductive Cells
- Immersed and Coolable Detectors

MISSILE & SPACE VEHICLE INSTRUMENTS
- Tracking Sensors & Systems
- Horizon Sensors
- Satellite Radiometers
- Satellite Spectrometers
- Space Navigation Sensors
- Star Trackers

ELECTRO-OPTICAL ALIGNMENT INSTRUMENTS
- Photoelectric Autocollimators
- Azimuth Alignment Theodolites
- Flexure-Monitoring Systems

INFRARED CAMERAS

SCANNERS
- Single-line Scanners
- Multi-element Scanners

FIELD MEASUREMENTS EQUIPMENT
- Photometers
- Sequence Spectrographs
- Ballistic Cameras
- Airborne Radiometers
- Atmospheric Transmissometers
- Calibration Systems
- Multi-Image Wedge Cameras

OPTICAL COMPONENTS & SYSTEMS
- Reflective Objectives
- Refractive Objectives
- Interference Filters
- Collimators
- Special-Purpose Systems

ULTRAVIOLET INSTRUMENTATION
- Photometers
- Spectrometers
- Spectrographs
- Optics

COMPONENTS & ACCESSORIES

SPECIAL SERVICES
- Research
- Development
- Manufacturing
- Field Engineering
- Optical Design

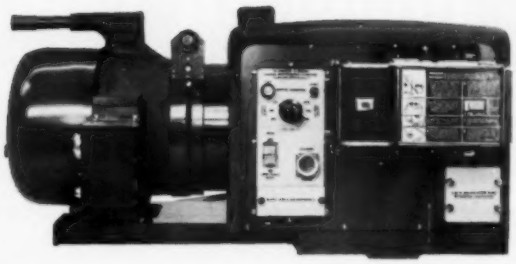

Infrared Camera for thermal photographic studies and quantitative analysis of extended areas. Request Bulletin 12-600.

Temperature-Controlled Infrared Radiation Reference Standards for laboratory and field use. Request Bulletin 11-010.

Radiometers, surface and airborne models, for military and scientific applications. Request Bulletin 1201.

Thermistor Bolometer Detectors — fast, sensitive, rugged and with uniform spectral response from the ultraviolet through the far infrared. Request Bulletin 2-100.

Barnes Engineering Company

Defense and Space Division

Main Office: 30 Commerce Road, Stamford, Connecticut, Area Code 203 FI 8-5381
In Europe: H. Dauber Associates, Inc., Leopoldstrasse 27, Munich 23, Germany

Announcing

HARSHAW LASER MATERIALS

Calcium Fluoride with various activators

★ Available from stock
★ Available as polished LASER rods
★ Proven LASER action

The Harshaw Chemical Company's entry to the LASER field is based on established excellence in crystal growth supplemented by a competent Research and Development team of chemists and physicists in their Crystal-Solid State Division. Proven crystal production know-how is now backed up by theoretical studies and careful experimental measurements of LASER materials. Additional LASER materials (tungstates, molybdates, etc.) and electro-optical materials suitable for modulation of LASER beams will be announced as they become available.

FEATURES:

- Specified activator type and concentration
- Specified activator valence state
- Charge compensation
- Measured absorption spectrum
- Measured fluorescence emission spectrum

SERVICE: Harshaw will grow experimental LASER and optical crystals to customer specification.

ADDRESS INQUIRIES TO:
The Crystal-Solid State Division
The Harshaw Chemical Company
1945 East 97th Street, Cleveland 6, Ohio

HARSHAW

The 60-in. (152-cm) Astrometric Reflector of the U.S. Naval Observatory

K. Aa. Strand

The 60-in. (152-cm) Astrometric Reflector has been designed primarily for high precision celestial photographic work. The telescope is basically a Newtonian type with a paraboloidal primary and a flat secondary, but the optics are arranged like a Cassegrainian telescope with the focal plane behind the primary. The description covers the materials, the design and the support system of the optics, and the mounting, dome, and support system of the telescope. A brief description follows of the environment of the telescope, which is so essential for effective utilization of such an instrument.

Introduction

The Astrometric Reflector of the U.S. Naval Observatory has been designed primarily for astrometry of faint stars.

What astrometry entails is not generally known outside the circles of the professional astronomer, but according to Webster it is defined as "That branch of astronomy dealing with the measurement of planets, stars, etc., and their positions and movements." More specifically, the main observing program of the new telescope will be the determination of the distances to the intrinsically faint stars within 30 parsecs (933 million million km) of the sun. These stars, classified as red dwarfs, white dwarfs, and subdwarfs, are of great astronomical interest, because they differ drastically in their physical properties from solar type stars. To determine these properties it is necessary to know the energy radiated from these objects, which can be evaluated only after their distances are known.

The distances of the stars are determined from their annual or heliocentric parallax, which is defined as the angle at the star subtended by the unforeshortened radius of the earth's orbit. The annual parallax is, in other words, the semimajor axis of the small ellipse which the star describes on the sky in the course of a year, reflecting the earth's annual motion around the sun.

These angular shifts, measured against a background of more distant stars, are for even the nearer stars only a small fraction of a second of arc, only a few microns in terms of scale in the focal plane of even the large telescopes, and these small quantities must be determined with probable errors of a fraction of a micron. To do so requires the use of photography with telescopes of sufficiently large focal length, preferably 10 m or more, having optics stable enough to preclude any material changes over periods of several years.

Since the beginning of this century, distance determinations of stars from their trigonometric parallaxes have been carried out almost exclusively with long-focus refractors such as was first done by Frank Schlesinger with the largest existing visual refractor at the Yerkes Observatory, which has a focal length of 19.4 m and an aperture of 102 cm (40 in.).

The effective limiting magnitude of even the largest refractors now in existence is of the order of 13.5. Since most of the stars in the categories mentioned above are fainter than this limiting magnitude, this means that there is at the present time no telescope available which can be satisfactorily used for determining the trigonometric parallaxes of these objects.

Since the mounting of the objective in the refractor definitely limits its size to that of existing refractors, a further extension to fainter magnitudes would require either photographic emulsions of considerably greater speed than any now on the market or it would require the use of image tubes for image intensification.

The development of a photographic emulsion of drastically increased speed seems doubtful at the present time. Similarly, it seems unlikely that image tubes will be available within a reasonable length of time which would provide undistorted fields over a sufficiently large area to permit their use for astrometric work of the kind indicated.

The author is at the U.S. Naval Observatory, Washington 25, D.C.

Received 1 September 1962.

Five percent of the nearly 11,000 trigonometric parallaxes which have been determined so far were obtained by Adriaan van Maanen with the 152-cm (60-in.) and 254-cm (100-in.) reflectors of the Mt. Wilson Observatory. The 152-cm was used at the Cassegrain focus, while the 254-cm was used at the Newtonian focus. These results proved that both instruments are suitable for high precision astrometric work when confined to small fields with coma free images, which in the case of the 254-cm is only 7 min of arc. Thus we find that the parallaxes of the fainter stars with nearby reference stars are in excellent agreement with the refractor parallaxes.

It has been the tendency in recent years to decrease the *f*-ratio of large reflectors from the traditional *f*/5 primary to values as small as *f*/3.3 for the 508-cm (200-in.) Palomar telescope and *f*/2.75 for the Kitt Peak 213-cm (84-in.) reflector.

The chief factor in favor of the small *f*-ratio is the lower cost of the completed facility, effected by the construction of a less massive telescope, and especially by the need of a smaller dome.

The disadvantage of the small *f*-ratio for astrometric work is the small size of the coma free field, which for the 508-cm Palomar telescope is less than 12.5 mm in diameter. This makes it necessary to use coma correctors such as devised by Ross[1] and Maksutov[2] if a wider coma free field is desired. The coma correctors for the prime focus of telescopes of small *f*-ratios show distortion and variation of scale with color, which are not permissible in astrometric work of high precision.

In order to obtain sufficient accuracy in astrometric work of high precision an equivalent focal length of at least 10 m (33 ft) is desirable. This can be obtained with a sufficient amplification factor of the Cassegrain secondary. However, it should be realized that the collimation of a telescope becomes increasingly difficult as the *f*-ratio decreases and the secondary magnification increases. In this respect a flat secondary and a primary of sufficient focal length becomes an ideal optical system for astrometric work, if the mirrors are kept aligned.

Optical Materials

The ideal situation for obtaining plates of a star field to be used in a parallax series is to observe the field on the meridian with the sun setting in the west or rising in the east. This can be seen from simple geometrical considerations. While such a situation is never realized, the early evening and late morning hours for observing are essential in a parallax program.

The early evening drop in temperature frequently produces distortion in the figure of the optical mirror to the extent that the star images formed by the system are useless.

For this reason it is essential to use a mirror material with a low coefficient of expansion and with high thermal conductivity.

To achieve the last property would require the use of a metal mirror. However, it was not felt that the state of the art of producing metal mirrors with high optical performance had been sufficiently developed to permit serious consideration of such a material at this time.

Low-expansion glass, such as Pyrex with a coefficient of expansion of 25–30 $\times$ 10^{-7} per °C, was introduced with the 508-cm telescope and has since become the generally used material for large optics.

Attempts to produce quartz which has a coefficient of expansion of only 6 $\times$ 10^{-7} per °C for optical mirrors are well known in connection with the development program of the 508-cm telescope. Although the program did not succeed in producing the desired disk for the primary mirror it did much to advance the production of fused quartz.

The process developed by Corning Glass Works of making fused quartz from gaseous silica appears at the present time the most successful of the various processes now being used, especially as applied to large mirror disks.

The 92-cm disk produced by Corning Glass Works for the Princeton Stratoscope project convinced the writer that this firm should be approached in an attempt to obtain silica rather than Pyrex mirrors for the new telescope. After a preliminary meeting Corning Glass Works was in a position in May 1960 to quote prices for delivery of fused silica blanks.

The specifications called for a primary solid mirror blank with a minimum diameter of 158 cm and 26.8 cm thickness. Since the manufacturing process limited the thickness of the silica blanks to approximately 8.9 cm, the specifications permitted the blank to be of a laminated design using 4 plates with 3 seals.

The blank, weighing 1360 kg, was successfully manufactured and delivered to Davidson Optronics in West Covina, California, for rough grinding and testing in May 1961.

After grinding the rough blank it appeared that the largest possible dimensions would be 6.3 mm less in both diameter and thickness than the specifications called for.

A polarimeter test showed a strain pattern which indicated that the blank was well and uniformly annealed. Maximum strain in the entire blank was found to be 20 to 22 nm per centimeter of thickness which was within the tolerance of 30 nm per centimeter set forth in the contract.

The late Don Hendrix, upon examining the strain pattern, remarked that he had never seen a large telescope blank with such a uniform strain pattern and with such low strain in it.

Careful examination of the top surface of the blank indicated that there would be approximately 30 bubbles

of 0.25 mm size in the area exposed to the stars, which was well below the maximum allowable inclusions of 10 per 100 cm² of sizes not exceeding 0.2 mm in diameter.

In Fig. 1 is shown the 158-cm blank after rough grinding and covered with refractive oil to render it transparent. The elongated 17.8-cm bubble shown at nine o'clock is at least 3.8 cm below the proposed polished surface and is not considered to cause any trouble.[3]

Since the 158-cm blank was the largest quartz blank so far produced by Corning Glass Works it was gratifying to have it come out so well.

The blank for the secondary mirror, 89 cm in diameter and 14 cm thick, weighing 204 kg, was produced well within the specified tolerances with a strain pattern not exceeding 10 nm per centimeter of glass thickness.

Optical Design

The basic optical design of the 152-cm telescope consists of a paraboloidal primary with a nominal focal length of 15 m, and a flat secondary reflecting the light through a perforation of the primary to the Cassegrainian focus.

With a focal length of 15 m, the scale is 13.″5/mm.

Using the simple theory of coma, we have

$$K'' = \frac{3}{16}\left(\frac{D}{F}\right)^2 \beta'',$$

where β is the angular distance of the star from the axis of the mirror, D is the aperture, and F is the focal length of the mirror. K is the total length of the comatic image.

Assuming under good seeing conditions an optimum photographic image size of 1.″2 for the axial image as compared to 1.″62 for the comatic image, we find from the above formula that the coma is first detectable for $\beta = 864'' = 14.'4 = 64$ mm. The total field with no coma is then 28.′8 as compared to 2.′9 for the 508-cm telescope.

The large secondary mirror increases the intensity of the first and second diffraction ring. Theoretically, the first dark ring appears at 0.″092 from the center of the image and the third dark ring at 0.″25. If the second bright ring contributes a perceptible amount to the image intensity, the theoretical image of 0.″50 is well within the photographic image size. The question is still open as to how this will affect micrometer observations of close binaries.

Specifications for the 152-cm optics call for 80% of the light within a 0.025-μ diameter circle or 0.″33. For comparison, the 508-cm has 80% of the light within 0.″7 diameter circle. The general surface quality has been specified to be such that the maximum angle of deviation from the true paraboloid will be less than 0.10 sec of arc.

The optical system will have a built-in collimation system which will provide check on proper alignment of the two mirrors. Collimation will be carried out by mechanically adjusting the secondary mirror by means of motors controlled from the eye end of the telescope.

Fig. 1. The 62-in. (157-cm) quartz blank after rough grinding. Reproduced by permission of the Corning Glass Works. (*Photo Vanda Roberts, Interstate Photographers.*)

Since the secondary mirror is an optical flat, it is only required that its surface be normal to the optical axis of the primary mirror for proper alignment. This of course precludes major shifts in the secondary which might introduce effects due to vignetting.

The optical system incorporates a coma corrector to be used when a larger field is desired for other purposes than high precision astrometric work.

The corrector lens assembly is located 15 cm in front of the face of the primary mirror and is motor driven to fold in and out of the optical path in a plane parallel with the mirror. No vignetting is caused by the corrector in its out position because it is hidden in the shadow of the secondary.

The Mirror Support System

The mirror support system is based upon an air tight cell housing for both mirrors.

The axial support of the primary mirror is provided by a layer of compressed air 125 μ thick on the back of the mirror, with a variable air pressure applied depending upon the position of the mirror. The pressure varies in range from zero when the mirror is in a vertical position to a pressure equal to the weight of the mirror when in its horizontal position.

Fig. 2. Photograph of a scale model of the 60-in. (152-cm) Astrometric Reflector. (*Official U.S. Navy Drawing.*)

Axially, the mirror is defined by 3 pads located in the rear of the cell.

The radial support of the mirror is provided hydrostatically on two buoyant neoprene tubes filled with mercury. One tube surrounds the perimeter, the other the inside hole in the center of the mirror. The mercury-filled tubes, in addition to "floating" the mirror axially, also seal off the pressure chamber at the rear of the mirror.

The three radial defining pads are located around the hole in the center of the mirror.

The mirror support system for the secondary is similar to the system just described for the primary except a vacuum is applied equal to the weight of the mirror when in the horizontal position and zero when it is in a vertical position.

The mirror support system is provided with a pressure supply and regulating system to deliver the correct pressures for both mirrors.

For the primary we have a pressure of $+42.4 \sin A$ (mm Hg) and a vacuum of $+22.2 \sin A$ (mm Hg) for the secondary where A is the altitude of the telescope above the horizon.

The chief advantage of the mirror support system described above is its simplicity, as compared to the more conventional lever system used in the larger modern reflectors. Final adoption of the system, however, depends upon the outcome of tests made with dummy steel mirrors.

The axial support system actually employs an old idea first put into practice by Foucault, who used a pig's bladder to carry the mirror.[4]

Since both mirrors are thicker than usual for their diameter, the axial support problem is less difficult to solve. According to Schwesinger[5] the second harmonic in the Fourier spectrum of the edge pressure distribution should be avoided. The neoprene tubes eliminate this term if they are entirely filled with mercury and for all practical purposes have zero stiffness.

The Telescope Mounting

As shown in Figs. 2 and 3, the mounting of the 152-cm Astrometric Reflector is the fork type. It resembles the 305-cm reflector of the Lick Observatory with its unequal-armed parallelogram truss of the Serrurier type for the tube. The compensated truss structure allows the primary mirror cell to deflect under gravity the same amount as the secondary cell.

The secondary mirror support struts are seamless steel tubings 5.2 m long, 20.3 cm in diameter, with 4.8 mm walls, holding the secondary cage support ring of the same material.

The primary mirror support struts are seamless steel tubings approximately 1.22 m long, 12 7 cm in diameter, with 12.7 mm walls, supporting an annular steel casting 2.24 m in diameter, to which the cell of the primary is mounted.

The distances from the center of the declination axis to the mirror cells of the primary and secondary mirrors are 1.83 m and 5.8 m respectively, using a nearly one-fourth-point balance position.

The total weight about the declination axis is 14,750 kg, while the primary and secondary mirrors with their support systems weigh 5000 kg and 750 kg, respectively.

Since only the primary focus is being used, it is essential that enough working space is left between the mirror cell and the fork to allow the observer access in all positions of the telescope.

It is also essential that the stiffness of the fork be preserved by not making it unduly long.

The total length of the fork from the center of the declination axis to the face of the fork bearing is 4.72 m, allowing a maximum working space of 1.22 m between focal plane and fork when the telescope is directed towards the north pole.

The fork is a welded steel structure constructed of 2.5 cm steel plates reinforced by internal stiffening partitions (Fig. 4).

Telescope Drive and Support System

In place of separate wheels for slewing and tracking, the right ascension drive for the 152-cm telescope consists of a single worm wheel used for both motions. Al-

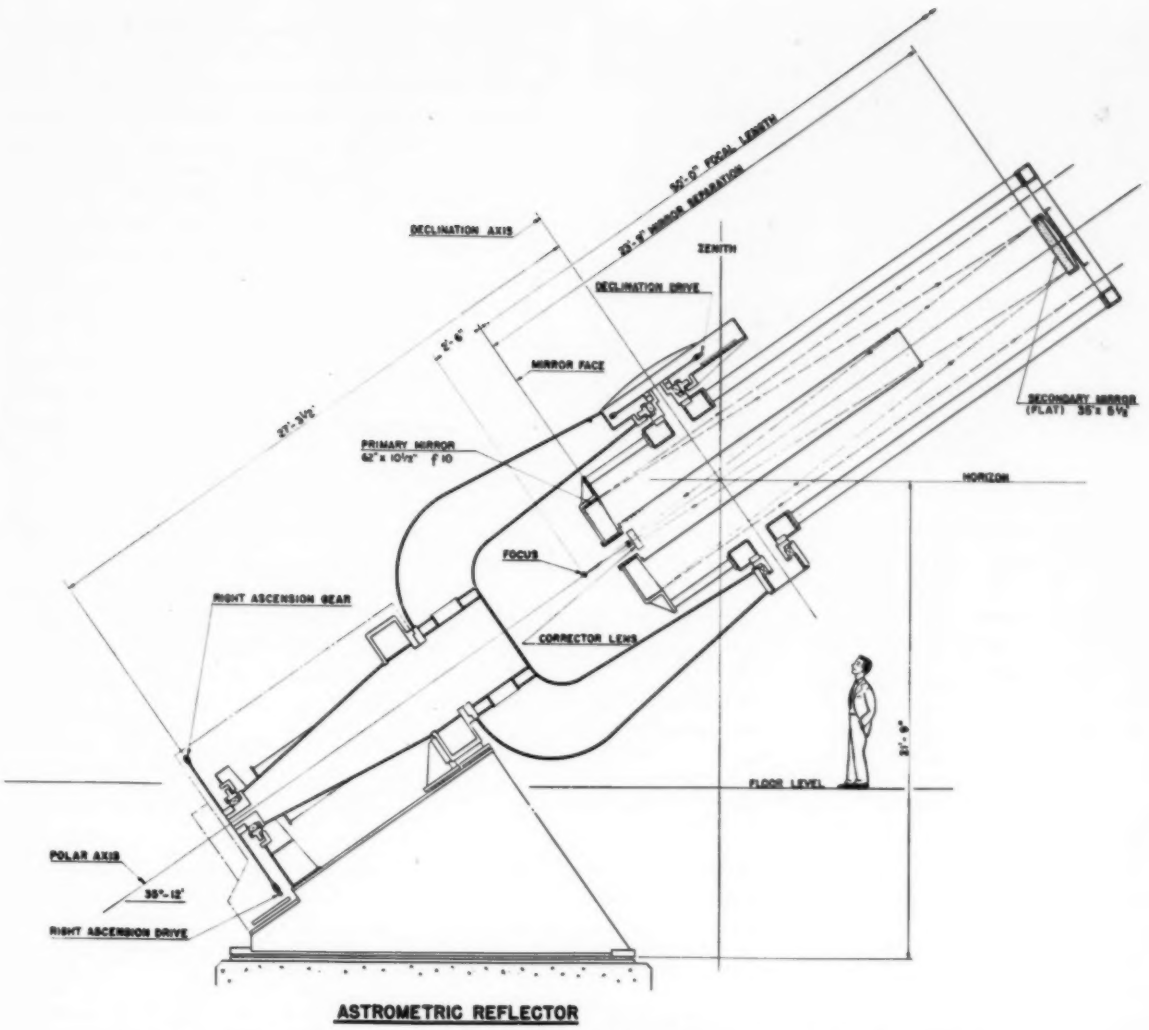

Fig. 3. Section of the 60-in. (152-cm) Astrometric Reflector. (*Official U.S. Navy photograph.*)

though this places an additional load upon the wheel and worm in slewing, it was felt that the dimensions of the telescope were still within the limits permitting the use of a single wheel and that proper lubrication of the worm would give a satisfactory lifetime of the wheel.

With the telescope primarily being used within two hours of the meridian there is a possibility that the corresponding section of the wheel will receive greater wear than the remainder of the wheel. For this reason provisions have been made to rotate the worm wheel with respect to the polar axis, and in this way avoid any excessive wear on one particular sector of the worm wheel.

The right ascension worm gear, 2.29 m in diameter with 720 teeth, is driven by a worm of 8.9 cm pitch diameter. The maximum tooth to tooth and total composite errors have been specified as 5 μ.

The right ascension drive consists of two basic drive units, a fine drive unit, and a slewing unit. The fine drive unit mounted on an adjustable defining plate includes the tracking motor, setting motor, and guiding motor. The three motors are interconnected by two differentials to the drive worm. All of the motors may be operated simultaneously or separately. When a motor is not running it is locked against rotation. A magnetic clutch couples the drive to the worm and is spring opened to disengage the drive if there is a power failure or the slewing motor is operating.

The slewing motor is geared directly into the fine drive coupling clutch and never disengages from the

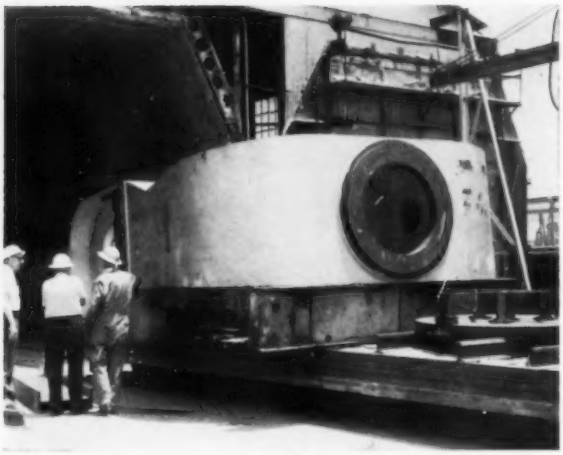

Fig. 4. Fork fabrication of 60-in. (152-cm) Astrometric Reflector on cart prior to going into the stress relieving furnace. (*Photograph by L & F Machine Company.*)

right ascension worm. The slewing drive is wired in such a way that the fine drive unit is disengaged from the right ascension worm whenever the slewing motor is energized. Smooth starting and stopping of the slewing motion is secured by equipping the slew motor with both a flywheel and a drag brake.

The slewing motion is performed by a 250 W 1140 rpm motor, while the setting and tracking motors are 38 W 48 rpm and 10 W 1800 rpm, respectively.

Corrections to the guiding of the telescope will be made directly through the right ascension and declination drives by means of 11 W guide motors. The guiding can be controlled by hand or be carried out automatically by means of a transistorized version of the Weitbrecht type, which uses a pyramid shaped prism and four 1P21 photomultiplier tubes as position indicators.[6]

The adopted engineering specifications and allowable errors are as follows:

Slewing rate	120°/min
Setting rate	1°/min
Guiding rate	0".5/sec
Sudden error	±0".25/sec
Pointing error	±1′ over the sky
Tracking accuracy	0".5 in one revolution of worm (2 min)

The declination worm gear, 1.52 m in diameter with 480 teeth, is driven by a worm with 6.35-cm pitch diameter. The same tolerances are specified here for worm-gear precision as for the right ascension drive.

The rotating weight of the telescope about the polar axis is 36,300 kg, and is carried by a combination of oil pad and standard ball bearings.

The north-polar bearing consists of three oil pads supporting the majority of the weight of the telescope both radially and axially.

The average operating pressures of the oil, which has a high viscosity index, are 54 kg/cm² for the radial bearing pads and 48 kg/cm² for the thrust pad. Under dynamic conditions the flow is 10 l/min. Duplicate pumping and filtering systems are provided with 2.25 kW motors with variable speed drives used on each pump.

Each pad consists of a cylindrical surface, matching the journal surface with a recessed control cavity with a diameter of half that of the pad. The oil under high pressure flows into the cavity and is allowed to flow out to the collection channel around the edge of the pad. The oil-film between the journal and the surface of the pad ranges in thickness from 75 μ to 125 μ. The total oil capacity of the system is 416 l. The two radial bearing pads and the thrust pad are all circular in shape with an actual supporting area of 0.2 m².

Special needle valves, one for each pad, allow adjustment of the oil film thickness for the particular temperature conditions prevailing during a normal night's observation period.

The telescope is now under construction in California as a joint venture of L and F Machine Company in Huntington Park, and Boller and Chivens, Inc., in South Pasadena. It is expected that it will be completed in June 1963.

Building and Site

The Astrometric Reflector will be housed in a new observatory building (see photograph of model on cover) located at the Flagstaff Station of the U.S. Naval Observatory, approximately 8 km west of the city of Flagstaff, Arizona.

The station has an elevation of 2300 m above sea level, and has excellent observing conditions in regard to the number of clear nights, transparency, and seeing.

The observatory building has been designed with the principal aim of minimizing the deleterious effects of higher daytime temperatures upon nighttime operation of the telescope. For this reason the dome has double walls with air space and insulation in between. Similarly, the stationary structure of reinforced concrete below the dome is protected against the daytime heat by a cellular glass insulation and an aluminum shield spaced 15 cm from the wall to allow free flow of air. The ample sized dome, 20 m in diameter, and observing floor level 10 m above the ground provide added protection against bad "seeing" effect.

The planning, funding, and construction of a major astronomical project usually extends over a period of many years. The Astrometric Reflector project differs in this respect. Preliminary engineering for funding purposes started as late as in the fall of 1959. The quick passage of the appropriation for this project by Congress in July 1960 was without doubt the result of recognition of the scientific need for this instrument. Several international conferences, including the Cosmic Distance

Scale Conference at the University of Virginia in the spring of 1956 and the General Assembly of the International Astronomical Union in Moscow, U.S.S.R., in the summer of 1958, adopted resolutions supporting the project.

Over the years the author has had the privilege of discussing the planning of the project with many astronomers and engineers experienced in telescope construction and operation. He is particularly indebted to Ira S. Bowen, the Director of the Mt. Wilson and Palomar Observatories, and his associates over many years, the late Walter Baade, the late Frank E. Ross, Bruce Rule, and the late Don Hendrix for their wise counsel and to Vice Admiral J. T. Hayward, U.S. Navy, for his enthusiastic support as Deputy Chief of Naval Operations (Development).

It is a pleasure to acknowledge the expert management of engineering and contracting and supervision of construction by the Director of the Southwest Division, Bureau of Yards and Docks, Rear Admiral T. R. Davis, C.E.C., U.S. Navy, and his staff. Much credit goes to C. W. Jones of Los Angeles and his firm, which was awarded the preliminary and final engineering and architectural contracts.

References

1. F. E. Ross, Astrophys. J. **81**, 156 (1935).
2. D. D. Maksutov, *History of the Telescope* (Sky Publ. Corp., Cambridge, Mass., 1944).
3. Report from Davidson Optronics, Inc., to: Corning Glass Works, 11th Naval District Contracting Office, K. Aa. Strand, dated August 10, 1961.
4. G. M. Sisson, *Vistas in Astronomy*, A. Beer, ed. (Pergamon Press, New York, London, Oxford, Paris, 1960), Vol. 3, p. 100.
5. G. Schwesinger, J. Opt. Soc. Am. **44**, 417 (1954); also private communication dated July 27, 1962.
6. R. H. Weitbrecht, Rev. Sci. Instr. **28**, No. 2, 122 (1957).

Meeting Reports

47th Annual Meeting of the Optical Society of America, Manger Hotel, Rochester, New York, October 3–5, 1962

Reported by D. L. MacAdam, Eastman Kodak

The 47th Annual Meeting was preceded on October 2 by trips to the new Physics Laboratory of the Eastman Kodak Company, to Bausch & Lomb, Wollensak, the new Xerox Plant at Webster, and to the Eastman Kodak Company's Camera Works. On Tuesday evening the members present were guests of the Institute of Optics at the University of Rochester where they inspected the new wing of the Physics Building and the various research projects being carried on by the Institute of Optics. A panel discussion on the professional needs in optics of the United States and of the educational program needed to satisfy the demand was held in Hoyt Hall, the spectacular new auditorium at the University of Rochester. The speakers were Rudolf Kingslake, Wallace R. Brode, Van Zandt Williams, and Robert E. Hopkins. The discussion was thrown open to all present and became very lively. Dr. Williams reported that a survey he had made indicated that a minimum of three thousand people would need to be trained to at least a B.S. level in optics or optical engineering during the next five years. Dr. Kingslake mentioned that considerably fewer than three hundred people had been given such training at the Institute of Optics during the thirty-three years of its existence. Professor Hopkins confirmed this estimate and asked what other universities and colleges are or can be interested in providing such training. No answers were available to this and the many other questions that were asked.

W. A. Weyl of the Pennsylvania State University opened the session Wednesday morning with an invited paper on "Liquid Structures and Glass Formation." This was followed by a full three-day session of 104 contributed papers and five other invited papers by Ralph Evans, Winfield W. Salisbury, Nicholaas Bloembergen, and the Mees and Ives Medalists—Alfred Kastler and Max Herzberger.

The 1962 Ives Medal was awarded at the Banquet on Thursday evening to Dr. Herzberger, Eastman Kodak, for his outstanding contributions to the theory of optical image formation. The first award of the C. E. K. Mees Medal was made to Professor Kastler of École Normale Supérieure, Université de Paris, Paris, France. Professor Kastler's work on optical pumping is basic to current developments in the maser field, and he told of his most recent findings, in his enthusiastically received lecture on "Energy Levels of Atoms Displaced by Light." In making the presentation of the Mees Medal the President called attention to the fact that the medal bears the motto, "Optics transcends all boundaries." In commenting on the fact that the medal is for award to optical scientists regardless of nationality, and that the committee for selection of the medalist must always include at least one scientist from abroad, the President expressed

Max Herzberger, the Ives Medalist (left), and Alfred Kastler, the first recipient of the Mees Medal, receiving their awards from the then OSA President David L. MacAdam, during the Rochester Meeting.

the hope that the medal, and the recipients whom it honors, may serve to bring closer the day when men shall know no boundaries. Twenty-nine members, who had been named Fellows by action of the Board of Directors, were called forward to receive their Fellowship certificates at the Banquet, and then Crawford H. Greenewalt, Chairman of the Board of Directors of E. I. du Pont de Nemours, presented color slides of humming birds and high-speed motion pictures of them in action. His informal comments on these pictures added immeasurably to the pleasure of the members.

There were 491 guests at the banquet and 782 registrants at the meetings. Interest was sustained throughout the contributed as well as the invited papers. The former were of the usual high quality, with unexpected surprise announcements occurring in several instances. The discovery of laser action with Raman-displacement lines of several organic liquids was announced by F. J. McClung in a paper which he substituted for the one announced in the program. The significance of this discovery was the subject of lively discussion during the remainder of the meeting.

International Conference on Precision Electromagnetic Measurements, NBS, Boulder, Colorado, August 14–17, 1962

Reported by N. Bloembergen, Harvard

About three sessions out of ten of the International Conference on Precision Electromagnetic Measurements were devoted to topics which also belong to the field of quantum electronics. One whole day was devoted to atomic frequency and time. Many different types of atomic clocks were discussed; the hydrogen maser, the ammonia maser, the cesium beam and thallium beam atomic clock, and the rubidium vapor cell which utilizes optical pumping techniques. These devices are in a neck to neck race to be elected as a new standard of time by 1966. They all utilize an atomic resonance in the microwave region as the frequency determining element. Reproducibility settings of one part in 10^{12} and short-term stabilities of one part in 10^{13} were quoted.

The only optical device that can boast figures of comparable order of magnitude is the helium neon gas laser. A. Javan reported that he had observed a beat note between gas lasers during 3–5 seconds with a stability of one part in 10^{13}. The frequency drift was less than 100 cps. Since the frequency determining element in the optical maser is the distance between the two Fabry-Perot plates, the frequency is very sensitive to mechanical vibrations, seismological disturbances, etc. With the help of seismologists and geologists, a quiet spot was located on MIT property: the wine cellar of the Round Hill estate on Cape Cod, Massachusetts. When there is no storm blowing, the above quoted result may be obtained. The reproducibility in frequency setting is at present only two parts in 10^9. It depends on pressure and power level of the laser. It could probably be improved by an order of magnitude with further careful experimenting. The neon gas laser has thus become the leading candidate for a new standard of length.

J. P. Gordon discussed the fundamental quantum noise limitations on the transmission of information. He proved in a fundamental way that, in linear amplifiers and attenuators, the noise and signal properties can be treated independently. In the important limit that the incident signal plus noise contains on the average much less than one quantum per electromagnetic mode, the quantum counter has greater information capacity than the linear amplifier. A. L. Bloom discussed the use of the optically pumped rubidium vapor cell as a magnetometer. A detailed account appeared in the first issue of this journal.* R. C. Mockler proposed to modulate ultrasonically the source and detector in a Mössbauer experiment. By varying the distance between source and detector, "fringes" in the number of recoilless absorption processes of γ-quanta would be observable. The velocity of light, i.e., of γ-quanta, could thus be measured with an estimated precision of three parts in 10^7. Microwave modulation of visible light offers a similar, competitive method. K. D. Froome at the National Physical Laboratory has an experiment of this kind under way. These and other precision determinations of "c" were discussed at a special evening session, presided over by N. F. Ramsey. H. S. Boyne described a proposal of the National Bureau of Standards to use a high-frequency beat between two neon lasers — $\Delta\nu \sim 1.6 \times 10^{12}$ cps—oscillating near 1.207 μ and 1.199 μ, respectively. The wavelengths of the two lasers would be compared with the Kr wavelength standard in a Michelson interferometer. The frequency difference would be measured as a modulation of the photocurrent from a cathode, on which the two laser beams are focused. The beam would be modulated also at 10^{10} cps with a known microwave frequency. A distinct pattern would result if the beat frequency is exactly an integral number, 160, times the microwave frequency. $c = \Delta\lambda/\Delta\nu$ could probably be determined to a few parts in 10^9.

Another topic of interest for *Applied Optics* readers was the discussion by N. Bloembergen of the determination of the nonlinear part in the index of refraction. The nonlinear properties of optical media can be studied with available high-intensity laser beams. At present the precision is poor and the determination of nonlinear properties is not better than one part in one and a half. The topic, therefore, hardly belonged at this conference, but the theory of nonlinear effects is well understood and rapid experimental progress may be expected soon.

* A. L. Bloom, Appl. Opt. **1**, 61 (1962).

(Reproduced by kind permission of the Editor of New Scientist.)

"It makes me feel more significant."

Problems of Long-Focus Photographic Astrometry

Peter van de Kamp

A survey is given of astronomical problems utilizing the techniques and methods of long-focus astrometry, and of the sources of errors and the currently attainable accuracy in this field of applied optics. Particular attention is paid to the astronomical problems of parallax and orbital motion, to errors due to atmospheric dispersion, and to the astrometric effects of coma, if present in an achromatic objective. A brief outlook follows on current progress in techniques and future expectations.

Section I

A number of astronomical problems involves the measurements of minute angular displacements. The positions of the stars on the celestial sphere have been studied for over two millenniums. We are not concerned here with these positions as such, but rather with changes in relative positions. Historically the problems of positional astronomy have developed in the following sequence. Appreciable changes in the equatorial coordinates of celestial objects are due to the *precession* of the equinoxes, which was discovered by Hipparchus as early as 125 B.C. because of its large angular value, 50″ yearly. The actual angular changes in position, or *proper motions* of individual stars, were not observed until 1718, when Halley noted the relative displacements of some bright stars from their positions recorded by Ptolemy in the second century A.D. Discovery and measurement of stellar proper motions are now commonplace procedures; the largest known proper motion, shown by Barnard's Star, amounts to 10″.31 per year.

Of primary interest are the relative *orbital motions* of the components of binary stars, first established by Herschel in 1803 for Castor and other double stars, and the *annual parallactic motion* first successfully measured in 1838 by Bessel for the double star 61 Cygni. By definition, the *annual parallax* of a star is the angle under which the unforeshortened semi-axis major of the earth's orbit around the sun would appear from the star; in other words the annual parallax is very nearly equal to half the major axis of the elliptical, parallactic orbit which the star appears to describe around its heliocentric position, such as would be observed from the sun. The largest stellar parallax thus far known is 0″.76 for the (nearest) star Alpha Centauri. A parallax of 1″ corresponds to a distance of one parsec, or 206,265 A.U., 1 A.U. of distance being very nearly the semi-axis major of the orbit of the earth around the sun, or 149,600,000 km. Hence a parallax of p'' yields a distance of $r = 1/p$ parsecs. One parsec equals 3.258 light years.

Parallax and orbital motion lead to further information. Parallax p yields distance r and hence *stellar luminosity* (absolute magnitude M), if the apparent brightness (magnitude m) is known:

$$M = m + 5 + 5 \log p$$

or

$$M = m + 5 - 5 \log r.$$

The analysis of the relative *apparent orbit* of the two components of a double star yields an angular value a'' of the semimajor axis of the unforeshortened *true orbit*, and of the period of revolution P. With known parallax p'' the linear value a of the semi-axis major, expressed in astronomical units, is found to be

$$a = \frac{a''}{p''}$$

and the *combined mass* of the two components follows from the harmonic relation

$$M_1 + M_2 = \frac{a^3}{P^2}$$

where the sun's mass is used as unit mass, and the period P is expressed in sidereal years (one sidereal year equals 356.2564 mean solar days). If the mass ratio of the two stars is known, the separate masses may be found.

The author is at Sproul Observatory, Swarthmore College, Swarthmore, Pennsylvania.

Received 30 August 1962.

the hope that the medal, and the recipients whom it honors, may serve to bring closer the day when men shall know no boundaries. Twenty-nine members, who had been named Fellows by action of the Board of Directors, were called forward to receive their Fellowship certificates at the Banquet, and then Crawford H. Greenewalt, Chairman of the Board of Directors of E. I. du Pont de Nemours, presented color slides of humming birds and high-speed motion pictures of them in action. His informal comments on these pictures added immeasurably to the pleasure of the members.

There were 491 guests at the banquet and 782 registrants at the meetings. Interest was sustained throughout the contributed as well as the invited papers. The former were of the usual high quality, with unexpected surprise announcements occurring in several instances. The discovery of laser action with Raman-displacement lines of several organic liquids was announced by F. J. McClung in a paper which he substituted for the one announced in the program. The significance of this discovery was the subject of lively discussion during the remainder of the meeting.

International Conference on Precision Electromagnetic Measurements, NBS, Boulder, Colorado, August 14–17, 1962

Reported by N. Bloembergen, Harvard

About three sessions out of ten of the International Conference on Precision Electromagnetic Measurements were devoted to topics which also belong to the field of quantum electronics. One whole day was devoted to atomic frequency and time. Many different types of atomic clocks were discussed; the hydrogen maser, the ammonia maser, the cesium beam and thallium beam atomic clock, and the rubidium vapor cell which utilizes optical pumping techniques. These devices are in a neck to neck race to be elected as a new standard of time by 1966. They all utilize an atomic resonance in the microwave region as the frequency determining element. Reproducibility settings of one part in 10^{12} and short-term stabilities of one part in 10^{13} were quoted.

The only optical device that can boast figures of comparable order of magnitude is the helium neon gas laser. A. Javan reported that he had observed a beat note between gas lasers during 3–5 seconds with a stability of one part in 10^{13}. The frequency drift was less than 100 cps. Since the frequency determining element in the optical maser is the distance between the two Fabry-Perot plates, the frequency is very sensitive to mechanical vibrations, seismological disturbances, etc. With the help of seismologists and geologists, a quiet spot was located on MIT property: the wine cellar of the Round Hill estate on Cape Cod, Massachusetts. When there is no storm blowing, the above quoted result may be obtained. The reproducibility in frequency setting is at present only two parts in 10^9. It depends on pressure and power level of the laser. It could probably be improved by an order of magnitude with further careful experimenting. The neon gas laser has thus become the leading candidate for a new standard of length.

J. P. Gordon discussed the fundamental quantum noise limitations on the transmission of information. He proved in a fundamental way that, in linear amplifiers and attenuators, the noise and signal properties can be treated independently. In the important limit that the incident signal plus noise contains on the average much less than one quantum per electromagnetic mode, the quantum counter has greater information capacity than the linear amplifier. A. L. Bloom discussed the use of the optically pumped rubidium vapor cell as a magnetometer. A detailed account appeared in the first issue of this journal.* R. C. Mockler proposed to modulate ultrasonically the source and detector in a Mössbauer experiment. By varying the distance between source and detector, "fringes" in the number of recoilless absorption processes of γ-quanta would be observable. The velocity of light, i.e., of γ-quanta, could thus be measured with an estimated precision of three parts in 10^7. Microwave modulation of visible light offers a similar, competitive method. K. D. Froome at the National Physical Laboratory has an experiment of this kind under way. These and other precision determinations of "c" were discussed at a special evening session, presided over by N. F. Ramsey. H. S. Boyne described a proposal of the National Bureau of Standards to use a high-frequency beat between two neon lasers — $\Delta\nu \sim 1.6 \times 10^{12}$ cps—oscillating near 1.207 μ and 1.199 μ, respectively. The wavelengths of the two lasers would be compared with the Kr wavelength standard in a Michelson interferometer. The frequency difference would be measured as a modulation of the photocurrent from a cathode, on which the two laser beams are focused. The beam would be modulated also at 10^{10} cps with a known microwave frequency. A distinct pattern would result if the beat frequency is exactly an integral number, 160, times the microwave frequency. $c = \Delta\lambda/\Delta\nu$ could probably be determined to a few parts in 10^8.

Another topic of interest for *Applied Optics* readers was the discussion by N. Bloembergen of the determination of the nonlinear part in the index of refraction. The nonlinear properties of optical media can be studied with available high-intensity laser beams. At present the precision is poor and the determination of nonlinear properties is not better than one part in one and a half. The topic, therefore, hardly belonged at this conference, but the theory of nonlinear effects is well understood and rapid experimental progress may be expected soon.

* A. L. Bloom, Appl. Opt. **1**, 61 (1962).

(Reproduced by kind permission of the Editor of New Scientist.)

"It makes me feel more significant."

Problems of Long-Focus Photographic Astrometry

Peter van de Kamp

A survey is given of astronomical problems utilizing the techniques and methods of long-focus astrometry, and of the sources of errors and the currently attainable accuracy in this field of applied optics. Particular attention is paid to the astronomical problems of parallax and orbital motion, to errors due to atmospheric dispersion, and to the astrometric effects of coma, if present in an achromatic objective. A brief outlook follows on current progress in techniques and future expectations.

Section I

A number of astronomical problems involves the measurements of minute angular displacements. The positions of the stars on the celestial sphere have been studied for over two millenniums. We are not concerned here with these positions as such, but rather with changes in relative positions. Historically the problems of positional astronomy have developed in the following sequence. Appreciable changes in the equatorial coordinates of celestial objects are due to the *precession* of the equinoxes, which was discovered by Hipparchus as early as 125 B.C. because of its large angular value, 50″ yearly. The actual angular changes in position, or *proper motions* of individual stars, were not observed until 1718, when Halley noted the relative displacements of some bright stars from their positions recorded by Ptolemy in the second century A.D. Discovery and measurement of stellar proper motions are now commonplace procedures; the largest known proper motion, shown by Barnard's Star, amounts to 10″.31 per year.

Of primary interest are the relative *orbital motions* of the components of binary stars, first established by Herschel in 1803 for Castor and other double stars, and the *annual parallactic motion* first successfully measured in 1838 by Bessel for the double star 61 Cygni. By definition, the *annual parallax* of a star is the angle under which the unforeshortened semi-axis major of the earth's orbit around the sun would appear from the star; in other words the annual parallax is very nearly equal to half the major axis of the elliptical, parallactic orbit which the star appears to describe around its heliocentric position, such as would be observed from the sun. The largest stellar parallax thus far known is 0″.76 for the (nearest) star Alpha Centauri. A parallax of 1″ corresponds to a distance of one parsec, or 206,265 A.U., 1 A.U. of distance being very nearly the semi-axis major of the orbit of the earth around the sun, or 149,600,000 km. Hence a parallax of p'' yields a distance of $r = 1/p$ parsecs. One parsec equals 3.258 light years.

Parallax and orbital motion lead to further information. Parallax p yields distance r and hence *stellar luminosity* (absolute magnitude M), if the apparent brightness (magnitude m) is known:

$$M = m + 5 + 5 \log p$$

or

$$M = m + 5 - 5 \log r.$$

The analysis of the relative *apparent orbit* of the two components of a double star yields an angular value a'' of the semimajor axis of the unforeshortened *true orbit*, and of the period of revolution P. With known parallax p'' the linear value a of the semi-axis major, expressed in astronomical units, is found to be

$$a = \frac{a''}{p''}$$

and the *combined mass* of the two components follows from the harmonic relation

$$M_1 + M_2 = \frac{a^3}{P^2}$$

where the sun's mass is used as unit mass, and the period P is expressed in sidereal years (one sidereal year equals 356.2564 mean solar days). If the mass ratio of the two stars is known, the separate masses may be found.

The author is at Sproul Observatory, Swarthmore College, Swarthmore, Pennsylvania.

Received 30 August 1962.

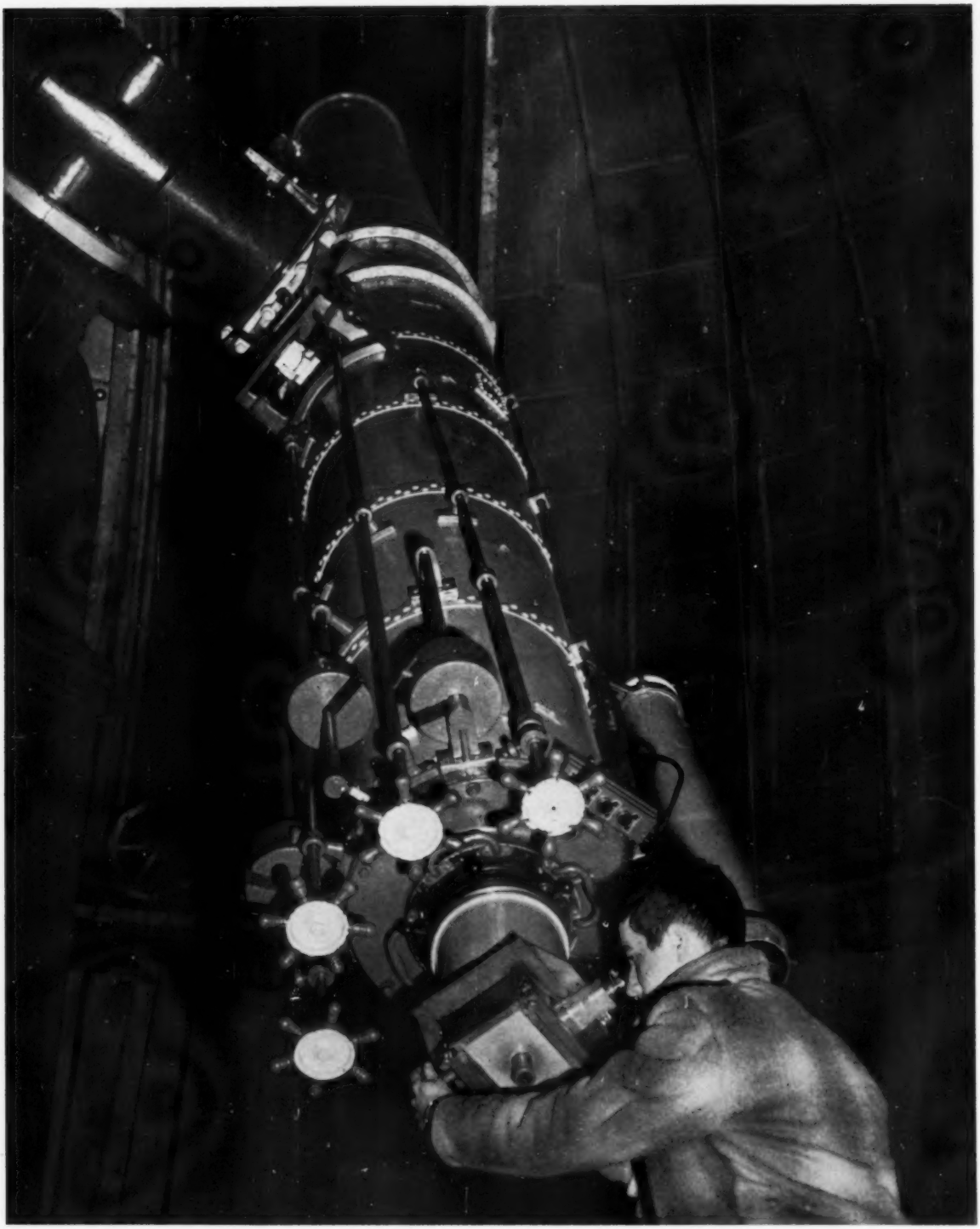

Fig. 1. Observer at the eyepiece of the 61-cm refractor of the Sproul Observatory, Swarthmore College.

Where only one component is visible the observed orbital motion, i.e., the *perturbation* in the observed proper motion, provides a clue to the existence and nature of the unseen companion of the primary star.

The orbital motion and parallax of stars were first measured in the nineteenth century, before the advent of photography. The minuteness of the quantities measured indicated the desirability of using long-focus instruments for these problems. The invention of photography paved the way for the ideal combination—long-focus telescope and photographic plate—for achieving the solutions to those problems which require the measurement of very small angular displacements. Long-focus photographic astrometry may be said to have begun early in this century with the successful work of Frank Schlesinger and of Ejnar Hertzsprung.

Schlesinger developed both techniques and methods as applied to the problems of *stellar parallax;* Hertzsprung did the same for photographically resolved *double stars*, i.e., the relative positions of binary star components as seen projected on the sky. Both astronomers reached a perfection in their techniques that so far has undergone only minor improvements. Both used a visual refractor, panchromatic emulsions, and a yellow filter, thus eliminating the blue light, to obtain sharp star images in the color range for which the objective was corrected. In his later years, Schlesinger also used refractors corrected for blue light directly, and thus used blue sensitive plates without filters. Both used precautions to minimize errors in comparing stars of different brightness.

The typical long-focus refractor used in this field has a focal ratio between $f/15$ and $f/20$. For example, the Sproul 24-in. achromatic visual objective has a full aperture of 24 in. (61 cm), a focal length of 36 ft (1093 cm), and a focal ratio of $f/18$. The scale value in the focal plane is defined as the number of seconds of arc per millimeter; for a focal length of F mm, the scale value is $206{,}265/F$ seconds of arc per millimeter. For the Sproul refractor the scale value is 1 mm = 18".87, or 0.053 mm for one second of arc.

The *photovisual* technique employing visual refractors is particularly advantageous inasmuch as residual dispersion caused by the objective and the atmosphere in comparing the positions of stars of different colors is greatly reduced.

The relative positions of the photographic star images on the plate are commonly obtained from measurements made with a precision long-screw measuring machine. The diameter of a well-defined, sharp, black star image is about one to two seconds of arc (incidentally, a quantity well above the visual resolving power). If a fine cross-wire is set on the centroid of the image, one obtains a position to an accuracy of about one percent. With the Sproul refractor the relative location of two star images is obtained with a probable error of ±0.002 mm or about ±0".04. An increase in the number of exposures on any one night permits a typical reduction in the accidental probable error to ±0".02. One may even reach ±0".01 if observations covering many exposures on several nights are combined.

Fortunately there are many significant positional problems for which the size of the observable phenomenon is well above the lower limit of 0".01. Over 49 stellar systems have parallaxes above 0".2. Hundreds of binary stars are known with orbital amplitudes over 2". Several perturbations with amplitudes of 0".02 or more have been observed.

To determine the parallax of a star, or stars, one measures the positions with respect to a background of, say, three or more virtually fixed, distant reference stars of, say, approximately the tenth magnitude. On current emulsions, stars of the tenth or eleventh magnitude are photographed in less than one minute. When necessary the brightness of the *parallax star* is reduced to that of an average reference star by means of a small rotating sector placed just above the center of the photographic plate. Up to four photographic plates, each with two to four exposures, are taken near the meridian on one night; this procedure is repeated at suitable intervals throughout the observing season in order to insure sufficient range in parallactic displacement. The path of the star is followed for several years. All the photographs may be reduced to a common scale, origin, and orientation by a linear reduction, using the method of dependences first developed by Schlesinger. A conventional parallax determination, based on some 20 to 30 photographs, each with 2 or 3 exposures extending over several years leads to a probable error of ±0".01 for the *relative annual parallax*. By increasing the observational material and by multiple parallax determinations at different observatories, one may reach even higher accuracy.

The *absolute parallax* is obtained by adding to the relative parallax a value for the parallax of the reference stars. This "correction to absolute" is usually obtained from statistical knowledge of mean parallaxes of faint stars; the resulting correction ordinarily ranges between +0".001 and +0".005.

Gliese[1] lists 915 stars with a total of 1094 components, known to have annual parallaxes over 0".05. For all these stars the parallaxes, and hence the distances, are known with a percentage probable error which may reach a maximum value of 20% at a distance of 20 parsecs. The parallaxes and distances of stars nearer than 5 parsecs are generally known with a percentage probable error of 2% or even less. Similar techniques and methods of reduction can be used to

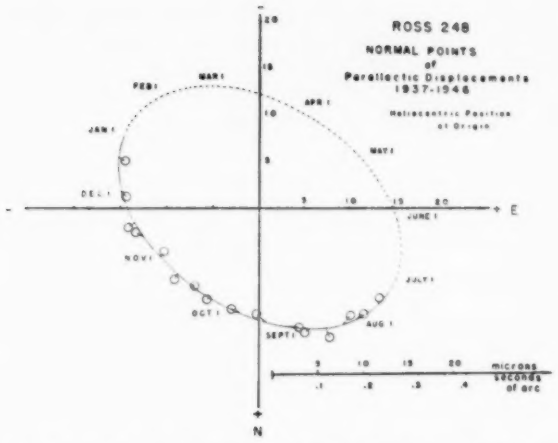

Fig. 2. The apparent parallactic orbit of the nearby star Ross 248 (distance 10.3 light years), resulting from the earth's orbit. The observations, made at the Sproul Observatory, have been grouped into 16 points, whose accuracy is represented by the radii of the small circles; these points clearly determine the part of the star's parallactic orbit accessible to observation. Since the observations are always made close to the meridian, the other half of the parallactic orbit corresponds to daytime culminations and is not observable.

establish the mass ratio of double star components, which is revealed through the uniform rectilinear motion of the center of mass, as observed relative to a background of reference stars. The mass ratio is revealed as the inverse ratio of the scales of the observed orbital displacements of the components relative to the center of mass. If the total mass of the binary system is known, the separate masses may thus be obtained.

Stellar luminosities and masses are basic desiderata in astronomical research, and, if only for this reason, the techniques and methods of long-focus photographic astrometry are therefore important. Accurate luminosities and masses are known for several dozen binary stars and have contributed to an accurate knowledge of the *mass-luminosity relation*.

Of particular interest are the discovery and subsequent observation of departures from uniform rectilinear motion for what appears to be a "single" star. These perturbations may be interpreted as caused by the gravitational effect of an *unseen companion*. In several cases the "unseen" companion has subsequently been "seen" with a larger telescope and has thereby extended our knowledge of the components of binary stars, particularly toward the fainter and less massive portion of the mass-luminosity relation. Whereas less than a decade ago the smallest known stellar mass was 16% the sun's mass, the smallest known stellar mass is now 4% that of the sun.

The search for unseen companion objects includes the search for *planetary companions* of stars. So far it cannot be said for certain that a planetary companion for a star other than for the sun has been discovered. We can say, however, that the gap between the visible star of the lowest known mass (4% of the sun) and the most massive planet Jupiter (0.1% of the sun) is currently being narrowed. Several unseen companions with estimated mass of 1% that of the sun have been found; there is observational evidence for the existence of even smaller masses. In many cases the observed perturbations have small amplitudes not far above the threshold accuracy of 0".01 so that care must be taken in appraising the significance of the results.

Another astrometric problem is the measurement of the *secular perspective acceleration* for a relatively nearby star having uniform rectilinear space motion, and with both appreciable proper motion and radial velocity, i.e., velocity in the line of sight. The yearly change in proper motion is proportional to the proper motion, to the radial velocity, and to the parallax. This secular perspective acceleration recently has been established by van de Kamp[2] for the second nearest star—Barnard's Star—for which the observed value of the acceleration 0".00119 ± 0".00004 (p.e.) agrees very closely with the predicted value of 0".00124 ± 0".00003.

Proper motions of the stars in *open clusters* permit the separation of cluster and noncluster stars. In a few cases, for clusters sufficiently near, the (annual) motions have been so accurate, probable errors of ±0".0005 or less, that internal motions have been established. Precise proper motions also yield information about the expansion of stellar *associations*.

A problem for the future is that of the orbital motion of very *wide double stars* and that of *distant companions* to existing single and multiple stars.

The total *space motion* of a star is obtained from its parallax, proper motion, and radial velocity. Accurate space motions yield information about groups of stars having common motion and therefore presumably common origin.

Apart from the various problems involving the measured path of a particular star on a background of stars, there is the problem of relative photographic positions of the components of *visual binaries*, as first considered by Hertzsprung and successfully continued by Strand and others. This method is particularly applicable to double stars whose components are well separated on the photographic plate, i.e., with a separation of more than 3" or 4". By the use of coarse objective gratings, magnitude (brightness) errors are reduced and a high accuracy is reached, amounting to about ±0".006 (p.e.) for a multiple exposure plate with 40 or 50 measured exposures. A probable error as low as ±0".002 is reached for a normal point based on six or more multiple exposure plates, thus reaching a precision well beyond that currently obtainable in star positions measured relative to an extended background of reference stars. An advantage is that the

images may all be photographed close to the optical axis, and field errors affecting the positional measurements of extended star configurations play virtually no role. The very high accuracy in turn permits the discovery and subsequent study of perturbations due to a "third" companion close to either of the two visible components. Several such discoveries have been made and, as in the case of the perturbations of the proper motion of single stars, have led to the discovery of unseen companions of low masses, such as the unseen companion in the binary system 61 Cygni.

Section II

The accuracy attainable by the techniques and methods of long-focus photographic astrometry is limited primarily by atmospheric, photographic, and optical effects. While the former eventually may be overcome by the use of space telescopes, they play a limiting role in all current work.

Atmospheric refraction lifts all star images by an amount which may be represented to a high degree of approximation by the formula

$$(\mu - 1)\tan\zeta$$

where μ is the index of atmospheric refraction at the observer's location and ζ is the zenith distance of the star. The above relation is usually written as

$$R\tan\zeta$$

where R, the atmospheric refraction at $\zeta = 45°$, is the *constant of refraction*.

Because of atmospheric refraction, any vertical angular distance suffers a minute contraction, whose first order term is represented by the factor $R(1 + \tan^2\zeta)$; any horizontal distance, measured along the great circle, suffers a contraction R. For a wide range of wavelengths in the visual spectrum R is close to 60″; hence the scale reduction in the zenith amounts to 0.00029. The constant of refraction R and its dispersion per 100 Å are given in Table I.

Each star appears as a spectrum, whose blue end appears closer to the zenith than the red end, the length of the spectrum being proportional to $\tan\zeta$. For stars

Table I. Atmospheric Dispersion

λ	R	Dispersion per 100 Å
4000	61″.34	−0″.108
4500	60.89	−0.072
5000	60.58	−0.050
5500	60.33	−0.037
6000	60.19	−0.028
6500	60.06	−0.021
7000	59.96	−0.017
7500	59.89	−0.014
8000	59.83	−0.011

of different spectral types the energy distribution is different: moreover, the spectra differ in brightness. Using a long-focus refractor, the astronomer reduces these spectral images to essentially "monochromatic" images by the combined choice of photographic emulsion and color filter with the telescope objective. The *photovisual* technique, favored by a rapid decrease of atmospheric dispersion toward longer wavelengths, is illustrated for the Sproul refractor. A minus-blue (No. 12) Wratten filter is used in contact with the 5 × 7 plate, eliminating practically all radiation on the blue side of approximately λ 5100. Eastman G-emulsion is used, for which the sensitivity is greatest at λ 5650, but extends little beyond λ 6000. Sharp, round star images are obtained in view of the fact that the effective radiation falls within Rayleigh's criterion that expresses the differences in focus between the marginal and paraxial rays as $4f^2\lambda$. Here f is the focal ratio and λ the wavelength corresponding to minimum focal length. Generally, for long-focus refractors Rayleigh's limit is between 0.5 and 0.7 mm; for the Sproul refractor it is 0.7 mm. The 61-cm objective consists of a negative meniscus flint-glass lens (approximate refractive index for green light, 1.61)—convex side forward—and a bi-convex crown-glass lens (approximate refractive index 1.51), the separation of the two lenses being 0.05 mm. The color dispersion of the flint component is about double that of the crown component. Proper choice of radii of curvature leads to a focal curve (also called "color-curve," "achromatization-curve," or "secondary spectrum") with minimum focal length at λ 5607. The effective wavelengths of the star images range only from about λ 5480 for a blue star of spectral type A to about λ 5525 for a red star of spectral type M. This corresponds to a small difference in the constant of refraction of 0″.017 at an altitude of 45°, the A star appearing comparatively that much closer to the zenith than the M star. In addition, the star's position depends to some extent on the star's brightness.

Hence, even with the best possible spectral compensation, small differences in effective wavelengths still remain in the measurement of relative star positions. In addition, this residual systematic error varies with the time of the night, due to the changing altitude and orientation of the stars as the telescope follows the rotation of the celestial sphere. Variations in the flexure of the objective may cause further prismatic effects having a net effect similar to that of refraction. For work which involves the measurement of differential displacements only, it is therefore advisable, in any one series of plates of a particular object, always to take photographs in the same position, preferably close to the celestial meridian. If a reflecting telescope is used, there is no secondary spectrum, but the effect of atmospheric dispersion remains the same.

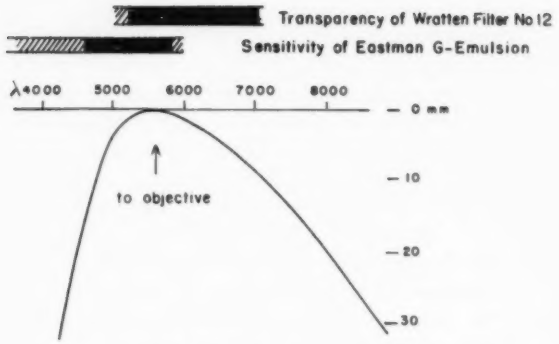

Fig. 3. Focal curve of the Sproul 61-cm objective.

Achromatic refractors, corrected for blue light, are also being successfully employed in this field.

Limitations in attainable accuracy in extended star fields are to a great extent due to *optical field errors* which may vary with the temperature. The principal off-axis aberration of many existing long-focus objectives is "coma." If one uses rectangular coordinates in the image plane, the intersection of any ray differs from the ideal point (θ, y_0) by quantities Δx and Δy, which are functions of ρ and θ, the polar coordinates of the point in the objective through which the ray passes. The coma is given by

$$\Delta x = \gamma y_0 \rho^2 \sin 2\theta$$

$$\Delta y = \gamma y_0 \rho^2 (2 + \cos 2\theta)$$

i.e., the rays passing through a zone of the objective of radius ρ intersect the image plane in a circle of radius $\gamma y_0 \rho^2$, whose center is at a distance $2\gamma y_0 \rho^2$ from the ideal image point $(0, y_0)$. Hence the "flare" due to coma varies linearly with the distance from the optical center and with the square of the diameter of the largest zone of the objective through which the light is allowed to pass. To obtain highest optical quality, therefore, if an objective regrettably has coma error, it is desirable to limit the size of the field, and a reduction of the aperture may prove even more effective.

Philip A. Ianna[3] has recently made a study of the Sproul objective. A comparison of plates taken on one night of the star cluster NGC 1039 with the Sproul refractor at full (61 cm) and at reduced (30.5 cm) aperture shows strikingly improved images, off-center, for the smaller aperture, accompanied by a scale reduction of 0.0005. Plans are under way for the installation of an iris diaphragm to permit the use of reduced openings for extended star fields. On-axis and off-axis Hartmann tests of the Sproul 61-cm objective have recently been made to investigate the aberrations of the objective as a function of the cooling of the lens and of the position of the telescope. The tests show appreciable variation in the objective during the course of a night. Longitudinal spherical aberration is positive and may be as large as seven times the Rayleigh criterion (0.7 mm), at the beginning of the night. It normally decreases to within the Rayleigh criterion in about six hours, and may even become negative in the morning hours if the dome temperature remains constant. Primary coma and astigmatism also vary with the state of temperature adjustment of the objective. The astigmatic difference remains less than 2 mm. Coma varies from slightly negative to positive values producing a comatic flare of the order of 0.5 mm in the corners of the field. Both off-axis aberrations tend to be large when the spherical aberration is large. Plates taken through a coarse-wire objective grating show a magnitude-coma scale effect of -0.00008 ± 0.00001 (p.e.) per magnitude at full aperture, and only -0.000015 ± 0.00001 at 30.5-cm aperture.

Errors due to photographic emulsions and measuring machines play a lesser role; however, particular care should be taken to insure constancy of measuring machine and measurer, whether personal or impersonal, particularly where measurements have to be carried out over prolonged intervals of time.

III. Looking into the Future

The rapid increase in the sensitivity of photographic emulsions has already resulted in a minor revolution over the past several decades, in that photographs are now obtained with exposure times only a few percent of those required three or four decades ago. The current image tube experiments indicate even greater breakthroughs in terms of exposure times. The advantages of greatly reduced exposure times are obvious—fainter stars may be reached, and multiple exposures may be made. Short periods of atmospheric stability may be utilized, leading, for example, to greater photographic resolving power for close double stars.

While the long-focus refractor up to the present time has appeared to be the instrument "par excellence" for problems of long-focus photographic astrometry, the construction of the new 152-cm quartz reflector of the U.S. Naval Observatory is ushering in a new era in this field. This telescope is described by Strand in the first paper of this issue. A reflector can cover the whole optical range of electromagnetic radiation. This particular instrument should have a more nearly constant optical figure than existing instruments. Because of its larger aperture and complete achromatism it should provide a vast increase in our knowledge of parallaxes and orbital motions of much fainter stars than can now be reached. It will undoubtedly lead to an extension of our knowledge of intrinsically faint stars and of stars of low mass.

The future will certainly put the current photographic method in a different perspective. Improved measuring

techniques are also to be expected. Meanwhile, the long-focus telescopes with either micrometer or interferometer attachments still continue to be significant in the visual realm, with their high resolving power, as the observer continues visual measurements of close double stars—a necessary supplement to the photographic method.

A new approach to the measurement of very accurate positions has recently been proposed by F. D. Drake[4] of the National Radio Astronomy Observatory. If a digital photoelectric analysis of the star image across a slit, and the accurate measurement of time intervals by means of a quartz crystal or equivalent means are combined, a potential positional accuracy of 0".0001 is indicated if the equipment were used above the earth's atmosphere. Clearly the attainment of an even comparable accuracy is beyond the wildest dreams of the current photographic methods. At the same time it would seem a miracle if the proposed photoelectric method would not meet the ever present limitations of the law of diminishing returns and would not be subject to systematic effects of various origins which normally frustrate all our efforts. However, even if the existing limitations in accuracy, as represented by a probable error of ±0".01, could be shifted to the next decimal, i.e., if a probable error of ±0".001 could be obtained, this would lead to a significant improvement in the accuracy and importance of stellar parallaxes; it might also lead to discoveries of very small perturbations—particularly among the nearby stars—such as might possibly be due to objects having planetary masses.

As Drake remarks, full advantage of his proposed method is expected to be reached only through the use of space telescopes. Undoubtedly space telescopes would benefit all methods: photoelectric, image-tube, photographic, and perhaps even visual.

To conclude: the photographic era, a revolutionary development only a century ago, has led to the current techniques and methods of long-focus photographic astrometry that are successfully being continued by surface observations. One cannot help but regard with renewed affection and appreciation nature's thoughtful provision of this stable observing platform, the earth, whose path, in addition, provides a useful baseline for determining stellar parallaxes. The climatic atmospheric limitations of our present space platform are being overcome gradually and effectively by the increased sensitivity of photographic emulsions, image-tube techniques, and very significantly, by the use of balloon telescopes only 25 km more or less, above the ground.

There is little reason to question the continued usefulness of long-focus telescopes mounted on platform earth, and it will prove interesting and instructive to witness the development of the comparative advantages and disadvantages of these and telescopes mounted on artificial space platforms.

References

1. W. Gliese, "Katalog der Sterne näher als 20 Parsek für 1950.0," Mitt. Astron. Rechen-Inst. Heidelberg, Ser. A, No. 8 (1957), pp. 1-89.
2. P. van de Kamp, Astron. J. **67,** 284 (1962).
3. Philip A. Ianna, Astron. J. **67,** 273 (1962).
4. F. D. Drake, Astron. J., in press.

Bibliography

P. van de Kamp, "Long-focus photographic astrometry," Popular Astron. **59,** pp. 65–79, 129–137, 176–191, 243–254 (1951); Contrib. I.A.P., Sér. A, No. 81, pp. 1–52.

P. van de Kamp, "Elements of long-focus photographic astrometry," Photogrammetric Eng. **22,** No. 2, 314–325 (1956).

P. van de Kamp, "Double Stars." Robert Grant Aitken lecture given at the Los Angeles meeting of the Astronomical Society of the Pacific, June 13, 1961. Publ. Astron. Soc. Pacific, **73,** No. 435, 389–409 (1961).

P. van de Kamp, *Astrometry with Long-focus Telescopes, Stars and Stellar Systems, Vol. II, Astronomical Techniques, Compendium of Astronomy and Astrophysics* (Univ. of Chicago Press, 1962).

The Sproul Observatory of Swarthmore College, 1958 (booklet).

---

continued from page 16

(c) to study specific areas of optics where there exists an inadequate research basis for the corresponding engineering program of national scope, and to recommend means by which an adequate research balance can be restored—perhaps the faculties and students in small colleges could be of assistance here; (d) to become fully familiar with the activities of the Institute of Optics of the University of Rochester, to assure its full backing by the OSA, and to determine whether similar programs can be seeded at other universities—this will involve a study of the whole area of optical engineering; (e) to investigate further the status of the undergraduate teaching of optics in the U.S. and to determine whether it meets the present requirements for persons trained in optics, and also to insure OSA cooperation with similar efforts now going on in Europe. In addition there should be one person to lead the task force who would monitor the total program and coordinate the areas of overlap that will surely show up among the several individual investigators and their tasks.

This is a most attractive program, but a very ambitious one. Its success clearly hinges upon locating a few individuals who are highly motivated toward the objectives of the program and who (through some miracle not as yet understood or realized) could arrange to spend a considerable fraction of their professional time on this study for a period of some months. Whether this can be effected, or whether we will have to be satisfied with only a partial program which can give only a partial solution, remains to be seen. In any case, our thanks go to Dr. Williams for his excellent appraisal of the situation and for describing it in such a trenchant and provocative fashion.

Editor's Note: This report has also been discussed in the Executive Office column in *J. Opt. Soc. Am.*

Applied Optics — Optical Activities in the Universities

reported by STANLEY S. BALLARD, Department of Physics, University of Florida, Gainesville, Florida. Professor Ballard hopes to receive news and comments for this column, which should be sent to him at the above address

The Optical Society of America properly takes a keen interest in the teaching of optics on all academic levels, and in the broad field of optics research, both pure and applied. These interests, and some of the associated activities, have been discussed in this column, in the January, March, and July issues last year [*Appl. Opt.* **1**, 84, 96, and 414 (1962)]. For several years there has been a standing committee on Teaching and Research in Optics appointed by the President of the Society, reporting its activities to the Board of Directors at its semiannual meetings. Additionally, interested individual members of the Society have submitted suggestions, and small groups of members have worked together to propose rather definite lines of action. Two of these have been referred to in the above-noted columns; they are what we have come to call the "Rochester proposal" to make a survey of the present status of optical education and of the needs, in both nature and extent, for more optically trained people in the academic community and in industrial and government laboratories; and the "Boston proposal" that a study be made of the need for a National Institute of Modern Optics to serve as a leader in the further development of our field at both basic and applied levels and as a catalyst for optics research on the postgraduate level. These two proposals have received a great deal of consideration, and many lengthy discussions have centered about them on the part of members of the OSA Board of Directors.

In order to bring the matter into sharper focus before specific lines of action are formed, it was decided, at the Board meeting held in Washington in March 1962, to appoint an *ad hoc* committee to make an intensive study of the whole situation, particularly the Rochester and Boston proposals, and to present a definite plan of action to the Board at its Rochester meeting of October 1962. This committee, which was known as the "Needs in Optics" committee, consisted of six members under the leadership of an extremely active Chairman in the person of Van Zandt Williams. Thus the report, which was presented to the Board on October 2, represented largely the work of Dr. Williams, although the recommendations were heartily concurred with by all members of the committee. Dr. Williams was assisted in some phases of the study by the Executive Secretary of the Society, Mary Warga, and he called on other members of the OSA to help him with specific items.

The report commences, appropriately, with a definition of the term "optics." It appears that much of the present confusion arises from the fact that this term is used in two quite different senses. Optics in its broader sense, and as currently used by the Editor of the *J. Opt. Soc. Am.* [see *J. Opt. Soc. Am.* **51**, 1042 (1961)], is defined as follows:

> Optics is the science which deals with radiant energy, its genesis, its propagation, the effects which it suffers, the effects which it produces, and all phenomena closely associated with it.

The report goes on to say: "Such a definition includes very broad areas of physics, engineering, chemistry, physiology, zoology, and biology. However, the word 'Optics' is often subject to immediate mental restriction when it occurs in such phrases as 'Education in Optics' or 'Research in Optics.' Here the accepted sense of Optics is largely limited to geometrical optics and component design; physical optics of electromagnetic wave propagation, coherence, diffraction, refraction, interference, scattering, fibers, etc.; and physiological optics. Academic people consider areas such as lasers, solid-state energy levels, atomic structure, communication, etc., as primary fields in which Optics is an important tool or technology. This distinction is an important one to make, even though the boundary line is not a sharp one. In view of this dichotomy, this report uses the term *Optics* in the broadest sense and the term *Optics per se* for the more restricted area."

A distinction between research and engineering is made, and it is noted that each of the *disciplines* of physics or engineering can conduct either research or engineering. This is a point that is seldom stressed.

Now let me quote from the Summary pages of the report: "The basic conclusion of this study is that Optics in the United States today is providing a vigorous, surging contribution to the field of science. The Optical Society of America is fortunate to be representative of such an active, useful area of science.

"It is evident that Optics is in a state of transition and redirection. The last few years have seen a dramatic intensification of research and space exploration. It is suddenly required that we see further and better, measure higher temperatures, time-resolve faster events, communicate more information, measure more accurately, peer deeper into materials, transfer power over longer distances, and compute more complex information. Optics and its principles are basic to all these needs.

"In this short period, the concept of Optics has enlarged from its early status as a mature field of physics research into a very broad spectrum of application. All the strains of such growth are evident. Optics has become an engineering responsibility, as well as of physics. The accumulation of basic knowledge is being used up rapidly, and a limitation of such knowledge is apparent. There is a numerical need for people trained in Optics that is much greater than the supply. An even greater concern is the fact that such supply as exists is not properly trained to meet the need, so the hard core of competence on which efficient growth and exploitation can be built is insufficient."

The body of the report gives evidence that the Needs in Optics committee has gone a long way in conducting at least the skeleton of the survey of optical needs and the status of optical education that was recommended in the Rochester proposal. Also, this brief survey has served to isolate specific areas where more must be learned about the present state of optics and the future needs. Thus the report recommends action by the Board of Directors of the OSA as follows: That a small task force (*not* a committee) be set up in which each person would have the responsibility for a certain area. The over-all scope would include the following: (a) To investigate optical companies and state educational organizations to see if some mutual program of optician and optical-technician training can be instituted; (b) to continue a study of the basic need for a National Institute of Modern Optics, or rather for several such institutes located in selected areas of the country;

continued on page 15

The Relationship Between Standard Coordinates of Stars and the Measured Coordinates of Their Images

Heinrich Eichhorn

The formation of a photographic image of a star on a plate by having a telescope assume the functions of the camera is described. The factors which contribute to the spreading of the light from a star on the emulsion, and those which bring about deviations from a "flawless" (usually gnomonic) projection of the stars onto the plate are analyzed. The amount by which the measured position of an image deviates from the position prescribed by the flawless projection depends on the position of the image on the plate, the intensity, and the spectrum of the star. Methods are given to show how measured positions can be freed from these deviations and thus reduced to "flawless" positions, and examples are quoted showing where and how these methods have been applied.

I. Introduction

All photographic astrometric work is either explicitly or implicitly based on fundamental relationships of the type

$$\xi = \xi(\alpha, \delta, \alpha_0, \delta_0)$$
$$\eta = \eta(\alpha, \delta, \alpha_0, \delta_0) \quad (1)$$

which are one-valued and have one-valued inverses:

$$\alpha = \alpha(\xi, \eta, \alpha_0, \delta_0)$$
$$\delta = \delta(\xi, \eta, \alpha_0, \delta_0) \quad (1a)$$

In (1) and (1a), α and δ are the right ascension and declination of the stars, α_0 and δ_0 are the right ascension and declination of that point on the sky for which $\xi = 0 = \eta$, and ξ, η are the "standard coordinates" of the images of the stars on the photographic emulsion. The emulsion is usually on a glass plate, but occasionally on film base. In what follows "plate" will be used synonymously with "photographic emulsion," no matter what the emulsion carrier material may be.

The form of (1) and (1a) is determined by the geometry of the projection of the celestial sphere on the plate. The model used in almost all cases is based on gnomonic projection as described for instance by König.[1] This projection assumes that the sky is projected by a pinhole camera onto a plane plate. This model cannot be used for Schmidt cameras, when the plate is not plane during the exposure. The formulas for the projection of the sky to a cylinder whose axis goes through the center of the celestial sphere were recently developed by Eichhorn.[2]

In order to obtain right ascensions and declinations (or the equivalents of these) of stars from measurements of the relative coordinates (x, y) of their images on the plate, relationships of the form

$$\xi = \xi(x, y, m, c)$$
$$\eta = \eta(x, y, m, c) \quad (2)$$

must be established, where m is a measure of the intensity of the image (determined mainly by the magnitude of the source star) and c a parameter describing the spectrum of the source star, i.e., a color index. The relationships (2), or at least the parameters in them, must be established empirically, because a purely theoretical determination would be too involved.

II. The Formation of the Image

Although the stars themselves are for all practical purposes ideal point sources of light, their images on the plate are spread over a certain area within which the intensity of the blackening is generally not symmetrical. This is due to the following factors:

A. The Atmosphere

From the outer limit of the atmosphere to the site of the camera, the index of refraction of the atmosphere increases steadily and varies, of course, for different wavelengths. This causes the star to be seen as a (short) spectrum (atmospheric dispersion) at a slightly

The author is at Van Vleck Observatory, Wesleyan University, Middletown, Conn.

Received 15 August 1962.

higher altitude than the true direction (refraction). Furthermore, the indices of refraction along the path of the light of the star through the atmosphere fluctuate (with periods that are short compared to the length of the exposure) constantly around the mean values. This causes the undisturbed refracted spectrum to become blurred and fluctuate itself around a mean position (bad seeing, shimmer).

B. The Camera

Owing to the action of the components of the optical system the cylinder of light from an infinitely distant point source of light is transformed into a ruled surface. The optical system is considered to perform the better, the more this surface resembles a cone (i.e., the more it converges toward an apex), the more uniformly it does this for cylinders of light hitting the front component from different directions, and the closer the locus of the "minimum diameters" of these ruled surfaces can be brought to coincide with the plate (which usually means a plane field and provisions for accurate focusing). In addition, the boundaries of the optical components and other objects in the path of the light (as for instance cells of secondary mirrors) produce a diffraction pattern which overlies the ruled surfaces. Thus, the image of even a point source will be spread over a finite area on the plate.

C. Guiding

In order to keep the light from any star always on the same spot on the plate during the exposure which for astrometric purposes usually lasts between fractions of a minute and more than an hour, the optical axis of the camera should always point to exactly the same spot in the sky. This is, however, not possible for two reasons:

Firstly, a conventional telescope drive can be regarded for only very few purposes as good enough to follow the apparent movement of the sky. Compensation for the small and well-nigh never completely avoidable irregularities of the drive must be made either manually by an observer or automatically by a photoelectric device in order to follow the stars as well as possible. Absolute perfection is here unattainable, but also not really necessary as long as systematic trends are avoided, i.e., as long as the points toward which the telescope is directed during the exposure are randomly and circularly symmetrically scattered around a mean point. (But even experienced observers occasionally get elliptical or even pear shaped images in the center of the field, particularly if the guiding star is faint.)

Secondly, the observed relative positions of the stars change during the exposure as the changing zenith distance of the guiding star changes the effect of the refraction. This means, assuming perfect guiding, that only those stars which during the exposure were always at the same zenith distance as the guiding star will appear as points on the plate; the others will produce short streaks. A similar effect will appear if the telescope is not set up perfectly, i.e., if the axis on which it rotates during the exposure does not coincide accurately with the direction of the refracted celestial pole.

Almost none of the factors discussed above is constant. While some, however, will change rather randomly (for instance, seeing and guiding), others will change perhaps stochastically as functions of certain parameters during the exposure. It has, for instance, been shown[3] that the coma effect produced by the Sproul Observatory Refractor changes with the temperature. It is just as probable that the optical properties of larger instruments depend also on the rate of change of the temperature and on the zenith distance toward which they are directed, but this remains to be investigated.

Owing to all these factors, the light of wavelength λ from a star will be spread on the plate over a certain area F centered on x,y [defined below in (5)] and produce a blackening, the distribution function of which is

$$\sigma(\lambda, I_0)\cdot S(\rho, \varphi, x, y, \lambda, I_0)$$

where I_0 is the intensity of the light source (essentially the star's apparent bolometric magnitude minus extinction), ρ, and φ are polar coordinates in the area F with x,y as pole and σ is a characteristic function for the plate depending on its gradation curve, the length of the exposure, etc.

The distribution function of the total density of blackening produced by a certain star is now given by

$$s(I, \rho, \varphi, x, y) = \int \sigma(\lambda, I_0)\cdot S(\rho, \varphi, x, y, \lambda, I_0)\cdot I(\lambda)d\lambda \quad (3)$$

where $I(\lambda)$ is the normalized spectral function of the star, i.e.,

$$\int I(\lambda)d\lambda = 1. \quad (4)$$

x and y are now defined in such a way that

$$\int s(\rho, \varphi_0)d\rho = \int s(\rho, \varphi_0 + \pi)d\rho \quad (5)$$

for all φ_0, i.e., such that the point defined by x,y corresponds to the center of blackening. x,y are actually the coordinates that would be measured on an automatic measuring machine. An experienced measurer using a visual measuring machine will also usually try to set on the center of blackening of an image.

From the above it is clear that the form of s depends —ceteris paribus—on the form of $I(\lambda)$ used in (3). From astrophysics it is well known that $I(\lambda)$ is a function that depends on only one parameter, say the

effective temperature or a color index, but that stars with the same effective temperature can have rather different functions $I(\lambda)$. This stage of sophistication has, however, not yet been necessary in photographic astrometry and as there is a close correlation between the spectrum $I(\lambda)$ and the color index with respect to a suitable chosen basis, we shall, in what follows, regard a color index c as an adequate description of $I(\lambda)$.

Taking all this into consideration, we can rewrite (2) as follows:

$$\xi = \xi_1(x, y) + \Delta\xi(x, y, m, c),$$
$$\eta = \eta_1(x, y) + \Delta\eta(x, y, m, c). \tag{2a}$$

The functions ξ, η, $\Delta\xi$, and $\Delta\eta$ contain, besides the arguments indicated, certain parameters which have to be determined empirically.

The split of ξ into ξ_1 and $\Delta\xi$ and of η into η_1 and $\Delta\eta$ is somewhat arbitrary, as we shall see presently, because $\Delta\xi$ and $\Delta\eta$ may also contain terms which depend only on x and y.

ξ_1 and η_1 are generally those parts of ξ and η which would describe a "flawless" projection. In the example of a gnomonic projection produced by a camera which is free from aberrations of any kind, we would have

$$\xi_1 = \frac{Ax + By + C}{\alpha x + \beta y + \gamma}$$
$$\eta_1 = \frac{ax + by + c}{\alpha x + \beta y + \gamma}. \tag{6}$$

In (6), usually, $|\alpha| \ll 1$, $|\beta| \ll 1$, and $|\gamma - 1| \ll 1$. We may then develop the denominator as a binomial series, and thus obtain

$$\xi_1 = Ax + By + C + px^2 + qxy,$$
$$\eta_1 = ax + by + c + pxy + qy^2. \tag{6a}$$

This is frequently done, but as p and q are small, the terms with p and q as coefficients are often incorporated into $\Delta\xi$ and $\Delta\eta$.

III. The Determination of $\Delta\xi$ and $\Delta\eta$

As we have pointed out earlier,[4] the corrections $\Delta\xi$ and $\Delta\eta$, which might suitably be called "aberration terms," can, in principle, be composed of terms of the following types:

$$\Delta\xi = \Delta_1\xi(x, y) + \Delta_2\xi(m, c) + \Delta_3\xi(x, y, m, c) \tag{7}$$

and analogously for $\Delta\eta$. To determine $\Delta\xi$ and $\Delta\eta$, trial formulas for Δ_1 etc. must be set up with enough parameters in them to keep them sufficiently flexible adequately to represent $\Delta\xi$ and $\Delta\eta$.

These parameters can be determined in two ways: (a) by comparison with reference stars, and (b) by comparison of positions which were obtained from different arguments (x,y,m,c), and, of course, by a combination of the methods indicated by (a) and by (b).

(a) The determination of $\Delta\xi$ and of $\Delta\eta$ by comparison with reference stars is quite straightforward. A sufficient number of stars should be selected, as homogeneously distributed as possible and covering the magnitude and color index ranges of all stars on the plate. Accurate and systematically correct positions must be available for these stars. From (1), their theoretical standard coordinates are computed and used in a pair of equations of the type (2a) for each one of these stars. The equations are then used as equations of condition to obtain the parameters of $\Delta\xi$ and of $\Delta\eta$ and also of ξ_1 and η_1 by a least squares adjustment.

(b) In order to obtain the parameters in $\Delta\xi$ and $\Delta\eta$ by comparing positions ξ and η of the same stars obtained from different arguments, the following possibilities exist:

A. Variation of the Coordinates

Let us assume that we can take plates under such circumstances that the functions $\Delta\xi$ and $\Delta\eta$ can be regarded as identical on them. This means, of course, that the origins of x and y must have the same positions on these plates: let us suppose they are at the geometrical plate centers. Also, the standard coordinates of the stars from all plates must be referred to the same origin. Let the part of the sky under consideration be covered by plates in such a way that every star is recorded on at least two plates. If x_i,y_i are the coordinates of the image of a certain star on the ith plate, we have the conditions

$$\xi(x_1, y_1, m, c) = \xi(x_2, y_2, m, c) = \ldots = \xi(x_i, y_i, m, c) = \ldots$$

and analogously for η. These equations can also be used as equations of condition for the determination of parameters in (2).

This procedure is subject to certain limitations. Parameters in terms of the type $\Delta_2\xi$ and $\Delta_2\eta$ as indicated in (7) can obviously not be determined by this type of comparison as they would affect the position of an image in the same way no matter where it is on the plate. Also, certain terms of Δ_1 and Δ_3 will be indeterminable for certain types of plate overlap patterns. If the overlap pattern is, for example, such that the edges of the plates are parallel and the edge of any one plate coincides with the central lines of its neighbors (i.e., if the centers of the plates are at the same declination and spaced at right ascension intervals corresponding to half a plate width; this is the pattern in which, for instance, the plates for the Yale catalogues were taken), it will be impossible to determine terms containing any power of y (assuming the y-axes to be in the directions of the meridians), to separate terms $t(m,c,y)$ from terms $x{\cdot}t(m,c,y)$ because $x_1 - x_2 = \text{const.}$, etc.

Whenever the plans for a photographic astrometric investigation are worked out, the overlap pattern should

be chosen carefully so as not to make the determination of suspected aberration terms impossible.

The other, and more serious, drawback of the determination of the parameters in $\Delta\xi$ and $\Delta\eta$ from plate overlaps is that these functions are never quite identical on two plates, in particular those terms which are caused by imperfect guiding. There is also evidence[5] that terms of the form $\Delta\xi\ (x,y,m)$ vary significantly from one plate to the next, taken with the same telescope.

An example for the determination of $\Delta\xi$ and $\Delta\eta$ by a combination of plate overlaps and comparison with reference stars was carried out by Eichhorn.[4]

By a simple artifice, even terms of the type Δ_2 can be determined by variation of the coordinates, provided that they remain sufficiently constant from plate to plate taken with the same telescope and are mainly produced by the properties of the optical system. A certain region is taken first with the telescope east of the pier and then a photograph of the same field is taken with the telescope west of the pier, so that the field is rotated by 180° with respect to the plate holder between the two exposures. Any terms of the type Δ_2 will then affect the positions on the two plates with different signs and can easily be determined. This seems, except for comparison with reference stars, the only way to determine terms of the type $\Delta\xi(c)$ and $\Delta\eta(c)$ for it is impracticable to vary the color of a star producing an image on a plate. (It is doubtful whether a practically useful procedure could be developed using differently colored filters for the filter to be used is more or less prescribed by the wavelength–focal length curve of the telescope and the wavelength–sensitivity curve of the emulsion.)

The procedure for a rigorous least squares determination of the parameters in ξ_1, η_1, $\Delta\xi$, and $\Delta\eta$ from a combination of plate overlaps and reference star comparisons was worked out by Eichhorn.[6]

B. Variation of the Magnitudes

The parameters of Δ_2 and Δ_3 in (7) can also be determined by placing close beside an image of a star another one of the same star, but with different intensity. This could be done by photographing the same field on a plate with two or more slightly displaced exposures of different duration, or by using a neutral filter between the exposures. The latter method would have the advantage that the magnitude difference between the two components of a pair of images is constant. The various exposures need not, of course, be made on the same plate as long as they are centered on the same point. If m_i is a measure for the total blackening of the image of a star for the ith exposure, the equations

$$\xi(x, y, m_1, c) = \xi(x, y, m_2, c) = \ldots = \xi(x, y, m_i, c) = \ldots$$

can be used as the equations of conditions for the determination of the magnitude dependent terms in Δ_2 and Δ_3. Terms involving color or the coordinates only cannot be determined in this way but must be established as described above. Also, obvious disadvantages of this procedure are the necessity of multiple exposures and the fact that, as pointed out above, certain terms, especially those depending on guiding, are necessarily different from one exposure to the next.

This appears, however, to be the only way to determine the terms of the type $\Delta\xi(m)$ and $\Delta\eta(m)$ in the positions of the various zones of the Astrographic Catalogue, because there are no reference stars available that go down to the magnitude limit of the Astrographic Catalogue.

IV. The Coarse Objective Grating

A coarse grating of evenly spaced and equally thick parallel bars in front of the objective will produce at the sides of every sufficiently strong image a series of pairs of diffraction spectra along an axis perpendicular to the bars. As these companion images are produced by the same exposure as the central image, guiding etc. will affect them in the same way, and the objections to the determination of $\Delta\xi$ and $\Delta\eta$ from different exposures do not apply here. From the theory of the grating (cf. Bucerius[7]) we know that in ideal circumstances the magnitude differences δ_i between a central image and a corresponding diffraction spectrum of the ith order are constant; these differences are called the "grating constants" for the diffraction spectra of the various orders. One must consider, though, that due to the photometric field corrections, a star of the same magnitude will not produce an image of the same blackening all over the plate. This means that owing to the nonlinearity of the gradation curve the difference in blackening (or image intensity) between a central image and a diffraction spectrum will not remain constant over the plate, even for stars of the same apparent magnitude. This effect is harmless, however, because it will be compensated for if the models for $\Delta\xi$ and $\Delta\eta$ are sufficiently flexible. In what follow, m_0 denotes the blackening of a central image and m_i that of a diffraction spectrum of the ith order. For not too critical investigations, these can be replaced by the magnitudes, with, thereby, neglect of the photometric field corrections and the nonlinearity of the gradation curve.

Owing to the very narrow wavelength bands commonly used to produce astrometric plates, the diffraction spectra of the first order are practically indistinguishable in appearance from a central image, and only the second and third order spectra are noticeably elongated. In practice, third order spectra are the last ones which are still more or less round in appearance and measurable.

Under the assumption that the mean of the positions of the components of a pair of diffraction spectra is astrometrically equivalent to that of a central image of the same intensity, we obtain an equation of condition

$$\Delta\xi(x, y, m_0, c) - \Delta\xi(x, y, m_i, c) = d_i$$

for every star for which a central image and a pair of diffraction spectra of the ith order are measured. d_i is the difference between the measured position of the central image minus the average of the measured positions of the corresponding ith diffraction spectra. (d_i must, of course, be expressed in units of ξ by application of the scale factor, which is always known with sufficient accuracy.) From these equations the parameters in $\Delta\xi$ and $\Delta\eta$ for all terms of the form $D(x,y,m)$ can be established. These are often the only ones which are significant. If the blackening of the individual images is not directly measured on the plates themselves (for instance by a photometer) but replaced by or computed from magnitudes taken from another source, particular care must be taken that these magnitudes refer to the same effective wavelength as corresponds to the wavelength interval which produces the images. Otherwise, systematic errors which depend on the stars' colors will be introduced.

In any case, $\Delta\xi$ and $\Delta\eta$ should be determined also from a separate analysis of the differences between the position of the central images and those of the mean of the diffraction spectra of each order. The expressions for the $\Delta\xi$ and $\Delta\eta$ obtained from considering different order diffraction spectra should agree within their errors. If this is not the case, and if we are sure that the reasons for the disagreement are not faulty grating constants or wrong values for the blackenings, we can assume that central images and diffraction spectra are not astrometrically equivalent. There is evidence from a recent study by Jefferys[8] that diffraction images behave astrometrically different from central images for long focus refractors.

The peculiarities of the astrometric behavior of images of each order can, however, be established from plate overlaps (i.e., variation of the coordinates) as described above, by overlapping grating plates and determing the $\Delta\xi$ and $\Delta\eta$ separately by always using one particular order image in the analysis of the overlaps. The results obtained in this way should be compatible with those from the analysis of the position differences between the central and mean of diffraction images. In this way, the corrections to be applied to the diffraction spectra to reduce them to "central image behavior" can be established. The procedure is straightforward enough to make a detailed description here unnecessary.

V. Applications

The fact that the varying image intensity can cause systematic errors in photographic positions has been known since around 1900. Most attention was paid to the "magnitude equation," i.e., an error of the form $\Delta\xi = \alpha m$, $\Delta\eta = \beta m$ where α and β are constant coefficients and m is the magnitude of the star. It was widely believed that these could be avoided by careful guiding; however, it is now evident that errors of this kind are partly due to badly aligned components of the photographic objective and cannot be avoided by even the most perfect guiding.

Furuhjelm[9] and Gill[10] noticed that the scale of the Helsingfors and Cape zones, respectively, of the Astrographic Catalogue depend on the magnitude (coma effect). The same effect was found by Schlesinger[11] who called it "magnitude distortion" for the plates used for some zones of the Yale Catalogue. Formulas for the removal of systematic and magnitude dependent errors from the Helsingfors zone of the Astrographic Catalogue were given by Eichhorn.[4] A simple formula, namely,

$$\Delta\xi = adx; \qquad \Delta\eta = ady$$

(a being a constant, d the image diameter) was established by Eichhorn[12] for the removal of the coma effect from the Hyderabad zone of the Astrographic Catalogue.

During the work on the Yale Catalogues[13] it was found that for some cameras the scale depends on the spectral type (color), i.e., that terms of the type $\Delta\xi = acx$ and $\Delta\eta = acy$ were present (color distortion). The same was found to be true for the Hamburg zone of the AGK2.[14] On the plates taken with one particular camera for the Yale Catalogue, terms $\Delta\xi = acmx$, $\Delta\eta = bcmy$ were found significant. More material on systematic errors is found in the introductions to the Yale Catalogues, the Cape Photographic Catalogues, and the AGK2 [Hamburg-Bergedorf, Vol. 10 (Heckman, 1952) and Bonn, Vol. 11 (Kohlschütter, 1959)].

In a study of the systematic errors of the Hyderabad zone of the Astrographic Catalogue (not yet published), Eichhorn[5] found that the terms in $\Delta\xi$ and $\Delta\eta$ involving magnitude vary significantly from plate to plate, while those involving only color can be regarded as constant for all plates, and therefore as characteristic for the optical system.

References

1. A. König, Handb. Astrophys. **1**, 502 (1930).
2. H. Eichhorn, Scientific Report No. 1, Contract AF19(604)-7330 (1962).
3. P. Ianna, Astron. J. **67**, 273 (1962).
4. H. Eichhorn, Astron. J. **64**, 2 (1959).
5. H. Eichhorn, not yet published.
6. H. Eichhorn, Astron. Nachr. **285**, 233 (1960).
7. H. Bucerius, Astron. Nachr. **246**, 33 (1932).
8. W. H. Jefferys, Astron. J. **67**, 532 (1962).
9. R. Furuhjelm, Thesis, Helsingsfors, 1906.
10. D. Gill, *Cape Astrographic Zones* (H.M.S.O., London, 1913), Vol. I, p. 38.
11. F. Schlesinger, Trans. Yale Astron. Observatory **4**, 22 (1925).
12. H. Eichhorn, Astron. J. **62**, 142 (1957).
13. F. Schlesinger and I. Barney, Trans. Yale Astron. Observatory **11**, 9, 10 (1939).
14. O. Heckmann, Zweiter Kat. Astron. Ges. **10**, E1 (1954).

Papers to appear in subsequent issues

We have had so many papers submitted for publication during the past year that we have already built up a backlog which is as embarrassing for a new publication as it is a demonstration of the need for this journal. We have done our best to publish papers as quickly as we can by bringing out bigger issues than had originally been intended last year, and **becoming a monthly in 1963.** The Editors wish to express their sincere appreciation to all contributors who have thus demonstrated their faith in *Applied Optics*.

Infrared Transmission through the Atmosphere—*Green and Griggs*
Performance Prediction of Range-Finder Systems—*Patrick*
Three-Dimensional Wavefront Reconstruction—*Meyer-Arendt*
Experimental Transfer Characteristics of Image Motion and Air Conditions in Aerial Photography—*Hendeberg and Welander*
Method of Inferring Single-Path Band Transmission Factors from Double-Path Measurements—*McKiernan and Wessely*
Thermal Radiation from a Hemispherical Source in Contact with an Infinite Plane—*Kester and Minardi*
Total Absorptance of Water Vapor in the Near Infrared—*Burch et al.*
Cloud Chamber for Optical Measurements of Aerosols—*Speyer*
Nine-Channel Polychromator for Observation of Time-Dependent Spectral-Line Profiles—*Spillman et al.*
Isocon Scan—A Low-Noise Wide-Dynamic-Range Camera-Tube Scanning Technique—*Cope and Borkan*
Design Theory for a Submersible Scattering Meter—*Tyler*
A Simple Grating Calibrator for the Visible and Vacuum Ultraviolet—*Hammer, Arakawa, and Birkhoff*
Comparison of AM and FM Reticle Systems—*Carpenter*
Modifications of a Beckman Spectrophotometer for Direct Measurements of Spectral Energy Distribution of Light Sources—*Grum*
Production and Use of Variable-Transmittance Sinusoidal Test Objects—*Lamberts*
A Simple Voltage Amplifier for Photovoltaic Cells—*Paix*
Generation of Sinusoidal Light Intensity—*Julich*
An Automatic Rapid-Scanning Spectrophotometer to Study Thermoluminescence Spectra—*Ghosh*
Use of a Kaleidoscope to Obtain Uniform Flux over a Large Area in a Solar or Arc Imaging Furnace—*Chen et al.*
Photorefractometer I. Extension of Sensitivity and Range; II. Measurement of N and K—*Kapany and Pontarelli*
Faraday Rotation in FeNi Films—*Wieder and Collins*
Photographic Emulsions as Computer Storage Media—*Levi*
Lighting Parameters and Generalized Characteristics of Xenon Lamps—*Marshak*
Design of Superachromatic Lenses—*Herzberger and McClure*
Reflection and Transmission of Infrared Materials—*McCarthy*
A Null Corrector for Paraboloidal Mirrors—*Offner*
A Simple Grating Spectrometer Fore-Prism Drive—*Ferriso*
Multilayer Reflection Coatings on a Metal Mirror—*Youny*
Correlation of Output Spikes from Different Portions of a Ruby Laser—*Ready*
Enhancement in Mercury–Krypton and Xenon–Krypton Gaseous Discharges—*Grosof and Targ*
The Use of Polarized Infrared Radiation in Magneto-optical Studies of Semiconductors—*Palik*
A Multicolor Photoelectric Photometer for Artificial Satellite Observations—*Moore and Elliott*
A Method for Evaluating Laser Potentialities of Crystals—*Theissing et al.*
Focusing of Light by a Dielectric Rod—*McKenna*
Some New Aspects for Laser Communications—*Megla*
The Abundance of Nitrous Oxide, Methane, and Carbon Monoxide in Ground Level Air—*Bowman and Shaw*
An Optical Null Double Beam Double Pass IR Spectrophotometer—*Minami*
A Photomultiplier Circuit for Precision Spectrophotometry—*Budde*
Large Scale Photoelectric Planimeter for Leaves—*Carman*
Alteration of the Muscovite Absorption Spectrum by KBr Pellet Preparation—*Ruthberg, Barnes, and Noyce*
Wavelengths of Fe Lines Measured by a New Technique—*Smith and Baird*
Spectral Band Absorptance for Atmospheric Slant Paths—*Plass*
Optical Design for Two Telescopes, Parts A and B—*De Vany*
A New Method for High-Speed Motion Picture Photography of Transparent Drops—*Pfeiffer*
Reduction of Scattered Light in the Coronograph—*Newkirk and Bohlin*
Photometric Accuracy of Infrared Spectrophotometers—*Stewart*
Absorption by Ozone in the 4.75μ Region of the Solar Spectrum—*McCaa and Shaw*
Exploding Wire Blast Shutter—*Chace and Fish*
Laser Operation at 3.39μ in a Helium-Neon Mixture—*Bloom et al.*
Auxiliary Optical Systems for the Kitt Peak Telescopes—*Schulte*
A Dual-Channel Pulse-Counting Astronomical Spectrophotometer—*Rodman*
A New Type of Shearing Interferometer for the Measurement of Transfer Functions of Microscope Objective—*Tsuruta*
Tests of Photomultipliers for Astronomical Pulse-Counting Applications—*Rodman and Smith*
The Effect of Protective Coatings of MgF_2 and SiO on the Reflectance of Aluminized Mirrors—*Bennett et al.*
Image Orthicon Astronomy at the Dearborn Observatory—*Powers and Aikens*
Concave Gratings for Astronomical Spectrographs and Spectrometers—*Liller*
The 15–26μ Sky Emission Spectrum at Jungfraujoch (3570 m)—*Bolle*
Measurements and Interpretation of Laser Beam Divergence—*Evtuhov and Neeland*
Infrared Dispersion of Some Oxide Glasses—*Malitson et al.*
A Liquid Calorimeter for High Energy Lasers—*Damon and Flynn*
Study of the Fabrication of Aspherical Surface—*Sakurai and Shishido*
Planetary Telescopes—*Baker*
Low Sun Phenomena—*Feibelman*
Theory of Optical Information Storage in Solids—*van Heerden*
A New Optical Method of Storing and Retrieving Information—*van Heerden*
One and Two Dimensional Processing in Line Scanning Systems—*Callahan and Brown*
Helium Continuum Light Source for Photoelectric Scanning in the 600–100Å Region—*Huffman, Tanaka, and Larabee*
Asymmetry of an Integrating Sphere—*Olson and Pontarelli*
Isosceles Total Internal Reflectors as Optical Elements—*Rothstein*
Direct Recording of Integrated Band Intensities from a Linear Wavelength Spectrometer—*Schurin, Williamson, and Clough*
Jet Controlled Arc—Excitation of Second Spectra—*Thygesen and Moore*
Milestones in Optics II—Thomas Young—*Barr*
Test of Theoretical Absorption Band Model Approximations—*Burch and Williams*

NEW SUBSCRIPTION ORDER

APPLIED OPTICS

Please enter my/our subscription* and continue until countermanded:

- ☐ OSA member rate $6.00 per year
- ☐ Other AIP Societies' rate $8.00 per year
- ☐ Regular rate $10.00 per year
- ☐ Please send OSA membership information
- ☐ check enclosed ☐ bill me
- ☐ Single copy of issue $2.00
- ☐ **MASERS Supplement** published December 1962 .. $5.00

Name ..... Membership No. .....

Address .....

.....

*Subscriptions entered for calendar year only.

NEW SUBSCRIPTION ORDER

APPLIED OPTICS

Please enter my/our subscription* and continue until countermanded:

- ☐ OSA member rate $6.00 per year
- ☐ Other AIP Societies' rate $8.00 per year
- ☐ Regular rate $10.00 per year
- ☐ Please send OSA membership information
- ☐ check enclosed ☐ bill me
- ☐ Single copy of issue $2.00
- ☐ **MASERS Supplement** published December 1962 .. $5.00

Name ..... Membership No. .....

Address .....

.....

*Subscriptions entered for calendar year only.

FIRST CLASS
Permit No. 18297
New York, N. Y.

BUSINESS REPLY MAIL
No postage stamp necessary if mailed in the U. S. A.

POSTAGE WILL BE PAID BY

APPLIED OPTICS
American Institute of Physics
335 E. 45th Street
New York 17, N. Y.

Attention Miss J. Raimondi, Circulation

FIRST CLASS
Permit No. 18297
New York, N. Y.

BUSINESS REPLY MAIL
No postage stamp necessary if mailed in the U. S. A.

POSTAGE WILL BE PAID BY

APPLIED OPTICS
American Institute of Physics
335 E. 45th Street
New York 17, N. Y.

Attention Miss J. Raimondi, Circulation

Limitations à la Qualité des Images d'un Grand Télescope

Jean Texereau

It is possible to construct a telescope achieving about two meters of aperture and still capable of yielding an essentially normal Airy disk. Atmospheric turbulence can spread out this image to where the central maximum of the diffraction pattern can easily be ten times larger. Nevertheless the photographic resolution of a large telescope is always better than that of a smaller instrument if the exposure time is not too short. The characteristics of the two-meter Haute Provence telescope are described.

I. Les Défauts du Miroir au Laboratoire

Considérons par exemple les aberrations résiduelles du miroir de 193 cm; $F = 960$ cm; taillé au Laboratoire d'Optique de l'Observatoire de Paris pour un télescope de l'Observatoire de Haute-Provence. Le tableau ci dessous est extrait d'une étude plus complète que nous avons effectuée par la méthode de Hartmann sous une forme voisine de celle décrite par A. Danjon et A. Couder[1]; les notations sont les mêmes: h désigne la hauteur d'incidence; λF l'aberration transversale au foyer, mesurée dans le plan du cercle de moindre aberration; u est l'angle entre l'élément de surface d'onde considéré et l'onde sphérique de référence.

L'écran Hartmann comprend deux rangées de trous alternés de 50 mm, disposées symétriquement au voisinage du diamètre horizontal du miroir ϕ_1, puis ϕ_2 apres une rotation de 90° du miroir. Les chiffres du tableau sont les moyennes de deux essais complets A, puis B après retournement de l'écran, ceci permute les trous pairs et impairs et dégage mieux l'aberration zonale des inclinaisons accidentelles du mamelonnage primaire.

Les aberrations transversales λF sont à comparer à ρ: rayon linéaire du disque d'Airy:

$$\rho = 1.22\,\lambda\,\frac{F}{D}.$$

Ici $F/D = 5.0$ et pour $\lambda = 0.56\ \mu$ on a $\rho = 3.4\ \mu$. Or la confrontation des séries A et B fait justement ressortir un écart moyen de $3.5\ \mu$ sur les déterminations individuelles des λF. La même méthode appliquée à un miroir de 80 cm conduit à une dispersion de l'ordre du micron seulement. La différence est due principalement à l'effet aléatoire prépondérant que prend le plus faible mamelonnage d'un grand miroir. Nous avons déjà signalé plusieurs fois[2,3,4] que la précision du surfacage optique comporte une limite physique que l'on peut exprimer par une pente caractéristique entre les éléments de surface d'onde réelle et une surface d'onde moyenne idéale. Cet angle est d'autant plus petit que la technique est meilleure, il est indépendant des dimensions du miroir. Un bon surfacage à la poix conduit à des défauts dont les pentes peuvent être inférieures à 1×10^{-6}. L'écart moyen mentionné plus haut correspond sur l'onde à des pentes de $3.5 \times 10^{-3}/9600 = 3.6 \times 10^{-7}$ donc 1.8×10^{-7} sur le miroir. Un tel mamelonnage, visible sur le Foucaultgramme sensible Fig. 1(a), correspond à 18 mμ ou $\lambda/30$ pour ces accidents d'environ 50 mm; on peut le considérer comme faible et difficile à réduire et nous admettons pour l'instant qu'un miroir d'environ 2 mètres de diamètre à $F/D = 5$ constitue une limite au delà de laquelle il devient difficile de répondre d'une figure de diffraction à peu près normale. Notre miroir de 193 cm donne sensiblement 70% de l'énergie dans le disque d'Airy.

Par ailleurs les angles $-u \times 10^6$ des deux dernières lignes du tableau donnent par intégration graphique (Fig. 2) les deux demi sections méridiennes de l'onde émergente. Les écarts de ces courbes par rapport aux traces des ondes de référence sont agrandis un million de fois sur l'épure originale à l'échelle grandeur. L'on constate des défauts zonaux atteignant 81 mμ ou $\lambda/6.9$ sur Φ_1 et 74 mμ ou $\lambda/7.6$ sur Φ_2. Ces zones se voient également sur le Foucaultgramme Fig. 1(a). Il ne serait pas bien difficile d'abaisser ces défauts mais le bénéfice pour l'image serait discutable car la limite sur les λF signalée plus haut subsisterait.

The author is with the Laboratoire d'Optique de l'Observatoire de Paris et Observatoire de Haute Provence.

Received 19 July 1962.

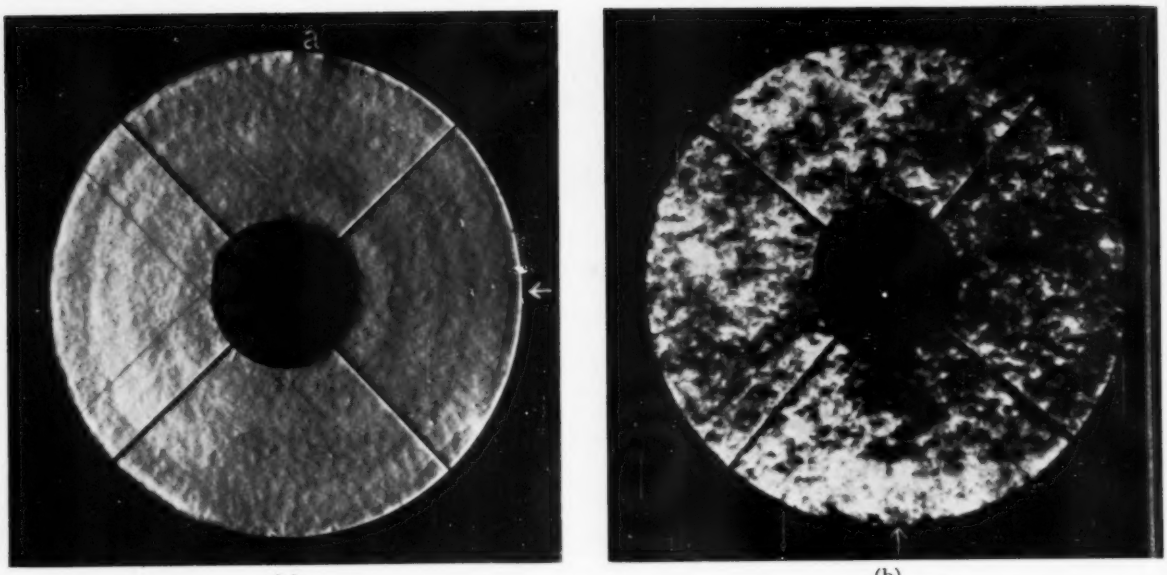

(a)
pose 2 min

(b)
pose 1/10 sec

Fig. 1. Foucaultgramme du miroir de 193 cm (couteau à droite).

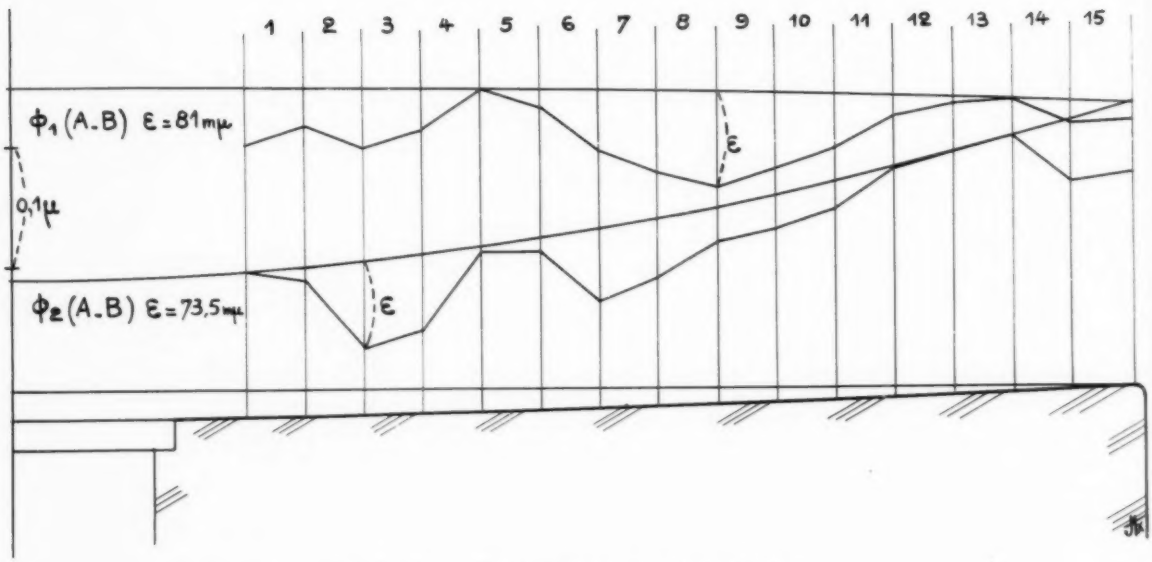

Fig. 2. Ecarts de tautochronisme du miroir de 193 cm.

II. Les Défauts du Miroir dans le Télescope

Nous nous contenterons de constater ici qu'il n'est pas trop difficile en pratique de conserver les résultats acquis au laboratoire dans les conditions d'emploi réelles de l'instrument. Dans le télescope de 193 cm de l'Observatoire de Haute Provence les flexions du miroir dans son plan sont compensées par un dispositif conçu par A. Couder[5] et réalisé par G. M. Sisson[6] comprenant, outre les 3 appuis dorsaux fixes, 30 supports astatiques répartis sur 3 couronnes. Notre Foucaultgramme Fig. 1(a) montre la bonne efficacité du système; l'instrument pointait Véga dans un angle horaire de 2 h 30, un appui latéral fortement chargé est responsable des

deux bosses marquées "a" en haut de la figure. Ce défaut n'affecte pratiquement pas l'image et l'on peut admettre que le miroir, malgré sa faible épaisseur de 175 mm, est encore convenablement supporté sans dispositif répartissant la composante parallèle à son plan.

C'est un point de vue trop simpliste que de décrire les effets thermiques simplement liés au coefficient de dilatation de la matière. La mesure des effets réellement présentés par les grands disques souligne en particulier l'importance de la répartition des tensions dûes à la trempe. Habituellement ces tensions croissent de manière continue en approchant du bord, un miroir qui se refroidit montre le plus souvent de la surcorrection sphérique assez régulière pour permettre une compensation par un dispositif expérimenté par A. Couder.[7] Dans le cas du 193 cm ce dispositif est rarement utile car l'effet thermique observé est petit et généralement de signe contraire; cette sous-correction est vraisemblablement liée à la distribution de la faible trempe résiduelle qui change trois fois de signe le long du rayon.

Nous retiendrons de cet aperçu qu'il serait techniquement possible d'obtenir le pouvoir séparateur théorique d'une ouverture de 2 m si l'instrument pouvait être installé en dehors de l'atmosphère, le but principal de ce travail est de décrire expérimentalement la dégradation considérable de l'image dûe à la turbulence atmosphérique.

III. La Turbulence Atmosphérique

Un phénomène aussi compliqué—et dont les conséquences sont aussi graves pour l'astronomie a fait l'objet de nombreux travaux que nous ne chercherons pas à analyser. Remarquons seulement que le plus souvent un aspect particulier du phénomène est examiné; par example: mesure de la *scintillation* au moyen d'un récepteur photoélectrique; estimation de *l'altération* de l'image de diffraction d'un petit instrument dans une échelle arbitraire; mesure de *réfractions* lentes sur une trainée photographique d'étoile. La dégradation de l'image d'un grand miroir dépend bien de tout cela mais la complexité de la grande surface d'onde est un facteur essentiel justifiant une analyse faite avec le grand télescope lui même.

Le Foucaultgramme Fig. 1(a) fut exposé 2 min pour bien intégrer les accidents turbulents et montrer les défauts propres au miroir, mais une étoile de magnitude zéro permet de réduire le temps de pose à $^1/_{10}$ de seconde sur une image plus petite; l'on obtient la Fig. 1(b) qui commence à donner une idée de la complexité de l'onde. Cette image n'est pas une simple figure de stries à haute altitude vues sous forme d' *ombres volantes* sur une plage extrafocale. Le couteau de Faucault montre avec un fort contraste les accidents de la couche d'air à basse altitude, celle qui a rencontré les obstacles au sol, c'est un véritable fleuve qui trans-

Table I.
Aberrations Residuelles du Miroir de 193 cm

Zones	1	2	3	4	5	6	7	8	9	10	11	12	13	14	15
h (mm)	225	275	325	375	425	475	525	575	625	675	725	775	825	875	925
$\lambda F(\mu)\Phi_1 A.B$	−3.1	+3.7	−2.9	−6.7	+3.1	+7.5	+3.4	+2.3	−3.0	−3.2	−5.3	−1.9	−0.8	+3.9	−0.6
$\lambda F(\mu)\Phi_2 A.B$	+1.2	+11.3	−3.0	−12.6	0.00	+8.1	−3.8	−5.7	−1.9	−3.1	−6.6	−2.7	−2.8	+7.7	−1.4
$-u \times 10^6(\Phi_1)$	+0.32	−0.39	+0.30	+0.70	−0.32	−0.78	−0.35	−0.24	+0.31	+0.33	+0.55	+0.20	+0.08	−0.41	+0.06
$-u \times 10^6(\Phi_2)$	−0.12	−1.18	+0.31	+1.31	0.00	−0.84	+0.40	+0.59	+0.20	+0.32	+0.69	+0.28	+0.29	−0.80	+0.15

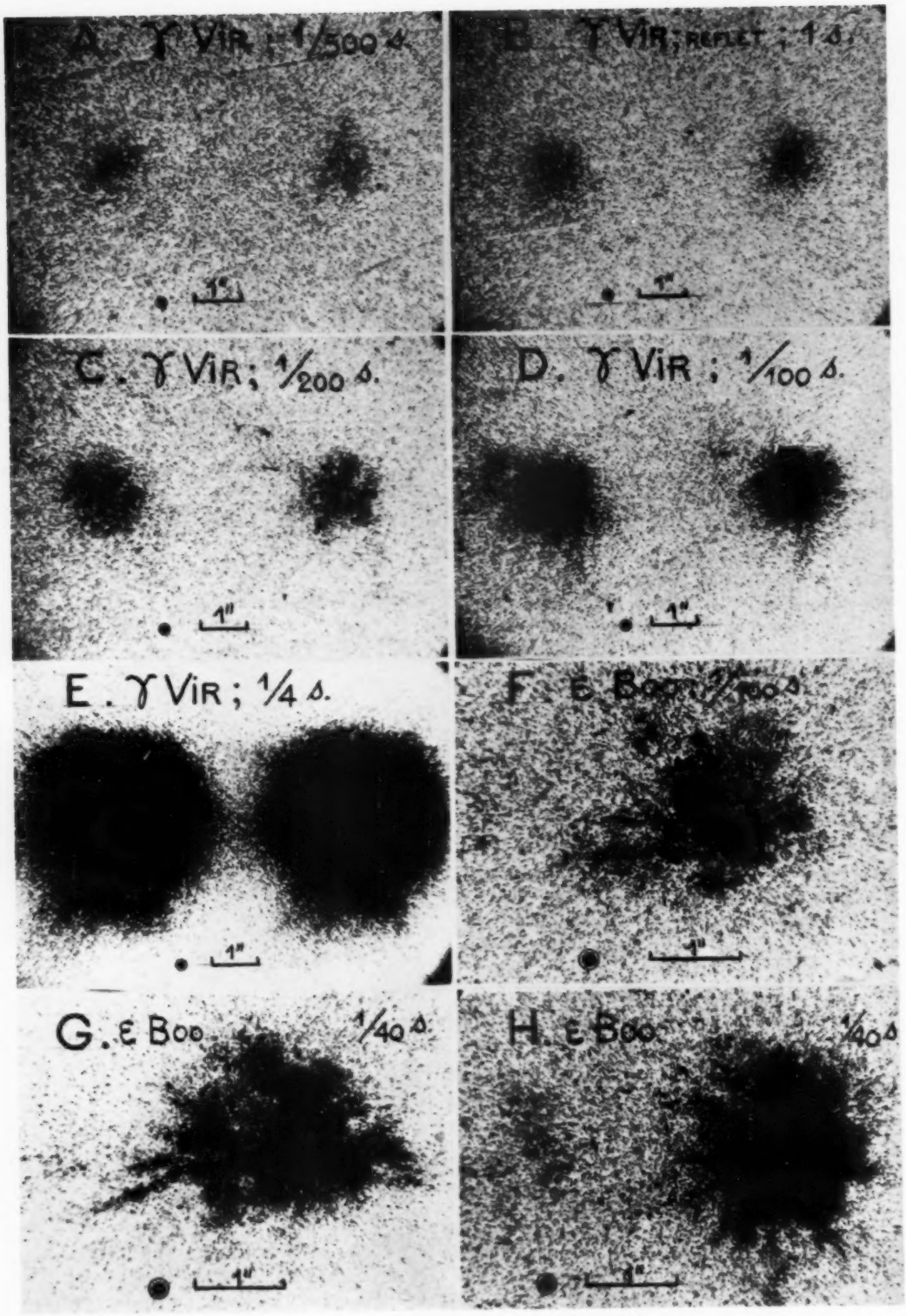

×46 pour *A.B.C.D.E.*

Fig. 3. Images d'étoiles doubles

×87 pour *F.G.H.*

porte rapidement des accidents de dimensions relativement constantes, ici 3 à 5 cm. Ce système subit des déformations à plus grande échelle, elles peuvent intéresser une fraction importante de la surface d'un grand miroir mais conservent un caractère accidentel.

L'altération de l'image ne peut être vraiment comprise si l'on ne tient pas compte des propriétés d'une surface d'onde aussi complexe et deformée. Nous avons affaire à un *réseau de phase* comparable à celui crée par le mamelonnage primaire du miroir mais cette fois infiniment plus destructeur car les pentes types sont de l'ordre de plusieurs 10^{-5}, les écarts de tautochronisme dépassent couramment $\lambda/2$ enfin et surtout ce réseau irrégulier, ce chaos d'accidents perpétuellement renouvelés, est cependant suffisamment périodique pour diffracter l'énergie suivant une loi stable caractéristique tant qu'un changement notable de la micrométéorologie locale ne vient pas modifier les dimensions des accidents types du réseau. La notion de réseau de phase résulte des travaux bien connus de F. Zernike et B. Lyot elle a déjà été mentionnée par E. Gaviola[8] à propos de la turbulence dans les grands télescopes. Il serait cependant imprudent de pousser l'analogie avec le cas simple d'un réseau de spectrographie diffractant rigoureusement la lumière dans les spectres des différents ordres. La superposition des accidents de tous les étages turbulents de l'atmosphère s'oppose à une theorie simple tendant à expliquer tous les résultats. Il nous paraît plus directement utile d'étudier expérimentalement la répartition de l'énergie dans l' image ou, si l'on préfère, le spectre d'ordre zéro et son brouillard de lumière diffractée.

IV. Etude Photographique de l'Image

Nous avons déjà décrit qualitativement l'image stellaire[9] observée visuellement au télescope de 193 cm. Trois nuits de Mai 1961 ont donné l'occasion d'une vérification photographique quantitative qui offre en outre l'avantage de situer le phénomène pour les applications les plus importantes.

Le foyer Newton à $F/D = 5$ est porté à $F/D = 19.4$ par une lentille de Barlow calculée par M. Paul.[10] La longueur focale résultante de 37 m devient suffisante pour permettre la résolution photographique de détails contrastés comparables à la tache de diffraction. Une lame séparatrice placée à demeure à 45° prélève 20% de l'énergie pour un oculaire latéral de guidage et de mise au point ($G = 1480$). Le traitement anti reflet de la face dorsale de la lame ne peut être complètement efficace dans un grand intervalle spectral, sur émulsion panchromatique l'on observe un reflet 350 fois plus faible que l'image directe soit 6.4 magnitudes de plus. Ceci permet la comparaison mentionnée plus loin. La chambre photographique est un boitier 24 × 36 Leica dont l'obturateur à rideau assez précis donne les temps de pose de $^1/_{1000}$ à 1 sec, les poses plus longues sont déclenchées au chronomètre. Dans ces conditions l'étoile double γ Vir. de magnitude 3.6 et 3.6 donne une image significative à partir de $^1/_{1000}$ de seconde sur film 35 Agfa Isopan Record; l'émulsion Kodak Tri-X est moins sensible mais résoud en $^1/_{100}$ de seconde tous les détails accessibles.[11] Par ailleurs la distance actuelle[12] du couple: 4".96 donne l'échelle des images et permet la vérification des réfractions différentielles. Les 36 poses d'un chargeur 24 × 36 sont prises en un quart d'heure environ et les poses rapides sont répétées tout le long du film pour le contrôle de la stabilité du phénomène.

V. Structure des Images

Les agrandissements négatifs d'images de la Fig. 3 sont donnés par des objectifs de microscope Planapo Zeiss Winkel × 10; O.N. 0.32 et × 25; O.N. 0.63. Il est en effet nécessaire de disposer d'une ouverture numérique suffisante pour donner une représentation assez fidèle du grain de l'émulsion qui constitue l'image. Chaque agrandissement porte un disque d'Airy dessiné à l'échelle à gauche de la longueur représentant une seconde d'arc.

A. *γ Vir.*, $^1/_{500}$ *sec:* Seuls les granules les plus intenses de ce que nous avons nommé paquet central[9] contribuent à un noircissement irrégulier de la plage. Cette nuit la l'on ne peut obtenir d'image bien formée de moins de 0".95 de diamètre.

B. *γ Vir. reflet 1 sec:* Le reflet, dont la magnitude apparente est 10, donne en une seconde une image légèrement plus dense que la précédente mais la structure est complètement différente. Les granules ont eu le temps de s'agiter en tous sens dans les limites du paquet central et le noircissement de la plage est bien régulier. Il y a bien eu quelques écarts anormaux mais trop rares pour affecter notablement le diamètre résolvant qui reste égal à 0".96 sur ces images. La même nuit sur le même film nous avons obtenu en 5 min de pose des étoiles faibles de l'Amas M 13; certaines d'entre-elles ne dépassent pas 0".93.

Ceci est très important, les millions d'accidents simultanément présents sur une grande surface d'onde déterminent avec précision la répartition d'énergie dans l'image et réduisent à une valeur très petite les fluctuations de position du pic central. Les réfractions accidentelles ne sont pas totalement éliminées dans un grand télescope mais elles sont "tellement accidentelles" qu'elles n'augmentent pas le diamètre des images à longue pose.[9]

C. *γ Vir.*, $^1/_{200}$ *sec:* l'énergie devient suffisante pour donner une meilleure définition des granules, malgré leur déplacement; les détails sont malheureusement un peu empatés sur Isopan Record.

D. *γ Vir.*, $^1/_{100}$ *sec:* l'énergie extérieure au paquet central commence à apparaitre avec un caractère aléatoire assez marqué. Souvent les deux composantes,

à quelque secondes d'arc de distance, sont affectées parallèlement mais ce n'est pas du tout une règle générale. Ici la composante de gauche est dédoublée vers la gauche, celle de droite est peu affectée. Sur d'autres images les distortions sont complètement indépendantes. Il ne faut pas tenir compte de l'aigrette en bas des images dûe à la coma, elle constitue bien entendu une cause d'étalement systématique; nous n'avons pas le temps matériel de retoucher à ce moment l'inclinaison du grand miroir, qui impose dans cet instrument la reprise des jeux des 30 leviers astatiques. La diffraction du réseau de phase est toujours affectée de fortes discontinuités si l'on considère un champ un peu étendu. Les plages d'inégales définition sur les photographies de grains de riz photosphériques comme sur les photographies lunaires sont bien connues.

E. γ Vir., $^1/_4$ sec: développement régulier du halo diffracté, seule la cause systématique de déformation: la coma extraaxiale, subsiste.

F. ϵ Boo., $^1/_{100}$ sec: cette image très fine et agrandie donne une bonne idée des granules du paquet central. Quelques uns d'entre eux sont inférieurs au disque d'Airy. L'émulsion Tri X suffit donc pour résoudre les détails bien contrastés avec le rapport $F/D = 19$. Le temps de pose est encore insuffisant pour donner des éléments significatifs du compagnon bleu de la "Pulcherrima" ($m = 6.3$).

G. ϵ Boo., $^1/_{40}$ sec: Exemple de forte perturbation accidentelle dûe au passage d'un front turbulent donnant une déformation d'ensemble au réseau de phase. Paquet central très allongé et image du compagnon anéantie malgré le temps de pose suffisant.

H. ϵ Boo., $^1/_{40}$ sec: Image normale pour cette nuit l'énergie est régulièrement concentrée et les granules les plus marquants du compagnon commencent à laisser leur trace.

VI. Mesure des Images

Les négatifs originaux sont mesurés sur une petite machine à chariots croisés de la Société Génevoise, grossissement du microscope 25.

La distance des composantes de γ Vir. se pointe sur des images régulières telles que B avec une erreur moyenne de 0".02. Les poses courtes, sensibles aux écarts accidentels, conduisent à des dispersions de 0".07. Les poses plus longues sont affectées d'un effet Kostinsky notable[13]; si l'on attribue les 4".96 à la moyenne des images posées $^1/_{500}$ et $^1/_{200}$ sec, les poses $^1/_{100}$ sec donnent 5".03 et les $^1/_4$ sec 5".12.

Les diamètres de toutes les images sont mesurés de la même manière au moyen d'une simple croisée placée à la limite du palier de densité des plages. Pour chaque temps de pose t: $^1/_{1000}$, $^1/_{500}$, $^1/_{200}$, $^1/_{100}$, $^1/_{40}$, $^1/_8$, $^1/_4$, $^1/_2$, 1 sec; 6 sec, 15 sec; 1 min on forme les moyennes exprimées en secondes d'arc et portées en fonction de $\log (t_0/t)$, l'unité est le temps t_0 juste suffisant

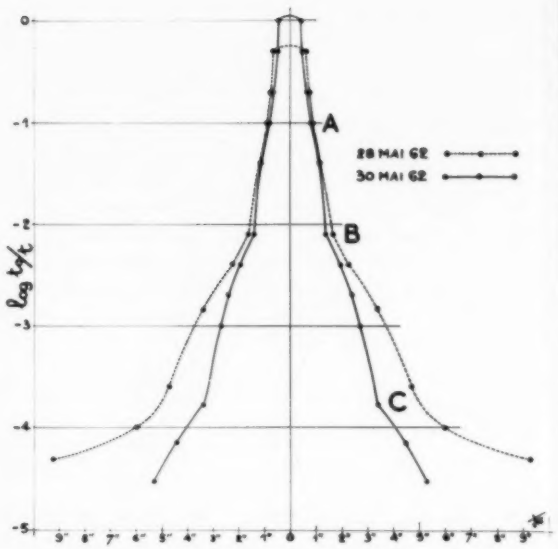

Fig. 4. Répartition de l'énergie dans le spectre de diffraction produit par le réseau turbulent.

pour donner une image mesurable. La Fig. 4 montre la courbe obtenue avec γ Vir. pour deux nuits différentes.

Ceci n'est pas à proprement parler le profil photométrique du spectre de diffraction produit par le réseau de phase. Les causes d'erreurs de ce procédé simplifié ne sont cependant pas considérables étant donné l'importance du phénomène. L'erreur de réciprocité de l'émulsion reste faible dans l'intervalle de luminations considéré où la courbure de la chaînette de Kron est petite. L'étalonnage de l'obturateur serait nécessaire en seconde approximation. Une nuit à absorption variable fut rejetée. Enfin l'enregistrement microphotométrique de plages d'un film calibré donnerait des pieds de courbe nettement plus évasés par l'incorporation inévitable de la diffusion photographique, écartée des pointés visuels.

Trois paliers $A - B - C$ de plus en plus marqués se distinguent. Ce que nous appelons le paquet central, y compris ses réfractions, reste de diamétre inférieur au palier A dont le niveau est voisin du dizième de celui du centre. Les paliers B et C, 100 fois et 5000 fois plus faibles respectivement que le pic, correspondent chacun à une classe d'accidents caractéristiques du réseau de la nuit étudiée, ils sont très sensibles à un changement de conditions météorologiques, ils représentent une part d'énergie gaspillée notable et variable.

En 1955 nous avions proposé de prospecter par cette méthode les sites envisagés pour l'installation d'un télescope austral de 350 cm. Avec des instruments de cette importance l'idée tenace "d'instants de parfaite

images" doit être absolument abandonnée pour un point de vue plus réaliste situant l'efficacité de l'instrument dans les *conditions courantes*. Un cassegrain de 50 cm monté sur un remorque pourrait suffire. Faute d'un réseau de phase assez grand il ne donnerait pas une courbe semblable à la Fig. 4, la part des réfractions accidentelles serait plus grande mais un étalonnage serait possible au voisinage d'un grand instrument en service opérant simultanément. Les possibilités des sites étudiés de cette manière apparaîtraient immédiatement en fonction des applications demandées au grand instrument. Pour les travaux à haute résolution, la photographie à grande echelle, le spectrographie à grande dispersion, seul compte le diamètre du paquet central: 0".95 le 30 Mai 1".31 le 28 (Fig. 4). Si l'objet est faible on prendra le palier B comme largeur de fente. La photométrie précise par contre ne pourra se faire qu'avec un trou de diamètre au moins égal à C. C'est à dire 7" le 30 Mai; 11" le 28; il faudra s'attendre à des surprises en cas de changement de vent au sol.

VII. Faut-il Construire des Grands Télescopes?

Une personne non prévenue pourrait conclure de la Fig. 4 qu'il est inutile de construire des grand miroirs très soignés. Puisque la figure de diffraction d'une ouverture de 28 cm n'est pas plus grande que le paquet central observé le 30 Mai pourquoi employer un miroir de 193 cm? Un observateur armé d'un récepteur très sensible, comme le caméra électronique de Lallemand, peut effectivement obtenir de temps en temps une image

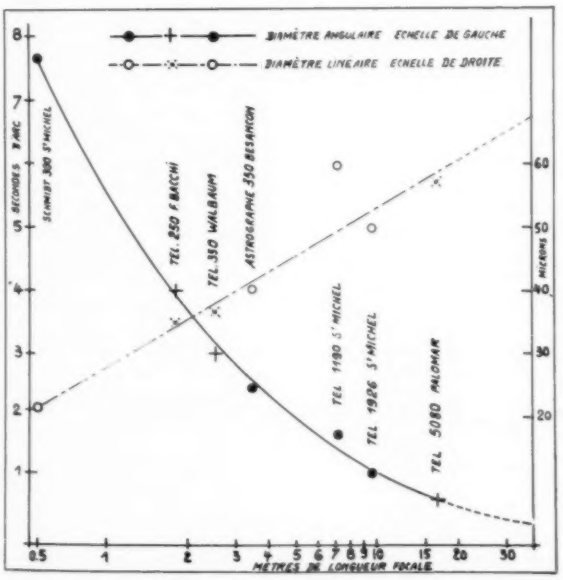

Fig. 5. Diamètres des plus petites images photographiques d'étoiles en fonction des dimensions de l'instrument.

présentable du disque d'Airy, d'un instrument moyen, avec un *temps de pose court;* c'est pratiquement utopique avec une ouverture de deux mètres. Par contre à chaque fois qu'une pose *assez longue* est nécessaire la supériorité du grand télescope est certaine; il y a trois raisons au moins à cela nous nous excusons de le répéter:

1. Le disque d'Airy, centre de dispersion de l'énergie est plus petit.

2. Le grand réseau de phase, composé d'accidents très nombreux donne un paquet central plus net, plus homogène, dont la section au niveau du seuil de l'émulsion a un diamètre plus faible.

3. Le pic central fourni par un grand miroir est pratiquement insensible aux réfractions contrairement à la figure de diffraction d'un petit instrument.

Les plus petites images de diffusion photographique sur émulsions astronomiques rapides 103*aO*, II*aO* ont un diamètre voisin de 25 μ. La limitation imposée par la turbulence apparaît nettement sur les photographies à longue pose, même prise directement au foyer d'un faisceau à $F/D = 3$ seulement d'un instrument modeste.

Sur la Fig. 5 les points noirs représentent les plus petits diamètres d'images d'étoiles que nous avons pu atteindre avec différents instruments de qualité sûre et bien réglés. L'argument est la dimension du télescope repérée sur une échelle logarithmique par la longueur focale.* Les croix concernent des mesures faites sur les meilleurs clichés de deux amateurs: Bacchi (25 cm) et Walbaum (33 cm). La dernière croix est plutôt une estimation—nous ne disposions pas du cliché original—d'une photographie de NGC 205 obtenue par Baade au télescope Hale, dont la qualité semble également difficile à dépasser. La résolution angulaire ne croît pas linéairement avec l'ouverture, comme le voudrait la diffraction en l'absence de turbulence; cependant elle croît et c'est spécialement important quand il s'agit de très grands instruments si l'on veut effectivement atteindre la magnitude limite accessible. En effet, outre la turbulence, il existe une autre limitation atmosphérique: la luminance du fond du ciel nocturne dont la magnitude d'après Baum[14] est 22 par seconde carrée. Non seulement le grand télescope collecte suffisamment de photons mais *il est seul capable de les concentrer en une image assez petite angulairement pour donner un palier de densité significatif par rapport au fond.* L'extrapolation de la courbe aux dimensions d'un télescope de 10 m d'ouverture permet d'espérer des images de 0".4; le gain de 1.5 magnitude—par rapport au télescope Hale serait donc encore vérifié.

* L'homothécie, au moins approximative, est implicitement admise; bien entendu l'augmentation du diamètre détermine seule l'amélioration de pouvoir résolvant photographique pourvu que la longueur focale soit suffisante pour rendre la diffusion photographique petite devant la turbulence.

Bibliographie

1. A. Danjon et A. Couder, *Lunettes et Télescopes* (ed. Rev. opt., Paris, 1935), § 115.
2. J. Texereau, Ciel et terre **56,** nos. 3–4, (1950).
3. J. Texereau, *Le Contraste de Phase et le Contraste par Interférences* (ed. Rev. opt., Paris, 1952), p. 172.
4. J. Texereau, *How to Make a Telescope* (Interscience, New York, 1957), p. 83.
5. A. Couder, Thèse, Paris (1932).
6. G. M. Sisson, Nature **179,** 937 (1957).
7. A. Couder, *Vistas in Astronomy* (Pergamon Press, Oxford, 1955), Vol. I, p. 372.
8. E. Gaviola, Astron. J. **54,** 155 (1949).
9. J. Texereau, *La Construction du Télescope d'Amateur*, 2e ed. (Paris, 1960), p. 267.
10. M. Paul, Rev. opt. **14,** 169 (1935).
11. P. Guérin, L'Astronomie **76,** 102 (1962).
12. P. Muller, J. Observations **36,** 89 (1953).
13. S. Kostinsky, Mitt. Nikolai Hauptsternwarte Pulkovo **1,** no. 11 (1906).
14. W. A. Baum, Sky and Telescope **14,** 188 (1955).

From the Editor

In several editorials last year we have remarked that we would turn soon to our correspondence. In spite of our repeated invitations for letters it is still a small correspondence; perhaps half a dozen critical letters. (We do not plan to discuss here the noncritical letters, although we appreciate them just as much as the critical ones.) So far these letters have dealt with four principal subjects: comments on format, comments on content, comments on terminology and units (in particular the use of the metric system), and finally a few comments concerning scientists and engineers. Let us consider these subjects in turn. We will quote occasional passages from our mail.

There have been a few remarks about our use of filler material. "I bind my journals and I hate to think that I am binding in this extraneous material along with the timeless material." Your Editor also saves his back journals; in fact he cannot afford to have them bound, so he saves them entire, even including the advertisements. At such times as he has pondered the injustice of this arrangement he has usually concluded that even among the contributed scientific papers of undoubted worth in his back journals there are a rather large number that he didn't read when the journal was new, that he doesn't plan to read later, and that in all probability he never will read; and yet there they are, occupying space on the bookshelf. Not everything that we devour is palatable, nutritive, or even digestible, and some roughage supposedly helps. Your Editor can only admire those austere and ascetic scholars among us who wish to deny and exclude the trivial and nonessential; they are scientific monks and most of us are but poor sinners.

We mentioned once before that we were trying, as an experiment, to start each article on a right-hand page. The filler material has been largely used to fill the gaps that then occur between articles. We felt vindicated in this policy when, at a recent meeting of the Publications Board of the American Institute of Physics, it was announced that a cost analysis had been run on the relative merit of starting each article on a right-hand page compared to the present system in AIP journals of beginning on either page but then having to reset the left-handed articles when preparing reprints (which provide a substantial portion of the journals' operating income). The cost analysis indicated the Institute would be ahead if they began articles on the right-hand side, even if a few left-handed pages in each issue were then left blank. If it offends you that an occasional page of filler occupies space on your shelf, how will you react to these blank pages? As material for the filler we have our University and Industry Columns, Book Reviews, Meeting Reports, Patents Reviews, timeless editorials such as this, and our news notes, pictures, squibs, and quiddities concerning optics people, and events. There are those who assert that the presence of some such material in the same journal as genuine scientific papers somehow detracts or degrades the worth of those papers. We are aware that a sense of proportion and moderation is required here. When we attend a scientific meeting some go just to hear papers and to rejoice in the science of it all but most of us also enjoy seeing and talking to our friends and colleagues and some of us even occasionally smile. Suffice it to note that for every one of you who wants none of this material there appear to be many more who find it interesting.

A few readers have not liked the use of pictures as fillers. Too much like *Physics Today*. Your Editor himself happens to be rather fond of *Physics Today* so that this particular analogy somewhat eludes him. Let us digress a moment and consider certain more "popular" or less "technical" journals: *Physics Today, American Scientist, Sky and Telescope, Scientific American*. There are many more, but these are the ones that we often read. *Scientific American*, we would say, is popularizing science, and is aimed at the lay audience rather than the technical audience. *American Scientist* deals more with the general trends and philosophical undercurrents of science. It is aimed at the scientific audience although it does not delve into the technical depths of any one discipline. It emphasizes the philosophic, rather than the professional aspects of scientists. Journals such as *Sky and Telescope* and *Physics Today* attempt to evoke our professional spirit, and hence the meeting reports, book reviews, and many pictures of personalities and events of one profession. It is possible to be an excellent scientist and feel no professional responsibilities. Most of us, however, feel a kinship with our fellow workers, and out of this feeling grow professional societies, which in turn serve the profession in various ways such as by publishing journals. We feel that these filler pictures of optics people and events in *Applied Optics* help to identify optics as a profession, and these same pictures, if they appeared in, say, *Physics Today*, would not do this. If you have informal snapshots of colleagues or events that should appeal to our audience, lend them to us.

One or two have remarked that some of the columns favor one side of controversial issues or one man's personal views. If you would read the fine print above these columns you will see that reader contributions and suggestions are invited, and news material is welcomed from whatever source. In those columns that are signed (such as this one) any opinions are certainly those of the writer; if they happen to differ from your opinions why not let us know. (Let us try, however, to confine ourselves more or less to optical matters.) In this Editorial column we feel disposed to try to say something: we have opinions and this journal has a purpose, a raison d'être which we wish to discuss here.

JOHN N. HOWARD

A Direct Analyzer for Stellar Images

Stanley H. Zisk and Robert A. Fish

Double star and polarization studies are being conducted at Lick Observatory with an image analyzer. The instrument scans the telescopic image with a slit 6 sec by 0.18 sec of arc at a frequency of 103 cps. Scans alternate between orientations 90° apart. Light transmitted by the slit is sensed with a refrigerated 1P21 phototube. After appropriate ac circuitry the signal is displayed on the intensity axis of an oscilloscope. The trace position is swept downwards over a period of several minutes. Photographs of the oscilloscope face consist of parallel vertical streaks whose width and brightness show the image structure.

I. Introduction

The study of visual binary stars is of importance to astronomy in at least three respects.* First, the visual binaries have supplied mass estimates for the stars, and thus established the relationship between mass and luminosity of main-sequence stars as a fundamental checkpoint in the study of stellar interiors.[1] Second, the stars of a visual binary are co-eval, and observation of evolutionary indicators in the better understood members has provided information on the state of evolution of their less familiar companions.[2] Third, visual binaries have been found to be so abundant among the nearest stars (25 of the 48 stars nearest the sun are members of visual binaries or triples) that the mechanism for the formation of these systems is now regarded as an integral part of the mechanism of star formation.[3]

Of course there are unfinished tasks in this field, as in any other. Some consist of continued measurements of many binaries available to present-day techniques, but for which orbital computation would now be premature. But there are many problems that cannot even be approached without studying systems beyond the capabilities of today's instrumentation (Fig. 1).†

The luminosities of long-period variable stars cannot be obtained from a study of visual binaries with present techniques, because only two cases, X Ophiuchi and R Hydrae, are known where the companion is a normal star whose absolute magnitude can be estimated, while only a few others are known cluster members. Many more binary systems would be required to establish a magnitude-period or a magnitude-amplitude relation that would allow these stars to be used as distance indicators analogous to the Cepheids.

It seems likely that some long-period variables will have K-type main-sequence companions that are now escaping detection because of the large magnitude difference that exists between the two stars, even at minimum light. The discovery of such pairs alone would not suffice to provide a magnitude calibration for these variables. We should like to measure Δm in two colors and combine it with a value for the B-V color for the pair, whence a value of B-V for the secondary might be deduced. For main-sequence stars the photovisual absolute magnitude is a known function of B-V, and the absolute magnitude of the primary follows directly.

The nature of the components of astrometric binaries—detected by variability of their proper motion—cannot be determined either, because of present limitations in dealing with close stars of great magnitude differences. For astrometric pairs one cannot distinguish whether the orbital displacement of the photocenter from the barycenter is due to a planetary companion of negligible luminosity, or a more massive stellar companion of higher luminosity.[4] Direct observation of the companion would be of obvious usefulness here.

Stanley H. Zisk is a National Science Foundation Predoctoral Fellow at the Radio Astronomy Institute, Stanford University, and Robert A. Fish, a Fellow of the Miller Institute for Basic Research in Science, is at the Lick Observatory, University of California.

Received 1 September 1962.

Lick Observatory Bulletin No. 580.

* The term visual binary usually refers to a double star system whose orbital motion is detectable by positional, rather than radial velocity, measurements.

† We were guided in the preparation of this figure by the comments of W. H. Van den Bos and H. M. Jeffers.

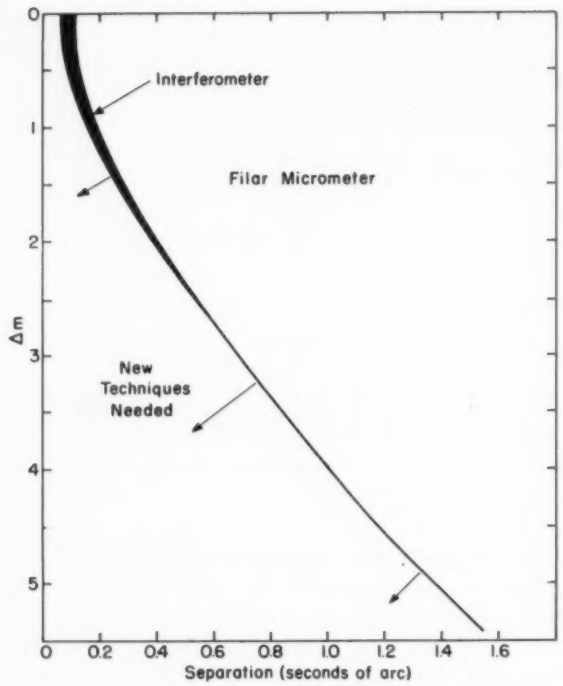

Fig. 1. Domains of present-day measuring techniques as applied to double star measurement at the Lick Observatory 36-in. (91-cm) refractor. The filar micrometer is usable in the region above and to the right of the curved line of demarcation. The interferometer can measure stars separated by half as much as the best that can be measured by micrometer for $\Delta m = 0$, but loses its advantage for larger values of Δm. Its domain of unique usefulness is the black area above $\Delta m = 2.5$. The interferometer is also used for close pairs that are accessible to the micrometer as well. Photographic p.a. and separation measurements are useful principally for pairs wider than 2 seconds of arc, hence lie off the right-hand edge of the diagram. The domain reading "New Techniques Needed" is inaccessible to present-day nonelectronic instruments. The image analyzer was constructed to operate in this latter domain, although at present we have successfully resolved and measured stars only when they lie well inside the micrometer domain (see text).

And as a final example, the current observational techniques offer no hope for progress with the orbits of some important, nearby systems, because the companion star approaches the primary too closely to be observable during large portions of the orbit. Examples of this type of binary are α Ursae Majoris, β Scorpii, ρ Geminorum, and 11 Leo Minoris. Since the position angles and separations obtained from the observable portions of the orbit establish the orbital areal constant $\rho^2 d\theta/dt$, an accurate determination of θ as a function of time for the unobserved arc could markedly improve the orbit. Good measurements of ρ would be useful as a check, even though they are somewhat difficult to achieve.

These examples suggest that there is a need for a new instrument for measuring double stars with magnitude differences and separations beyond the capabilities of present techniques. In addition, if the accuracy of the measurements of position angle and separation were competitive with the filar micrometer, then impersonal measurements by relatively untrained persons could be used to supplement the efforts of the dwindling number of skilled visual observers.

II. Techniques of Double Star Analyzing

Let us examine the reasons for the limitations of present-day observing techniques that will bear on the problem of designing a new instrument. The human eye, working with the filar micrometer, is more susceptible to magnitude illusions than to any other failing. It overestimates magnitude differences, responds more slowly to motions of a faint star than to a brighter primary (and thus sees a "rocking" in position angle), and cannot see the duplicity of close binaries at all when the brightness difference becomes large (Fig. 1). These deficiencies are caused by a combination of retinal scattering and retinal desensitization due to the brighter star.

Photographic methods, which are ideal for stars separated more than 2–3 seconds of arc, or alternatively for astrometrical determinations of an orbit in which only one circular image is visible, are subject to large, systematic errors in the intermediate range where images are noncircular but unresolved. One problem that arises with photography is blurring of the image, caused by motions of the seeing disk, although preliminary studies suggest that this problem can be reduced by automatic selection of instants of exposure.[5] Photography is also limited in the magnitude differences

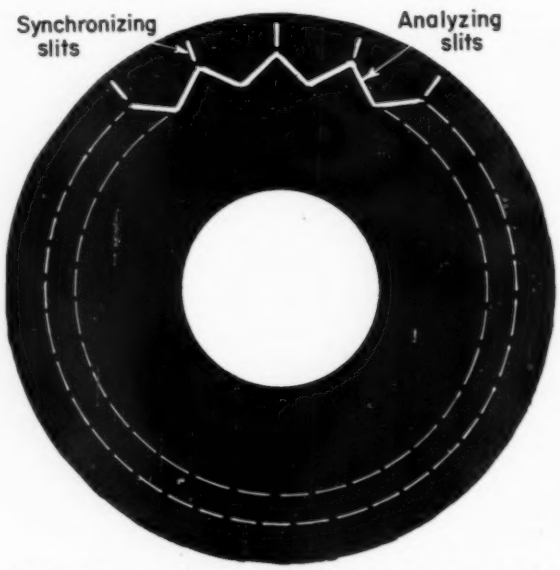

Fig. 2. Schematic drawing of the slit disk (slit pattern is at the correct radius, but greatly enlarged).

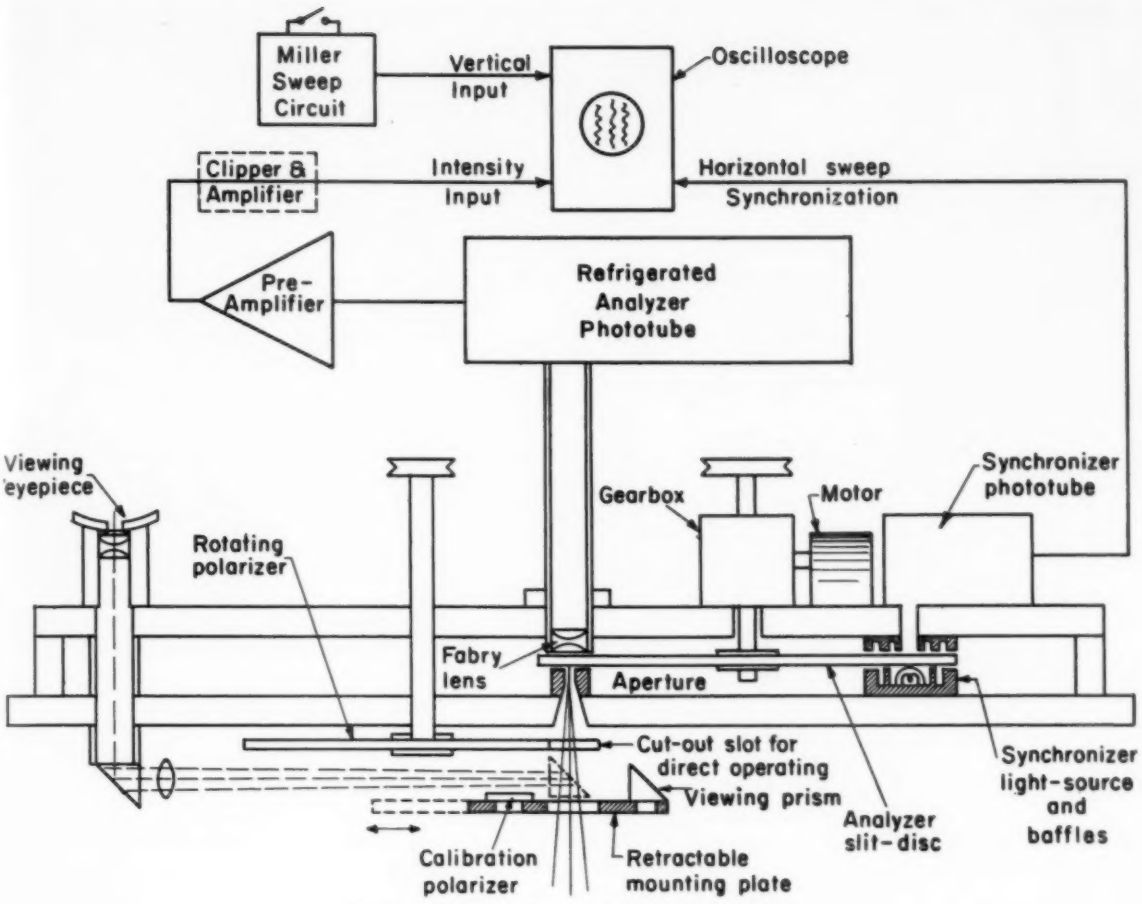

Fig. 3. Schematic diagram of the image analyzer.

that are accessible, due to the growth of the image of the brighter star caused by scattering in the emulsion and chemical migration effects.

The eyepiece interferometer can measure equal magnitude pairs of smaller separation than can be attained by the filar micrometer and is restricted principally by its dependence on the visibility of interference fringes. Its usefulness is somewhat restricted by its limited capabilities in dealing with stars differing in brightness by more than one and a half to two magnitudes.[6]

In addition to these traditional techniques of observation, we must take note of the electronic image-conversion devices which are assuming an important role in astronomical research.[7] The image scale and screen brightness can be controlled arbitrarily to eliminate photographic effects and to shorten exposure times down to the point where blurring is eliminated. Short exposures entail a reduction in the number of photons responsible for the image, and for stars fainter than eleventh magnitude the statistical fluctuations in individual 1/100th sec exposures become intolerable. Longer accumulation times can be achieved by feeding data into a high-speed computer instructed to correct for motion of the image and to integrate, but the cost and complexity are unattractive. Image orthicons are also affected to some extent by scattered light in the photocathode, as well as scattered and induced charges in the collecting medium.

Image Scanning

In all these techniques we find that image degradation occurs between the focal plane of the telescope and the analysis of the image. If one scans the image with a slit at the focal plane and converts the physical distribution of light across the image into a time varying intensity as suggested some time ago by Lacroute and Bacchus,[8] the instrumental degradation of the image can be reduced. Also, with conversion of the luminous intensity into a time-varying voltage, various electronic processes may be applied to improve the usability of the information.

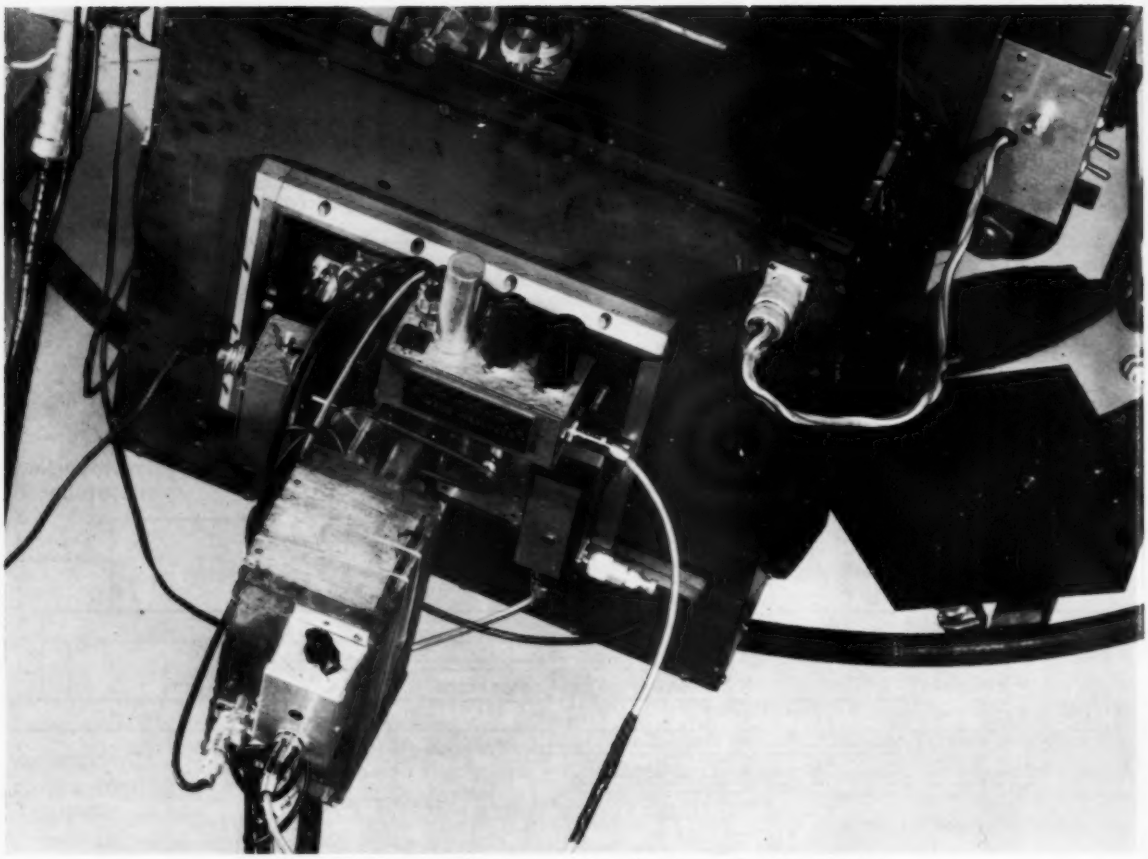

Fig. 4. The image analyzer, mounted on the 91-cm refracting telescope

In addition, scans with a slit can be made in a sufficiently short time (0.01 sec or less) that there is no appreciable motion of the image during any one scan. By repeating the scans we obtain an ac signal that permits the use of ac circuitry. Information obtained from successive scans can be processed to minimize image motion. In this way one can obtain relatively long integration times without the loss of information to be expected from direct superposition. It is also a simple matter to alternate the scans in position angle, so that the ac signal carries two channels that may be compared without any need for an external reference.

III. The Image Analyzer

In designing the image analyzer we decided upon the zig-zag slit pattern diagrammed in Fig. 2. This geometry seemed preferable to an oscillating slit which would introduce vibrations. It was also preferred to a slit requiring placement of the image at the center of rotation, since we wished to minimize distortion of the wave shape of the output voltage caused by motions of the image.

A schematic diagram of the image analyzer is shown in Fig. 3, and a photograph in the operating position in Fig. 4. The slit disk scans the image in two perpendicular directions alternately, at a scanning rate of 720 times the rotation rate of the disk (103 scans per sec). The radial slits are used for synchronization, and will be discussed later. The preparation of the slit disk is described in the Appendix.

The image plane is masked out except for a square aperture 0.47 mm on a side, positioned so that the slits cross the aperture parallel to a diagonal. The length of the diagonal of the aperture is 7.9 seconds of arc, identical with the length of a slit. This form of aperture exposes a constant area of slit, and eliminates an ac contribution from the sky.

A Fabry lens system is located beyond the slit disk. Its purpose is to maintain the illuminated spot in a fixed position on the photocathode, as the slit moves across the focal plane of the telescope.

The electrical signal from the phototube is preamplified at the telescope, in order to minimize hum and distortion in the long transmission cable. The preamplifier employs 40 dB of negative feedback which results in a stable gain of 1000 and an output impedance of less than 5Ω. Saturation occurs at an output level of 30 V peak-to-peak, which is high enough to drive the in-

tensity axis of the oscilloscope, if no other processing is used.

The light intensity curve is displayed on the oscilloscope, using the internal sweep, and starting each sweep by a signal from the radial slits on the analyzing disk. A light source is mounted behind the disk, and the signal is picked up by a separate photomultiplier. Thus, the beginning of each sweep corresponds to the same point in the image plane of the telescope. The duration of the horizontal sweep can be varied in order to display an arbitrary number of scans on each sweep. At the conclusion of a sweep the screen remains blank until the next synchronizing signal.

A trace is thus displayed on the oscilloscope screen whose intensity at each point represents the integrated brightness of the image along the slit at a corresponding point on the image plane.

In order to separate successive traces, a slow vertical motion is applied to the trace from a Miller sweep circuit. This procedure converts the alternating bright and dark portions of a trace into bright and dark vertical streaks on the oscilloscope screen. The resulting display is photographed with a Polaroid camera, employing a time exposure.

The horizontal coordinate of the resulting pattern represents a projection of the image upon a line perpendicular to the slit, while the vertical coordinate represents elapsed time. For a perfectly stationary image centered in the aperture we see pairs of vertical bright streaks, corresponding to scans in orthogonal directions. The width of a streak represents the size of the image in the direction of scanning, so that for an

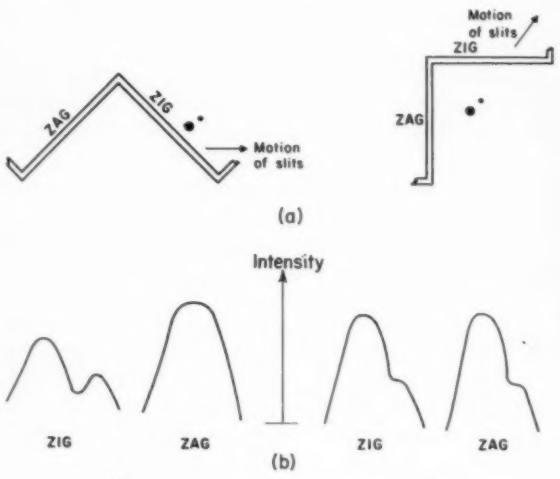

Fig. 5. Zig-zag slit scanning of a double image. (a) Slit geometry; (b) light output from slits: (*i*) Double star perpendicular-parallel to slits. (*ii*) Double star at 45°-45° to slit. After a photograph is made with the image analyzer, the instrument is rotated to produce a new angular relationship between the stellar image and the slits.

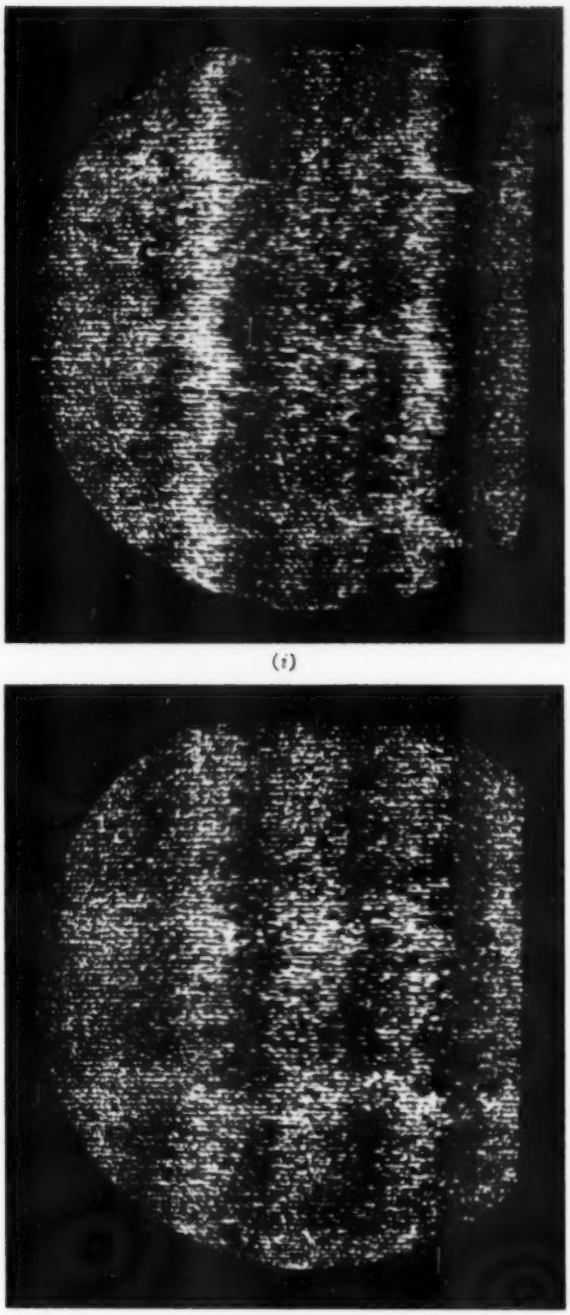

Fig. 6. Zig-zag slit scanning of Zeta Aquarii (refer to Fig. 5). (*i*) Double star perpendicular-parallel to slit. The last half of the first perpendicular streak is at the left of the figure, and two complete sets of parallel-perpendicular streaks follow from left to right. (*ii*) Double star at 45°-45° to slit. The last half of one 45° streak is at the left of the figure, and two complete 45°-45° sets follow. Thus a rotation of the instrument by 45° produces a change in the pattern from 6(*i*) to 6(*ii*), and a further rotation by 45° would give a pattern of type 6(*i*) once again (though with altered phase).

elongated image oriented parallel to one slit, the streaks will clearly alternate between narrow and wide. Motions of the image will cause the pattern to shift; the streaks will then assume a jagged shape, which the eye will tend to smooth out during the measurement of the photographs (Fig. 5).

IV. Observations

In Fig. 6 we can observe an example of the type of display just described. Figure 6(*i*) shows a photographic record of the double star ζ Aquarii (4.4–4.6 m, 1.9 sec separation) that was made on August 15, 1962, with the image analyzer oriented so that the slits scanned the image alternately perpendicular and parallel to the known position angle of the pair. Figure 6(*ii*) shows the pattern obtained upon rotating 45°. In the one position angle every other streak shows a clearly resolved double pattern, while in the other the difference between adjacent streaks virtually disappears. The separation can be measured knowing that the separation between a given phase of the pattern and its repetition further to the right is 7.9 seconds of arc on the sky.

The general procedure for observing double stars includes making photographs at intervals of 15°, and observing the progression of patterns from minimum to maximum and again to minimum difference with a periodicity of 90°. Although 4 such cycles may be observed in rotating through 360°, no redundancy exists because the order of the patterns is different in each quadrant. One need only progress through a little more than one quadrant to obtain a position angle estimate to about ±5°. This requires 6–10 photographs, which, including the initial setting-up, can be obtained in 40–50 minutes. Because the analyzer is so sensitive to image elongation, however, it is important to work within about 45° of the zenith, using a rather narrow band-pass filter, in order to minimize refractive effects. At the latitude of Lick Observatory (37°N) one is limited, therefore, to studies inside the declination limits $-8° < \delta < 82°$.

Two other modes of operation are sometimes employed instead of the direct viewing observations just described. In one case a fixed and a rotating polarizer are introduced into the light train (see Fig. 3), producing a $\sin^2\omega t$ modulation in the intensity at the focal plane. The whole display in this case shows horizontal bands, representing intensity variations during the vertical sweep. This mode is used to calibrate the photographic densities obtained from various relative intensities of illumination. In this way the nonlinear effects of pulse shaping, signal clipping, cathode-ray tube transconductance characteristic, phosphor brightness, and characteristic curve of the emulsion can be taken into account at once.

In the other mode only the rotating polarizer is in the light train. This mode is useful for carrying on studies of the distribution of polarization across the surface of small, resolved sources whose radiation is suspected to be polarized. Examples include radio-emitting stars such as 3C196 and 3C48, recently identified by Matthews at the California Institute of Technology, and the nuclei of extragalactic nebulae.

For a polarized source, a periodic alteration of light and dark will be observed in whatever portion of the vertical streak corresponds to a polarized portion of the image. The amplitude of the modulation is a measure of the percentage polarization.

Our recording system is restricted in its ability to encompass stars of greatly differing brightness, so long as the data is in the form of microsecond pulses whose number is proportional to the stellar brightness. A record of the pulses makes little use of the gray scale of the film, and "blooming" of excessively bright spots on the oscilloscope screen will expose and therefore mask large areas on the photograph. So stars differing in brightness by $1^1/_2$ magnitudes—a factor of 4—are barely within the range of the recording system.

We have adopted various circuits to counteract these two effects. By integrating the pulses for a time constant of 10^{-4} sec, which is long compared to that of a single pulse but short enough to preserve the spatial resolution of the system, we can smooth the wave shape and record it as a variable density of the film. By "clipping" the signal we can mute the influence of a bright star on the detectability of a faint neighbor. The optimum clipping level is one which eliminates all the voltage-amplitude of the bright star above the peak voltage amplitude of the companion. In these two ways we have been able to augment the detectability of faint companions to the point where stars differing in magnitude by $\Delta m = 3$ and separated by 2 seconds of arc are of nearly equal recorded brightness. Further improvement in this respect seems possible.

V. Efficiency of the Instrument

Potential Resolving Power of a Scanning-Slit of Nonzero Width

Let us now investigate the broadening of the observed image by the slit, which is one of the limitations of this form of image analysis. Consider the two-dimensional distribution of light in the image plane, $B(x, y)$. An infinitely long slit of width d, centered at x_0, allows light-energy to pass in the amount

$$E(x_0) = \int_{x_0-d/2}^{x_0+d/2} \int_{-\infty}^{+\infty} B(x, y)\, dy dx \qquad (1)$$

$$= \int_{x-d/2}^{x+d/2} C(x) dx,$$

where $C(x)$ is the projection of the two-dimensional dis-

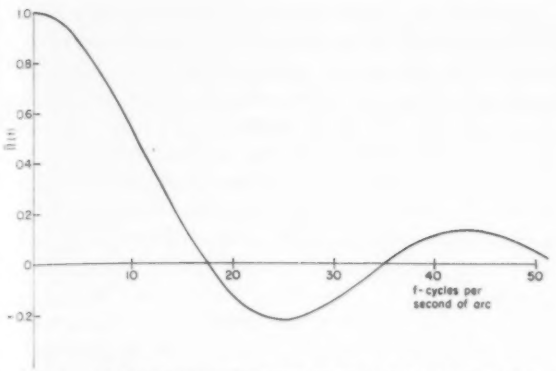

Fig. 7. Relative spectral transmission of a 0.18-second slit.

tribution $B(x,y)$ into a line distribution in the x direction. Equation (1) is seen to reduce to*

$$E(x) = \int_{-\infty}^{+\infty} C(X)\,\Pi\,[(X-x)/d]\,dX. \tag{1a}$$

One may observe the effect of slit-scanning in a qualitative way by transforming the brightness distribution into a spectrum of spatial frequencies. Let the notation $\bar{C}(f)$ indicate the Fourier transform of $C(x)$. Write the transform of Eq. (1a)

$$\bar{E}(f) = \bar{C}(f)\cdot\bar{\Pi}(f), \tag{2}$$

where the operation of convolution transforms to one of multiplication. The transform of $\Pi(x/d)$ can be shown to be

$$\bar{\Pi}(f) = \frac{\sin \pi f d}{\pi f} \tag{2a}$$

and is plotted in Fig. 7. Thus, the slit-scanning has drastically altered the spectrum of the image at frequencies above $1/d$, which is not unexpected. From Fig. 7 we can obtain the characteristics of an electrical filter, which could in theory reshape the light-intensity curve to its original contours. In practice, it would be preferable to operate on images whose spatial frequencies are restricted to the region below the first zero of the slit-spectrum of Fig. 7. This is equivalent to the intuitive criterion that the slit be much narrower than the narrowest feature of the image to be scanned; however, should this criterion be exceeded somewhat, it is clearly possible to build an electrical filter to restore a part of the spectrum of Fig. 7.

Let us next consider the specific case of a slit whose width is equivalent to 0.18 sec of arc, when used with a telescope whose theoretical resolving power is 0.14 sec. Under very good seeing conditions, the image of a star can be approximated by a two-dimensional Gaussian of half-intensity width 0.26 sec (0.022 mm at the focal plane of the telescope).

* $\Pi(x) = 1$ for $|x| \leq 1/2$; otherwise, it is zero.

$$B_s(x,y) = K_1 e^{-\pi(x^2+y^2)/0.022}. \tag{3}$$

For two stars of equal magnitude and spaced a distance s apart on the x-axis, we have

$$B_D(x,y) = K_1 e^{-\pi y^2/0.022}\,[e^{-\pi(x-s/2)^2/0.022} + e^{-\pi(x+s/2)^2/0.022}] \tag{3a}$$

In the x- and y-directions, the projections of the image are

$$C_D(x) = 0.022K_1[e^{-\pi(x-s/2)^2/0.022} + e^{-\pi(x+s/2)^2/0.022)}], \tag{4a}$$

$$C_D(y) = 0.044K_1(e^{-\pi y^2/0.022}). \tag{4b}$$

The separation of the Gaussian components in the image plane is seen to be identical with the separation of the Gaussian components of the projection.

Figure 5(b) showed the result of slit-scanning a stellar brightness distribution of the form of Eqs. (4a) and (4b); the omission of Gaussian wings in the schematic drawing was inadvertent. Scans at an acute angle to the centerline of the double star will exhibit a pattern between these two extremes. One measure, therefore, of the accuracy of determining the position angle of a symmetrical double is the ratio of the half-intensity widths of the curves of Fig. 5(b); a maximum ratio less than about 1.2 would not be considered capable of furnishing a reliable indication of position angle.

Figure 8 is a graph of the ratio of the observed half-widths, $W_\parallel/W_\perp$, as a function of the spacing between the stars. There is only a small discrepancy between the effectiveness of the finite and infinitesimal slits, in spite of the fact that the finite slit width equals more than half the width of the stellar image. On the basis of Fig. 8, the limitation imposed by the resolving

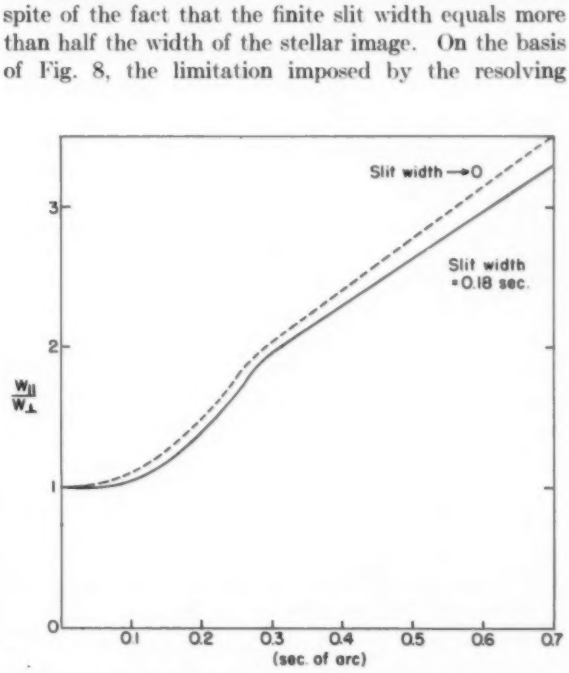

Fig. 8. Ratio $W_\parallel/W_\perp$ of the scan widths for a symmetrical double star, as a function of the separation of the binary, assuming a seeing disk diameter of 0.26".

power of the telescope and subsequent slit-scanning appears to be a minimum spacing of 0.16 sec of arc for a 91-cm telescope objective.

Noise Limitations on Observability of an Image

We would also like to gain some understanding of the role that various noise sources will play in limiting the detectability of faint features of composite images by means of the image analyzer. To do this we adopt the following parameters for the instrument as it is in use at Lick Observatory.

Diameter of seeing disk d = 0.26 sec, chosen as typical of the best ten percent of observing nights during the summer.

Diameter of objective = 36 in. (91 cm).

Loss in optics = 30%.

Effective width of bandpass = 1000 Å (5000–6000 Å).

Slit length l = 7.9 sec of arc.

Slit width w = 0.18 sec of arc.

Sweep frequency = 103 cps.

Time required for slit to cross aperture = 0.01 sec = t_s.

Cathode efficiency (λ5500) = 0.028 photoelectrons/photon.

The average number of signal photoelectrons emitted from the photocathode as the slit makes a single passage across a detail in the image will be given by $2wt_s/l \times N_{\text{feature}}$, the product of three quantities, $2dt_s/l$ being the time for the slit to move across the feature, N_{feature} being the number of photoelectrons per second that would result if the photocathode looked at the feature continuously, and w/d being the proportion of the seeing disk that can be transmitted by the slit. The combination $2wt_s/l$ is just the time for the slit to travel its own width (=1/2000 sec). For an isolated feature of eleventh visual magnitude, where $N_{\text{feature}} = 10^4$ with the efficiency parameters given,[9] a marginally detectable signal-to-noise ratio of 1.5 on a single sweep will be obtained. The "noise" in this case is the fluctuation in photon arrival time from the feature (dark current and sky background being negligible). When the feature of interest is superposed on the seeing disk and scattered light from a brighter image, then the photoelectron fluctuations are larger and S/N decreases.

We have considered the S/N ratio for a single sweep, because it is the 103 cps frequency of the slit sweeps that defines the maximum "stopping power" of the slit-scanning technique. The combination of information from successive sweeps increases the certainty of detection of a faint feature, but at a slower rate than the square root of the number of sweeps that would be the case in the absence of image motion. The reason that a slower rate applies is that some of the information is used in removing sweep-to-sweep changes in the image position.

In our visual data presentation scheme the required single-sweep S/N ratio seems to decrease approximately as $\sqrt[4]{n}$, while for a computer that was programmed to maximize the autocorrelation between sweeps the dependence might be the order of $\sqrt[4]{n}$. The practical result of employing the order of 10^4 sweeps seems to be to permit the use of S/N ratios of the order of 1/10 rather than unity, enabling us to look at features five magnitudes fainter than would be seen on a single sweep.

VI. Conclusions

The results obtained so far from the image analyzer suggest that a relatively simple instrument can be used to make electronic double star measurements that compare favorably with micrometer observations (Table I). Only pairs with small values of Δm are included because it is these that give separate, measurable streaks for both components that permit direct measurement of separation. In these cases the results are consistently satisfactory. While pairs with magnitude differences up to Δm = 3.5 have been "resolved" —that is to say, give one streak that is asymmetrical and clearly broader than the adjacent streak—the measurement of separation in these cases requires reconstructing the intensity distribution in the image. We are not satisfied that our calibration technique permits us to do this with sufficient accuracy as yet.

We can at this point only make measurements of pairs that are not difficult for a visual observer. There do exist possibilities for improvement that might permit the instrument to operate in the range of magnitude difference or separation difficult or impossible for the visual observer.

Table I[a]

Pair	Photovisual magnitude	Separation		Position Angle		Micrometer reference
		Image analyzer	Micrometer	Image analyzer	Micrometer	
ADS 1831	8.6–8.7	2.92″	2.92″	250° ± 10°	252–255°	Aitken[10]
α Psc	4.3–5.5	2.14″	2.06″	295° ± 5°	296°	Van den Bos[11]
μ Cyg	4.7–5.8	1.67″	1.77″	290° ± 5°	284.7°	Van den Bos[12]
ζ Aqu	4.4–4.6	2.05″	1.93″	258° ± 10°	259.4°	Van den Bos[12]

[a] These examples represent the last four double stars measured before submission of this paper, and for which resolution into separate streaks was unmistakable.

The data display that we have adopted is simple, and permits continuous monitoring of the image signal, both as it is affected by observing conditions and by experimental processing systems. In addition, the photographic record is immediately available for study. However, the data processing could well be improved at some sacrifice of simplicity. An electronic computer could process the original signal and subsequently give a more precise curve of image brightness distribution. It seems likely that, if a refined instrument were constructed, improvements could be effected in the following ways: by replacing the photographic disk with a ruled aluminum-on-glass disk, by mounting the instrument so that it could be rotated without rotating the telescope tailpiece, and by recording the signal and synchronizing pulses in a form suitable for computer programming with the oscilloscope display system being retained solely for monitoring purposes.

We are greatly indebted to A. E. Whitford for making the 36-in. (91-cm) telescope available to us for this project, and for providing us generously with assistance from the machine shop, photographic shop, and optical shop of the Lick Observatory. We are grateful to him for helpful technical discussions, especially concerning information-handling in stellar photometry. We should like in addition to acknowledge considerable support from Charles Seeger and the Stanford Radio Astronomy Institute. We should like to thank staff members at Lick Observatory and the Stanford Radio Astronomy Institute for their suggestions, and particularly wish to mention help in engineering design from Raymond Greeby, photographic advice and assistance given by Ronald Watson, and assistance in electronics from John Oliver. W. H. Van den Bos provided us with valuable guidance in discussions of double star measuring techniques and in suggesting systems of unusual interest, and S. Vasilevskis and David Cudaback also made comments that were of considerable value. And we must thank the National Science Foundation and Miller Institute for Basic Research in Science for Fellowship support.

Appendix

Preparation of the Slit Disk

The disk that scans the stellar image operates at the focal plane of the 91-cm refractor of the Lick Observatory. No magnification of the image is employed, so the scale at the focal plane of the instrument is 11.9 sec of arc per mm. In order to utilize the full resolving power of the 91-cm objective we should like to employ a slit with a width of only 12 μ.

Perhaps an ideal base material for such a disk would be glass coated with a thin layer of aluminum. Precision ruling techniques could then be employed to obtain uniform smoothly bounded lines of the desired dimensions. A disk of this sort would have cost several times the total amount available for the entire instrument. We therefore resorted to photographic procedures.

A 180 times scale negative drawing of a single zig-zag and associated synchronizing slit was prepared, and reduced 15 times photographically. The resulting positive transparency was projected upon an Eastman *649-0* high-resolution spectrographic plate mounted upon a precision rotary table to which had been fitted adequate light baffles. After each exposure the disk was rotated 1 degree with a probable error of placement of about 6 seconds of arc, until the circle was completed. The resulting master disk was then printed upon *649-0* plates and these were cut into doughnut shapes for use as slit disks.

The finest line width that could be obtained with satisfactory uniformity and freedom from veiling was 15 μ, and it was decided that this would give useful results despite some sacrifice of resolving power. The length of an individual zig or zag is 0.665 mm or 7.9 sec of arc, which places an upper limit of 5.6 sec on the diameter of image that can be analyzed. The separation between the repeating patterns on the oscilloscope represents 7.9 sec of arc along the image, which sets the scale for measurements of double star separation and image diameter.

References

1. H. N. Russell and C. E. Moore, *The Masses of the Stars* (University of Chicago Press, Chicago, Ill., 1940).
2. W. P. Bidelman, Publ. Astron. Soc. Pacific **70,** 413 (1958); J. Fernie, Astrophys. J. **130,** 611 (1959); C. B. Stephenson, Lick Observatory Bulletin No. 563 (University of California, 1959).
3. W. H. Van den Bos, *Vistas in Astronomy*, A. Beer, ed. (Pergamon Press, New York, 1956), Vol. 2, p. 1035.
4. P. van de Kamp, *Handbuch der Physik*, S. Flügge, ed. (Springer-Verlag, Berlin, 1958), Vol. 50, p. 187.
5. J. R. Platt, Astrophys. J. **125,** 601 (1957).
6. W. S. Finsen, Popular Astron. **59,** 399 (1951).
7. L. W. Fredrick, Astron. J. **65,** 345 (1960); G. Wlerick, J. Rösch, and M. F. Dupré, Internatl. Astronom. Union XI, Report of Comm. 9a (1961).
8. P. Lacroute and P. Bacchus, Compt. Rend. Acad. Sci. Paris **234,** 408 (1952).
9. A. E. Whitford, *Handbuch der Physik*, in press.
10. R. G. Aitken, *New General Catalogue of Double Stars* (Carnegie Inst. of Washington, Washington, D.C., 1932).
11. W. H. Van den Bos (private communication).
12. W. H. Van den Bos, Astron, J. **67,** 141 (1962).

The Optical Society of America

Officers of the Society

President	STANLEY S. BALLARD, Department of Physics, University of Florida, Gainesville, Fla.
President-Elect	RICHARD C. LORD, Spectroscopy Laboratory, MIT, Cambridge 39, Mass.
Past President	DAVID L. MACADAM, Research Laboratories, Eastman Kodak Company, Rochester 4, N.Y.
Executive Secretary	MARY E. WARGA, OSA, 1155 16th Street N.W., Washington 6, D.C.
Treasurer	ARCHIE I. MAHAN, Applied Physics Laboratory, 8621 Georgia Avenue, Silver Spring, Md.
Editor of the Journal of the Optical Society of America	DEANE B. JUDD, National Bureau of Standards, Washington 25, D.C.
Editor of Applied Optics	JOHN N. HOWARD, Geophysics Research Directorate, AFCRL, Bedford, Mass.

Directors-at-Large

* *Term expires December 31 of the indicated year.*

RUDOLF KINGSLAKE (63)* Eastman Kodak Company, Rochester 4, N.Y.
EARLE K. PLYLER (63)* Department of Chemistry, Florida State University, Tallahassee, Fla.
DAVID RICHARDSON (63)* Bausch & Lomb, Inc., Rochester 2, N.Y.
GEORG H. HASS (64)* ERDL, Fort Belvoir, Va.
R. CLARK JONES (64)* Polaroid Corp., Cambridge, Mass.
E. D. MCALISTER (64)* Scripps Institution of Oceanography, La Jolla, Calif.
W. LEWIS HYDE (65)* J. W. Fecker, Inc., 4709 Baum Boulevard, Pittsburgh, Pa.
JOHN A. SANDERSON (65)* Naval Research Laboratory, Washington 25, D.C.
GEORGE WALD (65)* Biological Laboratories, Harvard University, Cambridge 38, Mass.

Local Sections

Rochester
JOHN L. TUPPER, *President*
JOSEPH L. ROOD, *President-Elect*
SHELDON PHILLIPS, *Secretary*
Eastman Kodak Co.,
Rochester 4, N.Y.
MANUEL KINER, *Treasurer*

Detroit
RICHARD MAJKOWSKI, *President*
CARL LEISTNER, *President-Elect*
DANIEL L. HARMON, *Secretary*
16152 Parkside, Detroit 21, Mich.
SAMUEL COHEN, *Treasurer*

Niagara Frontier
E. SCHUSTIK, *President*
THOMAS FROST, *President-Elect*
CALVIN W. YOUNG, *Secretary*
Carborundum Metals Co.,
Box 32, Akron, N.Y.
RAY ANNINO, *Treasurer*

New England
DAVID S. GRAY, *President*
CHARLES KOESTER, *Vice-President*
GEOFFREY HARVEY, *Secretary*
Itek Corporation,
10 Maguire Rd.,
Lexington, Mass.
WILLIAM J. DAVIS, *Treasurer*

Texas
CHARLES S. WILLIAMS, *President*
P. O'B. MONTGOMERY, *Vice-President*
HARRY J. AUVERMANN, *Secretary-Treasurer*
LTV Research Center
P.O. Box 5003,
Dallas 22, Tex.

Delaware Valley
F. J. WARZAK, *President*
J. E. TUDOR, *Secretary*
General Electric Company MSVD
3316 Spring Garden Street
Philadelphia, Pa.
M. CONSHERRY, *Treasurer*

Chicago
FRED CLARKE, *President*
DONALD PONTARELLI, *Vice-President*
RICHARD STECK, *Secretary*
4556 North Oakview,
Chicago 31, Ill.
HOWARD PADGITT, *Treasurer*

Southwestern Connecticut
LEONARD EISNER, *President*
ROBERT C. GORE, *Vice-President*
MARTIN ROME, *Secretary*
Machlett Laboratories, Inc.
1063 Hope Street
Springdale, Connecticut
EDWARD SPEYER, *Treasurer*

Southern California
R. HENRY FRELS, *President*
ERNEST DAVIDSON, *Vice-President*
CLIFFORD O. THOMAS, *Secretary*
10 Miramonte Drive,
Fullerton, Calif.
W. S. GALLAWAY, *Treasurer*

Northern California
ANDREW L. JORGENSEN, *President*
CLYDE C. SHAW, *Vice President*
HARVEY MORTON, *Secretary-Treasurer*
Tinsley Laboratories,
2448 Sixth Street,
Berkeley, Calif.

National Capital
RICHARD TOUSEY, *President*
FREDERICK W. PAUL, *First Vice-President*
HARRY K. HAMMOND, III, *Secretary*
National Bureau of Standards
Washington 25, D.C.
RICHARD S. HUNTER, *Treasurer*

San Diego
JOHN E. TYLER, *President*
Other officers to be announced

The Optical Society of America was organized in 1916 "*to increase and diffuse the knowledge of optics in all its branches, pure and applied, to promote the mutual interests of investigators of optical problems, of designers, manufacturers and users of optical instruments and apparatus of all kinds and to encourage cooperation among them.*" The Society invites to membership all who are interested in any branch of optics, either in research, in instruction, in optical or illuminating engineering, in the manufacture and distribution of optical goods of all kinds, or in physiological and medical optics. Further information may be obtained from the Executive Secretary of the Society. **Annual Dues:** Regular members and Fellows, $17.00; Associate members, $13.00; Corporate members, $125.00. These dues include subscription to the Society's official journal, the *Journal of the Optical Society of America*, but not to its other publications.

Optical Problems of Television Recording of the Moon and Planets from Approaching Spacecraft

E. P. Martz, Jr.

The type and quality of scientific information desired from television cameras on spacecraft approaching the moon and nearby planets are reviewed. The desired accuracy of the optical data is compared with that presently secured from earth-based telescopes. The fundamental limitations due to the vibration and shock of the rocket launch and to the vacuum, radiation, and temperature environment of interplanetary space are considered. The influences of solar illumination, phase angle, and altitudes of recording on the resolution obtained are discussed. Optical television systems employed on certain lunar and planetary probes are described. Methods of improving optical television images received on earth by reduction of the background noise are noted.

Introduction

Modern rockets are launching astronomical instruments in spacecraft that will closely approach or impact the moon and the nearby planets. These instruments will be remote from the optically imperfect atmosphere of the earth and will record the lunar and planetary bodies from effective distances several orders of magnitude closer than can be viewed optically from earth-based observatories. It appears therefore that observational data received from these instruments concerning the surfaces of our neighbors in space should be marked by improvement over that collected at present by astronomers from the surface of the earth.

I. Basic Type and Quality of Information Desired

Surface Resolution

Primarily, more fundamental scientific information is desired about the topographic structure and constitution of the lunar and planetary surfaces than that presently available from terrestrial observations. For example, on the moon our best photographic telescopic resolution from earth is about 0.8 km (0.4 sec of arc) with visual observations under the very best conditions yielding up to perhaps 0.2 km resolution.[1] The best terrestrial observations of Mars resolve perhaps 30 km on the surface (0.1 sec of arc). In order properly to plan and engineer future instrumented and manned spacecraft for landings on the moon or planets we need to have advance knowledge of the surface structure to at least 1-m resolution or better. This implies an optical surface resolution requirement several hundred times better than presently available from terrestrial observations of the moon and some 30,000 times better than presently secured on Mars. Clearly, closely approaching spacecraft and/or long focal length, high resolution optical systems are mandatory.

Mapping—Cartography

In order to assure that our spacecraft to the moon, both instrumented and manned, land in an area where they can later be located precisely from earth, and to assist our first roving vehicles and man in the lunar surface exploration, it is necessary that we establish really accurate cartographic maps of the landing areas and determine the true elevations of the local topography prior to landing. The best present lunar cartography from earth-based photographs addended by visual observations yields the relative positions of points on the lunar surface to perhaps 1 km and altitudes to ± 100 m in localized areas or ± 1000 m in areas some hundreds of kilometers apart.[2] To ensure the safety of lunar explorers and proper evaluation of the telemetered information from landed instrumented spacecraft we must know the relative positions and altitudes of medium scale surface features to within at least a few meters, or several hundred times better than at present. Aerial topographic mapping from lunar orbiters and impacting spacecraft is the obvious answer, but this depends upon the proper solution of a great number of

The author is at the Jet Propulsion Laboratory, California Institute of Technology, Pasadena, California.

Received 3 August 1962.

This paper presents one phase of work performed by the Jet Propulsion Laboratory, California Institute of Technology sponsored by the National Aeronautics and Space Administration. It was presented to the International Commission for Optics in Munich, August 1962.

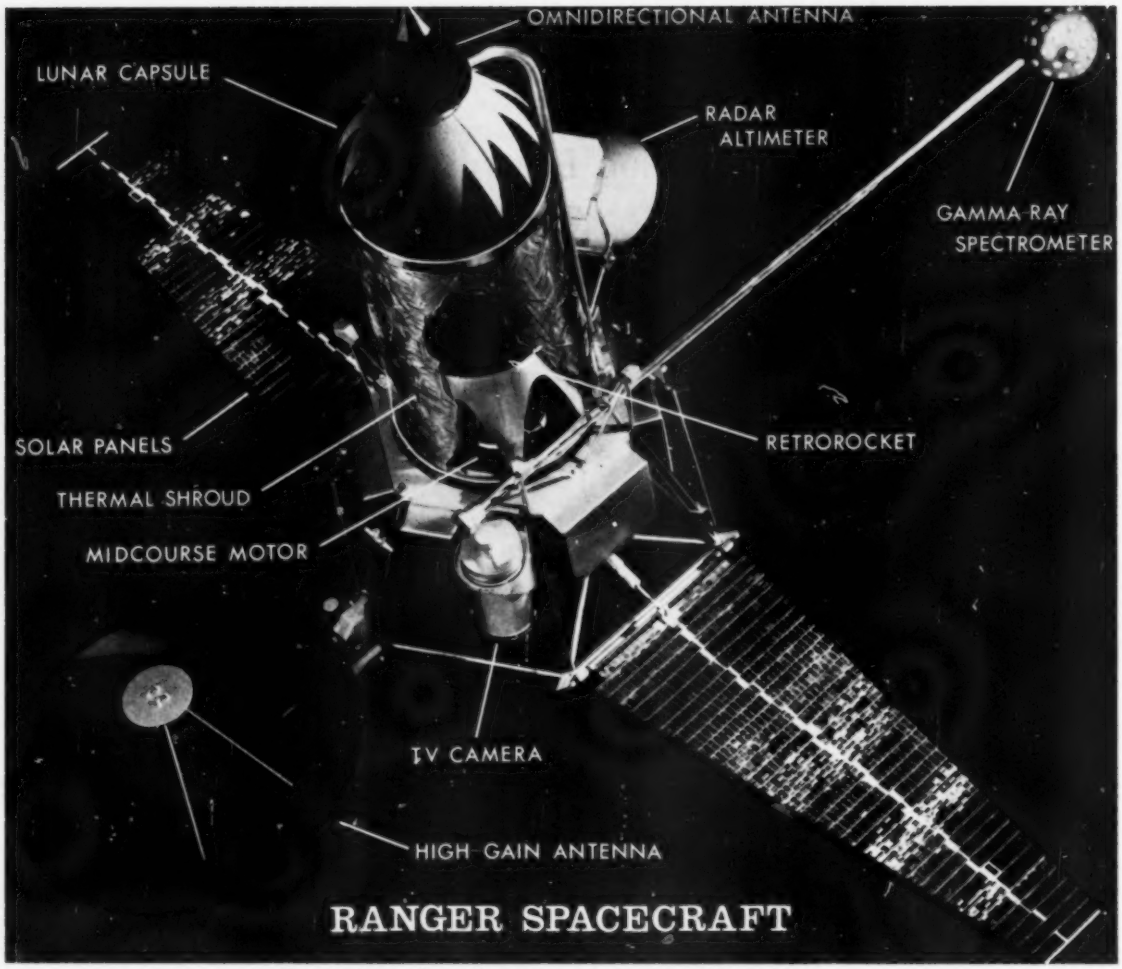

Fig. 1. Lunar impacting spacecraft showing vidicon telescope.

closely interrelated design and geophysical parameters. Existing aerial photogrammetry from altitudes of 6000 m over the earth is capable of position accuracies of 5 m, so the basic approach seems sound, provided some solution to the problem of providing accurate control points on the lunar surface is reached.

Geomorphology

Immediately after a landing has been made on the surface of the moon or a planet, we will be concerned with the local geology and geomorphology. If, as has been proposed, the lunar surface is covered by a thick layer of dust, we will obviously have to find some means of preventing the spacecraft from sinking deeply into it! Or, if the surface is very hard and barren, like solidified volanic lava, then a landing approach and first exploratory contacts must be planned keeping this in mind. Though a great deal has been hypothesized about the geology of the moon from terrestrial observations, the hypotheses often differ radically and we actually know very little for certain about the true geological conditions on the lunar surface. Efforts have been made to evaluate the probable geomorphology from photographs, and attempts to identify characteristic rock materials have been undertaken from heterochromatic, spectrographic, and goniophotometric data, but with indifferent success to date. Similarly, very little is firmly established about the geological condition of the surface of Mars, and practically nothing observationally about the surface of Venus for it is doubtful if we have ever seen it optically through the thick cloud layer.

II. Fundamental Spacecraft and Space Environment Limitations on Optical Recording Instruments of the Television Camera Type

Weight and Power

With the presently available rocket boosters for our lunar and planetary probes the amount of instrumental

payload possible is relatively small. However, with microminiaturization and weight-saving materials and proper design techniques the type and quality of information desired can still be achieved. For example, the total weight of one of our television telescopes for recording the moon or Mars with the quality of resolution needed is 9 kg, of which about 5 kg is the optical telescope and spacecraft mounting fixture. The television imaging tube and camera electronics weigh about 4 kg, exclusive of the data transmission equipment and antenna. The low input power required for operating the television camera and shutter is of the order of 5–10 W. This is furnished by a combination of solar panels and storage battery cells.

Vibration and Shock

The high thrust of present day rockets is obvious to anyone who has seen one launched. This mechanism initiates severe vibrations in the entire rocket structure including the scientific instrument and television telescope package. Though the time duration of these vibrations, and those of succeeding rocket stages, may be only several minutes, they can have adverse affects on improperly designed optical telescopes. As an example, the present telescopes are tested for sinusoidal sweeps from 40 to 1500 cps up to a 6g rms level, and white Gaussian noise up to a 15g rms level. Under these conditions, the optical elements may vibrate and rotationally oscillate in their mountings by as much as ±3 mm or more even in apparently rigid mechanical structures. If, as has been observed in some telescopes tested under these conditions, the optical elements do not return precisely to their original positions following vibration, a Cassegrainian telescope of 1 m focal length may end up as much as 1 cm out of focus. Unfortunately, we *cannot* at present refocus in space after launch! Tilting of the optical elements due to launch vibration conditions will clearly cause serious deterioration of the image even if the mounting and optical materials have themselves survived actual shattering and breakage.

In addition to the vibrations one must, in the optical-mechanical design, include the ability to withstand severe momentary shocks transmitted to our instruments by separation of the various rocket stages and by pyrotechnique device explosions which actuate certain operations of the spacecraft. These shocks may rise to a 200g level for a few milliseconds of time. If the optical elements are not properly mounted, the danger of breakage or misalignment is very serious.

Sterilization

An additional requirement of optical, mechanical, and electronic instrument components is that they must undergo prelaunch sterilization to kill all terrestrial bacteria and growths within or adhering to them. This requirement is imposed, of course, by our sincere desire to avoid contaminating the surfaces of the moon or the planets with terrestrial micro-organisms, in the event that our spacecraft impact or land on them. Such micro-organisms, by encapsulation, might well survive the trip through space. Their active presence would render useless our attempts to determine if the moon or planets harbor their own forms of life, and our study of the origins of life on the earth and in the universe. To ensure that we do not contaminate the other bodies of our solar system, before man arrives, the scientific instruments and all portions of the spacecraft are heated internally for 36 hr at +145°C. In addition, to kill bacteria that may have adhered to the outside surfaces from the air following the heating, the entire spacecraft package and scientific instruments are submitted to saturation in ethylene oxide gas for 24 hr. The heating noted does not damage most optical glasses or mechanical materials, but it does have a deteriorating effect on some of the instrument sensors employed, such as photographic emulsions and television vidicon tube target surfaces, which must be subsequently checked.

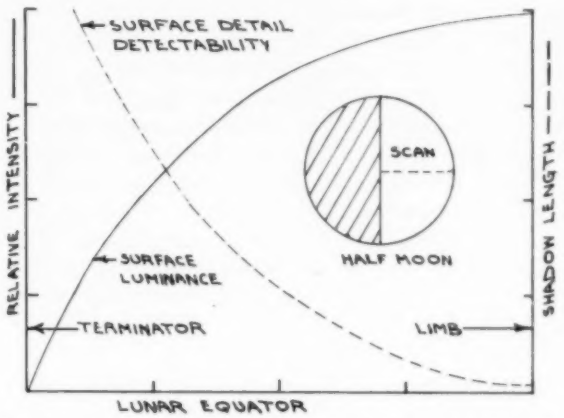

Fig. 2. Surface luminance and effect of shadow length on detectability of surface detail at half moon.

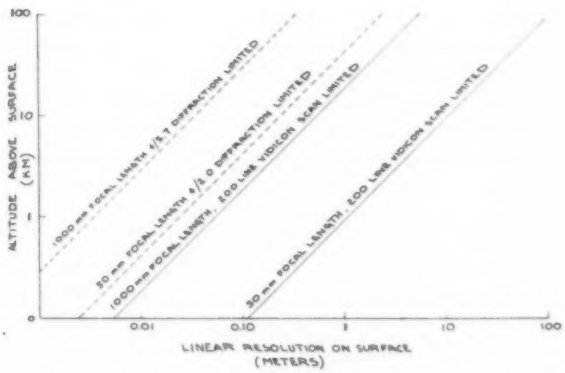

Fig. 3. Resolution on the surfaces of the moon and planets as a function of viewing altitude and objective focal length.

Experience has shown that ethylene oxide gas will *not* attack fused quartz and aluminized optical surfaces, or magnesium fluoride low reflection films on lenses. It does not leave any residue or blemishes on optical surfaces.

Temperature Environment

In space, between the earth and the moon or planets, the temperature of the spacecraft and scientific instruments will depend upon the rate of absorption of radiation from the sun on one side and its re-emission into deep space on either side. In spin stabilized spacecraft and some artificial earth satellites this ratio of absorption to emission is usually fairly well in balance, owing to the spin, and thus a fairly constant internal temperature is maintained. However, our present spacecraft to the moon and planets are axially stabilized by vernier jet thrusts to maintain earth contact with high gain antennas, the direction of pointing of optical guidance sensors, and the direction of pointing of the scientific instruments aboard. This, then, gives us a condition of solar heat on one side of the spacecraft and uncompensated deep-space cold on the opposite side throughout the flight. In addition, in any thermal analysis of the scientific instrument package the influence of internal heating due to the electronic operating equipment, and its rate of retention or dissipation of heat to space, must be evaluated. Spacecraft temperatures in the range from $-10°C$ to $+65°C$ have been anticipated for flights to the moon. In the case of one lunar probe a structural temperature of $+32°C$ was actually observed when the spacecraft was relatively close to the moon. However, the temperature *difference* between the primary and secondary mirrors of a small Cassegrainian telescope, open to space, was then computed to be 57°C! Clearly, careful attention must be paid in optical-mechanical design to employ materials and design techniques which will overcome such temperature extremes and maintain good optical focus and imagery. One approach, which is obvious, is to employ materials of low thermal coefficient of expansion, such as fused quartz, for *both* the optical and mechanical structural elements. Another approach is to fabricate both telescope mirrors and mounting structure out of a light material of high thermal conductivity, such as aluminum or beryllium, to reduce thermal gradients. An additional aid is to coat exterior instrument surfaces with a film of good emissivity characteristics, such as gold, to help maintain the internal temperature balance. The use of Invar alone is not sufficient to overcome the temperature differentials from end to end of the telescope. Techniques of compensation with materials of opposing thermal coefficients of expansion are also employed. In some cases sandwich construction and direct thermal control with shielding and internal heating are feasible approaches.

Particles and Gases in Space

The density of meteoritic dust in interplanetary space has been estimated[3] at 10^{-18} to 10^{-22} g/cm^3. Similarly, the abundance of individual particles of the order of 1–100 μ in diameter has been recorded[4] at 10^{-15} per cm^3. There appears to be a significant cloud of micrometeoritic particles surrounding the earth up to at least 160,000 km, with gradual thinning out to 10^6 km.[5] Spacecraft, and their optical systems, must pass through this on their way to the moon and the planets. Admittedly, these space densities appear very low and would normally not be alarming. But, when we consider that spacecraft present a cross-sectional area of some square meters and that they move through the interplanetary dust cloud at very high velocities, we cannot ignore the possibility of eventual impacts and possible deterioration of optical and other exposed surfaces. The obvious solution, where spacecraft telescopes are concerned, is to install a cover over the optical system, to be removed automatically just before recording on approach to the moon or planets. This is being done where the optical surfaces are not otherwise protected. The meteorite "bumper" cover over the telescope aperture performs an additional useful function in helping to maintain a constant moderate temperature within the telescope structure up until some time before its actual recording operation. It also prevents accidental line-of-sight contact with the sun from flooding and saturating the vidicon tube television sensor.

An additional point which must be considered is that high performance refracting or catadioptric systems must be designed for operation within the near vacuum of interplanetary space on the object side, and on the image side also, if the optical system is not internally pressurized.

High-Energy Radiation in Space

Less than half of the solar radiation between 0 and 50,000 Å impinging on our spacecraft is in the visible region. The solar radiation includes soft x rays and high-velocity protons and electrons yielding a space density of approximately 600 electrons/cm^3.[6] In addition, we know that cosmic rays from whatever source, Van Allen radiation, and other high-energy particles will be acting on spacecraft and their attached optical instruments throughout the flight to the moon and planets. In the flight to the moon this is for only $2^1/_2$ days, but to Mars the duration of exposure may be as much as eight months or more. Primarily, there arises the danger of exposure and fogging of photographic emulsions, and perhaps electronic television vidicon and image orthicon type sensitive surfaces if they are not shielded from this radiation. Available information indicates that photographic emulsions are more sensitive

than photoconductors to such radiation damage. In addition, it is known that such radiation can cause fluorescence, phosphorescence, and fogging of optical glass lenses and windows over long flight times. It is apparent that the radiation environment cannot be overlooked if we are to expect the optical systems and sensors to perform properly when they reach their destination. Lead shielding of the sensors is a clear-cut partial answer to the problem but introduces the serious difficulty of the added weight of the lead to an already limited permissible payload. Heavily leaded glass windows will reduce the impact of high-energy radiation on the interior optical and sensor surfaces but will also seriously reduce the transmission and amount of light available for exposure of the lunar and planetary surfaces. In addition it will modify, perhaps seriously, the relative color balance of the optical-sensor system and will again increase the weight according to the degree of protection achieved.

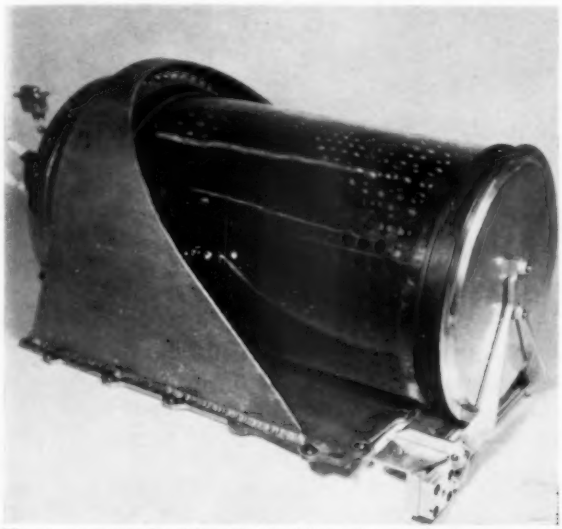

Fig. 4. 1-meter focal length television telescope for lunar spacecraft showing aperture cover.

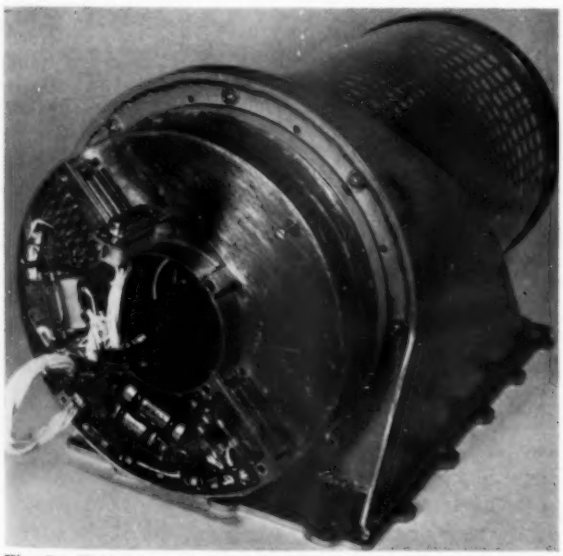

Fig. 5. Television telescope for lunar spacecraft showing electronics.

Illumination of the Moon and Planets

The relative luminance of sunlit areas on the moon may vary from perhaps 100–2300 millilamberts depending upon the albedo of the area and the lunar phase illumination.[7] On Mars the surface luminance may be approximately 1000 mL at full phase.[7] These values can be compared with luminances of daylit outdoor scenes on earth, judged suitable for conventional photography, which range from perhaps 100 to 3000 mL.[8] It appears that there would be sufficient light from the moon and Mars for photography or television recording with more or less conventional optical systems. The situation is made complex by consideration of the relative surface illumination at different phase angles and angles of approach and by the variation of resolution achieved with variation of the relative contrasts on the planetary or lunar surface. Further, the exposure times employed must be consistent with the surface illumination at the particular time of approach, with the sensitivity of the sensor, and with the blurring or "smear" of the image due to spacecraft motion.

We are all familiar with the marked difference in telescopic appearance of the half moon compared to the full moon owing to the improved contrast of extensive mountain ranges and craters. These are made visible by their long shadows at increasing phase angles. Because of the nature of the porous lunar surface these areas show greater contrast with lower sun angle and longer shadows, thereby improving the resolution of fine surface details. However, owing to this same porous surface the light from the moon drops off exponentially with increasing phase from full moon, and at half moon the integrated light is only one-ninth that at full, though the apparent illuminated area has only been cut in half.[9] Thus, just when the shadows become longer and surface detail more detectable, the luminance falls rapidly and we are forced to record at lower sensitivity levels of our sensors. Figure 2 illustrates this situation. This, then, forces our image down into the background noise level of the sensor system and as a result the resolution drops. The alternative of using a longer exposure time to record the fainter surface is ruled out because of the image blur due to spacecraft motion. Also, long focal length optical systems are desired for finest surface detail at closest approach, just when the image smear would be worst. Similarly, use of a high speed, low f/number optical system to record the fainter surface is limited be-

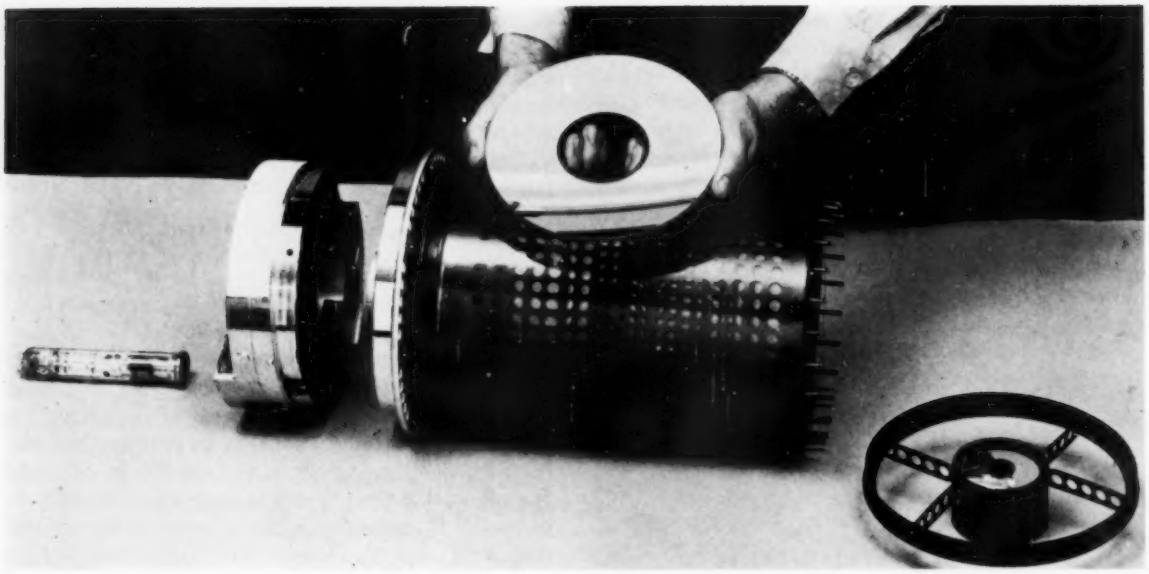

Fig. 6. Television telescope for lunar spacecraft disassembled.

cause of the aberrations introduced or of the complexity of a fully corrected system, and because of the added weight of such systems of the size of an astronomical telescope.

Field of View and Resolution

The surface field of view presented to television type telescopes recording the moon and planets from space is dependent upon the objective system focal length, the scanned area of the television sensor, and the distance from the surface being recorded. Our basic limitation is presently in the diameter of the sensitive photocathode surface and the scan frequency from the viewpoint of communication limitations. So called "1-in." vidicon television tubes presently in use have a usable scan aperture of only 1 cm square. With a 50 mm focal length lens this provides a field of view of 12°.6 or 22 km on the surface of the moon from 100 km altitude. However, the presently usable television scan rate on this vidicon tube, owing to bandwidth limitations on the transmittal of information to earth from space, may range from 200 to 800 television lines under different flight circumstances. This, then, would yield us a resolution of 112 to 28 m on the lunar surface, which is considerably less than our immediate goal of 1 m or better. A 1-m focal length telescope objective at 100 km altitude would give us television resolutions approaching those desired but at the expense of reducing the field of view on the surface to about 1 km. With such narrow fields of view we immediately run into the problem of identifying the area that we have photographed inasmuch as our present telescope resolution from earth is of the order of only 1 km on the moon. Admittedly, we could include a second, low resolution, very wide angle television camera to give us our pointing information, but at the expense of added weight and operational complexity leading to possible failure. If the spacecraft attitude can be maintained constant during descent to the surface, then successive photographs, starting with a wide field of view which can be identified, will nest, and knowledge of the location of the final high resolution narrow field images will be possible. Figure 2 demonstrates the optical and the vidicon scan limited surface resolution as a function of altitude and focal length.

III. Some Approaches Employed for Recording the Surface of the Moon and Planets

Impacting Lunar Probe Telescope

It can be demonstrated that with a 1-m equivalent focal length telescope employing a 200 TV line scan at 4000 km from the moon, the resolution on the lunar surface will just about equal the best secured from earth-based telescopes. There is, therefore, little purpose in attempting recordings at greater distances from the known side of the moon. One of our impacting lunar probe television telescopes will transmit from 4000 km down to a final line scan transmittal at 24 km altitude where earth contact with the high gain transmitting antenna will probably be lost because of other operations of the spacecraft. The recorded field of view of the lunar surface will vary from an area 45 km square at 4000 km to an area 0.7 km square at the last fully scanned picture exposed at 59 km altitude. The surface resolution secured will range from 0.2 km to 3 m. The

total recording time will be approximately 30 min during which about 100 TV photographs will be transmitted. These will be roughly nested into each other during spacecraft descent so that the location of the final narrow angle photographs on the lunar surface can be identified.

Optical System

The optical telescope which forms the image of the moon on the vidicon photoconductor surface is an 18-cm aperture Cassegrainian reflecting system of 1-m equivalent focal length operating at $T/6.3$. The optical resolution is 5 sec of arc on axis and 14 sec of arc 0°.3 off-axis at the edge of the square vidicon aperture. This corresponds to a linear resolution of 40 optical line pairs/mm on axis and 14 line pairs/mm at 0°.3, which is better than that afforded by the 200 line scan vidicon camera system (9 line pairs/mm). With resolution limited by the vidicon scan rate there was no reason, in this particular system, to employ other than conventional paraboloidal primary and hyperboloidal secondary Cassegrain telescope mirrors. With higher vidicon scan rates and better resolution it would be necessary to use a Ritchey-Crétien or some other type of aplanatic mirror system, or catadioptric corrector plate systems to maintain the required resolution over the field of view. This is being done with a similar telescope for recording Mars from a fly-by probe with a 400 line vidicon scan. Multiple element photographic objectives are attractive for their wide fields of view but they introduce excessive weight in such long focal lengths. Moreover, a proper edge mounting of such large lens elements would have difficulty in surviving the vibration and shock of launch.

Mechanical Design

In this particular lunar probe television telescope the significant deviations from usual astronomical tele-

Fig. 7. Television telescope showing offset secondary mount spider.

scope design consisted in the use of fused quartz for the telescope mirrors, Invar for all temperature sensitive metallic parts, and, of even greater importance, the use of a 20-cm diameter fused quartz tube as the basic rigid structure separating the primary and secondary mirrors. The fused quartz tube is 2 mm thick, 30 cm long, and is kept loaded under longitudinal pressure by 24 springs. These features permit both survival through the launch vibration and maintenance of optical-mechanical alignment and focus in the temperature extremes of over 50°C experienced by the instrument in space.

Normal reflecting telescope design employs three or four radially symmetrical spider supports for holding the secondary mirror mount in front of the primary mirror. In the case of our lunar probe telescope the four spider arm supports are offset in two parallel pairs forming a double couple to provide greater torsional rigidity. The radial symmetry is sacrificed for this rigidity. Two differently designed Cassegrain telescopes with conventional radial symmetry of the secondary mirror support structure did *not* survive the flight approval vibration test owing to their inability to hold the secondary mirror rigidly in place. The offset spider support does introduce broadening and multiplication of the diffraction line patterns across the field of the telescope. However, because we are not looking for close double stars but rather at extended areas on the bright moon the effect on the optical imagery is negligible.

Camera Shutter

A mechanical rotating sector shutter operating on inertial principles with solenoid actuation and spring tension release has been located near the focal plane at the vidicon tube face. The 45° pie-cut shaped aperture is similar to that in conventional motion picture cameras. This provides an exposure time of 20 msec on the photoconductor surface with a uniformly illuminated field. This exposure time is adequate with the particular ruggedized vidicon tube employed to record an exposure level range of 0.1 to 1.0 m candle seconds on the moon with the $T/6.3$ telescope. This is the illumination level expected near half moon in the impact area. The shutter will prevent blurring of the optical image of the lunar surface caused by vibration and motion of the spacecraft during the exposure time and will also provide a closing of the optical system during the 13 sec scan and erase operation of the vidicon electronic system.

Short-Focal-Length Lunar Probe Camera

Later lunar probe spacecraft will continue television photography of the lunar surface down to impact. They will employ conventional high quality photographic lenses of 75-mm focal length operating at $f/2$. These particular lenses have two plastic cemented elements. However, they have passed all the take-off vibration and shock tests and the temperature and vacuum space environment testing without damage. Several sets of these cameras will operate in tandem on the same spacecraft. One set will employ a full photoconductor area scan of the "1-in." vidicon tube at 800 TV lines equivalent with a field of view of 8°.4. The other set will employ a scan of only half the photoconductor diameter at 200 TV lines for the purpose of transmitting back some close-up high resolution information in the very limited time just before destructive impact. The full field scan cameras will provide a photograph 250 km square on the moon from an altitude of 1300 km, 10 min before impact, when recording will begin. One image every 2.5 sec will be secured and resolution of 350 m on the lunar surface is anticipated at the start. The partial scan cameras will continue recording on down to near impact a few hundred meters above the lunar surface. The field of view will then be about 20 m square with a surface resolution of a fraction of a meter. Five images per second will be recorded and transmitted at the final downward velocity of 2700 m/sec. The resolution of the vidicon TV scan will be approximately 35 line pairs/mm whereas the optical resolution of the photographic lens employed will be nearly 100 line pairs/mm, thus affording a good optical advantage.

It should be noted that the equivalent resolution of any optical sensor system will vary inversely as the summation of a root of all the contributing elements. That is[10]:

$$\frac{1}{R_{eq}^n} = \frac{1}{R_1^n} + \frac{1}{R_2^n} + \frac{1}{R_3^n} + \dots .$$

Thus, the element of lowest resolution does not automatically set a lower limit to the final resolution attained. Any improvement in each element of the system will improve the final result. Therefore, our optical imaging systems should, if possible, be better than the television sensor. Some considerations indicate that a factor of at least three times is desirable.

Mars Probe Telescope

Present planning for future probes to Mars visualizes the inclusion of a long focal length telescope for recording details of 1-km resolution on the surface from fly-by distances of the order of 10,000 km or greater. A 1-m focal length Cassegrain telescope operating at $T/5$ would accomplish this with the present vidicon television tubes. The field of view would be approximately 1°, only 1/40th the apparent diameter of the planet from such a distance. A second short-focal-length wide-angle camera will, in addition, indicate the direction of pointing and take heterochromatic color photographs of Mars from blue to red to yield valuable low-resolution

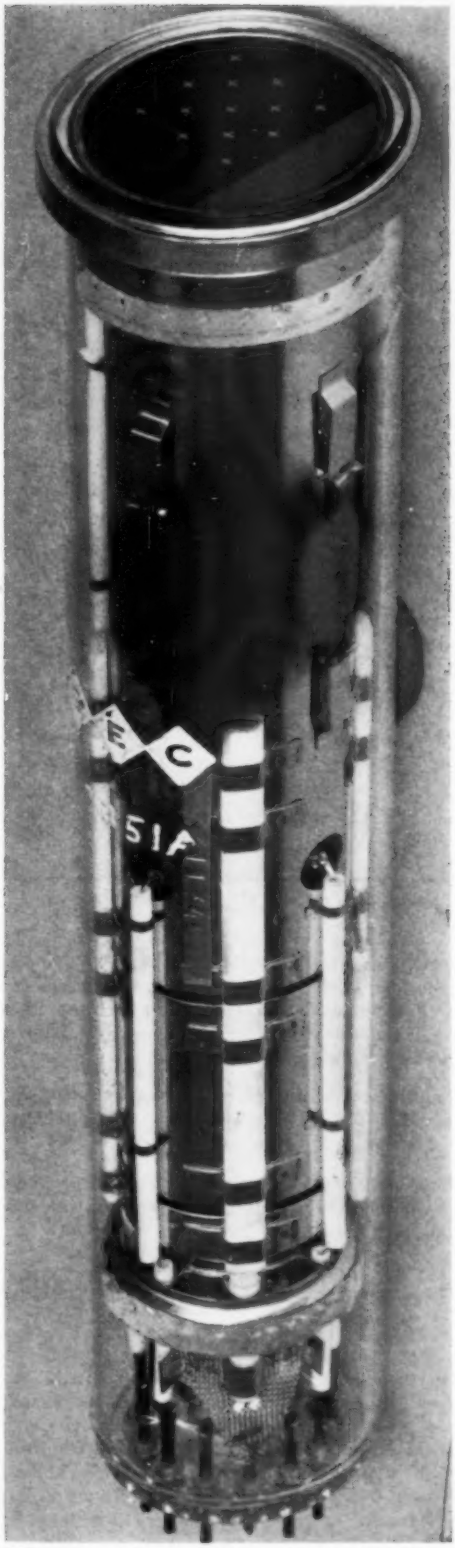

Fig. 8. Television telescope vidicon tube showing grid reference marks.

information on the blue atmospheric haze and on the color of the surface markings.

Background Noise and Methods of Reduction

It is clear, from space to earth recordings received to date, that the basic limitation on resolution of fine details on the moon and planets in pictures transmitted from our spacecraft will be the presence of irregular and unpredictable background electronic noise arising in the sensing instrument, in transmission to earth through the ionosphere, and in the terrestrial receiving equipment. When the illumination level of the area being recorded is too low or when the speed of the optical system and sensor are insufficient, we are forced to record at a level which forces us into this noise background. Extensive testing on present vidicon television cameras being employed for lunar and planetary photography from space has indicated that anything under 15 dB signal-to-noise ratio will be of little value as far as identification of fine surface detail is concerned (i.e., peak-to-peak signal/rms noise).

Even in the presence of excessive background noise several possibilities are open for improving the final optical image quality. These all involve suitable measurement and evaluation of the information received in terms of specific image points as they relate to adjacent image points in space and to the same points in successive pictures in time. Proper application of Fourier transform analysis permits us to separate the background noise from the desired signal and to clear up the image by elimination or reduction of the noise. Application of recent pattern recognition and extraction research approaches should make possible the enhancement of image edge contrast and further improvement of the final optical image being examined and interpreted. There are at least four specific types of instrumental approach which can be employed to improve the image in this way:

(1) Conventional multiple photographic printing with masking of several overlapping images of the same area and at the same scale, where these are available.[11]

(2) Electronic filtering of the vidicon television camera system to attenuate and mask out the background noise.

(3) Digital computer reading and comparison of the information from previous calibration tape recordings of the vidicon scans to print out images minus the noise and with confirmed configurations.

(4) Optical spatial filtering in the vidicon telescope and at the terrestrial receiving station to mask out the noise background and improve the image quality.[12] The removal of a fixed and repetitive moiré pattern, such as the television line scan raster, by such filtering is easily done. The removal of noise varying in both time and location is another matter!

None of these approaches is simple or theoretically and experimentally completely straightforward. However, each of these will help us achieve better qualitative and quantitative information about the surfaces of the moon and the planets, toward which we are striving today.

References

1. G. P. Kuiper, *Photographic Lunar Atlas* (University of Chicago Press, Chicago, 1960), Addended booklet, p. 3; R. J. Hackman and R. W. Carder, Photogrammetric Eng. **27**, 377, 389 (1961).
2. R. W. Carder, Photogrammetric Eng. **27**, 389 (1961).
3. M. Dubin, *Space Research* (COSPAR) (Nice, Italy, January 11–16, 1960), p. 1057; D. B. Beard, Nature **191**, 33 (1961).
4. L. D. Jaffee and J. B. Rittenhouse, J. Am. Rocket Soc. **32**, 336 (1962).
5. F. L. Whipple, Nature **189**, 127 (1961).
6. A. Behr and H. Siedentopf, Z. Astrophys. **32**, 19 (1953).
7. G. de Vaucouleurs, "Photometric Parameters of Mars," Harvard College Observatory Final Report under NASA-JPL Contract **950014**, (30 June 1961). (Column M1 in Table 3 must be multiplied by 10 to give mL.) (This report is an ASTIA document.)
8. L. A. Jones and H. R. Condit, J. Opt. Soc. Am. **39**, 126 (1949).
9. H. N. Russell, R. S. Dugan, and J. Q. Stewart, *Astronomy* (Ginn and Co., Boston, 1926), Vol. I, p. 173.
10. A. H. Katz, J. Opt. Soc. Am. **38**, 605 (1948); R. Kingslake, *Lenses in Photography* (Case-Hoyt Corp. for Garden City Books, Garden City, N.Y., 1951), p. 72.
11. G. W. W. Stevens, Phot. J. **87B**, 74 (1947).
12. E. L. O'Neill, IRE Trans. on Information Theory **IT 2-3**, 56 (1956); G. F. Aroyan, Proc. Inst. Radio Engrs. **47**, 1561 (1959).

Information for Contributors

Scope: Papers are welcomed in the broad areas of applied optics, in disciplines related to optics and employing optical techniques. Papers should be sent to *The Editor, APPLIED OPTICS, 1155 Sixteenth St., N.W., Washington 6, D.C.* Manuscripts may be submitted in English, French, German, or Russian, and the presentation should be as succinct as comprehension will permit. In general, the metric system of units is preferred. One original and one carbon copy of the manuscript, with two sets of all illustrations, must be sent in. Manuscripts should be typed double or triple spaced on one side of 22 × 28 cm (8½ × 11 in.) paper, leaving a 3.8 cm (1½ in.) margin all round. Papers on the more fundamental aspects of experimental and theoretical optics should be sent to *The Editor, JOURNAL OF THE OPTICAL SOCIETY OF AMERICA, National Bureau of Standards, Washington 25, D.C.*

An **abstract,** adequate as an index and a summary, of not more than 100 words should appear at the beginning of the paper after the *title, author's name, affiliation, and address.* In the case of papers in a non-English language, they must be accompanied by an abstract in English as well as an abstract in the language of the paper. It should be borne in mind that this abstract may be used in toto by the abstracting journals, therefore it should be self-contained.

Figures suitable for printer's use should be sent. Bear in mind that illustrations will normally be reduced to column width (8.4 cm—3⅜ in.—20 picas). *Halftones:* two sets of glossy prints are needed, which should be mailed flat, with any proportion or framing indicated on a working copy. *Line drawings* should be suitable for reproduction and be not larger than 22 × 28 cm (8½ × 11 in.). *Captions* should be listed on a separate sheet in addition to each caption appearing on each illustration.

Tables should be typed on separate sheets and the data therein be intelligible, by title, without reference to the text. Tables should include a minimum of vertical ruling.

References must be typed on a separate sheet, be numbered consecutively in the order of their appearance in the text, and follow this form:

1. F. C. Brown, Phys. Rev. **12**, 345 (1821).
2. J. Culpeper, *Space Optics* (Georgetown Institute of Technology Press, Washington, D.C., 1861), pp. 12, 345.

A list of abbreviations for the names of journals is published in the American Institute of Physics *Style Manual.* To make for uniformity of presentation generally, the *Style Manual,* second edition, should be used. In general, *APPLIED OPTICS* differs from the *Style Manual* only inasmuch as footnotes appear at the bottom of the page of text, while references are listed numerically at the end of the paper.

Letters to the Editor should follow the above suggestions, but no abstract is required.

Temperature Effects in Photomultipliers and Astronomical Photometry

Andrew T. Young

Temperature coefficients are reported for photomultiplier tube types used in astronomy. For 1% stability of gain and color response, temperature regulation of 1°C or better is generally required. This is nearly an order of magnitude better than what is usually achieved at the telescope, but careful use of a well-designed cold box should make 1°C temperature stability possible. For maximum stability and reproducibility, ordinary blue-sensitive tubes should be avoided at wavelengths longer than 5000 Å, and trialkali cathodes should not be used beyond 6500 Å.

Introduction

Users of photomultipliers are universally familiar with the fact that cooling is very effective in reducing a tube's thermionic dark current and the accompanying undesirable shot noise, but some of them are not aware that the sensitivity of the photomultiplier has a large, wavelength-dependent temperature coefficient. However, one can predict from published data in the physics literature[1] that temperature variations of one to four degrees Celsius can cause systematic errors exceeding one percent ($\approx$ 0.01 mag.) in most astronomical photometry. While photoelectric observers commonly claim an accuracy of 0.01 mag. or better, they rarely mention the existence of temperature effects, and no numerical values for temperature coefficients have ever been published in the astronomical literature. Furthermore, there is a widespread belief among observers that the use of dry ice as a refrigerant is so effective in stabilizing the behavior of the tube that temperature effects can be ignored in a refrigerated tube.

The purpose of this paper is to estimate the degree of temperature regulation actually achieved at the telescope, to present new data on tube types used in astronomy, and thus to assess the importance of temperature effects in astronomical photoelectric photometry.

Temperatures of Refrigerated Tubes

Average Cathode Temperatures

Kron[2] has published measurements of the dark currents of several photomultipliers with Ag-O-Cs (S-1) cathodes. Because of the low work function, the dark currents of these cathodes are extremely temperature-dependent; therefore the dark current measurements can be inverted to estimate temperatures.

Kron's tubes were "encased in well-built, hermetically sealed containers, filled with dry air, and mounted inside a thermally insulating box." Two of the tubes were cooled with "a stiff slurry of pulverized dry ice in isopropyl alcohol" as well as with plain dry ice. When dry ice alone was used as a refrigerant, the dark currents fell below the value at room temperature by a factor of about 10^7. When the alcohol was also used, the dark currents were about six times lower. The logarithm of the dark current is roughly a linear function of the temperature, although the slope is greater at the higher temperatures. The additional cooling produced by adding the alcohol to the ice must therefore be at least

$$\frac{(\log 6)}{(\log 10^7)} \times (\text{room temperature} - \text{dry ice temperature}),$$

or 11°C. Because of the curvature of the log I vs T relation, 15 or 20 degrees would be a better estimate.

The writer has repeated this experiment with two Farnsworth FW-118 tubes (which also have S-1 cathodes) mounted in an astronomical photometer, very similar to those used by H. L. Johnson.[3] The cold box of this photometer will be considered typical of cold boxes in general astronomical use, and will be referred to as a "Johnson-type cold box" in the remainder of this article, although similar cold boxes have been used by others. Because alcohols become very syrupy at low temperatures, ethyl acetate was used as the heat-transfer liquid. This ester remains quite fluid at −78°C. In these tubes, which seem

The author is at Harvard College Observatory, Cambridge, Mass.

Received 10 August 1962.

This work was supported by a grant from the National Aeronautics and Space Administration.

to be slightly less temperature-sensitive, the dark current fell by about 10^5 on cooling with dry ice alone, and by an additional factor of 5 when the ethyl acetate was added; again a decrease of about 15°C is indicated.

These data show clearly that the use of dry ice alone in the usual cold box fails to cool the cathode to dry-ice temperature. They also raise the question of how much above −78°C is the temperature of the cathode, even when a heat-transfer liquid is used. This question can be roughly answered by measuring the change in the *rate* of cooling (based on the slope of the dark current vs time relation) in the two cases. The increase in cooling rate when the liquid is used is about 50%. Let us assume that the differences between dry ice and the final cathode temperatures T_d and T_w in the dry and wet cases, respectively, are inversely proportional to the rates of cooling. Then

$$\frac{T_d - T_{CO_2}}{T_w - T_{CO_2}} = 1.5.$$

Since we have already determined that $T_d - T_w = 15°$, we have

$$T_d - T_{CO_2} = 45°C \text{ and } T_w - T_{CO_2} = 30°C.$$

This means that the average cold box cools the photomultiplier cathode only about two-thirds of the way from ambient temperature toward the −78°C of the dry ice. This conclusion is supported by the experiments of Hogg,[4] who has measured the cathode temperature directly with a thermocouple.

Why is the photomultiplier cathode some 40°C hotter than the metal walls of the cold box a few millimeters away? To answer this question, one must look at the heat budget and thermal conductivities of the tube and its container. The details of the calculation depend on the particular tube type. For an end-on EMI tube, the thermal conductivity to the box walls is limited primarily by heat conduction across the end window from the center to the edge. This window is made of fused quartz 3 mm thick and 25 mm in radius, which corresponds to a heat flow of about 6 mW/°C of temperature difference between center and edge. Heat transfer across a 1-mm air space between the sides of the tube and the walls of the box amounts to about 28 mW °C^{-1}/cm of length along the tube, and conduction along the 1-mm-thick glass side walls is about 13 mW°C^{-1}/cm temperature gradient along the length of the tube. The resultant heat flow from cathode to box walls is a few milliwatts per degree Celsius of temperature difference between cathode and box. Even for the RCA 1P21 this is the order of magnitude of the heat conductivity, because the metallic connection between the cathode and the base has a very small cross section.

The amount of heat conducted in from the base should be small if the voltage-divider chain is kept away from the tube socket. Since the thermal conductivity between the dynodes and the cold box is of the order of 1 mW°C^{-1} per stage (the nickel alloy wires between dynodes and base are about 1 mm in diam and 5 cm long) and the maximum power dissipated in the dynodes is about 1 mW/stage, the internal tube currents are a negligible source of heating, and the dynodes should be nearly at dry-ice temperature.

This leaves only the entrance window of the cold box as a source of heat. This window is generally at or near room temperature; it is often heated slightly to prevent dewing. At 300°K a blackbody radiates about 45 mW of thermal energy per square centimeter; a typical window has an area of about 3 cm^2. Evidently the thermal radiation alone is enough to account for most of the cathode heating, even if convection currents between the tube and the window are neglected.

If the above explanation of the cathode heating is correct, then the cathode should be brought much closer to −78°C by placing a transparent radiation shield in front of the photomultiplier. Experiments show that placing even a single layer of Saran Wrap inside the cold chamber ahead of the tube produces a significant improvement in cathode cooling. However, an ideal heat shield should not only absorb the incident thermal radiation, but should be thick enough to conduct it to the dry ice instead of reradiating it to the cathode. A 1-cm slab of fused quartz serves this purpose very well, if it is no larger in diameter than necessary and is mounted in a metal ring in good thermal contact with the walls of the cold box. Tests made with such an arrangement indicate that the cathode temperature will fall to within 5°C of the refrigerant temperature after several hours of cooling.

The heat shield need not be a simple window, but can be an active part of the optical system. In some cases, it may be convenient to use a field lens as the heat shield inside the cold box. However, one should remember that a thick lens will conduct more of the heat flux to the box walls than a thin one, and that fused quartz is a better heat conductor than glass.

Temperature Variations at the Telescope

At first sight, it might appear that the temperature regulation achieved in the ordinary cold box would be adequate; if the cathode is cooled two-thirds of the way to dry ice temperature, then two-thirds of the ambient temperature variation should be eliminated. However, since the cathode is heated by radiation and cooled by conduction, the problem is not so simple. If the cathode is 40°C warmer than the dry ice, a 1°C change in cathode temperature requires a 2.5% change in heating; but a 1° change in window temperature at 300°K causes a 1.3% change in heat radiated to the cathode. Thus the cathode suffers about 53% of the

change in ambient temperature. This figure is directly proportional to the temperature difference between the cathode and the refrigerant; in a properly designed cold box with an internal cold window, this difference should be 5°C or less and the cathode should show less than 7% of the fluctuation in window temperature.

In addition to this variation, however, one must add the variation in cathode temperature which results from allowing insufficient time to establish thermal equilibrium in the box between the initial addition of dry ice and the beginning of observations. The author's experience with Johnson-type cold boxes shows that this time interval should be at least two to three hours. Also, for a 1P21, Engstrom[5] says that "When accurate temperature of the cathode has to be known, it is necessary to hold the tube at a constant temperature for several hours to allow the parts inside the tube itself to reach equilibrium." However, in one of the most precise and careful photometric investigations ever carried out, Serkowski[6] reports that the dry ice was put on the 1P21 only $1^1/_2$ hr before beginning observations. From this cause alone one can expect the cathode temperature to have been at least 5°C warmer at the beginning than at the end of the night.

Finally, the temperature of the cathode can depend on the orientation of the photometer, both because of the presence of convection currents in the air around the tube, and because of the shifting of the dry ice in the box. The amount of this effect can be large, at least 10°C; however, a more typical value at the telescope might be 5°C because the telescope is generally moved at frequent intervals from one position to another. This is a particularly serious problem, because it can produce systematic errors in the observations that depend directly on zenith distance and/or declination. These errors therefore will appear undiminished in the final results, while other temperature effects may be partly eliminated in the correction for extinction and reduction to the standard system. Fortunately, the use of a cold inner window should practically eliminate any convection currents, and the use of ethyl acetate on the dry ice drastically reduces the effect of the shifting of the dry-ice load in different positions.

On the whole, then, one can expect cathode temperature variations of 5–10°C and somewhat smaller dynode temperature variations during a few hours when using conventional equipment and observing techniques. It should be possible to reduce these variations to about one degree by observing the following precautions:

1. Use a cold inner window in the cold box to block the heat flow from the heated outer window.
2. Always use ethyl acetate or some similar fluid (e.g., acetone or methylene dichloride) on the dry ice to insure good thermal contact with the box.
3. Fill the box with dry ice *at least* 3 hr before beginning observations, and keep it full during the night. It would be best to keep the box loaded with dry ice 24 hr a day.

If these precautions are not observed, the temperature variations of a refrigerated cell may easily exceed those of an unrefrigerated cell. In other words, the use of dry ice as it is usually employed probably does not significantly reduce the temperature fluctuations of the photomultiplier cathode.

Table I. Listing of Tubes Subjected to Measurement

Tube type	Cathode		Dynodes
EMI 6256 A	Sb-Cs (S-13)	13 stage	Venetian blind Sb-Cs
RCA 1P21	Sb-Cs (S-4)	9 stage	Focused Sb-Cs
EMI 9558 C	"Trialkali" (S-20)	11 stage	Venetian blind Sb-Cs
Farnsworth FW-118	Cs-Ag-O (S-1)	16 stage	Box-and-grid Mg-Ag

Magnitudes of the Temperature Effects

The first data on temperature effects in the commonly used Sb-Cs cathode surface were published over a decade ago.[7] In 1957, Kinard[8] discovered the negative temperature coefficient of Sb-Cs dynode surfaces. In 1959, Lontie-Bailliez and Meessen[1] added their own experimental results to all the previously published data in a comprehensive review of the subject. Some data have also been published on the important new "trialkali" cathodes.[9,10] However, some of the published data are rather conflicting, and none of the tube types used by astronomers has ever been measured. Therefore, the temperature effects for a number of tubes of astronomical interest were measured in this study.

Experimental Procedure

Table I gives the tube types which were tested; two of each type were used. The EMI 6256 is identical to the more widely used type 9502, except that it has a quartz window.

Table II. Characteristics of Filters Used in Experimentation

Central wavelength (Å)	3200	3570	3933	4170	4550	5000	6250	7300	8600	>1μ
Bandwidth at half-peak transmission	200	70	60	200	100	250	300	350	170	—
Blocked to at least λ	8500	8500	1.2 μ	1.2 μ	1.2 μ	1.2 μ	1.2 μ	1.2 μ	1.2 μ	—

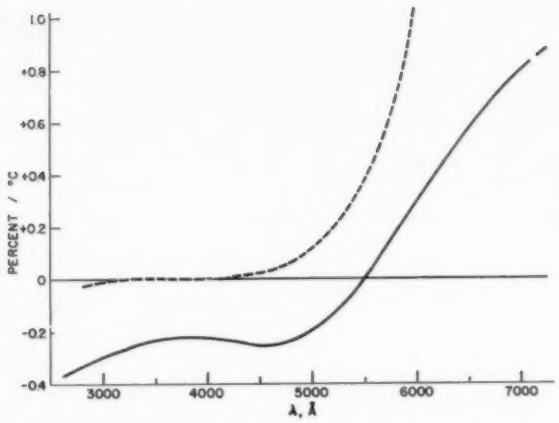

Fig. 1. Temperature coefficient of Sb-Cs cathodes as a function of wavelength (after Lontie-Bailliez and Meessen[1]). Solid curve: T = +20°C. Dashed curve: T = −80°C.

The optical part of the experimental apparatus consisted essentially of a voltage-regulated 100-W light bulb, the set of interference filters listed in Table II, and a Johnson-type cold box with a heated quartz outer window, containing the end-on photomultiplier under test. The voltage-regulating transformer used reduced the short-term fluctuations in the light output of the bulb well below 1%, even at λ 3200. The photomultiplier voltage divider consisted of precision deposited-carbon resistors, all of the same type, mounted outside the cold chamber.

For the 1P21's, the window was a layer of Saran Wrap, and a voltage divider of ordinary carbon resistors was contained in the cold chamber. The transmission of the Saran Wrap was measured and proved to vary by only 2% over the wavelength range from 3200 to 7300 Å.

The power supply for all the photomultipliers was a Northeast Electronics type RE-2003, which has a long-term stability of about 1 part in 10^4 and a short-term stability, under the actual conditions of operation, of about 1 part in 10^5. The anode currents were amplified by a General Radio type 1230-A electrometer and recorded on a Bristol strip chart recorder. The measured deviations from linearity in the amplifier-recorder combination are less than 0.1%. The inherent accuracy of measurements made with this system is a fraction of a percent, and is chiefly due to errors in reading the chart paper. Errors caused by long-term changes in the light bulb may amount to a few percent, but are surely less than 1% for periods of the order of a day or two. Thus, data for a single tube should be accurate to about 1%, and comparisons between different tubes should not be worse than a few percent.

All the tubes were measured with the box at room temperature and at dry-ice temperature (−78°C). In addition, the trialkali tubes and one of the infrared-sensitive tubes were measured with the cold box at some intermediate temperatures and at liquid-nitrogen temperature (about −190°C). Ethyl acetate was generally used on the dry ice to promote cooling, but most tests were made before the importance of using an inner cold window was discovered. Therefore the cathode temperatures were warmer than the box temperatures.

Sb-Cs Cathodes

In their survey article, Lontie-Bailliez and Meessen[1] put together a large number of observations on different Sb-Cs cathodes. Their results can be summarized as follows: (1) In the blue, the temperature coefficient of the Sb-Cs cathode is about −0.25%/°C at room temperature and is roughly independent of the wavelength. (2) For λ > 5000 Å, the temperature coefficient rapidly becomes more positive with increasing wavelength, at a rate of about 6×10^{-6} °C^{-1} Å^{-1}. That is, for every 100 Å we move to the red, the tem-

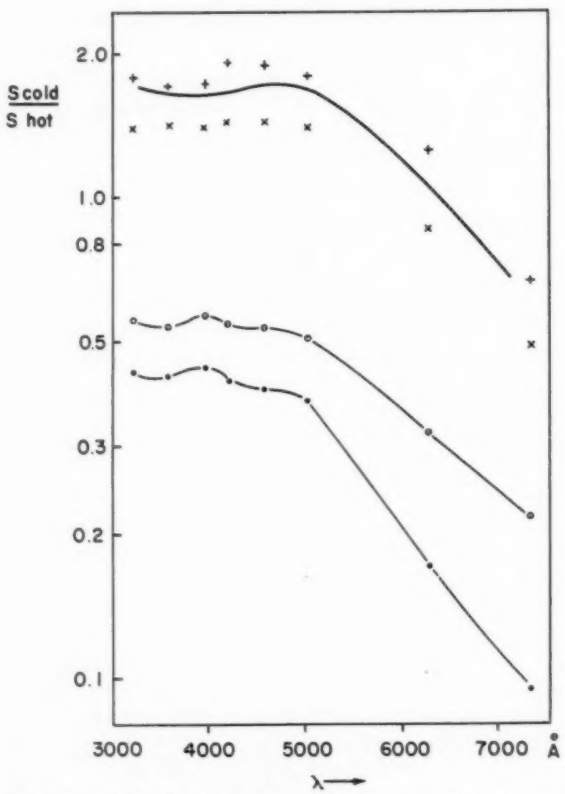

Fig. 2. Ratio of cooled to room-temperature anode sensitivity as a function of wavelength for EMI 6256 (crosses) and RCA 1P21 (dots) photomultipliers. The solid curve is the predicted ratio for a cathode temperature of −40°C and a dynode temperature of −70°C. The 1P21 points are anomalously lowered by condensation on the window. Cold box temperature = −78°C (dry ice).

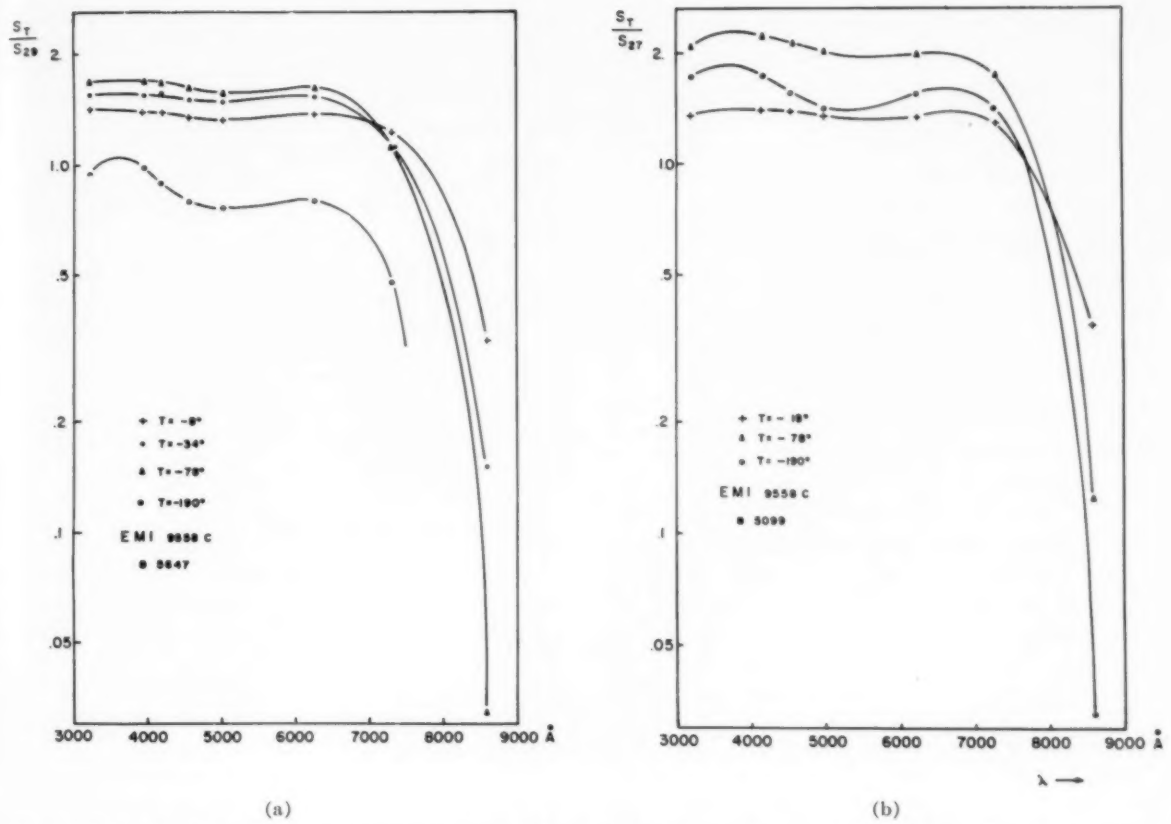

Fig. 3. Ratio of cooled to room-temperature anode sensitivity for two EMI 9558 photomultipliers and various cold box temperatures. Cf. Fig. 2.

perature coefficient increases by 0.06%/°C. (3) As the temperature is lowered, the plot of temperature coefficient against wavelength retains practically the same shape, but becomes more positive at every point (Fig. 1). This means that for any wavelength shorter than 5500 Å, there is some temperature below room temperature at which the Sb-Cs cathode has maximum quantum efficiency. At λ 4500 this is very nearly dry-ice temperature; however, the fractional increase in quantum efficiency from room temperature to dry ice is only about 15%. The efficiency falls off much more steeply on the cold side of the maximum than on the hot side. Thus, at λ 4500, about 40% of the maximum sensitivity is lost at liquid nitrogen temperature. (4) The temperature coefficient of the dynodes is $-0.04\%/°C^{-1}$ per stage on the average, but the values for individual tubes vary from zero to $-0.1\%/°C^{-1}$ per stage. For a given tube, the dynode temperature coefficient is practically independent of both temperature and operating voltages.

With the assumption that the temperature coefficients for Sb-Cs cathodes and dynodes given by Lontie-Bailliez and Meessen are applicable to the EMI 6256, the expected ratio of refrigerated to room-temperature response has been calculated as a function of wavelength. In accordance with the discussion of cold-box properties given above, the cathode was assumed to be cooled 60°C, and the dynodes, 90°C. The resulting function is plotted as the solid line in Fig. 2, and the experimental data for the two 6256's are represented by crosses. The agreement is quite satisfactory, especially considering that the dynode temperature coefficient (which affects the height of all points regardless of wavelength) is known to be widely variable from tube to tube. Data are also given in the figure for two RCA 1P21's; the curves are lowered because condensation on the unheated Saran Wrap window of the 1P21 cold box blocked part of the light to the refrigerated tubes. The shape of the 1P21 curves shows that the thermal properties of 1P21 cathodes are similar to those of other Sb-Cs cathodes.

Trialkali Cathodes

Figure 3 shows the effects of cooling two EMI 9558 C photomultipliers to various temperatures. As in Fig. 2, the ratio of anode response at a given box

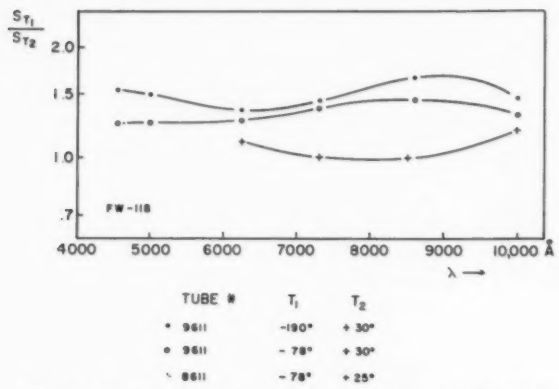

Fig. 4. Ratio of cooled to room-temperature anode sensitivity for two Farnsworth FW-118 photomultipliers cooled with dry ice and with liquid nitrogen.

temperature to that at room temperature is plotted. Tests of the two tubes operated as diode photocells show that the cathode sensitivity is unaffected by dry-ice cooling in the range 5000–6000 Å; in the blue the quantum efficiency is raised by cooling, and in the red it is sharply reduced. The dynode temperature coefficients for these tubes are about twice as large as the average reported by Lontie-Bailliez and Meessen.

The anode dark currents of these photomultipliers increased by about a factor of two when liquid nitrogen was used instead of dry ice. At such low temperatures the large negative temperature coefficient of the multiplier section overwhelms the diminishing positive temperature coefficient of the cathode dark current. The curves taken with liquid nitrogen as refrigerant probably have been affected by window icing and are too low; nevertheless, there is a genuine drop in cathode response at temperatures below about −100°C, just as in the case of the Sb-Cs cathode.

Ag-O-Cs Cathodes

The infrared-sensitive FW-118's were tested in the same way as the Sb-alkali-metal tubes. Figure 4 shows the results. Since the dark current noise masked the weak signals for λλ 4550 and 5000 at temperatures above 0°C, an extrapolation was made to estimate the room-temperature response at these wavelengths; the error made is probably less than 5%. The one FW-118 tested at a box temperature of −190°C was strongly influenced by window icing, and the data taken at this temperature have arbitrarily been multiplied by 50 at all wavelengths to make them comparable to the data taken at −78°C. Some error may have been introduced if the iced window did not transmit all wavelengths equally; however, even a layer of water 0.2 mm thick would cause less than 1% of actual absorption anywhere in the wavelength range considered here. The effect of the window frost must therefore be primarily a neutral geometrical shadowing. While the figures probably show correctly the effects of nitrogen cooling on the relative spectral response, the measurements need to be repeated with an experimental setup especially designed for work at temperatures below −100°C, with particular attention given to the problem of measuring the true cathode temperature.

One would expect the extreme infrared response to fall off with cooling, but the data taken do not extend to long enough wavelengths to show this. The changes in spectral response and in anode sensitivity are of the order of 30% for a 100°C temperature change. These tubes have Ag-Mg dynodes, which have been found[1] to have rather more variable temperature coefficients than Sb-Cs dynode surfaces.

Very-Low-Temperature Effects

The drop in sensitivity below −100°C which is shown by semitransparent antimony-alkali cathodes has been blamed on their low electrical conductivity at such temperatures.[11] As a corollary, some workers have claimed that the 1P21 cathode, being plated on a metallic base, does not lose sensitivity when cooled with liquid nitrogen.

Suppose that the resistance of the cathode is sufficient to cause an appreciable drop in cathode-to-first-dynode potential; the effect should be roughly equivalent to connecting a large resistor in series with the cathode. If the voltage drop in this resistor is large enough to affect the photoelectron collection efficiency by a factor of two, it must amount to some tens of volts. Then if we double the light input to the tube, the increased cathode current must cause a further large drop in K-D1 potential and collection efficiency, partially offsetting the increase in photoelectric emission. Additional increase in cathode current will soon use up all the available K-D1 supply voltage in the series resistance, and a saturation current must exist. In this regime, the cooled cathode must be very nonlinear in its apparent response to light. On the other hand, if we decrease the illumination by a factor of ten, the potential drop in the series resistance falls to a few volts, and no appreciable loss in collection efficiency or apparent cathode sensitivity is produced. Below this level the tube's response to light will be linear. No such nonlinearity has ever been observed, however; the data complied by Lontie-Bailliez and Meessen[1] from a wide variety of sources agree reasonably well at the lowest temperatures, and show that at 5000 Å the Sb-Cs cathode drops to about 30% of its peak sensitivity when cooled with liquid nitrogen. Likewise, the sensitivity loss of the EMI 9558 tubes at the lowest temperatures reached does not show any dependence on

cathode current. Finally, published data on the resistivity of cooled cathodes[12] show that cathode resistive voltage drops in photomultipliers—where cathode currents are generally below 10^{-12} A—can be neglected. Therefore the effect is inherent in the cathode material and should also be present in the case of the 1P21.

There is, in fact, direct evidence that the 1P21 cathode also falls to about one-third of its normal sensitivity at λ 5000 when cooled by liquid nitrogen. Engstrom's data[5] show a loss in anode response of about 2 dB in going from room temperature to liquid nitrogen; if his 1P21 had a normal dynode temperature coefficient, this indicates a reduction to 39% of the room temperature cathode sensitivity.

The fact that 1P21's and other Sb-Cs cathodes have been operated with liquid nitrogen cooling,[13,14] without showing any loss in cathode sensitivity, simply demonstrates the ineffectiveness of the usual astronomical cold box; if the cathode is not cooled below −130°C, it should show very nearly its room temperature sensitivity to blue light. However, it is better to use a properly designed cold box with dry-ice cooling, not only because the temperature stability is much improved and because the maximum quantum efficiency is reached, but also because the dark current is so insensitive to temperature near −100°C that the difference in temperature will not increase the dark current by more than about 50%.

Individual Differences

It is well known that different tubes of the same type show different spectral sensitivities, but there is very little in the published literature to indicate how much variation the user can expect. To give some idea of the tube-to-tube variation, we have plotted the *ratio* of the responses of the two tubes of each type, expressed in stellar magnitudes, in Fig. 5. Because some observers have been reluctant to use the end-on EMI tubes for U,B,V photometry, the ratio of the mean EMI 6256 response to the mean 1P21 response is also plotted. It appears that systematic differences between EMI and RCA tubes are no larger than the individual differences between 1P21's. In this respect it is worth recalling that Mikesell[15] tested 38 1P21's and found that the ratio of blue response to response at λ 6100 varied by a factor of 16. Considering the lower leakage, larger gain, and higher quantum efficiencies which are available in tubes such as the 6256 it seems preferable to use end-on tubes in place of the 1P21.

Two comments can be made about the curves shown in Fig. 5. First, the ratio of the S-1 cathodes shows an extremum at about 8000 Å. Since the S-1 surface itself has a bump in its spectral sensitivity at this wavelength, it appears that one of these tubes has a much larger bump than the other.

Second, the antimony-alkali-metal cathodes all show large variations in the red, but are generally well-behaved in the blue. The 9558 (S-20) tubes show a phenomenon which is also present in all four Sb-Cs tubes: the cathodes with the largest relative far-red sensitivity also show the smallest temperature coefficients at long wavelengths. This correlation is understandable in terms of Spicer's description[9] of such cathodes: the far-red sensitivity is due to loosely filled acceptors (impurities) in these *p*-type semiconductors, and the distribution of impurity states increases "in something like an exponential manner above the top of the valence band. If such were the case, the slope of the yield curve [logarithm of photon response plotted against photon energy] should increase by about a factor of 4 on cooling from 300° to 77°K. Such an increase was found...." In other words, tubes with sharp red cutoffs become even sharper when cooled, while those with long red tails of low slope—and hence higher relative far-red sensitivity—lose a smaller fraction of their long-wavelength response on cooling.

Finally, it is evident that Sb-Cs cathodes have similar spectral response and small temperature coefficients for λ ≤ 5000 Å, but become unreliable at longer wavelengths; similarly, S-20 cathodes are well-behaved out to only λ 6000 or 6500. Photometric systems intended to have high accuracy and reproducibility should not push to the red of these limits. Thus, for the highest precision, a wavelength band at 7500 Å should be measured with an S-1 cathode, even though the S-20 cathode has (on the average) five times as much

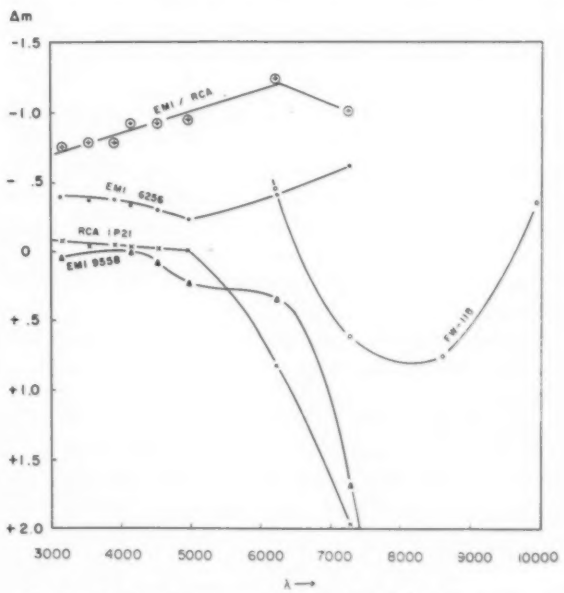

Fig. 5. Ratios of responses of two tubes of the same type, as a function of wavelength. For the EMI 9558's, the ratio is in the sense (tube No. 5647)/(tube No. 5099); cf. Fig. 3. The curve marked EMI/RCA is the ratio of the mean of the 6256's to the mean of the 1P21's.

sensitivity at this wavelength. Stability and reproducibility must be considered when selecting a photocathode; sensitivity alone is an insufficient criterion.

Astronomical Effects

General Considerations

Since photoelectric observers commonly claim an accuracy of 0.01 mag. or better, temperature effects should be kept below 1% in all photoelectric investigations. In fact, it would be desirable to keep photocell changes below 0.1%, since observers sometimes report observations to this accuracy. In the following discussion, 1% stability is adopted as a minimum standard. For comparison, typical cathode temperature fluctuations of 7°C and dynode variations of 3°C are here assumed for a conventional cold box.

Gain Stability

The trialkali tubes tested had over-all temperature coefficients larger than $-1\%/°C$ in the blue, and Sb-Cs tubes typically have temperature coefficients of about $-0.7\%/°C$. Evidently a minimum requirement for 1% stability of response is a temperature regulation of the order of 1°C—a value which is certainly *not* realized in most photometers. However, most of the gain variations arise in the dynode section of the tube. Since the dynodes probably suffer somewhat smaller temperature variations than the cathode, one can expect over-all sensitivity fluctuations of about 3% in ordinary circumstances. If a standard light source is not used, these 0.03 mag. errors can enter directly into the determination of extinction and will appear as both systematic and random errors in the results. Several photoelectric observers, both in this country and abroad, have abandoned the use of standard light sources because they show both temperature and hysteresis effects. However, according to data furnished by the U.S. Radium Corporation, the temperature coefficients of most radioactively excited phosphor light sources are about five times smaller than those of photomultipliers. The use of such sources to check gain variations in the photomultiplier is therefore recommended. For the highest accuracy, the source should be carefully thermostated.

The effects of dynode gain variations can be partially eliminated by the use of pulse-counting techniques. However, the quantum efficiency of the cathode is still temperature dependent, and sensitivity variations of nearly 2% may still occur with the conventional cold box. Careful operation with a properly designed box can reduce this figure by a factor of 5 or 10.

Pulse-counting should also reduce the influence of the "fatigue" effects which appear when anode currents larger than one microampere are drawn from the tube. These effects occur in the last few dynode stages, and

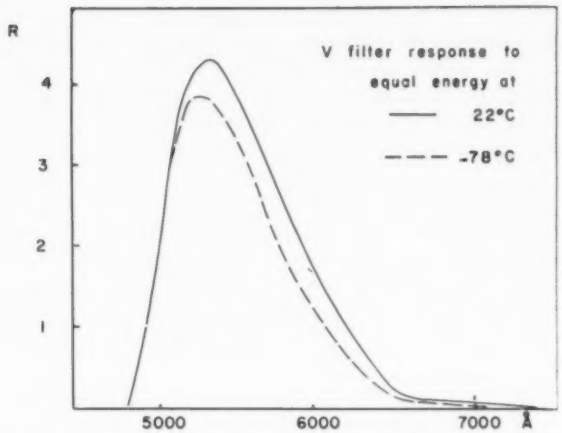

Fig. 6. Response curves for V band of U,B,V photometry using a cooled (dashed curve) or uncooled (solid line) photomultiplier. The refrigerated cathode is assumed to be cooled 60°C below room temperature (cf. Fig. 2).

are independent of the light intensity at the cathode—i.e., they depend only on the electron currents in the last few stages. Engstrom[5] has found a 20% decrease in sensitivity after drawing 5μA from a 931-A for 40 min, and both positive and negative sensitivity changes have been reported for 1P21's.[6] All of the end-window tubes in the present study showed a gain in sensitivity of the order of 5 or 10% in ten minutes for 5μA anode current; the change was rapid at first and then leveled off. When the anode current was reduced, the tubes very slowly returned to their original sensitivity. These high anode currents correspond to very high counting rates, of the order of 10^7 pulses/sec, but equipment is beginning to become available for these ranges.

Color Stability

In all photometric investigations, it is assumed that the color zero point of the photometer remains fixed during a night's observations; indeed, it is often assumed that the instrumental color system is constant for days or weeks at a time. Thus, Weaver[16] says that "the zero-atmosphere colors and magnitudes of the extinction stars are constants and should have the same numerical values each night," and Hardie[17] bases his method of determining extinction on the assumption that "the zero-point term [in the colors] was constant over many nights." However, temperature variations at the cathode can seriously change the color systems.

For the U, B, V system the temperature effects appear most strongly in the visual band. Figure 6 shows the V response curves for Johnson's 1P21 measured at room temperature[18] and calculated for the same tube cooled with dry ice in a conventional cold box, on the

assumption that the tube behaves according to the curves of Fig. 2; the response curves have been normalized for $\lambda < 5000$ Å. The effect of cooling is to reduce the relative V response by 0.18 mag. and to reduce the effective wavelength by about 50 Å, which reduces the B-V color baseline by about 4%. Since the standard stars of the U, B, V system were measured with the photocell refrigerated,[19] we should expect that the B-V colors of stars calculated from the published response curves and theoretical stellar energy distributions would be 0.18 mag. redder than the observed colors. The actual discrepancy[20] is slightly less, and amounts to 0.13 mag. on the average. The difference, if significant, may mean that Johnson's 1P21 was unusually red-sensitive, or that his cold box was unusually inefficient.

In any case, we can say that the temperature coefficient of the B-V zero point is 0.003 mag./°C, and that the ordinary cold box will allow this zero point to wander by at least 0.02 mag. A cathode temperature regulation of 3°C or better is required to hold the U, B, V color system fixed to an accuracy of 0.01 mag., even if a standard source is used to measure the dynode gain variations. Even in the blue and ultraviolet, one should *never* reduce together observations made with a cooled and an uncooled photomultiplier—as at least one spectrophotometric observer has done!

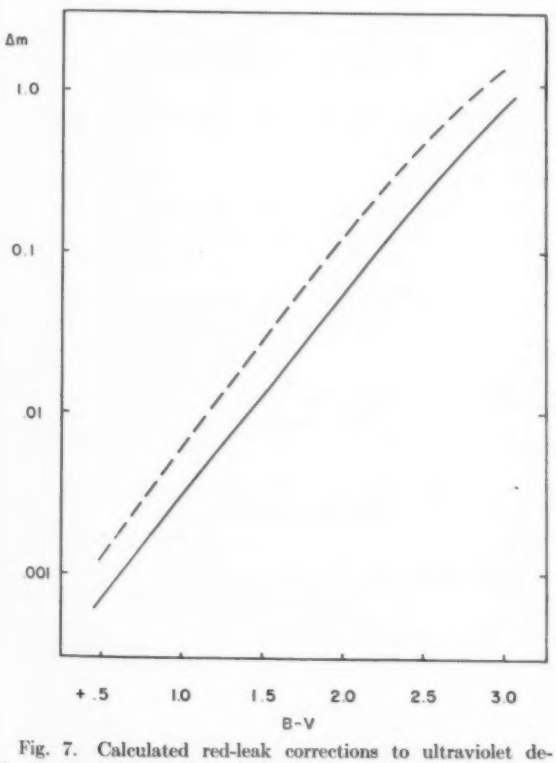

Fig. 7. Calculated red-leak corrections to ultraviolet deflections for Johnson's U,B,V photometer. Solid line: 1P21 refrigerated with dry ice. Dashed line: 1P21 not refrigerated.

The temperature-color effect also enters into U, B, V measurements in another way. Johnson[19] says that the ultraviolet deflection of DS Peg required a correction of 0.25 mag. because of the red leak in the ultraviolet filter. Since the effective wavelength of the leak is about 7000 Å, it must be very temperature-dependent. If we make the rather poor assumption that these red stars radiate as blackbodies, we obtain the correction curves of Fig. 7 for cooled and uncooled photomultipliers. The curves are not to be taken literally, but serve to illustrate the magnitude of the red leak and its temperature dependence. Cooling the photocathode has the desirable effect of reducing the leak, but one can expect very large variations—perhaps a factor of 30—from tube to tube.

A serious temperature effect is also present in the recent photometry of Borgman,[21] who used a dry-ice cooled 1P21 at 5200 Å and 5800 Å. His λ 5200–λ 5800 colors show a scatter of about 0.03 mag. The cathode temperature coefficients at these two wavelengths differ by nearly 0.4%/°C, so that a temperature variation of about 8°C should suffice to account for the scatter. This value is about what one can expect for the usual cold box. Borgman's difficulties serve to emphasize the unreliability of Sb-Cs cathodes to the red of 5000 Å.

Finally, the data for S-1 tubes (Fig. 4) show that a temperature regulation of about 3°C is required to stabilize the response of these tubes to 1%. This figure is very similar to the temperature regulation required for U, B, V photometry.

Conclusion

If 1% stability is taken to be a minimum requirement for an astronomical photoelectric photometer, then most existing photometers fail, by a factor of about 3, to achieve an adequate degree of temperature regulation. Careful use of dry ice as a refrigerant in a properly designed cold box *can* reduce temperature effects well below 1%, but it is doubtful that a stability of 0.1% can be reached without the use of a closed-loop thermostat system, in which the cathode temperature is measured and used to control the refrigeration.

With existing photometers, the use of a standard source to monitor instrumental gain and color changes is almost mandatory if 0.01 mag. accuracy is to be reached. Pulse-counting techniques can help reduce the effect of temperature-induced gain variations, but the temperature-color effect remains as a fundamental property of the photocathode.

Even the most carefully regulated photomultiplier, however, can display significant sensitivity variations as a result of "fatigue," aging, and short-term fluctuations of unknown origin. The need for a really reliable standard light source is likely to become even more

pressing as we try to go from hundredth of a magnitude accuracy to 0.001 mag., and temperature control of the light source will be as important as temperature control of the photomultiplier.

The author wishes to thank M. S. Roberts and H. C. Ingrao of Harvard College Observatory for providing the 1P21's and a cold box to fit them. He also wishes to thank Mr. Ingrao for providing references to the physics literature.

References

1. M. Lontie-Bailliez and A. Meessen, Ann. soc. sci. Bruxelles **73,** 390 (1959).
2. G. E. Kron, Publ. Astron. Soc. Pacific **70,** 285 (1958).
3. H. L. Johnson, *Astronomical Techniques*, ed. W. A. Hiltner (Univ. of Chicago Press, 1962), Chap. 7.
4. A. R. Hogg, private communication.
5. R. W. Engstrom, J. Opt. Soc. Am. **37,** 420 (1947).
6. K. Serkowski, Lowell Obs. Bull. No. 116.
7. N. Schaetti and W. Baumgartner, Helv. Phys. Acta **24,** 614 (1951).
8. F. E. Kinard, Nucleonics **15,** 92 (1957).
9. W. E. Spicer, Phys. Rev. **112,** 114 (1958).
10. G. Frischmuth-Hoffmann, P. Görlich, and H. Hora, Z. Naturforsch. **15a,** 1014 (1960).
11. W. E. Mott and R. B. Sutton, *Handbuch der Physik*, S. Flügge, ed. (Springer-Verlag, Berlin, 1958), Vol. 45, p. 93.
12. W. J. Harper and W. J. Choyke, J. Appl. Phys. **27,** 1358 (1956).
13. H. L. Johnson, Sky and Telescope **17,** 558 (1958).
14. W. J. Harper and W. J. Choyke, Rev. Sci. Instr. **27,** 966 (1956). (The Sb-Cs curve labeled −175°C in this paper actually corresponds to a temperature of only about −110°C.)
15. A. H. Mikesell, Astron. J. **54,** 191 (1949).
16. H. Weaver, Astrophys. J. **116,** 638 (1952).
17. R. Hardie, Astrophys. J. **130,** 663 (1959).
18. H. L. Johnson and W. Morgan, Astrophys. J. **114,** 522 (1951).
19. H. L. Johnson and W. Morgan, Astrophys. J. **117,** 313 (1952).
20. A. D. Code, *Stellar Atmospheres*, J. L. Greenstein, ed. (Univ of Chicago Press, 1960), Chap. 2.
21. J. Borgman, Bull. Astron. Inst. Netherlands **15,** 255 (1960) *ibid.* **16,** 99 (1961).

Future Issues

Each issue will specially feature one area of applied optics in addition to the usual contributed papers, shop and technical notes, reports of meetings, Letters to the Editor, book reviews, Meetings Calendar, and special columns. The feature subject of each issue is the responsibility of the named editor.

1963		
February	**Astronomy II**	James G. Baker
March	**Optical Instruments**	W. L. Hyde
April	**Image Evaluation**	F. Dow Smith
May	**Interferometry**	R. A. Woodson
June	**Super Achromats**	—
July	**Spectroscopy**	Mary E. Warga
August	to be announced	
September	**Lens Design and Computers**	D. P. Feder
October	**Bubble Chamber Optics**	S. Rosin
November	**Coblentz Commemoration**	E. K. Plyler
December	**Chemical Optics**	M. Kent Wilson
1964		
January	**Photographic Optics**	George C. Higgins
February	**Atmospheric Optics**	D. Q. Wark
April	**Visibility**	S. Q. Duntley
June	**Fiber Optics**	C. W. Peters
July	**Optics in Japan**	R. A. Oetjen
December	**Solar Optics**	G. Newkirk Jr.
1965		
February	**Plasma Radiation**	L. M. Branscomb

FUTURE MEETINGS

OPTICAL SOCIETY OF AMERICA

1963 25–27 March, Spring Meeting,
Robert Meyer Hotel,
Jacksonville, Fla.

23–25 October, 48th Annual Meeting,
Sherman House Hotel,
Chicago, Ill.

1964 1–3 April, Spring Meeting,
Sheraton Park Hotel,
Washington, D.C.

7–9 October, 49th Annual Meeting,
Statler-Hilton Hotel,
New York, N.Y.

1965 31 March, 1 and 2 April,
Spring Meeting,
Statler-Hilton, Hotel,
Dallas, Tex.

Executive Office

1155 16th Street, N.W. Washington 6, D.C.

The Effects of Telescopes on Astronomical Polarization Measurements

R. H. Miller

Systematic errors appearing in astronomical polarization measurements in the range of one percent and less are expected to be partly due to the telescopes used in making the measurements. A 6-parameter description of possible telescope polarization effects is proposed which can be reduced to a 4-parameter description in the practical case in which the telescope is to be used only for relative intensity measurements. The 4 parameters can be represented as 2 which describe the elliptically polarized telescope eigenstates, and 2 which are the relative phase-shifts and the ratio of absorptions of the orthogonal eigenstates. The effects of the telescope are presented in a 4 × 4 transformation matrix which transforms the Stokes parameters of the incident beam into those of the emergent ray. The empirical determination of the telescope parameters, the correction of polarization measurements once the parameters are known, and the problem of establishing stellar sources of known polarization for use in calibrating telescopes is discussed. No estimates of the magnitude of the possible effects are attempted.

This paper presents an analysis of the possible effects of an astronomical telescope producing systematic errors in measurements of the polarization of starlight. The interest in this problem arises because recent attempts to measure small polarizations (less than 1%) have shown effects which are commonly regarded as systematic. These effects are at least partially ascribed to the telescopes used in making the measurements. The methods and results are more generally applicable, however.

In recent years, several formulations using matrices to describe the action of optical devices on radiation passed through them have appeared in the literature.[1,2] However, the 2 × 2 coherency matrices introduced by E. Wolf[3] have been shown by Parrent and Roman[4] to yield a matrix formulation of the action of optical devices which is easy to apply to practical systems, and which forms the basis of the present paper. The conditions under which the coherency matrix formulation is valid are discussed by Parrent and Roman. The determination of the telescope parameters is facilitated by transforming the result to a 4 × 4 matrix of real elements which transforms the incident to the emerging "Stokes vector" (Mueller Matrix[5]).

The approach used in this paper is to postulate the existence of polarization eigenstates of the telescope. These are states of polarization such that an incident beam in that state of polarization will produce an emergent beam in the same state of polarization—the amplitude and phase may be changed, but the axis ratio, sense of rotation, and inclination of the axes of the characteristic ellipse are the same. Projection operators are introduced which project out these polarization states, and the telescope is pictured as producing a simple linear combination of these states. While the projection operators are singular, the linear combination will not be singular except when one of the coefficients is zero. Thus, the telescope acts as a partial polarizer, and a transformation matrix is developed which represents the effect of the telescope on an incident beam of arbitrary polarization. Methods for determining the parameters of the telescope, and of correcting for the effect of the telescope, are then discussed. Finally, the problem of establishing a set of standard polarized sources which would permit any telescope to be easily calibrated for its polarization effects is discussed.

Transformation Matrix

For purposes of analysis, the telescope is regarded as a "black box" in the sense of circuit theory. The effect of the telescope on the incident light can be expressed as a 4 × 4 matrix transforming one set of Stokes parameters into another set. A convenient device for calculating the transformation matrix is provided by the coherency matrix.[4] In this formalism, the telescope can be regarded as having an eigenstate of polarization, which implies that the orthogonal

The author is in the Department of Astronomy and Institute for Computer Research, The University of Chicago, Chicago, Illinois.

Received 11 December 1961.

state is also an eigenstate.* The two eigenstates will be transmitted by the telescope with different amplitude and phase factors. The general eigenstates will be elliptically polarized, and will have their axes inclined at some angle to the (arbitrary) reference axes.

One of these states can be described by a projection operator (for the right-elliptically polarized state with its major axis at an angle θ to the reference x axis):

$$\Pi_+ = \frac{1}{1+a^2}\begin{pmatrix}[\cos^2\theta + a^2\sin^2\theta] & [(1-a^2)\sin\theta\cos\theta + ia] \\ [(1-a^2)\sin\theta\cos\theta - ia] & [\sin^2\theta + a^2\cos^2\theta]\end{pmatrix}. \quad (1)$$

The orthogonal eigenstate has its major axis perpendicular to that of the other state, and rotates in the opposite sense:

$$\Pi_- = \frac{1}{1+a^2}\begin{pmatrix}[\sin^2\theta + a^2\cos^2\theta] & -[(1-a^2)\sin\theta\cos\theta + ia] \\ -[(1-a^2)\sin\theta\cos\theta - ia] & [\cos^2\theta + a^2\sin^2\theta]\end{pmatrix}. \quad (2)$$

Here, a is the axis ratio of ellipticity; $0 < a < 1$; $a = 0$ corresponds to linearly polarized states, and $a = 1$ corresponds to circular polarization. These projection operators may be constructed from the evident operators for linear and circular polarizations by applying a rotation operator as indicated in ref. 4, and have the usual properties of projection operators:

$$\begin{aligned}&\Pi_+\Pi_+ = \Pi_+, \quad \Pi_+\Pi_- = 0 = \Pi_-\Pi_+, \\ &\Pi_-\Pi_- = \Pi_-, \quad \Pi_+ + \Pi_- = I.\end{aligned} \quad (3)$$

With the help of the projection operators, a "telescope operator" can be formulated:

$$T = (\alpha\Pi_+ + \beta\Pi_-) = \alpha I + (\beta - \alpha)\,\Pi_- = \beta I + (\alpha - \beta)\,\Pi_+. \quad (4)$$

Here α and β are complex numbers, $\alpha = e^{-(\eta_+/2)}e^{i(\delta_+/2)}$ and $\beta = e^{-(\eta_-/2)}e^{i(\delta_-/2)}$, where η_+ and δ_+ are, respectively, the absorption parameter and phase shift associated with Π_+, and η_- and δ_- are similarly associated with Π_-. These terms will, in general, be different for the two eigenstates. It is this difference which produces the telescope polarization.

The transformation of the incident coherency matrix is given by[4]:

$$\mathcal{J} = T\,\mathcal{J}_0\,T^+, \quad (5)$$

where T^+ is the Hermitian adjoint to T. The relation with the Stokes parameters is $\mathcal{J} = \frac{1}{2}\sum_\alpha \sigma_\alpha\sigma_{\dot\alpha}$, where σ_α are the Pauli matrices, with σ_1 diagonal, and $\sigma_0 = I$.

The number of parameters introduced to describe the telescope is 6—the real and imaginary parts of α and of β, and the ellipticity parameters a and θ. It is convenient to define other (real) parameters:

$$\begin{aligned}&C_1 = \alpha\alpha^*, \quad C_2 = \tfrac{1}{2}(\alpha\beta^* + \beta\alpha^*), \\ &C_3 = \beta\beta^*, \quad C_4 = \tfrac{1}{2}(\alpha\beta^* - \beta\alpha^*)i\end{aligned} \quad (6)$$

(α^* is the complex conjugate of α). Normally all these parameters will vary from point to point in the focal plane of the telescope, because different parts of the optics are used in slightly different ways at these different points. It is implicit in what follows that all measurements refer to a given point in the focal plane, so that the position dependence may be suppressed. The parameters will also be color-dependent.[6,*] The parameters to be used are suitable averages over the frequency bands.

For the case in which the telescope is not to be used for absolute intensity measurements, α or β can be factored out. Normally the factor of smaller absolute magnitude will be factored out. This permits the definition of $\gamma = \beta/\alpha$. Then

$$\begin{aligned}&C_1 = 1, \quad C_2 = Re\ \gamma, \\ &C_3 = \gamma\gamma^*, \quad C_4 = \mathcal{I}m\gamma,\end{aligned} \quad (7)$$

and the entire transformation matrix will contain a common factor $\alpha\alpha^*$, which can be ignored. The number of relevant telescope parameters is thus reduced to four.

With these definitions, the transformation matrix of the telescope can either be written immediately as a 2×2 matrix of complex elements in the form of Eq. (4), or, by operating on a state defined by one of the Pauli matrices according to the rule of Eq. (5), and decomposing the result into a linear combination of Pauli matrices, a 4×4 matrix of real elements which operates on a "Stokes vector" may be obtained:

$$\begin{pmatrix}s_0' \\ s_1' \\ s_2' \\ s_3'\end{pmatrix} = M\begin{pmatrix}s_0 \\ s_1 \\ s_2 \\ s_3\end{pmatrix} \quad (8)$$

with M as follows:

$$\begin{pmatrix}M_{00} & A\cos 2\theta & A\sin 2\theta & M_{30} \\ A\cos 2\theta & [C_2 + B(1+\cos 4\theta)] & (B\sin 4\theta - D) & (F\cos 2\theta + G\sin 2\theta) \\ A\sin 2\theta & (B\sin 4\theta + D) & [C_3 + B(1-\cos 4\theta)] & (F\sin 2\theta - G\cos 2\theta) \\ M_{30} & (F\cos 2\theta - G\sin 2\theta) & (F\sin 2\theta + G\cos 2\theta) & M_{33}\end{pmatrix} \quad (9)$$

* In the most general formulation the two eigenstates need not be orthogonal. This leads to an 8-parameter formulation unlike the 6-parameter formulation to be described. The remaining two parameters can be introduced as analogues of a and θ for the other state. The same methods can be used, and most of the qualitative features remain. Some of the details are changed. The 6-parameter formulation seems to be as general as is commonly used in optical problems. The principal reason for restricting consideration to the case of orthogonal eigenstates is that nonorthogonal eigenstates can lead to situations in which energy is not conserved. However, the energy conservation requirement strictly leads to an inequality because of the absorption present in realizable telescopes. This inequality provides a rather weak statement about the degree to which the eigenstates can be nonorthogonal. The ultimate test must be experimental.

* The quoted effects are mostly less than 1%.

$$
\left.
\begin{aligned}
M_{00} &= {}^1/_2\,[C_1 + C_2] \\
M_{30} &= \frac{a}{1+a^2}\,[C_1 - C_2] \\
M_{33} &= C_3 + \frac{2a}{(1+a^2)^2}\,[C_1 + C_2 - 2C_3] \\
A &= \frac{1}{2}\,\frac{1-a^2}{1+a^2}\,[C_1 - C_2] \\
B &= \frac{1}{4}\left(\frac{1-a^2}{1+a^2}\right)^2 [C_1 + C_2 - 2C_3] \\
D &= \frac{2a}{1+a^2}\,C_4 \\
F &= a\,\frac{1-a^2}{(1+a^2)^2}\,[C_1 + C_2 - 2C_3] \\
G &= \frac{1-a^2}{1+a^2}\,C_4
\end{aligned}
\right\} \qquad (10)
$$

The subsequent discussion is based on the 4-parameter relative intensity measurement.

Discussion

One point which this matrix brings out immediately is the role of elliptically polarized states in the determination of polarization. (These are the states involving s_3.) In particular, there are contributions to the measured linear polarizations from the incident ellipticity, and, conversely, contributions to the measured ellipticity from the incident linear polarization terms. It seems to be customary in astronomical polarization "measurements" to ignore the ellipticity present in the polarization. It is by no means clear that elliptical polarizations are unimportant in weakly polarized sources, as is claimed to be the case for some strongly polarized sources.[7] Further, ellipticities should be present in synchrotron sources, elliptical states being characteristic of such sources.[8] The determination of linear polarization states is only half the problem.

The complete specification of the telescope parameters requires measurements based on at least two known sources of different polarizations. For example, the complete determination of the emergent polarization produced from a completely unpolarized source permits the determination of C_1, C_2, a, and θ. (Either C_1 or C_2 is taken to be 1; which one depends on the sign of a.) No information on the relative phases of the eigenstates can be obtained from the measurement with an unpolarized source. This information is contained in the combinations $(C_1 + C_2 - 2C_3)$ and C_4. A measurement with a source of known polarization must be made to determine the phase difference terms. As always, it is best to overdetermine the parameters so that error estimates can be made.

Once the telescope parameters are determined, the correction of observations is direct. The inverse of the telescope operator, T^{-1}, is required. However, for α and β nonzero, the inverse to T is

$$
T^{-1} = \left(\frac{1}{\alpha}\,\Pi_+ + \frac{1}{\beta}\,\Pi_-\right). \qquad (11)
$$

Thus, by an obvious redefinition of C_1 through C_4, the matrix already given can be used to correct the directly measured polarizations. The errors in determining the telescope parameters can be propagated through the telescope matrix to determine the errors in the measurement of the polarization of the initial beam. However, care must be exercised to carry the correlated errors through correctly.

It is observed that normally telescopes do not introduce polarization effects greater than a percent or so.[6,9] The effects to be expected for metallic reflections even some 3° from normal incidence (as may occur in an $f/4$ reflecting telescope) are on the order of a percent or less, and the phase shifts to be expected are on the order of a degree or less. However, if an attempt is made to estimate the magnitude of these effects, it turns out that, owing to the symmetry of the telescope, the telescope eigenvalues α and β become degenerate and all polarization states are eigenstates. Thus, to observe an effect there must be imperfections in the metallic surfaces. It is almost impossible to guess what a poorly aluminized surface might do. However, the effects are not expected to be more than a few percent at most, principally because of the averaging over the large mirror surfaces. Until the age-dependence of telescope parameters is known, frequent redetermination may be necessary.

The smallness of the telescope polarizations gives rise to the hope that the corrections for telescope effects can be made more simply than by using the inverse of the telescope matrix. It is instructive to pursue such an approximation because it displays clearly the assumptions inherent in the corrections normally made in astronomical polarization measurements. If the following assumptions are made, it is possible to achieve such a reduction. (1) The polarization to be measured is small (of the first order), and (2) all telescope parameters like $(C_1 - C_2)$, $(C_1 + C_2 - 2C_3)$, and C_4 are small (of the first order). The second assumption actually involves three separate assumptions: first, that C_1 and C_2 are very nearly equal; second, that the relative phase shifts are small; and third, that the telescope ellipticity parameter is small. It then follows that $C_1 \approx C_2 \approx C_3 \approx 1$, and the matrix (retaining first-order terms in the resultant Stokes parameters only) reduces to the following form:

$$
\begin{pmatrix}
1 & 0 & 0 & 0 \\
A\cos 2\theta & 1 & 0 & 0 \\
A\sin 2\theta & 0 & 1 & 0 \\
M_{30} & 0 & 0 & 1
\end{pmatrix}. \qquad (12)
$$

Thus, the final Stokes parameters are the result of the telescope operating on an unpolarized beam and of the

polarization present in the entering beam. A simple subtraction of the effect of the telescope on an unpolarized beam suffices to determine the polarization state of the incident beam. The difficulties with this type of analysis are that it is not *a priori* clear that the complete set of assumptions regarding the telescope parameters is justified; and that the polarization parameters are determined only to first order, with no operational definition of what constitutes first order. A proper estimate of the accuracy of this method requires a set of standard objects of known polarization, and, effectively, a complete determination of the telescope parameters. It works in favor of this method that the fractional precision demanded of astronomical polarization measurements is low. It should be noted, however, that the determination of the so-called "position angle" of polarization (the angle of the line along which the *linear* polarization effects are maximal) essentially requires the use of second-order terms.

Establishment of "Standard" Polarized Stars

An important point in the determination of the telescope parameters is that the entire telescope must be illuminated in the same way as a star illuminates it.* A set of stars of known unvarying polarization would provide a convenient way to calibrate the telescope. However, the establishment of such a set of standard stars presents the principal problem associated with such a program.

If the parameters of a telescope have been completely determined, that telescope can be used to establish a set of standard stars which can be used for subsequent recalibrations of the original telescope or to calibrate other telescopes. The one telescope might be calibrated by using terrestrial sources of known polarizations. Two methods involving terrestrial sources appear possible: One is a diffuse reflector mounted on the telescope, which could be illuminated with light beams of prepared polarization states; and the other is a distant source of changeable but known polarization. Each of these methods has its inherent difficulties. The diffuse reflector will have its own polarization parameters (which can be treated by the same formalism as has been given) to be determined separately from those of the telescope; while the distant terrestrial source can have its polarization modified by atmospheric effects over a long sight-path. Of the two, the distant source looks more promising, because, in principle it can be made bright enough to have its polarization state measured at the telescope position without using the telescope. A direct comparison of the light seen with and without the telescope can thus be made with this method.

Use of Several Telescopes

Another method of establishing a set of standard stars involves the use of several telescopes, the comparisons of the results obtained with each being used to eliminate the telescope effects and solve for the polarizations of the stars. This method looks the most promising of any of those proposed. In principle, if many different stars are measured with each of several telescopes, the number of measured quantities exceeds the number of independent parameters to be determined, thus permitting the use of a statistical argument to solve for each of these parameters. For example, if N stars are measured with each of M telescopes, $3MN$ Stokes parameters will be determined. There are $3N$ Stokes parameters for the stars and $4M$ telescope parameters to be determined. It is assumed that the telescope parameters are different for each telescope. The problem is overspecified and can be solved in a self-consistent way which allows for the determination of errors if $3MN > 4M + 3N$. Thus, if two telescopes are used, 3 or more stars of differing polarization states are required. This procedure has the advantage of automatically yielding a set of standard stars. The errors in the polarization of the stars will be correlated, however. The use of the minimal set of parameters as here envisioned would mean solving a nonlinear problem involving a hunting procedure. This could be avoided by solving directly for the elements of the matrix of Eq. (9). The symmetry of that matrix is such that 13 distinct elements of the matrix enter linearly. These might be regarded as independent. The statistical problem could then be recast in terms of seeking $13M$ telescope parameters and $3N$ parameters referring to the stars, changing the inequality to $3MN > 13M + 3N$, requiring 9 stars on each of two telescopes for a minimal set. The 13 matrix elements for each telescope could be solved, in principle, for the 4 basic parameters, but since the 13 are in fact the desired result, there may not be much reason to solve for the 4 basic parameters.

A modification of this method would be to attempt to use existing data for such a determination, using the data on the polarization of starlight which exist in the astronomical literature at present (see ref. 9, for example). These provide only the components of linear polarization, or (s_1/s_0) and (s_2/s_0). Thus only two quantities are available per measurement. In this case, if the linear problem be considered, none of the elements of the transformation matrix referring to the third Stokes parameter will enter the problem, and only 7 elements of the matrix of Eq. (9) need be considered. This makes the inequality become $2MN >$

* It is equivalent to measure the reflectance and phase shifts over the entire mirror and integrate, as Gehrels has done (ref. 6). A proper average over the entire mirror must be taken.

$7M + 2N$ (with $2N$ instead of $3N$ because the third Stokes parameter is forced to zero. This hypothesis can be checked later). Thus if two telescopes are involved, a number of stars greater than 7 is required to yield an overdetermined problem. The resulting 7 parameters could then, in principle, be solved for the four basic parameters of the telescope, which could, in turn, be used to predict the remaining elements of the full 4×4 telescope matrix.

It would be desirable to use data taken by different workers with polarimeters of different design in an attempt to eliminate other instrumental errors. Otherwise these systematic errors will appear in the "standard" star determinations.

Rotatable Telescope

The possibility of using a rotatable telescope to cancel the telescope-produced polarizations has been suggested.[9] This is expected to be particularly helpful in finding a stellar source of zero polarization.

Two features involving this system emerge from the present analysis. First, measurements must be made at a minimum of four telescope azimuth settings at intervals of $\pi/4$ to cancel both the 2θ and 4θ terms. Second, having canceled them, all the telescope parameters except θ remain in the resultant matrix: (The notation is unchanged.)

$$\begin{pmatrix} M_{00} & 0 & 0 & M_{20} \\ 0 & C_2 + B & -D & 0 \\ 0 & D & C_2 + B & 0 \\ M_{20} & 0 & 0 & M_{22} \end{pmatrix}. \quad (13)$$

It should be noted that determinations of s_0, s_1, s_2, and s_3 must be separately summed over all azimuths before dividing out $\overline{s_0}$. Otherwise only a first-order cancellation of the angle-dependent terms will result.

There is a subtle complication in this method, however. Normally, the optical axis and mechanical axis of the telescope will not coincide exactly. This will have the effect of making the telescope parameters themselves a function of the azimuth angle to which the telescope is turned. This effect will probably be small because the misalignment is expected to be small. However, in order to be certain that the desired cancellation is obtained—or to know to what accuracy the cancellation is obtained—the full set of telescope parameters must be determined for each telescope azimuth.

A particularly troublesome feature which remains is expressed by the 12 and 21 terms of the telescope matrix. This is a rotation of the so-called "position angle" which is not canceled by a rotatable telescope.

The rotatable telescope is not particularly helpful in removing systematic effects in the determination of the third Stokes parameter (ellipticity of polarization).

It is a pleasure to acknowledge a grant from the National Science Foundation which has assisted in this work.

References

1. R. Clark Jones, J. Opt. Soc. Am. **46,** 126 (1956), and references given there.
2. K. C. Westfold, J. Opt. Soc. Am. **49,** 717 (1959).
3. E. Wolf, Nuovo cimento **12,** 884 (1954); **13,** 1165 (1959).
4. G. B. Parrent and P. Roman, Nuovo cimento **15,** 370 (1960).
5. H. Mueller, J. Opt. Soc. Am. **38,** 661(A) (1948).
6. T. Gehrels, Astron. J. **65,** 466 (1960).
7. J. S. Hall, Astron. J. **54,** 187 (1949); V. A. Dombrovsky, Astron. J. USSR **30,** 603 (1953).
8. See, for example, W. H. McMaster, Rev. Mod. Phys. **33,** 8 (1961). Also K. Westfold, Astrophys. J. **130,** 241 (1959).
9. J. S. Hall, Lowell Observatory Bulletin **4,** 264 (1960). (Especially the reports by A. Behr and K. Serkowski.)

---

continued from page 66

By comparison of Eqs. (1) and (3) one finds the relationships

$$I(X) = 1 - 2q, \quad (4)$$

where

$$X = X(q)/\sqrt{2}. \quad (5)$$

From the experimental value of I, one calculates q from Eq. (4). Then, using a polynomial approximation for $X(q)$ (see ref. 2, p. 191) one determines the initial approximate value of X from Eq. (5). The value of X so derived is introduced into another polynomial approximation (see ref. 2, p. 187), this time for the integral of interest, Eq. (1), and an approximate value of $I(X)$, I^*, is computed. Using the monotonicity of $I(X)$ and $I^*(X)$ regarded as functions of X, a comparison of $I(X)$ and $I^*(X)$ permits the forming of a sequence of nested intervals about the proper value of X. This sequence may be stopped at any given degree of accuracy, but determination of X to within $\pm 10^{-7}$ is within the accuracy of the other approximations and is currently being used. The entire computation of the inverse error function X is schematically represented in the flow chart illustrated in Fig. 1.

The program which we now have in operation† performs the over-all data analysis according to the method of Longsworth.[1] However, in addition to the computation of the diffusion coefficient corresponding to a particular elapsed time, $D(t)$, the intercept and slope of the least squares straight line formed by a plot of $D(t)$ vs $1/t$ are determined, providing, respectively, the diffusion coefficient at infinity time and the so-called zero time correction.

References

1. L. G. Longsworth, J. Am. Chem. Soc. **74,** 4155 (1952).
2. C. Hastings, Jr., *Approximations for Digital Computers* (Princeton Univ. Press, Princeton, New Jersey, 1955).

† All inquiries concerning the possible acquisition of a copy of this program should be addressed to S. A. Rice, Institute for the Study of Metals, University of Chicago, Chicago 37, Illinois.

Letters *continued on page 77*

Applied Optics

Letters to the Editor

Letters to the Editor should be addressed to the Editor, APPLIED OPTICS, 1155 16th St., N.W., Washington 6, D.C.

High-Speed Calculation of Diffusion Coefficients from Rayleigh Interference Fringes

Lee Hook, Warren W. Davis, and L. Kotin

University of Chicago, Chicago 37, Illinois.
Received 20 April 1962.

Mr. Hook and Mr. Davis are associated with the Operations Analysis Laboratory of the University. Mr. Kotin was at the Institute for the Study of Metals. His present address is Department of Chemistry, Washington University, St. Louis 30, Missouri.

This research was supported in part by grants from the National Science Foundation, the United States Public Health Service, and the Air Force Office of Scientific Research.

The determination of diffusion coefficients from Rayleigh interferometric data is a tedious and time-consuming task and therefore highly susceptible to human error. Mathematically, it is a straightforward problem to calculate a diffusion constant after the photographic plate containing the Rayleigh fringes has been analyzed, i.e., after the fringes have been numbered and their coordinates measured. However, due to the necessity of dealing with a rather large quantity of data, the arithmetical computations require an inordinately large expenditure of time to achieve the final result. It is for these reasons that we have constructed a program for the Univac I computer to perform the necessary data handling and computations.

The mathematical analysis of the optical data is well known[1] and need not be repeated here. A great part of the program involves questions of data manipulation and the performance of elementary algebraic operations, which require no special comment. However, it is pertinent to comment on one phase of the calculation which involves numerical analysis.

In the case of concentration independent diffusion coefficients to which we limit our considerations, the diffusion coefficient, D, is related to the fringe number, j, and the total number of fringes, J—both experimental quantities—by the equation

$$I(X) = \frac{2j-J}{J} = \frac{2}{\sqrt{\pi}} \int_0^X e^{-t^2}\, dt, \tag{1a}$$

$$X = \frac{x}{2(Dt)^{1/2}}, \tag{1b}$$

where x is the diffusion cell coordinate of fringe j and t is the elapsed time after the start of the diffusion process. Equation (1) is the essential link between the mathematical theory of diffusion and the experimentally observed Rayleigh fringes.

When diffusion coefficients are computed on a desk calculator it is customary to determine X by interpolation in a table of error functions. However, in programming the calculation for the computer it is highly desirable to avoid either the introduction into the program of a large number of X's which have been predetermined by interpolation or a table of error functions from which the computer will determine the X's. The prior calculation of the X's by interpolation is undesirable because of the considerable time and labor involved, and the table input is impractical because of the prohibitively large number of entries which must be stored in the computer. The course we have followed is the direct calculation of X and it is a discussion of the procedure employed to which we now turn.

The determination of X is most easily carried out by a trial and error technique which may be outlined as follows: A reasonably good estimate of X is made and the error integral in Eq. (1) is computed. The result is compared with the experimental quantity $I(X)$ and a new approximation is made for X, the modification determined by the degree of agreement with $I(X)$. In this manner the value of X may be determined to as high a degree of accuracy as is desired.

The numerical analysis we have employed requires the use of polynomial approximations for the error integral.[2] The initial estimate of X is determined by the following considerations: If q is defined by

$$q = \frac{1}{\sqrt{2\pi}} \int_{X(q)}^{\infty} e^{-t^2/2}\, dt, \tag{2}$$

then it is readily shown that

$$1 - 2q = \frac{2}{\sqrt{\pi}} \int_0^{X(q)/\sqrt{2}} e^{-t^2} dt. \tag{3}$$

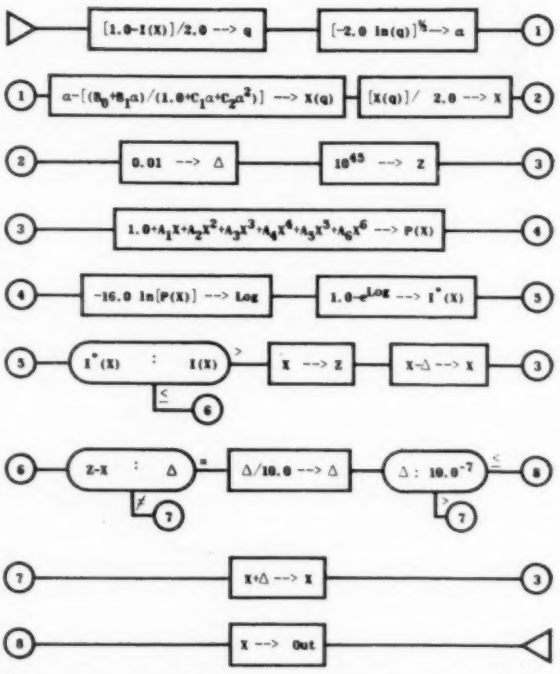

Fig. 1. Flow chart of the numerical computation of the inverse error function.

continued on page 65

The Wavelength Dependence of Polarization

Thomas Gehrels and Thomas M. Teska

Preliminary results are described of a program of polarimetry and photometry. Astronomical telescopes and a differential polarimeter are used with calibration by a Lyot depolarizer. The wide-band filters have effective wavelengths between 3250 Å and 9900 Å. The problems of instrumental polarization and depolarization are discussed; most of the instrumental effects can be avoided by proper aluminization of the telescope mirrors. The multiple molecular scattering of the sunlit sky and of the poles of Jupiter is closely represented by the Rayleigh-Chandrasekhar theory; the optical depth at the Jovian poles is 0.4–0.8. The same particle sizes that explain the interstellar reddening, 0.05–0.3 μ, are found from the interstellar polarization. Strong polarization-wavelength dependence is found for Venus and for lunar regions, but the detailed explanations require extension of the wavelength range. The range of wavelengths will be extended by using high-altitude balloons and spacecraft.

I. Introduction

The primary purpose of this study is to compare the particles that are between the planets with those between the stars. The sizes of these particles probably are near the wavelength of light, and the polarization of the light scattered by such particles is strongly wavelength-dependent (see ref. 1, pp. 152–153). Polarimetry over a wide range of wavelengths may therefore yield many parameters from which to study the particle size and refractive index. Colors are also determined, in addition to the amount and the orientation of plane-polarization. No measurements have as yet been made to distinguish elliptical polarization.

Strong wavelength dependence of the polarization was discovered on Venus and other astronomical objects. Apparently only little is known to date about the dispersion of polarization; the available references are given in the last paragraph of Section III. The present paper contains a summary of our results (the details are being published[2–5]), and of preparations for future work in order to extend the range of wavelengths.

II. Instrumentation

Techniques of polarization measurements have been discussed in a chapter by Hiltner,[6] who built and tested a two-beam polarimeter in 1951. Our photometer/polarimeter was assembled in 1958, and the equipment and reduction method have been described in detail.[7] A Wollaston-type prism, with two photomultipliers following it, is successively set at six or seven position angles. At each angle a pair of integrations is made with and without a Lyot depolarizer inserted in the incoming beam; thus a nearly simultaneous calibration is obtained. Lyot depolarizers have been described[8–10]; they consist of two quartz disks, with thicknesses e and $2e$, cut parallel to the optical axis; the two disks are put together with 45° between the axes.

Because of close calibration and simultaneous observation of both polarization planes, the measurements are not affected by flexure of the telescope and polarimeter, or by thin clouds and poor seeing (provided the seeing disk is smaller than the photometer diaphragm). When the objects are bright enough so that there are no statistical problems with dark current, the precision of the published results is with probable error $\pm 0.07\%$, or ± 0.0015 mag. (The percentage polarization being defined by $P = 100\,(I_1 - I_2)/(I_1 + I_2)$, or in astronomical magnitudes $p = 2.5 \log_{10}(I_1/I_2) \simeq P/46.05$; I_1 and I_2 are the intensities of electric-vector maximum and minimum, respectively.) A paper has been published[5] giving the details of the determination of the precision. The precision in a program on Venus is $\pm 0.055\%$.

The reductions for each position angle, μ, of the Wollaston prism are made with a simple least-squares solution of

$$\cos 2\mu\,(a \cos 2b) + \sin 2\mu\,(a \sin 2b) = f(m),$$

where $f(m)$ is a function of the tube outputs, a is the amount of plane polarization, and b is the position angle

---

Part of the work was done when the authors were at Indiana University; they are now at the University of Arizona.

Received 15 May 1962.

of the electric-vector maximum. A method of calibration of the position angle has been described.[7]

Four different telescopes have been used to date: the 82-in. (208-cm) and 36-in. (91-cm) Cassegrain telescopes of the McDonald Observatory, the 36-in. (91-cm) prime-focus reflector of the Goethe Link Observatory, and the 36-in. (91-cm) Cassegrain telescope of the Kitt Peak National Observatory.* A Barlow lens was used at the Goethe Link telescope, so that all observations were made at an f-ratio near $f/13$, with focal plane diaphragms of 4 to 30 sec of arc in diameter. The filters are combinations of standard Corning and Jena filter glasses with widths between 300 and 1400 Å (in exceptional cases as wide as 2700 Å). With the ultraviolet filters, solutions of nickel-sulfate and copper-sulfate are used to eliminate red leaks.[7] The present range of wavelengths is $1/\lambda = 1.01$–$3.08\ \mu^{-1}$ (9900–3250 Å). We use $1/\lambda$ in all wavelength designations, rather than λ, for it is the number of waves across the particle that characterizes the scattering properties.

After the description of the photometer was published[7] the following improvements were made to the equipment. In addition to RCA 7265 photomultiplier tubes for the ultraviolet, and RCA 7102 for the infrared, we now also use EMI 6255*S* tubes. The EMI tube has a fused silica window, and the nickel-sulfate filter was slightly modified (stock thickness Corning 9863 plus 8.7 mm thickness of a solution: 412 g $NiSO_4 \cdot 6H_2O$ plus 5.2 g $CuSO_4 \cdot 5H_2O$ plus 1 liter H_2O; and a disk of 1.6 mm thickness of fused silica). Spectrophotometer tracings have been made for our liquid filters at temperatures between 0°C and 45°C, and no shift in the effective wavelengths was found greater than about 20 Å. However, if one should use such liquids to determine precisely the filter characteristics, especially at the short-wavelength side, rather than in the present application to eliminate red leaks, one must indeed guard against temperature variations as they affect the filter width and over-all transmission. We are indebted to J. S. Neff for pointing out these effects, and to S. F. Pellicori for making the spectrophotometer tracings.

III. Checks of Reliability

The reliability of the polarimetric results is determined from laboratory checks, and from an intercomparison of the obtained results. Nonpolarized stars are observed during each observing session. These are near-by stars, and it is usually known from previous observations that they show very little polarization, if any. About ten stars per observing run are observed, chosen at various galactic longitudes so that their planes of polarization, if any, should be oriented approximately at random. The average of the observations on these ten stars is taken and, because of the supposedly random orientations, the average should be near zero.

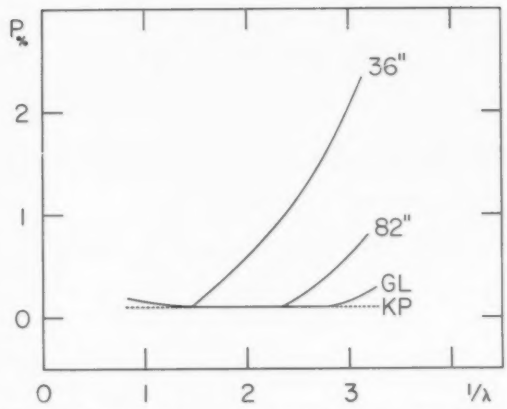

Fig. 1. Ordinates: percentage polarization. Abscissae: reciprocal of the wavelength in microns. Polarization introduced by the aluminized mirrors of the McDonald 36-in. (91-cm) and 82-in. (208-cm) telescopes (in 1959), the Goethe Link 36-in. (91-cm) primary mirror (1960), and the Kitt Peak 36-in. (91-cm) reflector (1961).

The findings on the instrumental polarizations caused by aluminized mirrors were published[2]; some mirrors have appreciable polarization, especially in the ultraviolet, as is shown in Fig. 1. The explanation is sought either in a diffraction effect, or in a differential absorption, in the crystalline structure of the aluminized layer. The effects are probably caused by asymmetric procedures during aluminization. The effects apparently can be avoided by using the glow discharge sparingly, preferably from electrode disks that are parallel to and slightly larger than the mirror surface. In Fig. 1, a residual polarization of 0.11% ± 0.03 appears common to all four telescopes with different position angles at different wavelengths. The residual polarizations, if real, apparently originate within the photometer.

At least as important as the tests for instrumental polarization are those for instrumental *de*polarization. We usually order two identical Wollaston prisms whenever one is needed. One of the two is, of course, installed in the polarimeter. During the test the second Wollaston is mounted in front of the telescope, or immediately in front of the polarimeter, and the light of one of its beams is observed. Should we be able to isolate one of the beams perfectly, the observed amount of polarization is 100%, provided, of course, that the mirrors, the Wollastons, and the polarimeter are perfect. It has been found before[2] that the aluminized mirrors of the McDonald 208-cm telescope were free of depolarization effects; the same conclusion is presently derived from a series of tests on the 91-cm mirror of the

* Recently, the 21-in. (53-cm) reflector of the Lowell Observatory has been used.

Goethe Link Observatory. Slight depolarization was found in the Wollaston photometer,[2] but some of this defect may not be real. Most of the instrumental depolarization previously reported[2] must be ascribed to multiple scattering by the air in front of the photometer, rather than to multiple scattering within the Wollaston prism. We have now succeeded in eliminating most, if not all, of such scattered light during the tests; we are indebted to R. E. Samuelson for his help. With various filters, 27 observations were made; the average of the observed polarization is 97.90% ±0.24 p.e. No wavelength dependence was found; all of the usual filters were employed except the one in the extreme ultraviolet, at $1/\lambda = 3.08$, for lack of a suitable light source. The deficiency of the depolarizer[2] is 1.20%. It follows that one Wollaston prism causes 0.45% depolarization. The photometer, that is one Wollaston plus depolarizer, then has 1.65% deficiency. For ease of conversion, a *correction factor* is defined, by

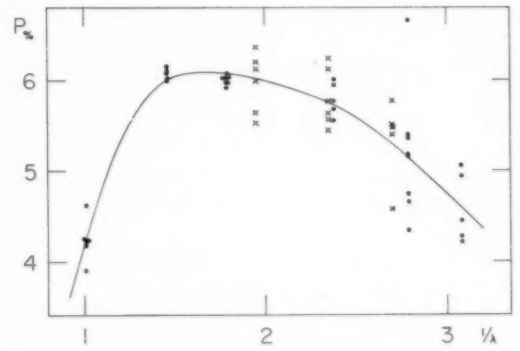

Fig. 2. Interstellar polarization, observed by Behr (crosses), and in the present program (filled circles). The apparent small scatter at $1/\lambda = 1.46$ and 1.79 is a result of the normalization process.

which all observed amounts of polarization are multiplied before publication. The presently determined correction factor is $100/(100 - 1.65) = 1.0168$. The polarization is now known in *absolute* amount; except for objects that are as strongly polarized as the sunlit blue sky, the accuracy is better than ±0.1% (±0.002 mag.).

Intercomparison of our observations indicates that the polarimeter gives consistent results. For instance, large amounts of polarization have been found for lunar regions near quarter phase, as shown below in Fig. 8. Toward zero phase, however, these polarizations uniformly vanish, as is expected from symmetry considerations. The position angles of polarization maximum were found on the sunlit blue sky[4] to be closely the same for observations made during various observing runs.

The agreement with the results of other observers is satisfactory. The polarizations observed with the green filter on lunar regions, Mars, Venus, and on Jupiter and its poles are in general agreement with those made visually by Lyot.[8] The present range of wavelengths is greater than that used by other observers, but, whenever observations were made at similar wavelengths, the agreement is good. The numerical agreement with Behr[12,2] on the amount of instrumental polarization of the McDonald 91-cm reflector is close, and that on the interstellar polarization[13,3] is good on the average, as is shown in Fig. 2. The comparison with observations made by Sekera on the sunlit blue sky[14,4] is good, and the same applies to the comparison with the work of Dollfus on Venus.[15,11] Agreement, allowing for phase differences, with the work on Mars by Treanor,[16] by Sobieski,[17] and by Dollfus[15] is seen below in Fig. 10, Section VIII. There is fair agreement with the position angles determined by other observers of interstellar polarization [3]

IV. Rayleigh Scattering

For the study of a complex planetary atmosphere such as that of Venus it appears valuable to study first the simpler case of the molecular scattering of the sunlit blue sky.[4] The polarization of the daytime sky has a maximum near 5500 Å, as is shown in Fig. 3. The decline in the ultraviolet is caused by multiple scattering, while in the infrared it is mostly due to ground reflection that is especially strong when green plants are present. The maximum was found near 75% polarization. The agreement of the Rayleigh-Chandrasekhar theory with the observations is good. The lack of complete polarization appears due to molecular anisotropy (6%), multiple scattering (6%), and ground reflection (5%), while there is a discrepancy between molecular theory and the observations, presumably due to aerosols (8%). At the time of sunrise, the polarization in the infrared was found to be as high as 84%, and

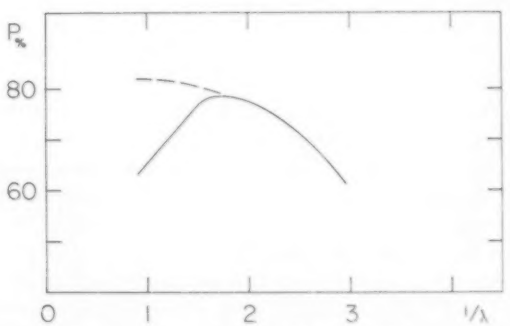

Fig. 3. Polarization of the clear blue sky 90° from the sun, observed on the morning of August 31, 1960, at the McDonald Observatory; with the sun 3° below (broken line), and 4° above the apparent horizon.

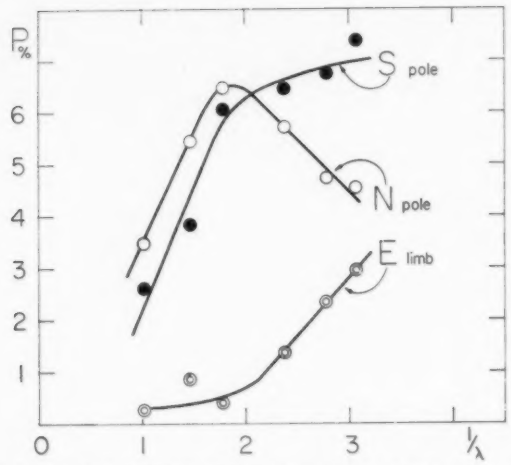

Fig. 4. Polarizations at the South Pole, North Pole, and East limb of Jupiter. Observations made with a 4 sec-of-arc diaphragm, in April 1960.

therefore greater than that in the green and in the ultraviolet. However, within about 20 min after sunrise the polarization in the infrared (for a clear sky but with vegetation around the observatory) was found to drop to 64%, which is appreciably less than the amounts in the green and ultraviolet. During the remainder of the day the polarization of the clear blue sky at 90° phase does not change appreciably.

It appears important to improve further the comparison between the observations and the theory of the sunlit blue sky. Since 1871, when Lord Rayleigh first attempted the comparison, the challenge has been recognized and progress has been made step by step. The main uncertainty presently lies in the unknown reflectivity of the ground and surface haze. We are therefore planning to repeat the measurements from a balloon, in order to include simultaneous measurements of the reflectivity of the ground and surface haze below the balloon. Thus the comparison between observations and the Rayleigh–Chandrasekhar theory may be improved, or a well-observed difference between observations and theory may allow us to determine the scattering by aerosols.

The polarization of the total disk of Jupiter is slight, but at the poles there always is up to 8% polarization, nearly independent of the planetary phase angle. Lyot[8] discovered the anomalous polarization and tentatively explained it by multiple scattering in the molecular part of the Jovian upper atmosphere. Other explanations have at times been proposed in the literature, by a thin fog or by meteoric dust particles. The wavelength dependence of the polarization[5] is shown in Fig. 4; again, as for the sunlit blue sky, the agreement of the Rayleigh–Chandrasekhar theory with the observations is close. Apparently, molecular scattering by the gas above the cloud layers explains the polarizations. From a comparison with the theory it is found that the optical thickness at 5500 Å lies between 0.4 and 0.8.

Effects similar to those for Jupiter have been observed on Saturn. In general, it appears that the wavelength dependence of polarization may be used for the detection of planetary molecular atmospheres. Even at small phase angles the polarization caused by Rayleigh scattering may still be appreciable. Such attempts for the detection of an atmosphere could be made with some effort for Pluto, Triton, Titan, etc. The results on the Jovian satellites I–IV so far have been inconclusive; the main uncertainty lies in scattered light within the telescope and earth's atmosphere from the bright disk of Jupiter.

V. Interstellar Particles

The wavelength dependence of the interstellar polarization is shown in Figs. 2 and 5. Details of this work have been published[3] (plots of two individual stars are in Fig. 3 of ref. 18). The wavelength dependence can be qualitatively interpreted by means of the calculations of van de Hulst (ref. 1, Chap. 15). The particles presumably are conglomerates of some 10^6 molecules each, the refractive index is about 1.5 (with imaginary component), and the diameters are of the order of 0.6 μ (although they are not spherical, but rather elongated particles).

The exact nature of the interstellar particles is still unknown as there is a complex set of parameters (e.g., size, refractive index, aspect) each strongly affecting the characteristics one might observe. Extension of the wavelength range of the observations is obviously important. Progress is being made by H. L. Johnson with infrared stellar photometry. It is seen (ref. 1) that an extension to wavelengths shorter than 3000 Å,

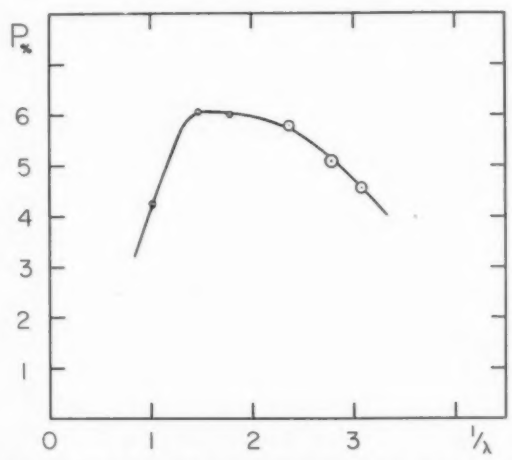

Fig. 5. Normalized average of interstellar polarization, observed on 8 stars that are at various galactic longitudes.

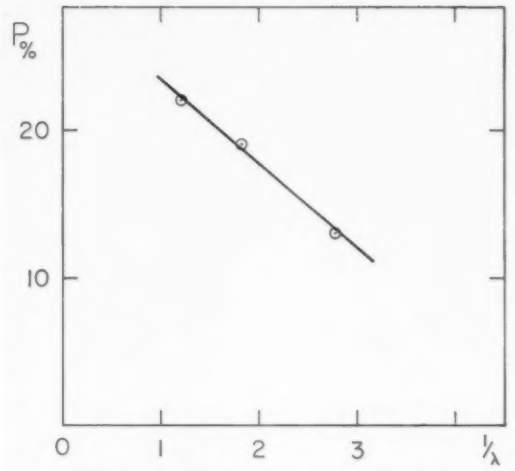

Fig. 6. Polarization in reflection nebulae, observed on small regions in NGC 7023 and NGC 2068.

especially for observations of interstellar reddening, could be especially important in resolving the nature of the particles. The measurements will have to be made at various galactic longitudes since Greenberg and Meltzer[19] have shown that differences in aspect also play a role.

Also on reflection nebulae the wavelength dependence of polarization is an effective tool in the study of interstellar particles. The light is scattered by particles that surround a star, the scattering angles are of the order of 90°, and the polarization phenomena are pronounced. The scattering should be mostly single because of low particle density so that the complications of multiple scattering need not be taken into account. The application of the Mie theory to a sufficient number of parameters of brightness and polarization at different wavelengths may yield the refractive index of the particles, the size, and perhaps even the size distribution. In actual practice it is difficult to observe with many filters at a wide range of wavelengths because the reflection nebulae are faint. The background sky-brightness must be carefully corrected for in order to avoid systematic errors. A preliminary result for two reflection nebulae, NGC 7023 and NGC 2068, is shown in Fig. 6, as obtained with three wideband filters; the electric-vector maximum is tangential with respect to the illuminating star. The measurements were made with a diaphragm 22 sec of arc in diameter, and we normalized to the amount of polarization at 38 sec of arc northeast of the central star in NGC 7023.

For the intercomparison of the particles between the planets with those between the stars it is important to observe the Zodiacal Light. As to the origin of the Zodiacal Light it is still uncertain whether it is due to scattering by particles or by electrons. The wavelength dependence of polarization, if it can be observed, may give the answer to this question. If no polarization dispersion is found, the Zodiacal Light probably is caused by electron scattering. Appreciable wavelength dependence, on the other hand, probably implies predominant scattering by small particles, and the particle characteristics may then be obtained from a fit of the Mie theory to the observations.

Observations of reflection nebulae and of comet tails are difficult to obtain free of systematic errors because of emission effects. Some of the emissions may be avoided by a choice of proper filters, and then the main problems are sky background and phototube noise.

VI. Venus

The atmosphere of Venus is complicated in that the scattering observed at different wavelengths is caused at different altitudes as well as by different constituents in the atmosphere. Figure 7 shows the percentage polarization as a function of phase, observed between the inferior conjunction of August 1959 and the superior conjunction of June 1960; a preliminary report has been published.[11] The curves are drawn closely through the observations that were made with six filters: Infrared (effective wavelength near 9900 Å), Red (6830 Å), Green (5600 Å), Blue (4200 Å), Ultraviolet (3590 Å), and a filter at 3250 Å, isolated by using a Nickel-sulfate solution. The scatter of the Venus observations about the mean curves corresponds to the observational precision (±0.055% p.e.), which indicates that Venus is remarkably steady from night to night. The N-curve is given with a dashed line so as to indicate that it has not yet been as well established as the other curves. The uncertainty may, however, be intrinsic in that the polarization of Venus at short wavelengths may be irregularly variab e.

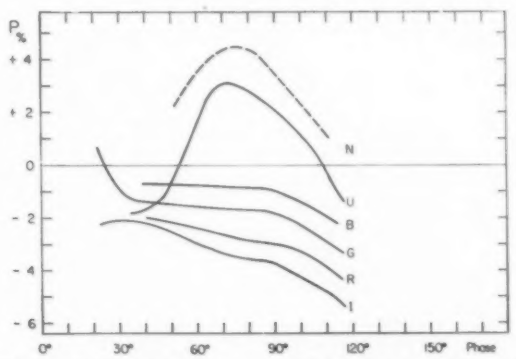

Fig. 7. Polarization of the total disk of Venus, as a function of phase: from 117° on October 8, 1959, until 19° on May 3, 1960. Observations with Infrared, Red, Green, Blue, and Ultraviolet filters, and with a filter near 3250 Å that uses a Nickel-sulfate solution.

The polarization at longer wavelengths is negative, that is, with the electric-vector maximum in the plane of the ecliptic. Predominant in visual light and at longer wavelengths probably is the scattering by large (micron-size) particles, crystals, or droplets. The polarization in the ultraviolet is entirely different, it has the electric-vector maximum perpendicular to the ecliptic and the phase dependence is strong. Predominant in the ultraviolet probably is molecular scattering or scattering by very small particles, or both.

Observations are needed at the shortest possible wavelengths, and they may be obtained with high-altitude balloons (*viz.* Section IX). With measurements made at wavelengths shorter than 3250 Å, it is expected that a detailed fit to the Rayleigh-Chandrasekhar theory will account for the contribution by the molecular scattering. The residuals will then be explained as due to the scattering by particles, and they may be compared with the Mie theory so as to obtain a determination of refractive index and particle sizes.

The range of wavelengths should be extended also into the far infrared. Since Venus is bright, the lack of sensitive detectors is not serious, and we are planning polarization measurements at 1.3, 2.2, and 3.6 μ. Beyond 3 μ there apparently are strong absorptions in the atmosphere of Venus, as the brightness of Venus at 3.6 μ is magnitudes fainter than that at shorter wavelengths.[20]

VII. The Moon and the Asteroids

Mercury, the asteroids, and most of the satellites, form a special category because of the lack of a molecular atmosphere. They may have a surface layer of fine particles, but effects of multiple scattering and of the background may complicate the phenomena. In preparation is a paper with observational results on colors and polarization of seven small regions on the surface of the moon over a large range of phase and also closely before and after a lunar eclipse. The observations were mostly made at the Cassegrain focus of the 208-cm McDonald telescope, and the lunar regions have a diameter of the order of 4 sec of arc. A preliminary result, published previously,[18] on one of the seven regions is given in Fig. 8, while the wavelength dependence is shown in Fig. 9.

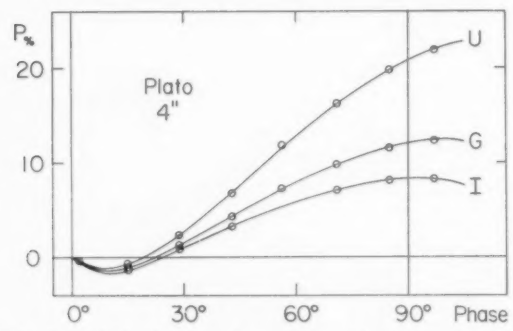

Fig. 8. Polarization of a 4 sec-of-arc region at the bottom of lunar crater Plato, as a function of phase. Observations made with the McDonald 82-in. (208-cm) telescope, April 23–30, 1959, with Ultraviolet, Green, and Infrared filters.

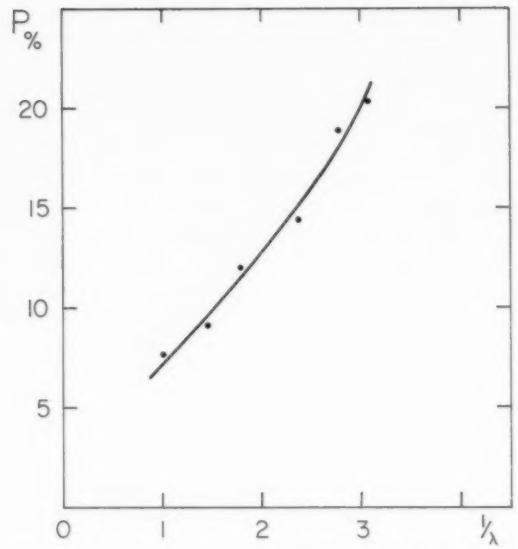

Fig. 9. Polarization of Mare Crisium near 90° phase.

Polarimetry is useful for intercomparisons between the surface of the moon and that of the asteroids, especially when combined with laboratory measurements.[8,15] Lyot concluded that the moon is covered with small particles having diameters of the order of 1 μ, for example, lava dust. This conclusion should not be misinterpreted as a proof of the existence of lava dust on the lunar surface, because other fine particles may give the same results. The choice of particles may be narrowed down by obtaining the parameters of polarization and intensity, both simultaneously, over a wide range of wavelength and phase.

As for the light variations of the asteroids one problem has not yet been solved. Is the brightness variation with rotation due to change of the projected area, that is, due to the shape of the asteroid, or is it due to the asteroid's body having different albedo at different parts of the surface, or to both? Polarimetry may give the answer to this question. It is known for the lunar surface that the dark areas have a larger amount of polarization than the bright areas. If the same is true on the asteroids, we would be able to observe a change in the amount of polarization with rotational phase. That is, as the asteroid is brighter, the polarization would be less, etc. A polarization curve would be observed as well as a light curve. Provin started this type of study and found little polarization–time variation for Iris.[15] It is essential, however, to obtain

the brightness–time variation simultaneously. Because of aspect variation Iris may have had small light curve amplitude at the time of Provin's polarization measures.[21] Our first polarization attempts have also given inconclusive results, which may mean that the bodies of the asteroids have rather uniform albedo over the surface and that the observed brightness variations are due to shape only. However, this is no more than a preliminary conclusion and further work is especially valuable on an asteroid with large amplitude of light variation and at large phase angle.

VIII. Miscellaneous Measures

A few miscellaneous measures are given in Table I. The phase angle is the angle subtended at the object between the radius vectors to the sun and earth. In addition to P, the percentage polarization, the position angle, θ_r, is given which is the position angle of the electric-vector maximum with respect to the normal to the plane through object-sun-earth (position angles are usually given between 0° and 180° only). The observations on comet Burnham are preliminary; a wide diaphragm was used, centered on the nucleus; no correction was made for emission effects. Colons in Table I indicate low quality of observation.

Table I. Miscellaneous Polarizations

Object	Date U.T.	Phase angle (deg)	1/λ	P (%)	θ_r (deg)
Comet Burnham (1959 k)	60.05.02	65	1.20	14.6	1
	60.05.04		1.20	14.4:	178:
	60.05.03		1.82	8.9:	171:
	60.05.03		2.38	8.3	5
	60.05.06		2.38	6.7:	177:
	60.05.03		2.78	8.4:	7:
Mars	59.04.24	33.4	1.01	1.08	1.4
			1.79	1.83	178.8
			2.79	6.88:	0.7
	59.04.25	33.3	1.01	1.05	3.5
			1.79	1.65	1.8
			2.79	6.74:	179.6
	59.04.28	32.9	1.01	1.00	4.2
			1.79	1.72	178.7
			2.79	6.32:	179.1
	59.08.04	8.0	1.46	0.89:	116.2:
			2.38	0.53:	94.6:
	59.08.10	7.4	1.01	0.38	149.2
	60.08.18	43.2	1.01	3.15	0.4
			1.79	3.47	2.0
			1.46	2.49:	7.7:
	60.08.22	43.3	2.38	4.93:	4.1:
			3.08	1.52:	1.7:
	60.08.23	43.3	1.01	2.52	179.2
			1.79	3.28	3.2
			2.79	0.06	1.4
	60.08.29	43.4	1.46	1.70	178.9
			2.38	4.28	5.7
			3.08	9.80:	2.2
	61.03.17	36.1	1.01	1.53	12.4
			1.79	1.94	175.9
			2.79	7.56:	172.2
Mercury	59.12.04	111	1.01	6.7	...
	59.12.09	86	1.46	7.09	...
	59.12.04	111	1.79	8.0	...
	59.12.09	86	2.38	8.7	...
	59.12.04	111	2.79	9.4:	...
	59.12.09	86	3.08	11.1:	...
	61.11.10	73	1.01	5.91	179.0

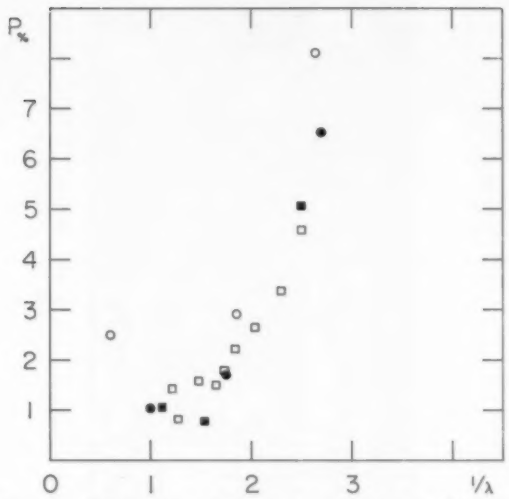

Fig. 10. Polarization of Mars, observed by: Dollfus, near 35° phase, 1949/1950 (open squares); Treanor, at 35°.5 phase, May 1961 (filled squares); Sobieski, at 36°.4 phase, March 1961 (open circles); and in the present program, near 33° phase, April 1959 (filled circles).

Mars has an increasing amount of polarization toward shorter wavelengths, as was discovered by Dollfus.[15] A similar wavelength dependence of the polarization was observed by P. J. Treanor[16] with interference filters at eight wavelengths from 4000 to 9000 Å. In addition, Treanor found that, to the red of 6500 Å, the polarization increases slightly. A minimum near 0.8 μ is also confirmed by very preliminary measures (not plotted in Fig. 10) made by S. Sobieski.[17] In Fig. 10, we plotted our observations and those by Dollfus, Treanor, and Sobieski. Even though these observations were made at different dates and phases, the polarization dispersions are closely the same. Dollfus[15] has explained the wavelength dependence of the polarization by the presence of the Martian atmosphere.

Mercury was found to have approximately the same wavelength dependence as that of the lunar surface. The measurements are difficult, especially at shorter wavelengths, because of the proximity to the sun.

An attempt was made to discover polarization of the flare-star system Krüger 60, during the time of no-flare, but the results are inconclusive. No polarization greater than 0.4% was detected. At the request of K. Aa. Strand, we also checked for possible light-variations during the time of no-flare. Krüger 60 was observed with respect to a near-by star from 1^h30^m

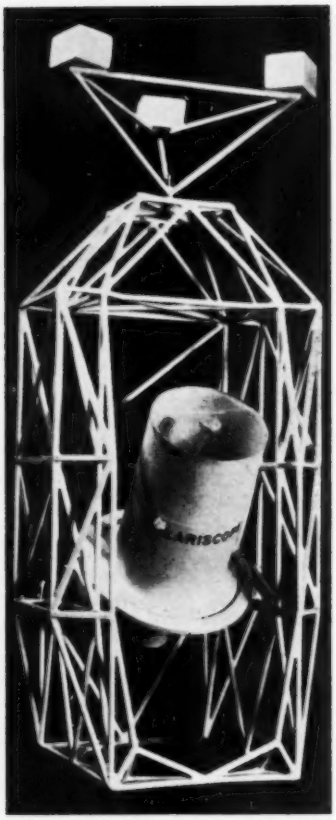

Fig. 11. Balsa-wood model of balloon gondola with 28-in. (71-cm) telescope.

until 8^h50^m on 19 October 1958 Universal Time. No brightness fluctuations were detected as the average deviation of individual measures from the mean light-level was ±0.005 mag, equal to the precision of such observations.[21] We would like to thank Dr. Strand for the loan of photometer equipment during the early stages of this program.

IX. Balloon Programs

We are presently preparing a balloon program, Project Polariscope, supported by the National Science Foundation, with the first flights scheduled for 1963. A model of the gondola and telescope system made by M. Diels is shown in Fig. 11. Figure 12 shows a diagram of the optical system. The primary is a 71-cm fused silica mirror, $f/2$; the Cassegrain focus operates at $f/13$ (Dall-Kirkham optics).

In addition to the system of Fig. 12, there is mounted a wide-angle polarimeter designed by a group working with Z. Sekera (see below), and a small telescope for photoelectric guiding. The attitude control is expected to hold to within ±20 sec of arc. The total weight of the system is of the order of 700 kg, and with a 10^7 ft^3 (3×10^5 m^3) balloon the estimated ceiling is near 35.4 km altitude. We are planning the following programs.

A. The Earth's Atmosphere and Albedo

In close collaboration with Z. Sekera of the University of California at Los Angeles, the relative intensity and the polarization at 5° intervals in the sun's vertical circle will be measured at various altitudes up to 35.4 km and over the greatest possible range of wavelengths. The telescope will be pointed below as well as above the gondola (except for 25° zenith distance obscured by the balloon). The main purposes are: (1) to obtain as closely as possible an intercomparison of the observations on the sunlit sky with the Rayleigh-Chandrasekhar theory (*viz.* Section IV); (2) to extend the study to that of aerosols in the earth's atmosphere; and (3) to determine reflectivities of clouds and of various parts of the earth's surface.

B. Measurements at Wavelengths Shorter than 3000 Å

The need for observations of the interstellar polarization and reddening and of polarization of the planet Venus at wavelengths shorter than 3000 Å is discussed in ref. 22 and in Sections V and VI of this paper. J. V. Dave recently supplied calculations of the attenuation due to molecular scattering, ozone, and oxygen above 33.5 km altitude. The calculations are

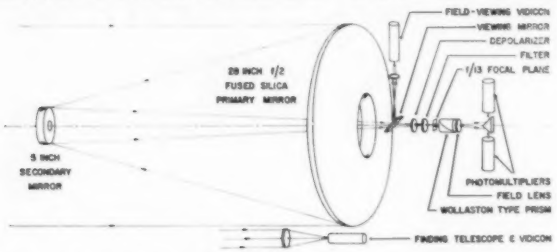

Fig. 12. Diagram of the 28-in. (71-cm) balloon telescope, the polarimeter, and the vidicons.

based on measurements during rocket flights[23] and on Tables 16-15, 16-16A, and 16-17 of the *Handbook of Geophysics*[24] (a factor 0.98 was used to obtain absorption coefficients for ozone at 245°K instead of the 291°K in the *Handbook*). With Dave's data, we compiled in Table II the extinction, in astronomical magnitudes $\Delta m = 2.5 \log_{10} I_1/I_2$, as a function of wavelength. The present calculations were made for latitudes near +35°. (We are indebted to Dr. Dave for his advice.) Wavelength intervals of 100 Å are used, and the calculations are for three altitudes, namely, 33.5, 36.6, and 39.6 km. The results are in general agreement with calculations previously obtained by other authors (see, for instance, ref. 25). The attenuations of Table II are typical values; above 33.5 km, the ozone concentration is less during the winter than during the summer. However, under unfavorable ozone conditions the totals in Table II may be greater by several magnitudes. A detailed analysis was made of the limiting magnitude of our polarimeter with a 71-cm

Table II. Attenuations at High Altitudes

Altitude	Constituent	Extinction, in magnitudes at $\sec z = 1$, at 2050 Å	2150 Å	2250 Å	2350 Å	2450 Å	2550 Å	2650 Å	2750 Å	2850 Å	2950 Å
	Scattering	0.05	0.04	0.03	0.02	0.02	0.02	0.01	0.01	0.01	0.01
	Oxygen	0.73	0.33	0.17	0.10	0.04	—	—	—	—	—
110,000 ft	Ozone (winter)	0.05	0.14	0.48	0.87	1.37	1.59	1.37	0.83	0.36	0.20
33.5 km	Ozone (summer)	0.21	0.58	1.67	3.56	5.59	6.52	5.59	3.40	1.48	0.47
20.8 miles	Sum (winter)	0.83	0.51	0.68	0.99	1.43	1.61	1.38	0.84	0.37	0.21
	Sum (summer)	0.99	0.95	1.87	3.68	5.65	6.54	5.60	3.41	1.49	0.48
	Scattering	0.04	0.03	0.02	0.02	0.02	0.01	0.01	0.01	0.01	0.01
	Oxygen	0.56	0.25	0.13	0.08	0.03	—	—	—	—	—
120,000 ft	Ozone (winter)	0.03	0.09	0.25	0.53	0.83	0.96	0.83	0.50	0.22	0.07
36.6 km	Ozone (summer)	0.17	0.45	1.32	2.80	4.40	5.13	4.40	2.68	1.16	0.37
22.7 miles	Sum (winter)	0.63	0.37	0.40	0.63	0.88	0.97	0.84	0.51	0.23	0.08
	Sum (summer)	0.77	0.73	1.47	2.90	4.45	5.14	4.41	2.69	1.17	0.38
	Scattering	0.02	0.02	0.02	0.01	0.01	0.01	0.01	0.01	0.01	0.01
	Oxygen	0.38	0.17	0.09	0.05	0.02	—	—	—	—	—
130,000 ft	Ozone (winter)	0.02	0.04	0.12	0.26	0.41	0.48	0.41	0.25	0.11	0.03
39.6 km	Ozone (summer)	0.12	0.31	0.90	1.92	3.01	3.51	3.01	1.83	0.80	0.25
28.4 miles	Sum (winter)	0.42	0.23	0.23	0.32	0.44	0.49	0.42	0.26	0.12	0.04
	Sum (summer)	0.52	0.50	1.01	1.98	3.04	3.52	3.02	1.84	0.81	0.26

telescope and with wide-band filters using selected photomultipliers. It appears possible, even during the most unfavorable ozone concentration, to observe the brighter stars and planets at 2200 Å, at altitudes above 33.5 km.

C. Other Studies

With a 71-cm balloon telescope there is a host of possible studies, such as: narrow-band photometry on absorption features due to water vapor, etc., in planetary atmospheres; ultraviolet and infrared photometry and spectroscopy; studies of cloud formations; polarimetry of the Zodiacal Light at various wavelengths; etc. If we do not lose the system in flight, it will be flown repeatedly, and also for programs of other investigators.

X. Polarimeters for Unmanned Spacecraft

The polarimeter/photometer of Fig. 12 may serve as a "pilot model" for space telescopes such as the NASA Orbiting Astronomical Observatories and those of the Kitt Peak National Observatory. Experience will be gained during the balloon flights with data acquisition, telemetry, etc.

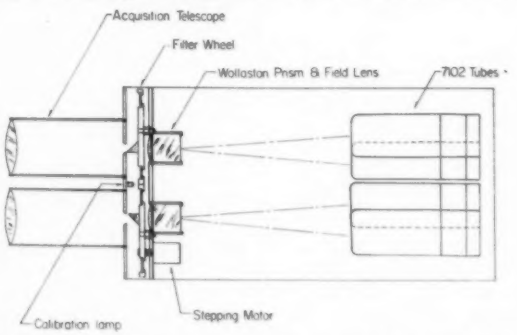

Fig. 13. A lightweight polarimeter/photometer for MARINER-type space probe.

Another type of polarimeter, shown in Fig. 13, was designed for lightweight planetary probes. The advantage of making polarization measures from a space probe lies in the possibility of making a detailed scan of the surface of the planet due to the close approach by the probe to the planet. Also, especially for Mars, large phase angles are possible by choice of a suitable fly-by. In principle the photometer is similar to the one used by us with telescopes on the ground; the modifications are dictated by weight limitations, by the automation, and by the need to have few moving parts. The design consists of two adjacent telescopes, two diaphragms, the filter and calibration wheels, the field lenses ("Fabry lenses"), the Wollaston prisms, and the phototubes.

The total weight of this system is under 4.5 kg, it is about 40 cm long, and it requires less than 5 W of power. Approximately the following effective wavelengths are proposed: 2900, 3500, 4300, 5600, 6900, and 9900 Å (having nearly equal spacings in $1/\lambda$). The prisms are calcite Wollastons, with butyl methacrylate cement; an alternate solution is to have ammonium di-hydrogen phosphate (ADP) with the halves in optical contact. Transistorized electrometer-type operational amplifiers accept the photocurrents, and a programmer follows the output of each phototube and pulses the stepping motor for rotation of the filter wheel after each observation. The disk of Mars, for instance, could be scanned at the rate of once per minute; the scans are proposed to be over the center of the planetary disk, with the scans in the direction of the motion of the space probe.

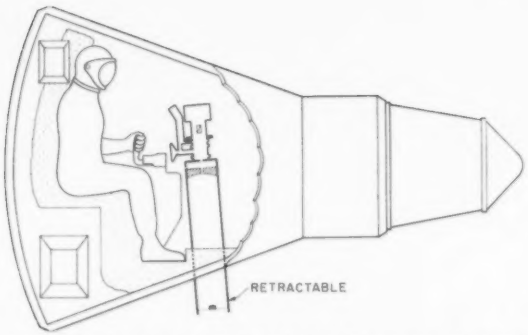

Fig. 14. The MERCURY capsule with a photometer/polarimeter instead of the original MERCURY periscope.

The space-probe polarimeter of Fig. 13 will be flown and used on board the balloon gondola described in Section IX. The special application on board the space probe will, of course, require detailed technical studies imposed by the environment and by the integration of the polarimeter with the space probe. The telemetry of the commands and observations will be a part of the general system of the probe.

XI. A Polarimeter for Manned Space Craft

The polarimeter that we have used extensively with telescopes on the ground can be used, after relatively minor modifications, in manned observations in a balloon gondola (e.g., the Stratolab gondola of the U.S. Navy), and in manned spacecraft (f.i., the Mercury, Gemini, and Apollo capsules). A sketch of such an arrangement is given in Fig. 14, while the details of the photometer are shown schematically in Fig. 15; the knobs will actually be at right angles to the eyepieces.

In 20 min or so the astronaut can make a set of measurements of polarization, photometry, and photography of Venus, for instance, at two or three different wavelengths in the extreme ultraviolet. A preliminary reconnaissance has been made of the engineering problems for mounting a polarimeter on board the Mercury capsule. (We are indebted to A. E. Lombard and M. Witunski of the McDonnell Aircraft Corporation for their technical assistance.) The most serious problem probably is that of close attitude control (±8 min of arc). It is, of course, of the greatest importance to make the photometer lightweight. The expected power requirement, 16 W or less, does not appear prohibitive.

XII. Concluding Remarks

Polarimetry is a powerful tool applicable to a wide range of subjects. A variety of techniques is possible, and they need not be complicated. We have not as yet undertaken a study of elliptical polarization; such a study appears to be an important challenge. No polarization-wavelength measurements have as yet been made of synchrotron radiation, for instance in the Crab Nebula. There is also a lack of polarization experiments in the laboratory. Lyot's laboratory work was done in visual light only, and progress may be expected from an extension to the greatest possible range of wavelengths.

This program has been supported by grants from the Office of Naval Research to Indiana University and to the University of Arizona. The following people have worked with us: S. F. Pellicori in the Electronics Shop; R. E. Samuelson, H. J. Wood, and A. U. Landolt at the telescopes; E. C. Olson and D. Fischel programmed routines for IBM 650 and IBM 709, respectively; and Mrs. D. J. Owings has made nearly all of the reductions. We would also like to acknowledge the cooperation of the Research Computing Center of Indiana University.

References

1. H. C. van de Hulst, *Light Scattering by Small Particles* (Wiley, New York; Chapman & Hall, London, 1957).
2. T. Gehrels, Astron. J. **65,** 466 (1960), Paper I.
3. T. Gehrels, Astron. J. **65,** 470 (1960), Paper II.
4. T. Gehrels, J. Opt. Soc. Am. **52,** 1164 (1962).
5. T. Gehrels, Astron. J. (1963), Paper III, to be published.
6. W. A. Hiltner, *Astronomical Techniques* (Univ. of Chicago Press, Chicago, Illinois, 1962), Chap. 10.

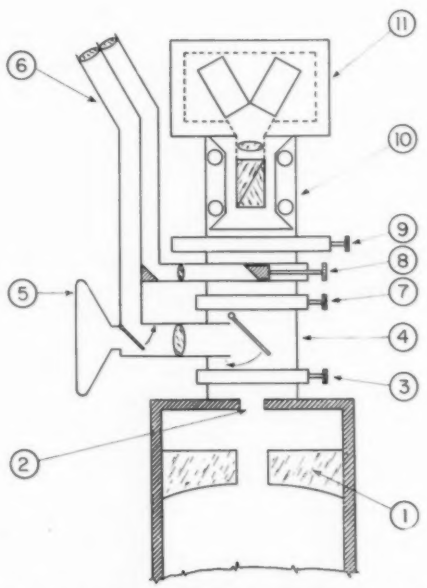

Fig. 15. Components of the photometer/polarimeter of Fig. 14: (1) 8-in. (20-cm) Cassegrain $f/10$ telescope; (2) quartz pressure-port; (3) Lyot depolarizer; (4) viewing mirror; (5) camera; (6) eyepieces, schematically drawn; (7) diaphragms; (8) viewing prism; (9) filters; (10) rotating assembly for Wollaston prism, field lens, and (11) electrically refrigerated phototubes.

7. T. Gehrels and T. M. Teska, Publs. Astron. Soc. Pacific **72,** 115 (1960).
8. B. Lyot, Ann. Obs. Paris (Sec. Meudon) **8,** Pt. 1 (1929).
9. J. S. Hall and A. H. Mikesell, Publ. U.S. Naval Obs. **17,** 10 (1950).
10. B. H. Billings, J. Opt. Soc. Am. **41,** 966 (1951).
11. T. Gehrels and R. E. Samuelson, Astrophys. J. **134,** 1022 (1961).
12. A. Behr, Lowell Obs. Bull. **4,** 292 (1960).
13. A. Behr, Z. Astrophys. **47,** 54 (1959).
14. Z. Sekera, *Advances in Geophysics*, edited by H. E. Landsberg (Academic Press, New York, 1956), Vol. 3.
15. A. Dollfus, *Planets and Satellites*, edited by G. P. Kuiper and B. M. Middlehurst (Univ. of Chicago Press, Chicago, Illinois, 1961).
16. Yearly Report, Yerkes Observatory, Astron. J. **66,** 496 (1961).
17. S. Sobieski, personal communication.
18. T. Gehrels, Lowell Obs. Bull. **4,** 300 (1960).
19. J. M. Greenberg and A. S. Meltzer, Astrophys. J. **132,** 667 (1960).
20. H. L. Johnson, personal communication.
21. T. Gehrels and D. Owings, Astrophys. J. **135,** 906 (1962).
22. T. Gehrels, Astron. J. **66,** 44 (1961).
23. H. E. Newell, Jr., *High Altitude Rocket Research* (Academic Press, New York, 1953).
24. *Handbook of Geophysics*, Rev. Ed. (Macmillan, New York, 1960).
25. K. Watanabe, *Advances in Geophysics*, edited by H. E. Landsberg and J. van Mieghem (Academic Press, New York, 1958), Vol. 5.

Letters to the Editor *continued from page 65*

Angular Measurements by Means of a Ronchi Ruling*

Jurgen R. Meyer-Arendt and Ellis D. Miner, Jr.

Physics Department, Utah State University, Logan, Utah.
Received 23 April 1962.

Highly accurate *linear* measurements are usually carried out by interferometry. The same principle can be applied to *angular* measurements. Two examples of interferential goniometers, both essentially modifications of a Michelson interferometer, are those described by Sugg[1] and Stroke.[2] Stroke's instrument is accurate to 0.1 sec of arc, with photoelectric recording even to 0.01 sec of arc, and has a range, without resetting the mirrors, of up to about one minute of arc.

Such accuracy is difficult to obtain with a conventional optical lever which represents the other approach frequently used for angular measurements. However, we have found that even a simple lever gives satisfactory results, with an accuracy of 2 sec of arc, if combined with a Ronchi ruling. The only comparable instrument combining an optical lever with a Ronchi grid is that designed by Jones[3]; this instrument, however, is also rather complicated and employs two grids which have to be carefully adjusted, and a photocell.

The schematic of our instrument, which is not so much an alignment device as has been described by van Heel[4] but a true goniometer, is shown in Fig. 1. Light from a source S is reflected by a right-angled prism cemented directly to the ruling R. The light passes through the ruling and through a converging lens located close to, but not in firm contact with, a plane mirror M. The mirror is attached to the system whose rotation is to be measured. Instead of the lens and mirror M, a concave mirror may be employed. The distance between the lens or mirror and ruling R is slightly less than the focal length of either one. The reflected light is observed through the grating intervals (which are parallel to the axis of rotation) by means of a telescope T. The resulting pattern seen in the telescope is due to a superposition of the Ronchi grid and its image and is highly sensitive to small rotations of the mirror.

The advantage of the system, besides its simplicity, is the fact that the readings are independent of any back-and-forth shift of mirror M. Only rotational motions are recorded, which is the same as in Stroke's design. Furthermore, if the distance between grid and mirror is kept constant and only the lens is moved along the optic axis, the fringes become closer or more widely spaced but the sensitivity does not change: that is, a turn through a given angle will produce the same fringe count passing a reference mark in the telescope or in a filar micrometer.

The sensitivity, however, increases with the focal length of the lens. Likewise, the fineness of the Ronchi ruling to be chosen depends on the application. Finer grids give greater sensitivity, but at the same time enhance diffraction. A grid with about 52 lines/cm (133 lines/in.) is best. The grating constant is then $d = 192\ \mu$ and, since the bars and intervals in the grating were of equal width, the clear intervals have a width of $d/2$. Using a lens of $f = 2$ m, the angular width of the intervals is $\sin\theta = (0.192/2)/(2 \times 10^3)$ mm $= 0.000048$, so that $\theta = 10$ sec of arc. A fringe shift in the image plane can easily be estimated to the closest one-fifth of an interval so that angular displacements can be measured which are as small as 2 sec of arc or about 10^{-5} rad.

The angular range over which the instrument can be used depends on the total width of the grid. For a Ronchi ruling 5 cm wide, an overlap will occur for twice this width so that the range will be almost 3°. Within this range, the readings will be a sufficiently linear function of rotation.

* Supported by a research grant from the National Institutes of Health.

References

1 R. E. Sugg, *An Improved Angle Interferometer* (Nat. Bur. Standards Handbook 77, Vol. 3, 1961), pp. 225/61–229/65.
2 G. W. Stroke, J. Opt. Soc. Am. **51,** 1340–1341 (1961).
3 R. V. Jones, J. Sci. Instr. **38,** 37–45 (1961).
4 A. C. S. van Heel, "Modern alignment devices," *Progress in Optics*, E. Wolf, editor (North-Holland Publishing Co., Amsterdam, 1961), Vol. 1, pp. 289–329.

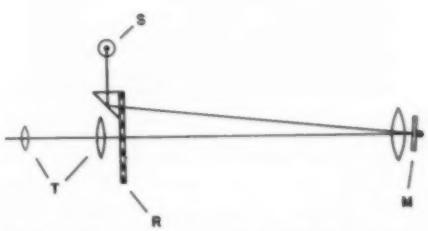

Fig. 1. Ray diagram of Ronchi ruling goniometer.

Shadowgraph of Self-Luminous Objects

M. A. Levine and J. C. Hegarty

Air Force Cambridge Research Laboratories, Bedford, Mass.
Received 18 August 1962.

The brilliance of self-luminous objects often obscures detail of a relatively dark area from within. A case in point is the exploding wire phenomenon. In part, the brilliance of a wire approaches the intensity of a source with a color temperature of 20,000°K, and at the same time some of the darker portions of the wire are of more scientific interest. To observe the behavior during the dark phases a shadowgraph system has been devised which optimizes the intensity of a backlight.

The use of the light from a back exploding wire to illuminate the early opaque stages of the exploding wire phenomenon is a common technique.[1,2] Recent advances in the theory of electrical conductivity[3] and physical phase changes[4] of wires have made it desirable to obtain more accurate and more detailed observations of the dynamic behavior of wires. To this end the backlighting system has been devised as shown in Fig. 1. This system is reminiscent of the Schlieren[5] system without interference effects, and consists of two conjugate planes as follows: (1) the object plane A of the back wire and an image plane A′ where a circular aperture is placed, (2) the object plane B of the exploding wire under examination and its image plane B′ where the shadowgraph appears. The circular aperture placed in the image plane of the backlight permits a maximum transmission of the backlight. At the same time it intercepts much of the light from the front wire. This aperture is adjusted to the image size of the back wire.

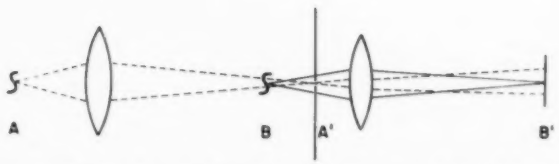

Fig. 1. Shadowgraph optical system. A—position of backlighting wire, B—position of wire under observation, A′—aperture in image plane of backlighting wire, B′—shadowgraph observation screen.

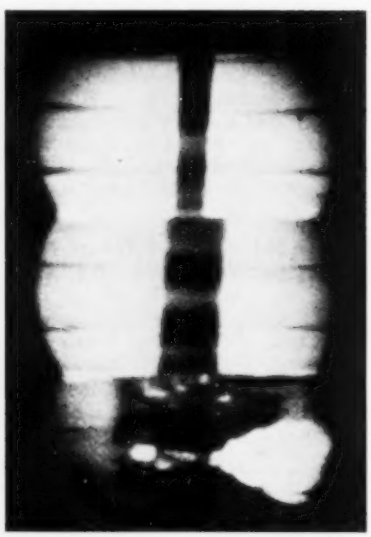

Fig. 2. Three frame sequence of #26 copper wire (0.4 mm diam) exploding using a STL image converter camera. First frame—T = 1.5 μsec (wire approximately initial size); second frame—T = 2.25 μsec; third frame—T = 2.75 μsec (wire in gaseous stage). (Note: Jetting of luminosity in generally opaque cloud.) Exposure time 0.1 μsec. (Horizontal lines are produced by image converter grid wires.)

The maximum contrast obtainable is set by the second law of thermodynamics. The backlight from a given temperature source can never outshine a wire of the same temperature. However, it is possible to bring the observed brightness for the same color temperature emitters to the same intensity. A simple calculation of relative intensity of the system described (neglecting lens reflections) indicates that this system gives the maximum shadowgraph contrast of one to one.

Some of the results obtained using the above-mentioned optical system are shown in Figs. 2 and 3. Figure 2 is a framed sequence of B&S #26 Cu as it explodes; Fig. 3 is a smear picture of the explosion of #26 Cu wire. The back illumination was provided by #26 wire at maximum brightness. Both pictures were taken with an STL image converter camera.

Frames 1 and 2 of Fig. 2 show the wire in the opaque stage of the expansion; frame 3 shows the wire becoming self-luminous in spots, yet the outline of the exploding wire is clearly visible. The smear picture again demonstrates that, despite the self-luminosity of the exploding wire, the detail of the expanding wire is very much in evidence.

The use of B&S #26 Cu wire for both the backlight and exploding wire was for convenience. The use of a more intense backlight in the form of an Al or W wire might permit more of the expansion process to be seen in detail.

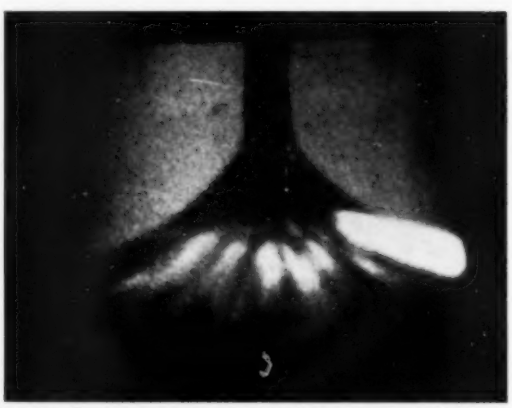

Fig. 3. Image converter streak picture, same optical system as in Fig. 2 using a narrow slit on the STL image converter photocathode. 5.0 μsec streak duration top to bottom.

References

1. W. G. Chace, Phys. Fluids **2**, 230 (1959).
2. T. Korneff, J. L. Bohn, and F. H. Nadig, *Exploding Wires*, W. G. Chace and H. K. Moore, eds. (Plenum Press, New York, 1959), Vol. I, p. 104.
3. C. P. Nash and W. G. McMillan, Phys. Fluids **4**, 911 (1961).
4. W. G. Chace and Howard K. Moore, *Exploding Wires* (Plenum Press, New York, 1962), Vol. II.
5. W. Müller, *Exploding Wires*, W. G. Chace and H. K. Moore, eds. (Plenum Press, New York, 1959), Vol. I, p. 186.

Letters *continued on page 87*

Spectromètre à Grilles

A. Girard

A gain of luminosity greater than 100 is obtained by replacing the entrance and exit slits of a spectrometer by a two-dimensional set of alternately transparent and nontransparent zones, the limit curves of which are regularly assembled equilateral hyperbolas having common asymptotes. One of the asymptotes is parallel to the slits of the conventional spectrometers. The general construction and, to some extent, the handling qualities of conventional spectrometers are not altered. The Littrow-type mounting is particularly advantageous. The examples of the results mentioned have been obtained with an apparatus having a focal length of two meters using the single-beam and single-pass principle.

I. Introduction

Parmi les appareils utilisés en analyse spectrale, il est maintenant classique de distinguer, d'une part, les spectromètres, où le spectre est exploré dans le temps, élément par élément et, d'autre part, les spectrographes qui permettent d'obtenir des informations simultanément sur tous les éléments du spectre. Les spectromètres présentent donc, par rapport aux spectrographes, la grave infériorité de ne fournir qu'une seule information à un instant donné. Leur emploi s'est pourtant généralisé, en même temps que celui des récepteurs photoélectriques, au détriment de l'émulsion photographique, d'ailleurs inutilisable au-delà de 1.2 μ.

Il est également bien connu que, pour des conditions de fonctionnement données, la précision de la mesure de l'intensité de l'élément spectral, directement liée au rapport signal-bruit, dépend finalement de la quantité d'énergie reçue et admise par l'appareil. Cette quantité joue un rôle fondamental: à pouvoir de résolution égal, deux appareils auront ainsi des performances très différentes suivant l'étendue du faisceau qu'ils admettent.

Diverses solutions existent actuellement pour réaliser des analyses spectrales dans des conditions de luminosité très supérieures à celles des spectromètres à fentes. Elles sont étudiées principalement par Jacquinot,[1,8] Chabbal,[2] Felgett,[3] P. Connes,[4] Gebbie,[5] J. Connes,[6] Mertz.[7]

Malgré sa très faible luminosité, le spectromètre à fentes reste, de très loin, l'appareil le plus utilisé. Cette situation paradoxale s'explique, au moins en partie, par la raison suivante: un spectromètre conventionnel possède, plus que tout autre, des qualités telles que commodité d'emploi, simplicité de fonctionnement, enregistrement direct du spectre, qui compensent, aux yeux de nombreux utilisateurs, sa très grave infériorité en luminosité.

Golay[9] a imaginé un dispositif qui conserve la disposition générale des appareils à fentes et dans lequel l'étendue du faisceau utile est considérablement accrue. Il est basé sur l'emploi de combinaisons de fentes et d'intervalles opaques dont les largeurs sont des multipler entiers de la largeur de fente dont on cherche à égale- le pouvoir de résolution. La surface totale des sys tèmes multifentes placés à l'entrée et à la sortie de l'appareil est divisée en deux parties différentes entre elles mais de surfaces égales, à l'intérieur desquelles les fentes sont disposées de telle sorte que le signal est la différence des flux émergents des deux parties du champ éclairé.

Le présent article expose le principe et quelques exemples des résultats obtenus avec un appareil qui est l'aboutissement de tentatives[10] faites pour concilier la recherche d'un gain très important de luminosité avec le maintien de la disposition générale des appareils conventionnels et, dans une certaine mesure, des qualités de maniabilité qui en justifient l'emploi.

II. Principe Général

On place à l'entrée de l'appareil un ensemble de zones alternativement transparentes et opaques constituant une grille G_E. L'appareil comporte ensuite, comme dans les appareils classiques un collimateur d'entrée, un système dispersif et un collimateur de

The author is at l'Office National d'Etudes et de Recherches Aeronautiques, Chatillon s/Bagneux (Seine), France.

Received 26 June 1962.

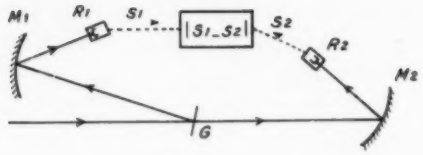

Fig. 1. Montage différentiel à deux récepteurs.

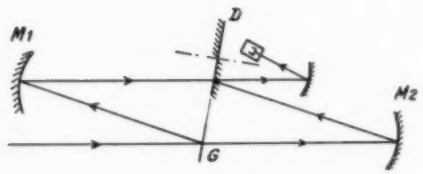

Fig. 2. Montage différentiel à un seul récepteur.

sortie. Enfin une grille G_s, image monochromatique de la grille d'entrée à travers l'appareil, est placée dans le plan focal du collimateur de sortie.

La grille de sortie se trouve donc superposée aux images monochromatiques G'_E de la grille d'entrée, décalées les unes par rapport aux autres en raison de la dispersion du spectre. Pour une position quelconque du système dispersif, il existe donc une radiation pour laquelle l'image de la grille d'entrée est exactement superposée à la grille de sortie. Cette radiation est appelée, dans la suite du texte, longueur d'onde de réglage. En effet, pour en changer, il suffit de faire défiler le spectre par des moyens habituels, tels que la rotation du système dispersif. Pour cette radiation, la grille de sortie transmet intégralement le flux qui tombe sur elle. Par contre, pour une autre radiation, G'_E est décalée par rapport à G_s, qui ne transmet alors qu'une fraction (50%) du flux qui lui parvient.

Si maintenant, l'une des grilles est remplacée par une grille complémentaire (ou négative) dans laquelle les zones opaques sont remplacées par des zones transparentes, et inversement, le flux transmis est nul pour la longueur d'onde de réglage et, pour chacune des autres radiations, s'élève comme dans le cas de deux grilles identiques, à 50% du flux qui parvient à la grille de sortie.

En réalisant les deux associations qui viennent d'être décrites (grilles semblables et grilles complémentaires), on obtient, après traversée de G_s, deux faisceaux émergents dont les compositions spectrales sont les mêmes pour toutes les radiations, sauf pour un intervalle spectral étroit autour de la longueur d'onde de réglage. La différence des flux transportés par ces deux faisceaux constitue donc une mesure spectrométrique portant sur cet intervalle spectral.

Pour mettre en oeuvre ce principe, il faut:

1. Obtenir les deux faisceaux à comparer grâce à la présence, à l'entrée ou à la sortie de l'appareil, de deux grilles images positives et négatives d'une troisième grille placée à l'autre extrémité de l'appareil.

2. Faire la différence des flux transportés par ces faisceaux émergents de l'appareil.

3. Réaliser, grâce à une constitution convenable des grilles, l'égalité des flux transportés sur les deux faisceaux pour toute radiation différente de la longueur d'onde de réglage, en y incluant les radiations les plus proches possibles de cette longueur d'onde de réglage. En désignant par E la largeur d'une grille suivant la direction d'étalement du spectre et x le décalage linéaire entre G_s et G'_E pour une radiation quelconque, la condition à satisfaire est la suivante: pour chacun des deux faisceaux, le flux émergent de G_s doit être égal à la moitié du flux qui parvient à cette grille de sortie, quelle que soit la valeur de x, au-delà d'une valeur $e \ll E$, qui caractérise la largeur de fente équivalente et, par conséquent, le pouvoir de résolution. Le gain de luminosité est voisin de $E/2e$ pour une grille ayant la même hauteur que la fente.

Ces trois points sont examinés successivement.

A. Production des deux Faisceaux à Comparer

Ils sont obtenus de la façon suivante: les intervalles opaques d'une grille sont réfléchissants, de sorte que cette grille fonctionnant par réflexion est l'image négative, ou complémentaire, de la même grille fonctionnant par transmission. Cette grille unique se comporte donc comme l'ensemble de deux grilles complémentaires imbriquées l'une dans l'autre. Le signal est la différence des flux émergents de l'appareil lorsque cette grille fonctionne par transmission et par réflexion.

Il est également possible d'obtenir les deux faisceaux en plaçant sur la surface S disponible à l'une des extrémités de l'appareil deux demi-grilles complémentaires de surface $s/2$.

Mais cela entraîne deux inconvénients: La luminosité est deux fois plus faible. Il est indispensable que l'éclairement soit rigoureusement uniforme sur l'ensemble de la surface s.

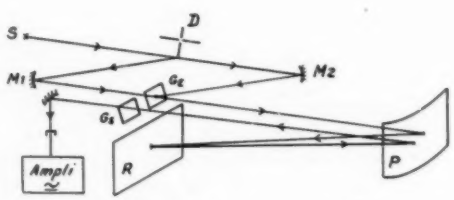

Fig. 3. Schéma optique d'un appareil réalisé. S—source; D—disque modulateur; G_E—grille d'entrée; G_S—grille de sortie; R—réseau; P—mirror parabolique taillé en dehors de l'axe.

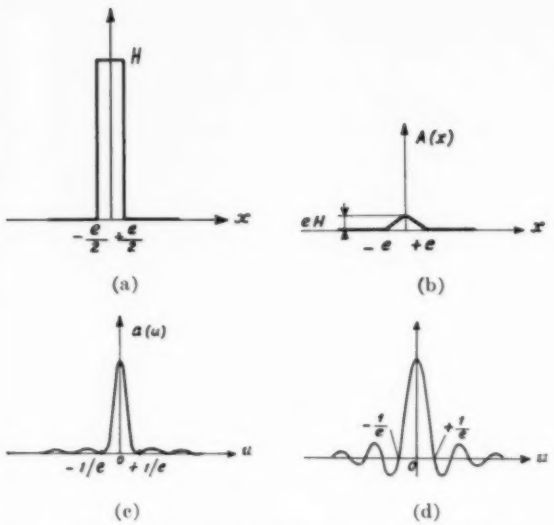

Fig. 4. Fonctions caractéristiques d'un appareil à fentes, en l'absence de diffraction.

(a)—Fonction fente. (b)—$A(x)$. (c)—$a(u)$. (d)—$[a(u)]^{1/2}$

B. Comparaison des Faisceaux

Les deux schémas indiqués Figs. 1 et 2 sont utilisables pour faire apparaître la différence des flux transmis et réfléchis. Ils ont déjà été décrits.[10] Dans le montage Fig. 1, deux récepteurs sont utilisés qui reçoivent respectivement le flux transmis et le flux réfléchi par la grille de sortie. On fait apparaître la différence des signaux grâce à un montage différentiel des récepteurs. Dans le schéma Fig. 2, les deux faisceaux tombent alternativement sur le même récepteur par l'intermédiaire d'un disque échancré D dont les pales sont des miroirs. Le signal est obtenu par l'intermédiaire d'un amplificateur alternatif centré sur la fréquence de commutation des faisceaux. Il ne comprend donc que la partie du flux modulé à cette fréquence.

Pour éviter d'être gêné par le rayonnement du disque modulateur, il est préférable de placer la grille réfléchissante à l'entrée de l'appareil. Le schéma de l'appareil réalisé sur ce principe est représenté Fig. 3.

Il est à noter que ce dispositif est favorable à l'élimination de la lumière parasite. En effet, le commutateur optique ne fonctionne pas comme l'obturateur périodique d'un appareil classique. Associé aux grilles G_E et G_s, il réalise une modulation sélective d'un domaine spectral étroit autour de la radiation de réglage. Le flux parasite diffusé, qui parvient au détecteur, est donc un flux continu et se trouve par conséquent éliminé.

Le coefficient de transmission en un point de coordonnées x, y d'une grille quelconque G, est une fonction $\tau\ (x, y)$ qui satisfait à la condition $0 < \tau < 1$ et peut se mettre sous la forme

$$\tau(x, y) = {}^1/_2[1 + f(x, y)] \text{ avec } -1 < f < +1. \qquad (1)$$

La loi de transmission de G_c, complémentaire de la grille G, s'écrit de même:

$$\tau_c(x, y) = {}^1/_2[1 - f(x, y)].$$

En faisant la différence des effets produits par les deux grilles G et G_c tout se passe comme s'il s'agissait d'une grille unique dont la loi de transparence s'exprime par la relation:

$$\tau - \tau_c = f(x, y) \text{ avec } -1 < f(x, y) < +1. \qquad (2)$$

C. Constitution des Grilles

La fonction enregistrée $F'\ (\lambda)$ fournie par l'appareil, est le produit de convolution de $F(\lambda)$ par la fonction d'appareil $A(\lambda)$:

$$F'(\lambda) = F(\lambda) * A(\lambda).$$

La fonction $A(\lambda)$ est la réponse de l'appareil lorsque le spectre étudié se réduit à une raie unique infiniment fine.

La loi d'étalement du spectre dans le plan de la grille de sortie, suivant la direction $0x$, confondue avec la direction $0x$ du plan des grilles, est liée à la variable d'espace x par la relation:

$$\frac{x}{\lambda - \lambda_0} = D.$$

$D = dx/d\lambda$ est la dispersion linéaire du spectre. λ_0 est la longueur d'onde de réglage de l'appareil pour $x = 0$.

Pour faciliter l'exposé du développement qui suit, la fonction étudiée est la fonction $A(x)$, liée linéairement à la fonction d'appareil $A(\lambda)$ par la relation précédente.

$a(u)$ transformée de Fourier de $A(x)$, est la fonction de filtrage des fréquences spatiales par l'appareil suivant la direction d'étalement du spectre. Ces notions générales s'appliquent au spectromètre à grilles.

Les performances de l'appareil sont donc déterminées par l'un ou l'autre des 2 fonctions $A(x)$, $a(u)$.

1. La Diffraction n'intervient pas

Les courbes 4b et 4c rappellent les fonctions $A(x)$ et $a(u)$ pour un appareil équipé de fentes de largeur e et de hauteur H, en l'absence d'aberrations et d'effets dûs à la diffraction. $A(x)$ est le produit de convolution de la fonction fente (Fig. 4a) par elle-même; $a(u)$ est le

carré de la transformée de Fourier (Fig. 4d) de la fonction fente.

Si l'appareil, équipé de grilles, est éclairé par une radiation unique et réglé de telle sorte que l'image de la grille d'entrée se trouve décalée de la quantité x par rapport à la grille de sortie, le flux émergent, en un point de la grille, est proportionnel au produit:

$$\tau(x' - x, y)f(x', y).$$

La fonction d'appareil est la fonction de x qui s' obtient en sommant ce produit sur la surface totale de la grille

$$A(x) = \int\int \tau(x' - x, y)f(x', y)dx'dy.$$

En tenant compte de (1), il vient

$$A(x) = {}^1/_2 \int\int f(x', y)dx'dy + {}^1/_2 \int\int f(x', y)f(x' - x, y)dx'dy.$$

La première intégrale est nulle à condition que la transparence moyenne de la grille fictive définie par (2) soit nulle; cette condition est remplie si les sommes des aires des zones utiles des grilles complémentaires G et G_c sont égales. La fonction d'appareil s'écrit donc:

$$A(x) = {}^1/_2 \int\int f(x', y)f(x' - x, y)dx'dy. \qquad (3)$$

En désignant par $\varphi(u, y)$, la transformée de Fourier en x de $f(x, y)$ on a la relation:

$$a(u) = {}^1/_2 \int [\varphi(u, y)]^2 dy. \qquad (4)$$

Les relations (2), (3), et (4) permettent de calculer $A(x)$ et $a(u)$ à partir d'une grille dont la loi de transparence est $\tau(x, y)$. Suivant les cas particuliers, il peut être avantageux d'effectuer le calcul de $A(x)$, soit directement par la relation (3), soit par l'intermédiaire de la transformation de Fourier.

Les grilles dont il faut équiper l'appareil pour remplacer de façon satisfaisante les fentes de largeur e, doivent être telles que la fonction d'appareil remplisse les conditions suivantes:

1. La largeur à mi-hauteur de la fonction d'appareil doit être égale à e—cette largeur caractérise le pouvoir de résolution de l'appareil.

2. La fonction d'appareil doit de plus décroître régulièrement à partir du maximum central et rester constamment négligeable pour toutes les valeurs de x supérieures à e.

La condition fondamentale à satisfaire pour obtenir un tel résultat est que la fonction $a(u)$ couvre le même domaine de fréquence que la transformée de Fourier d'une fente de largeur e. L'appareil est en effet un filtre linéaire et les résultats généraux de la théorie des filtres linéaires[12] lui sont applicables.

Par ailleurs, le problème de la réduction des maximums secondaires ("apodisation") a fait l'objet d'une étude générale,[11] qui comprend un chapitre relatif au dispositif décrit antérieurement.[10]

Il est commode de distinguer deux domaines:

1. *Apodisation lointaine* ($x > 10e$). Elle est obtenue en utilisant une fonction de filtrage $a(u)$ aussi régulière que possible, fonction continue avec un grand nombre de dérivées continues et bornées.

A ce point de vue, la loi $f(x, y) = \cos 2\pi K x^2$ proposée dans un article précédent,[10] n'est pas très satisfaisante. En effet, en négligeant les termes dûs aux dimensions finies de la grille, sa transformée de Fourier est le produit de la fonction:

$$\frac{1}{2K} \cos\left(\pi \frac{u^2}{2K} - \frac{\pi}{4}\right)$$

par une fonction rectangle nulle au-delà de la fréquence $1/p$. p étant le pas le plus fin de la grille (Figs. 12 et 13).

L'enveloppe de cette fonction a la forme souhaitée, mais le fait qu'elle prenne toutes les valeurs possibles entre -1 et $+1$ dans l'intervalle de fréquence utile, entraîne la présence de maximums secondaires dans la fonction appareil dont l'amplitude relative (de l'ordre de 1% du maximum central dans les cas pratiquement réalisés) est inadmissible pour de nombreux cas d'applications.

Le fait que la loi de transparence $\tau(x)$ ne soit pas

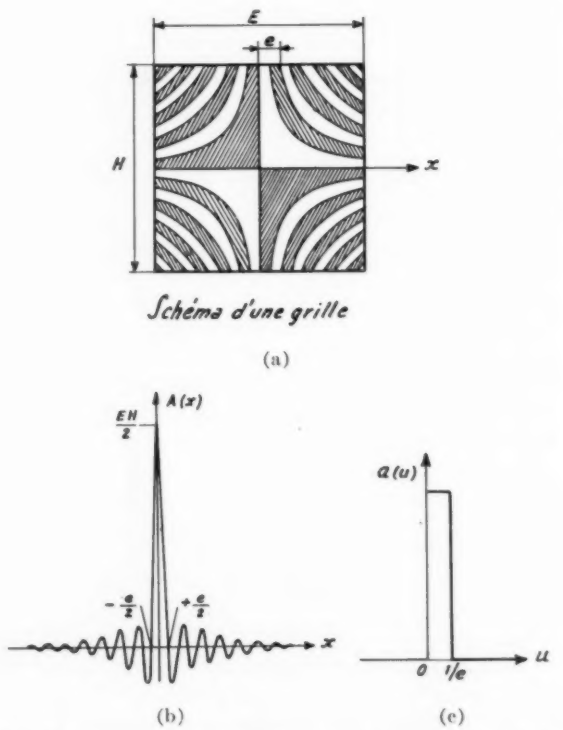

Schéma d'une grille

(a) (b) (c)

Fig. 5. Fonctions caracteristiques d'un appareil équipé de grilles, en l'absence de diffraction.

(a)—Schéma d'une grille. (b)—$A(x)$. (c)—$a(u)$.

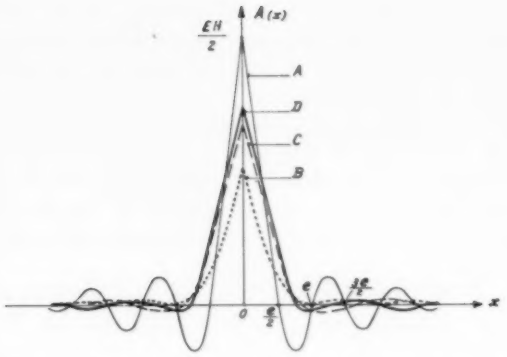

Fig. 6. Fonction d'appareil $A(x)$ pour différentes formes de grilles.

Courbe B

Fig. 7. Grilles à contour losangique.

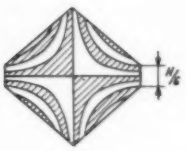

Courbe C

Fig. 8. Grille à contour hexagonal.

Courbe D

Fig. 9. Grille à contour suivant la courbe de Gauss.

représentable par une sinusoïde, mais par une fonction créneaux, aggrave considérablement ces difficultés. Un calcul rigoureux, effectué à l'aide d'un calculateur électronique, a confirmé les résultats expérimentaux obtenus.

D'autres fonctions $f(x, y)$ ont des propriétés plus favorables. Parmi celles-ci, la fonction

$$f(x, y) = \sin 2\pi Kxy \tag{5}$$

a été adoptée en raison de la simplicité des calculs qu'elle entraîne lorsqu'on applique les relations (2), (3), et (4). Les courbes d'égale transparence sont des hyperboles équilatères d'équation générale:

$$xy = c^{te}$$

Sur toute droite parallèle à l'une des asymptotes, les points de transparence égale sont équidistants.

La grille représentée Fig. 5a, a pour pas $p = e$ sur la droite d'ordonnée $y = H/2$. Son équation est donc

$$f(x, y) = \sin 4\pi \frac{xy}{eH}. \tag{5'}$$

Sur toute droite d'ordonnée y, le pas de la grille est $p = eH/2y$.[5] Par conséquent, le long de cette droite parallèle à la direction du défilement du spectre, la grille se comporte comme un filtre à bande passante étroite, de largeur $1/E$ (E largeur de la grille suivant $0x$) centré sur la fréquence $u = 1/p$. D'après (5') cette fréquence est proportionnelle à l'ordonnée y. Il en résulte que la courbe représentant la répartition des fréquences spatiales suivant $0x$ pour l'ensemble de la grille est de la forme représentée Fig. 5c: elle est sensiblement une fonction rectangle couvrant l'intervalle $0, 1/e$.

La fonction d'appareil (Fig. 5b), transformée de Fourier de $a(u)$ est la fonction:

$$A(x) = \frac{AH}{2} \frac{\sin 2\pi x/e}{2\pi x/e}.$$

Le calcul direct de $A(x)$ à partir des relations (2) et (3) ne présente d'ailleurs aucune difficulté.

Pratiquement, les grilles réelles se présentent sous la forme de zones alternées transparentes ou opaques et la loi de variation de transparence n'est pas une sinusoïde, mais une fonction créneaux. La fonction d'appareil ne s'en trouve pas modifiée dans le domaine de l'apodisation lointaine. Elle est légèrement améliorée dans la zone proche du maximum central (comme indiqué sur la Fig. 6,A par rapport à 5b).

2. *Apodisation proche* ($x < 10e$). La réduction des maximums secondaires proches du maximum central est obtenue en agissant sur le contour de la grille. Les courbes Fig. 6, B, C, et D, sont les fonctions d'appareil obtenues avec des contours losangiques (Fig. 7), trapézoïdaux (Fig. 8) et en forme de courbe de Gauss (Fig. 9). La valeur du premier maximum secondaire est d'environ 3%. Les suivants sont inférieurs à 1% du maximum central.

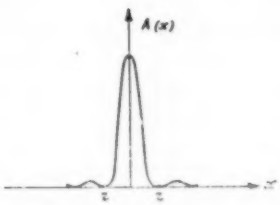

Fig. 10. Fonction d'appareil $A(x)$ pour un spectromètre équipé de grilles à contour rectangulaire, lorsque le pas le plus fin de la grille est égal au rayon r de la tache de diffraction.

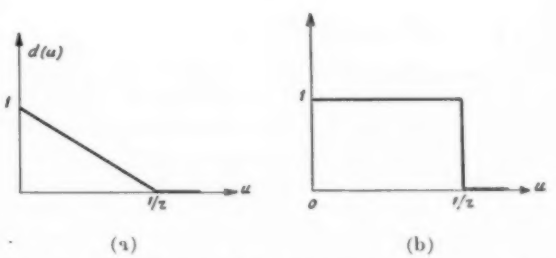

(a) (b)

Fig. 11. (a)—Fonction $d(u)$. (b)—Fonction $a(u)$ pour un appareil équipé de grilles à contour rectangulaire dont le pas le plus fin est égal au rayon r de la tache de diffraction.

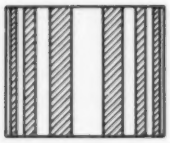

Fig. 12. Schéma d'une grille à bandes rectilignes.

2. Rôle de la Diffraction

La fonction d'appareil $A'(x)$ d'un appareil parfait est le produit de convolution de la fonction $D(x)$ représentant la répartition des intensités dans la tache de diffraction par la fonction $A(x)$ du paragraphe précédent.

$$A'(x) = A(x) \cdot D(x).$$

Dans l'espace des fréquences, on a par conséquent:

$$a'(u) = a(u) \cdot d(u).$$

$d(u)$ est la transformée de Fourier de $D(x)$.

Les courbes Fig. 10 et 11a représentent $D(x)$ et $d(u)$ pour un appareil à pupille rectangulaire, en éclairage incohérent r est le rayon de la tache de diffraction.

Il est bien connu que, même en l'absence de toute abérration ou de défaut de réglage, le pouvoir de résolution théorique, défini par la courbe 10, est une limite inaccessible puisqu'il nécessite l'emploi de fentes infiniment fines.

Par contre, ce pouvoir de résolution théorique est practiquement accessible si l'appareil est équipé de grilles convenables. En effet, la condition $a'(u) = d(u)$ qui entraîne $A'(x) = \mathrm{D(X)}$ est réalisée si la fonction $a(u)$ est une fonction rectangle limitée par une grille de contour rectangulaire dont le pas le plus fin est précisément égal à r. La fonction d'appareil obtenue alors est la courbe Fig. 10, dont l'ordonnée du maximum central est alors proportionnelle à $EH/4$.

L'emploi d'une grille comportant des intervalles plus étroits que r n'etraîne ni avantage, ni inconvénient: le pouvoir de résolution obtenu est le pouvoir de résolution théorique et tout se passe comme si ces intervalles très étroits n'existaient pas.

III. Description d'un Appareil Realise

A. Schéma Optique (Fig. 3)

Le montage Littrow a été adopté pour deux raisons:

1. La forme des grilles hyperboliques exclut tout montage dans lequel l'astigmatisme n'est pas corrigé et, en particulier, le montage Ebert-Fastie.

2. Il permet l'emploi du même couple de grilles (entrée et sortie) sur un intervalle spectral plus large que les montages à déviation non nulle. Ce point est développé dans le paragraphe "réalisation des grilles."

Les grilles d'entrée et de sortie sont placées au-dessus du réseau, dans le plan focal du miroir parabolique P, taillé en dehors de l'axe. La distance focale de ce miroir est 2 mètres. L'appareil est équipé d'un réseau de surface utile 180 × 135 mm. Il fonctionne en simple passage et simple faisceau.

La source lumineuse, le disque modulateur, le réseau et le récepteur sont situés dans des plans conjugués. Un éclairement uniforme de la grille d'entrée est obtenu en formant dans ce plan l'image du miroir condenseur qui suit immédiatement la source lumineuse.

B. Réalisation des Grilles

1. *Grilles d'Entrée*

Elles sont réalisées par photogravure à partir de la réduction photographique d'un dessin à grande échelle. Leur surface utile est 30 × 30 mm. Le pas le plus fin des grilles utilisées, pour obtenir les résultats présentés à la fin de cet article, est de 0.11 mm. Les matériaux suivants ont été utilisés comme support pour la photogravure: verre, CaF_2, NaCl, KRS5. Des grilles dont le pas minimum est 0.03 mm ont également été réalisées sur verre et sur fluorine.

2. *Grilles de Sortie*

La grille de sortie est l'image de la grille d'entrée à travers l'appareil. D'une façon générale, elle n'est donc pas rigoureusement identique à la grille d'entrée. Il est important d'examiner dans quelle mesure elle en diffère.

Soit θ l'angle d'incidence sur le réseau pour le faisceau lumineux issu de P (Fig. 14), foyer du miroir collimateur. La radiation λ de retour en P après diffraction sur le réseau, satisfait à la relation

$$K\lambda = 2a\sin\theta \qquad a = \text{pas du réseau} \tag{6}$$

Les centres 0 et 0′ des grilles d'entrée et de sortie G et G′ sont placés de part et d'autre de P (Fig. 14) dans le plan focal du collimateur. Il est commode d'exprimer les distances dans ce plan en les rapportant à la distance focale F du collimateur, de sorte que les coordonnées d'un point de ce plan sont des coordonnées angulaires. Soient α et φ les coordonnées d'un point A suivant $0x$ et $0y$ dans un système d'axe du centre P.

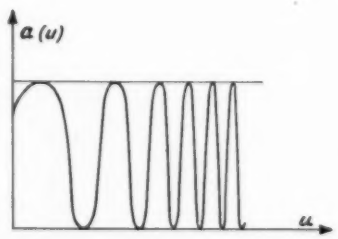

Fig. 13. Transformée de Fourier d'une grille à bandes rectilignes

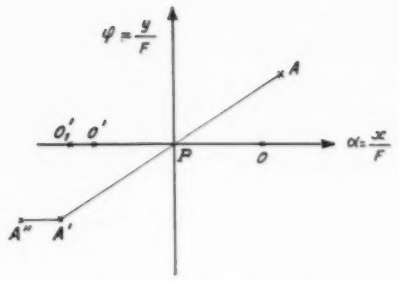

Fig. 14. Déformation geométrique de l'image dans le plan focal du collimateur d'un spectromètre à réseau.

Pour la radiation λ, les rayons issus de A convergent en A'', distant de A', symétrique de A par rapport à P de la quantité ϵ. A'A'' est parallèle à 0x direction d'étalement du spectre. La relation qui exprime que le couple de points A A'' satisfait à la relation fondamentale des réseaux s'écrit:

$$K\lambda = a\cos\varphi[\sin(\theta + \alpha) + \sin(\theta - \alpha + \epsilon)].$$

Compte tenu de (6), il vient:

$$\epsilon = 2\frac{\sin\theta}{\cos(\theta - \varphi)}\left[\frac{1}{\cos\varphi} - \cos\alpha\right].$$

En effet, α et φ sont petits et la relation s'écrit finalement:

$$\epsilon = (\varphi^2 + \alpha^2)\tan\theta = L^2\tan\theta \text{ avec } L = \overline{PA}. \qquad (7)$$

En particulier, l'image du centre O de la grille d'entrée se forme en un point O', tel que

$$O'O'_1 = \epsilon_0 = L_0^2\tan\theta$$

avec $L_0 = OO'/2$. Il est toujours possible de faire coïncider le centre de la grille de sortie avec le point O'.

Le terme de déformation résiduelle s'écrit alors:

$$\bar{\epsilon} = \epsilon - \epsilon_0 = (L^2 - L_0^2)\tan\theta. \qquad (8)$$

$\bar{\epsilon}$ ne dépend ni du pas du réseau, ni de l'ordre dans lequel il travaille, mais uniquement de l'angle d'incidence θ et de la disposition géométrique des grilles dans le plan focal du collimateur.

On compense pratiquement ces déformations en utilisant comme grille de sortie une photographie de la grille d'entrée, à travers l'appareil; la source utilisée pour effectuer cette opération est une lampe à vapeur de mercure isotopique. Des photogravures sont ensuite effectuées à partir de ces clichés sur les matériaux utilisables dans l'infra rouge.

En appelant E la largeur de la grille, la valeur de la déformation maximum $\bar{\epsilon}_M$ est de la forme:

$$\bar{\epsilon}_M \simeq EL_0\tan\theta.$$

Le terme $\bar{\epsilon}_M$, de même que sa dérivée en fonction de θ, sont proportionnels à L_0, angle de déviation du montage. Or, cet angle est environ 10 fois plus faible avec le montage de Littrow qu'avec le montage Ebert-Fastie. L'intervalle spectral couvert avec le même couple de grilles varie de la même manière.

La comparaison avec d'autres types de montages, tels que le montage de Pfund, serait encore plus favorable au montage de Littrow.

Pratiquement, l'appareil équipé de grilles ayant un pouvoir de résolution équivalent à celui qu'on obtient avec des fentes de 0.08 mm, et corrigées pour un angle d'incidence $\theta = 30°$ est utilisable entre $37° < \theta < 22°$, ce qui correspond à environ 6000 éléments spectraux, la distance focale de l'appareil étant de 2 mètres. La distance entre les axes des grilles d'entrée et de sortie OO' est de 35 mm.

C. Réglages

Etant donné la forme des grilles, l'appareil est beaucoup plus sensible que les appareils classiques à fentes à tout déréglage dans la direction 0y parallèle aux fentes. Un dispositif auxiliaire de contrôle visuel permanent de ce réglage a été adapté sur l'appareil.

L'appareil étant éclairé par une source monochromatique, des franges de moiré sont observables dans le plan de la grille de sortie, d'autant plus serrées que le décalage de la grille de sortie par rapport à l'image de la grille d'entrée est important. En l'absence de tout déréglage de l'appareil, ces franges de moiré sont rectilignes, équidistantes et parallèles à la direction d'étalement du spectre.

Par ailleurs, un peigne atténuateur est placé devant un des miroirs M_1 M_2 pour compenser les inévitables dissymétries résiduelles entre les trajets des faisceaux DM_1G et DM_2G (Fig. 3).

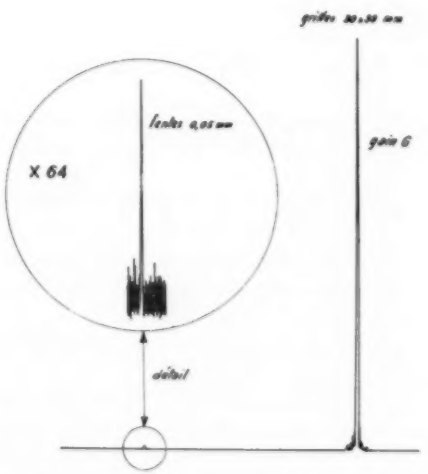

Fig. 15. Comparaison expérimentale des luminosités en grilles et fentes. Rapport des amplitudes: 130. Raie de l'hélium λ = 2.0580 μ.

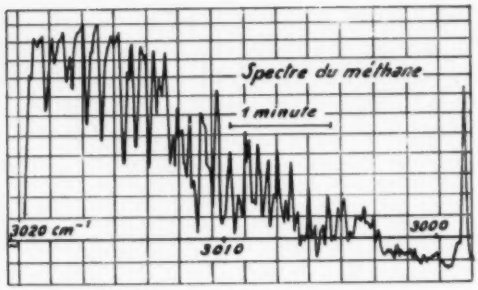

Fig. 16. Spectre du méthane, en absorption, vers 3.3 μ. Durée de l'enregistrement: 4 min. Cuve à gaz: e = 10 cm, p = 60 mm Hg. Source: SiC (globar) 1000°C. Détection simple f = 125 Mc.

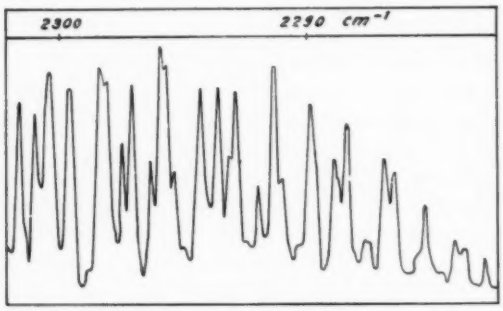

Fig. 17. Spectre du CO_2, en absorption, vers 4.3 μ. CO_2 atmosphérique. Epaisseur traversée: 10 mètres. Durée de l'enregistrement: 6 min. Source: SiC (globar) 1400°C. Détection synchrone f = 250 Mc.

D. Resultats

La Fig. 15 est une comparaison expérimentale des luminosités entre grilles et fentes, à pouvoir séparateur égal. Le rapport signal-bruit est 130 fois plus élevé, l'appareil étant équipé de grilles. Cette valeur n'est pas une limite supérieure et peut être considérée comme l'ordre de grandeur du gain de luminosité accessible sans difficultés spéciales.

Les enregistrements effectués jusqu'à présent couvrent le domaine des cellules photorésistantes PbS et PbTe.

Les quatre exemples présentés ont été obtenus avec un réseau à 300 traits par millimètre fonctionnant dans le 1er ordre. Le récepteur utilisé est une cellule au tellurure de plomb refroidie à la température de l'azote liquide.

Les Figs. 16 et 17 sont des exemples de spectres d'absorption.

La Fig. 18 est un spectre d'émission du gaz carbonique dans la flamme d'un bec Meker. Le pouvoir de résolution est d'environ 30.000 dans les trois cas.

La Fig. 19 est la même région du spectre du méthane que la Fig. 16, obtenue en émission.

IV. Conclusion

L'accroissement de la luminosité peut servir à obtenir des analyses plus fines, plus rapides ou plus précises suivant que le gain est réalisé sur le pouvoir de résolution, la bande passante de la chaîne de mesure ou le rapport signal-bruit. C'est ainsi que les vitesses d'enregistrement des spectres présentés sont nettement plus élevées que les vitesses d'enregistrement des spectres obtenus par les moyens classiques à un pouvoir de résolution du même ordre de grandeur.

Par ailleurs, la luminosité des appareils classiques est d'autant plus élevée qu'on utilise un système dispersif de grandes dimensions. C'est une des raisons pour lesquelles les appareils de hautes performances ont toujours des dimensions importantes; l'accroissement de luminosité dû à l'emploi de grilles peut être mis à

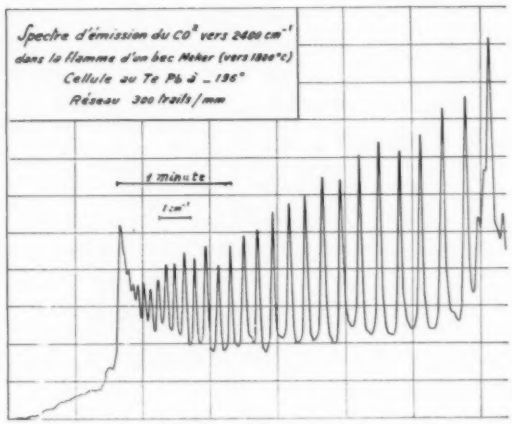
Spectre d'émission du CO² vers 2400 cm⁻¹
dans la flamme d'un bec Meker (vers 1900°c)
Cellule au Te Pb à – 196°
Réseau 300 traits/mm
1 minute
1 cm⁻¹

Fig. 18. Spectre du CO_2, vers 4.16 μ, dans la flamme du bec Mecker.

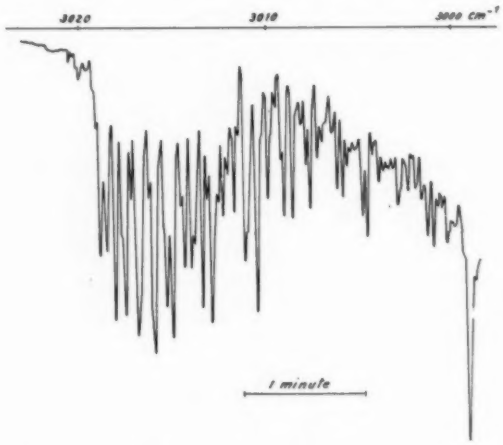

Fig. 19. Spectre du méthane, vers 3.3 μ. Emission à 300°C Cuve à gaz: longeur 15 cm, pression 50 mm Hg à 20°C.

profit pour réduire l'encombrement des appareils et, dans une certaine mesure, permettre leur miniaturisation.

L'application de ce principe dans le domaine d'emploi des photomultiplicateurs ($\lambda < 1.3\ \mu$) se heurte aux objections déjà exposées (1) à propos d'autres méthodes spectrométriques. Il semble toutefois que si le spectre étudié est peu dense (spectre de raies peu nombreuses, sans fond continu important), l'emploi de ce dispositif puisse conduire à une augmentation appréciable du rapport signal-bruit.

Par contre, le problème de la photogravure des grilles sur différents matériaux étant résolu, l'application de ce principe dans l'infra-rouge moyen ne pose pas de difficultés spéciales.

References

1. P. Jacquinot, J. phys. radium **19,** 223 (1958).
2. R. Chabbal, J. phys. radium **19,** 246 (1958).
3. P. Felgett, J. phys. radium **19,** 187 (1958).
4. P. Connes, J. phys. radium **19,** 215 (1958).
5. H. A. Gebbie, J. phys. radium **19,** 230 (1958).
6. J. Connes, J. phys. radium **19,** 197 (1958).
7. L. Mertz, J. phys. radium **19,** 233 (1958).
8. P. Jacquinot, J. Opt. Soc. Am. **44,** 761 (1954).
9. M. J. E. Golay, J. Opt. Soc. Am. **41,** 468 (1951).
10. A. Girard, Optica Acta **1,** 81 (1960).
11. P. Jacquinot et B. Roisen-Dossier, "Apodisation" dans *Progress in Optics*, publié sous la direction de E. Wolf (North-Holland, Amsterdam, á paraitre) Vol. 2.
12. J. Arsac, *Transformation de Fourier et Théorie des Distributions*, (Dunod, Paris, 1961).

Department of Fuller Explanation

In the Editorial of the July issue, in the course of discussing typical attitudes toward units and terminology, we hazarded to distinguish between scientists (specifically physicists) and engineers. We admitted such attempts are dangerous and can only result in a reductio ad absurdum: but we were led to opine that the engineer relies chiefly on his memory, and the physicist on his reason. One or two readers interpreted this as impugning the engineering profession. This we certainly did not mean to do. At the risk of embroiling ourself still further let us try again. In many schools it is possible to take training in physics or in a curriculum called "engineering physics." Why is the one considered a physicist and the other an engineer? The distinction supposedly is in the criterion which each applies to a problem. A physicist measures observables and tries to fit relations or theories to them (or vice versa), and his primary criterion is whether the phenomenon, or rather his description of it, appears to be true or false. The engineer must be more practical; his primary criterion should be whether it is useful or not useful. Philosophically, all these terms "true," "false," or "useful" have to be carefully defined, and even the philosophers divide into realists and pragmatists (and perhaps idealists). We do not wish to debate with philosophers. What we intended in our previous editorial was that the mental process of determining whether something is "true" or "false" is a function of the "reason," and the estimation of whether or not something is "useful" is measured against "experience," which we store in our "memory." It is not possible to have only one or the other: the senses, memory, and reason together form the intellect, of which we all have approximately equal amounts, if we are normal. Most engineers or physicists fall between the archetypes. Let us remember that this whole matter began while we were discussing "engineering units" and particularly as applied to optics. Even in the metric system the units used for engineering purposes (the MKS system) are commonly called "practical units." Perhaps we should retreat to an undisputed definition, such as "physics is what physicists do." We have an issue planned to feature chemical optics: we dread to think of the trouble we will get into in distinguishing between chemists and physicists, let alone chemical engineers.

Letters to the Editor *continued from page 78*

Operation of a Nd^{3+} Glass Optical Maser at 9180 Å *

R. D. Maurer

Corning Glass Works, Corning, New York.
Received 12 September 1962.

An optical maser employing the Nd^{3+} ion was first operated with a $CaWO_4$ host[1] and later with a glass host.[2] Following these, many crystals and glasses have been used to contain the Nd^{3+} ion. All these optical masers generate light of about 10,600 Å using the $^4F_{3/2}$—$^4I_{11/2}$ transition. This note describes the operation of a Nd^{3+} glass optical maser generating light of 9180 Å using a transition between crystal field components of the $^4F_{3/2}$ state and the ground state, $^4I_{9/2}$.

The base glass used in this study had the approximate composition by weight of 71% SiO_2, 15% Na_2O, 12% CaO, 1% Al_2O_3, 1% Sb_2O_3, and had a density of 2.56 g cm^{-3}. Various percentages of Nd_2O_3 were added keeping the weight ratio of the base glass oxides unchanged. Figure 1 shows the optical absorption near 80°K and near 300°K for the region around 9000 Å. This absorption corresponds to transitions from the $^4I_{9/2}$ to $^4F_{3/2}$ state.[3] Figure 2 shows the relative fluorescence intensity near 80°K and near 300°K after correcting for self-absorption and the apparatus response. These results are somewhat uncertain at wavelengths less than 9000 Å because of the large self-absorption corrections; the sample had a square cross section of side 0.5 cm. At room temperature there appear to be weak fluorescence bands near 8970 Å and 8680 Å which are not present at low temperatures. The main feature, however, is two prominent bands at 8860 Å and 9170 Å.

Figure 3 shows the proposed level scheme which accounts for the predominant features of these broad peak spectra characteristics of glasses. Presumably each "peak" contains several unresolved crystal field levels.[4] First, consider the optical absorption. At room temperature the prominent absorption occurs from the $^4I_{9/2}$ (1) level to the two $^4F_{3/2}$ levels giving two

* This work was supported in part by the Office of Naval Research.

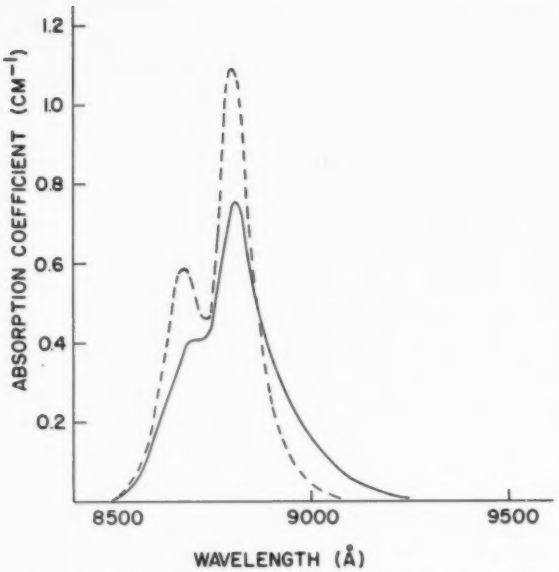

Fig. 1. Optical absorption versus wavelength for a glass with 3.1% neodymium oxide by weight. Solid line, 300°K; dashed line, 80°K.

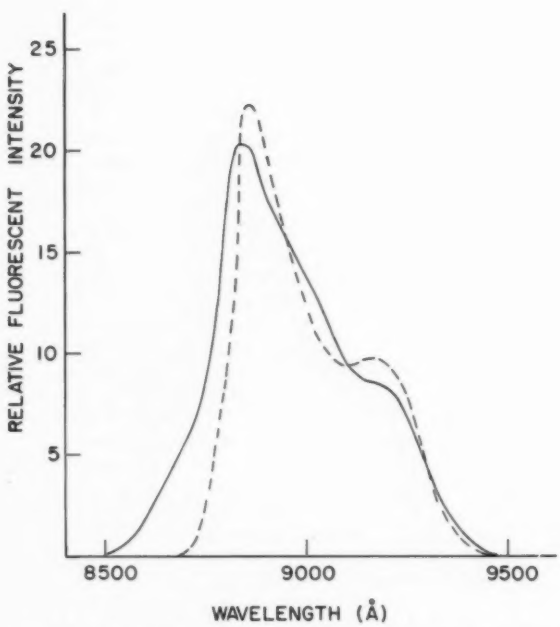

Fig. 2. Relative fluorescence versus wavelength for a glass with 6% neodymium oxide by weight. Solid line, 300°K; dashed line, 80°K. Resolution is about 20 Å.

peaks. In addition, there is some absorption from the $^4I_{9/2}$ (2) level but it is weak since only about 14% of the atoms are in this state. At 80°K, the main peaks have about the same peak height ratio as at 300°K; this is to be expected from the level scheme. However, the absorption at long wavelengths has disappeared since only about 10^{-3} of the ions are now in the $^4I_{9/2}$ (2) level. The energies of the two $^4F_{3/2}$ levels were determined from the two main absorption peaks. Next, consider the fluorescence. The two main peaks arise from transitions from the $^4F_{3/2}$ (1) level to the two $^4I_{9/2}$ levels. The lifetime is long enough for thermal equilibrium to be achieved in the excited states so about 30% of the excited ions occupy the $^4F_{3/2}$ (2) state at 300°K. The 8970 Å and 8680 Å bands are therefore weakened by the occupation of the $^4F_{3/2}$ (2) level. At low temperatures, the two weak peaks disappear since the $^4F_{3/2}$ (2) level is practically empty. There is an unexplained small wavelength difference between the fluorescence and absorption peaks, so the energy of the $^4I_{9/2}$ (2) level was obtained from the separation of the two main fluorescence peaks.

The level scheme suggests the possibility of inducing optical maser action at low temperatures with the $^4F_{3/2}$ (1)—$^4I_{9/2}$ (2) transition. Such oscillations were obtained using 5-cm long cylindrical samples with dielectric end coatings that suppressed the 1.06 μ oscillation. Transmissions of the ends at 0.92 μ and 1.06 μ were respectively <1% and >60% for one end and <2% and >80% for the other. Threshold at 80°K, deduced from the typical output "spikes" on the oscilloscope trace, was 700 J using an EG and G Laser Stimulator with the sample in a clear dewar cooled by the flow of nitrogen gas. Under comparable experimental conditions, threshold for the 1.06 μ oscillation would be of the order of 100 J. No oscillations were detected at room temperature with an input of 1100 J. At energies 50% above threshold, the stimulated emission spread over a range of about 80 Å centered near 9180 Å.

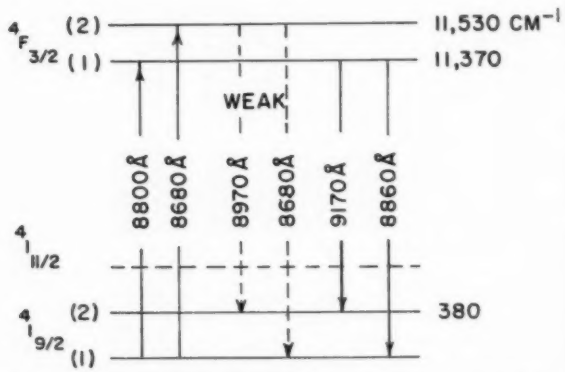

Fig. 3. Proposed level scheme to explain the fluorescence and absorption.

References

1. L. F. Johnson and K. Nassau, Proc. I.R.E. **49,** 1704 (1961).
2. E. Snitzer, Phys. Rev. Letters **7,** 444 (1961).
3. E. H. Carlson and G. H. Dieke, J. Chem. Phys. **34,** 1602 (1961).
4. W. A. Runciman, Repts. Progr. in Phys. **21,** 30 (1958).

Letters *continued on page 91*

A Sensitive Visual Photometer for Solar Research

Yngve Öhman

The paper describes one of the visual photometers which have been developed at the Stockholm Observatory and its solar station in Anacapri, in connection with the solar patrol which has been operating in these observatories for several years. The instrument, which uses a Savart polariscope as detector, can be used for measuring disk phenomena as well as limb phenomena, and is particularly well adapted for use as an auxiliary instrument when working with birefringent filters. It has proved useful in spectrophotometric measurements as well.

In connection with the solar flare patrol operating since 1952 at the Swedish Astrophysical Station in Anacapri and at the Stockholm Observatory in Saltsjöbaden since about 1947, considerable efforts have been made to develop simple auxiliary instruments for measuring areas and intensities of various solar phenomena, such as flares, filaments, and prominences. The first instrument (1) developed for this purpose consists of an orthoscopic eyepiece, where three holes in a transparent polaroid film are visible together with the solar image. The three holes correspond to the limiting sizes of flares of importance 1, 2, and 3. By turning the eyepiece with respect to a birefringent filter the solar image viewed in the eyepiece will change its intensity except for the small areas visible in the holes. In fact, the holes appear in this way as artificial flares which may be compared with real flares seen near the holes through the polaroid film.

A more refined instrument (number 2), based on a similar principle, was devised by the author in 1956[1] and has been used with great success at the Swedish Astrophysical Station in Anacapri.[2,3,4] In this photometer the polaroid film is cemented to a plate of calcite, the principal section of which is perpendicular to the vibrational direction of the polaroid. In this way two images are seen of the hole in the film, the intensities of which vary with different orientations of the eyepiece with respect to the birefringent filter. A setting θ which gives the extraordinary image of the hole (undisturbed part of the solar disk) the same intensity as that of the single image (ordinary) of a flare observed at the side of the hole allows the intensity of the flare i_f to be calculated according to the formula:

$$i_f = I_0 \left(1 + \frac{1}{a} \tan^2 \theta\right). \qquad (1)$$

Here I_0 is the intensity of the undisturbed solar disk and a a transmission factor which can easily be determined by comparing the two images of the hole. This method of solar flare photometry is particularly sensitive for objects of low contrast, as a consequence of the fact that the artificial bright object is added to the undisturbed solar surface as expressed by formula (1). Very bright objects and notably those with filamentary structure may be somewhat more difficult to measure, but a trained observer arrives at good accuracy also for such objects. Even dark filaments (prominences on the disk) have been satisfactorily measured with this device[5] by locating the filament on the hole.

In order to find an instrument which could allow accurate determinations even of flares with a filamentary structure and of flares and prominences situated outside the limb, experiments were started in 1960 with a modified photometer using a Savart polariscope as detecting device.[6] The experiments were very successful, and a new photometer was devised which has been found to give the same high accuracy as photometer number 2 described above but with still more possibilities. In fact from the extremely good experience we have had with this photometer (number 3) it might be worth trying it as a standard photometer in solar research. Its principle is as follows:

When the light has passed the birefringent filter M (Fig. 1) as plane polarized light, it is split into two beams polarized perpendicularly to each other in

The author is at the Stockholm Observatory, Saltsjöbaden, Sweden.

Received 14 August 1962.

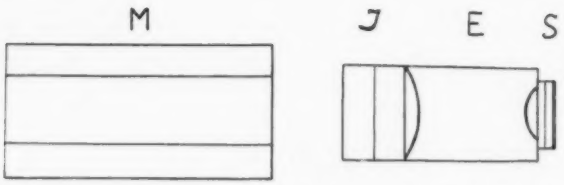

Fig. 1. Schematic plan of the photometer using a Savart polariscope as detecting device. M is a birefringent filter or ordinary polarizer, I a calcite plate, E the eyepiece, and S a Savart polariscope.

the calcite plate I connected with the eyepiece E, at the end of which is mounted the Savart polariscope S. With this arrangement the observer sees two somewhat displaced images of the sun. If the eyepiece is rotated with respect to the birefringent filter, the relative intensity of the two images will change. If the superimposed light of the two images, say of the central region of the undisturbed solar disk, shows no trace of polarization, that is, no trace of Savart fringes, the two images have evidently exactly the same intensity.

Suppose now that we have a solar flare in the field of view. With the same setting as before the Savart fringes are now well visible in both images of the flare. In order to make the fringes in one of the images disappear (Fig. 2) we turn the eyepiece an angle θ and obtain the intensity of the flare, i_f, expressed in the intensity of the neighboring solar disk, I_0, as unit, by means of the formula:

$$i_f = I_0 \tan^2 (45° + \theta). \tag{2}$$

In order for one to determine θ more accurately, the other image of the flare is now weakened by turning the eyepiece in a symmetrical position, so that the Savart fringes disappear in this image instead. The difference in the two settings gives the quantity 2θ.

When measuring objects which are fainter than the solar disk, say sunspots, filaments, or prominences outside the limb, the formula (2) will be replaced by:

$$i_p = I_0 \tan^2 (45° - \theta). \tag{3}$$

Figure 3 shows a photograph taken through the photometer when a setting has been made on a prominence outside the limb. As can be seen from this image the Savart fringes have completely disappeared in the prominence visible against the displaced solar disk of the fainter image. When such measurements are reduced, the apparent intensity ratio is generally transformed to one with the intensity in the center of the solar disk as unit. It is necessary therefore to make a determination of the limb-darkening function for the birefringent filter.

In the case of prominences and sunspots it is often necessary to apply a correction for stray light (atmospheric and instrumental). The photometer is very well adapted for such a procedure.[7] In fact stray light outside the limb can be observed in the same way that we observe a prominence. Suppose that K_s is the apparent intensity ratio found for the stray light and that K_p is the same for the prominence. The true intensity ratio for the prominence is then obtained as:

$$\frac{i_p}{I_0} = \frac{K_p - K_s}{1 - K_s}. \tag{4}$$

We have arrived at very good accuracy by this method, and have been able to establish small intensity variations in prominences which seem to be related sometimes to long distance disturbances from flares.[8]

The photometer has been found to be very convenient when used to measure sunspots as well.[7] Moreover it has been found useful for measuring equivalent widths of Fraunhofer lines.[7]

In the first instrument which has been in use now in Anacapri for about two years the calcite plate I has a thickness of 10 mm. In the same instrument the Savart polariscope has been so made that the fringes appear with a spacing of about 5 min of arc. This has been found very satisfactory when working with a solar disk formed by a lens with $f = 150$ cm and together with an eyepiece with $f = 25$ mm. In

Fig. 2. The importance 3 flare of July 15, 1961, observed through the photometer using a Savart polariscope. The Savart fringes are absent in the weaker (lower) image of the flare which is superimposed on the brighter and somewhat displaced image of the solar disk. This corresponds to a correct setting.

Fig. 3. Limb prominence of July 9, 1962, observed through the photometer using a Savart polariscope. The Savart fringes are absent in the stronger image of the prominence which is superimposed on the weaker and somewhat displaced image of the solar disk. This corresponds to a correct setting.

the Stockholm Observatory solar patrol instrument, which has a focal length of 189 cm, a polariscope is used which gives a separation of the fringes of about 8 min of arc. As the fringes are visible at infinite distance, a myopic observer must use his correcting glasses when working with the photometer.

A small improvement of the instrument may be made by placing a half-wave plate in front of the calcite plate. The measurements can then be made by turning this plate instead of the eyepiece. This method would particularly facilitate measurements of prominences because of the fact that a more or less radial displacement of the two images is preferable for such a purpose.

Though our photometer number 3 is similar in principle to the classical Wild photometer, it does not seem to have been used by other observatories. In our opinion it facilitates to a considerable degree the classification of solar flares, and could make possible a refined flare classification using two symbols, one expressing the area and the other one the intensity. It is worth noting in this connection that we have found no trace of systematic difference[9] between measurements made with this photometer and the photometer number 2 working according to formula (1). If the birefringent filters are of similar quality, we believe that different observatories would obtain very similar results. In this connection it should be mentioned that the accuracy found by us compares well with that of high quality photographic determinations.

References

1. Y. Öhman, Stockholms Observatoriums Ann. **19,** 4 (1956).
2. Kerstin Fredga, Stockholms Observatorium, Medd. 100 (1958).
3. F. Eleman, Stockholms Observatorium, Medd. 135 (1962).
4. Y. Öhman, Stockholms Observatoriums Ann. **22,** 4 (1962).
5. Kerstin Fredga, Stockholms Observatorium, Medd. 126 (1960).
6. Y. Öhman and Britt Ahnström-Sandgren, Stockholms Observatorium, Medd. 125 (1960).
7. N. J. Bergsjö, Stockholms Observatorium, Medd., in press.
8. Y. Öhman, A. Lindgren, and Ulla Lindgren, Stockholms Observatorium, Medd., in press.
9. Kerstin Fredga, Stockholms Observatorium, Medd., in press.

Letters to the Editor *continued from page 88*

An Unusual Property of MgF_2 Films in the Infrared

Milton Laikin

Pacific Optical Corporation, Inglewood, Calif.

Received 10 September 1962.

Evaporated MgF_2 films have long been used as antireflection coatings for glass parts,[1] and have also been used as a protective coating for aluminum mirrors.[2] Silicon monoxide is sometimes used as a protective coating for aluminum mirrors.[3] However, if the magnesium fluoride is baked at 250°C for 10 to 15 min, mirrors so protected are highly resistant to abrasion.[4] Magnesium fluoride is also used because of its ultraviolet transmittance as a protective coating on aluminum where high ultraviolet reflectance is desired.[5]

Referring to Fig. 1, curve 1 shows the reflectance of unprotected aluminum as compared to aluminum overcoated with a 250 mμ optical thickness (index of refraction times thickness as monitored with green light) of magnesium fluoride, curve 3. The reflectance is reduced at 16.5 μ by 15% due to the magnesium fluoride. Aluminum is first evaporated onto the cold glass block. The heaters are then turned on to raise the temperature of the work to 250°C and MgF_2 is then evaporated. All this is done at pressures of about 5×10^{-5} mm Hg.

Essentially the same curve is obtained if the MgF_2 is evaporated onto work which is at room temperatures and the heaters turned on immediately after the evaporation (while still under a vacuum).

However, a different reflectance is obtained, curve 2, if the heaters are not turned on at all while under a vacuum. The film is, of course, quite soft. Its reflectance has dropped by about 6% at 17.5 μ as compared to the plain aluminum. This reflectance

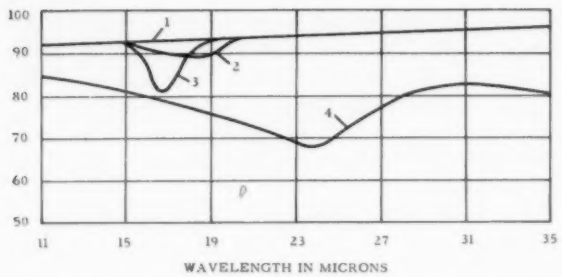

Fig. 1. Curve 1—reflectance of unprotected aluminum. Curve 2—reflectance of aluminum—MgF_2 protected—baked in air 24 hr later. Curve 3—reflectance of aluminum—MgF_2 protected—baked in vacuum. Curve 4—transmittance of CsI plate coated on both sides with MgF_2.

does not change even if the part is later placed in an oven (in air) at 250°C for 15 min. The MgF_2 film will now be quite hard.

Curve 4 shows the transmittance of 1.3 cm thickness of CsI coated with a 250 mμ optical thickness of MgF_2 on both sides of the plate. The transmittance of the CsI alone is 85% from 11 to 35 μ. The unusual thing here is that there is no lowered transmittance at 16.5 μ as might be expected from noting the reflectance curves.

The MgF_2 was applied to the plate while cold and then measured. Heating in an oven in air for 15 min at 250°C does not change the transmittance. At 2.9 μ there is an absorption band which lowers the transmittance by 6%. This also is unaffected by heating.

At 7.3 μ the absorption coefficient of single crystal MgF_2 is 1 cm^{-1}.[6] Since the total thickness of MgF_2 films on the CsI plate is approximately 365 mμ, the transmittance of the films is essentially unity. However, the absorption coefficient reaches a maximum at about 20 μ as indicated by the reflectance maximum here.[6] This is further indicated by the lowered transmittance as shown in curve 4.

The MgF_2 protected aluminum does not exhibit a lowered reflectance at 23 μ due to the standing wave pattern produced upon reflection.[7] The zero amplitude of the electric vector at the surface of the metal means that an absorbing film on the surface will have only little effect on reflectance.

At 16.5 μ, there is an absorbing film of extremely high absorption on the aluminum. Furthermore, this absorption is not due to the pure MgF_2 only. It appears as if the MgF_2 has reacted with the aluminum to produce this highly absorbing film. Silver also shows this reduced reflectivity when overcoated with MgF_2. Nichrome does this also, although to a lesser extent.

References

1. S. Bateson, J. Soc. Glass Technol. **31**, 170 (1947).
2. Mil-M-13508 Mirrors, Front Surfaced, Aluminum, For Optical Elements (June 1954). Off. Chief of Ordnance, Washington 25, D.C.
3. G. Hass and N.W. Scott, J. Opt. Soc. Am. **39**, 179 (1949).
4. D. A. Lyon, "Method for Coating Optical Elements," U.S. Patent 2,398,382 (April 1946).
5. P. H. Berning, G. Hass, and R. P. Madden, J. Opt. Soc. Am. **50**, 586 (1960).
6. A. Duncanson and R. W. Stevenson, Proc. Phys. Soc. (London) **72**, 1001 (1958).
7. Georg Hass, J. Opt. Soc. Am. **45**, 945 (1955).

Low Cost Noncontact Thickness Gauge

L. C. Lynnworth

Avco Corporation, Wilmington, Massachusetts.
Received 28 May 1962.

This note describes a new and economical solution to the recurring industrial metrology problem involving the measurement and control of the thickness of wet coatings. These coatings, for example, may be certain ablative-type plastics which are sprayed on missile and aerospace components to provide thermal protection during firing, ascent, or re-entry.

If the coating is too thin, heat shielding is inadequate. If the coating is too thick, excess weight seriously reduces range. In practice, tolerances of about ±0.005 in. (±125 μ) are commonly specified.

This accuracy requirement at first sight appears readily obtainable. However, the thickness measurement problem is complicated by the large, unwieldy structures being coated. Furthermore, it is desirable to measure the thickness while the coating is still wet, for two reasons. First, this sequence avoids the application of excess material, for which the cost of removal is high. Secondly, if too little material is applied, bonding of fresh extra coats to a cured substrate may be unreliable.

The shortcomings of three candidate inspection systems may be summarized as follows. Backscatter[1] methods, frequently used in industry to control sheet thickness of uniform materials, are sensitive to composition and density variations, and are generally expensive. Air gauges have been considered, but the thickness range per gauge is a fraction of a centimeter. Using an ultrasonic pulse echo system,[2] an ultrasonic transducer may be positioned a few centimeters from the wet surface. The pulse round trip transit time through air provides an accurate measure of thickness, but again the cost is several thousand dollars. Surprisingly, the cost of one proposed inspection facility to measure the coating thickness on a 1.5-m diam, 6-m long drum exceeded thirty thousand dollars.

A simple optical gauge has provided the most satisfactory solution to date. To illustrate the gauge's principle, Fig. 1 shows a 150 W projection lamp light source, reticle, 50 mm, f/4.5 lens, beam splitter, two masks, and two reflectors. The reticle, an "X" and an "I," is projected to the beam splitter. After splitting, the I is reflected from the left-hand reflector, and the X from the right-hand reflector. The X and I then converge to a

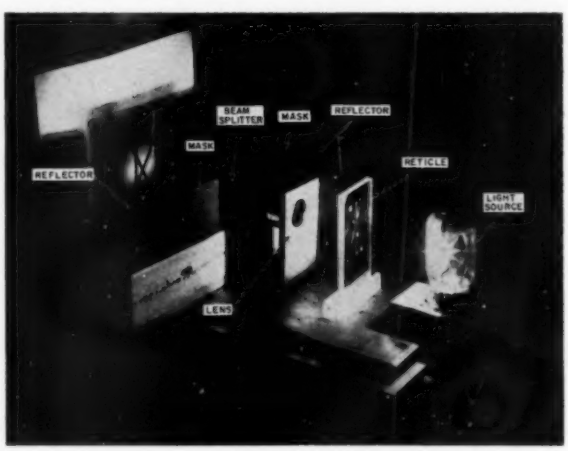

Fig. 1. Breadboard configuration of optics elements illustrates principle of noncontact thickness gauge.

continued on page 104

A Solar Observatory on Long Island

William A. Miller

A brief history of the solar observatory at Rocky Point, Long Island, New York, is presented herein. A topical semichronological account of the establishment of this observatory and the design and construction of the equipment follows. The results of the optical design and construction confirm our belief that the presently accepted tolerances (one-quarter wavelength limit, etc.) are too coarse and that all attempts at closer control of figure will be of benefit. A means of preventing mirror distortion due to exposure to the sun is described. The inter-relations between focal curve, emulsion sensitization, and filters are discussed. The excellent seeing conditions existing on Long Island and the observed meteorological situations accompanying the times of good seeing are described.

Introduction

Today there seems to be no scarcity of recommended techniques and procedures of optical design of the astronomical objective. Rather than repeat what is perhaps already well known, we shall place the emphasis on some of the major problems which were encountered. These problems arose in the attempt to establish a quite modest observatory whose sole purpose was the photography of the solar photosphere. Our solutions may be of some interest, if for no other reason than that they worked. Obviously, such solutions are not the only possible ones, but they may prove useful and interesting to others who may be facing the same or similar problems.

Historical Note

In 1950, RCA Laboratories, Rocky Point, L.I., New York, embarked on an attempt at providing information about the sun to those in RCA Communication, Inc., who were making predictions concerning HF radio propagation. Initially, it was intended that the effort would be limited to determining the daily sunspot number. Shortly after the first instrument was placed in operation in the spring of 1951 unexpected detail was found on the solar disk photographs. Then decisions were made to enlarge the observational program and to improve the quality of the instrumentation as much as was felt to be feasible.

This latter end was achieved by the design and construction, in 1952, of a 152-mm aperture, 12.27-m focal length ($f/80$) horizontal telescope used with a modified form of coelostat. In 1956, a 197-mm aperture, 3.55-m focal length ($f/18$) camera, also of our own design and construction, was put in operation. This instrument was equatorially mounted in a building with a 6.7-m diameter dome. Figure 1 shows both the horizontal and equatorial cameras in their respective buildings.

An extensive study of granulation and other solar disk features was carried on for several years until, in 1957, this program was considerably reduced in manpower and photographs were taken only on the days of best seeing. In 1959, this program was completely stopped. In 1961, when it was decided that the RCA Laboratories' facility at Rocky Point would be closed, these two instruments, the document files, and the plate collection were given to the Department of Physics, State University of New York, Long Island Center. This department hopes to have at least the horizontal camera in operation in 1963 at the University Campus, Stony Brook, Long Island.

Instrumentation

With the exception of the eyepieces used for testing the telescopes with stellar images, all optical and mechanical parts were designed and built at Rocky Point. The usual tolerable departure from sphericity of one-quarter wavelength in the yellow-green for achromat construction was changed to one-twentieth of the same wavelength. We found, during the con-

The author was at the RCA Laboratories, Rocky Point, New York. His present address is: Electronic Systems Division, Fairchild Stratos Corporation, Wyandanch, L.I., New York.

Received 28 June 1962.

The equipment program was totally supported by RCA Laboratories, while the observational program was partially supported by the Signal Corps.

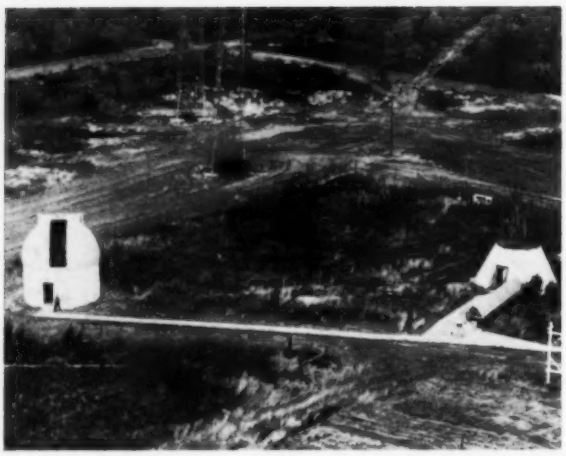

Fig. 1. Solar Observatory at Rocky Point ($f/18$ left–$f/80$ right).

struction of the $f/80$ objective, that as the departure from sphericity for each surface was reduced from the former to the latter value, the image quality improved.

The horizontal camera used the 12.27-m focal length achromat which was made of Bausch & Lomb BSC_2 and DF_2 glass. The optical design, after preliminary algebraic solutions, was completed using the procedures of Conrady.[3] The results of the design: the dimensions of the lens, spherical aberration curves, offense against the sine condition, and focal curve are shown in Fig. 2. It will be noted that the criterion for achromaticity (identity of focal length for C and F lines) is not precisely fulfilled, but the actual difference is so small that it is not important in view of the excellence of the correction for coma and spherical aberration not otherwise attainable.

Pyrex test plates of the proper radius of curvature were ground, polished, and tested by Foucault's[4] test. These test plates fit the design radius to ± 2.5 mm and depart from sphericity by no more than $^1/_{40}$ of the wavelength of the yellow helium line. The corresponding convex surfaces of the elements of the lenses were ground to the proper radii of curvature, polished, and figured until they fit their corresponding test-plate to better than $^1/_{20}$ wavelength of the D-line of helium. Before the final mounting of this objective, it was assembled in its cell, and a Foucault test was performed at focus by using a precision flat in front of the lens. A series of interference filters of 100 A bandwidth was used, together with a set of masks, to isolate the paraxial, zonal, and marginal regions. The tests were also made without stops. Such a system allowed us to measure the spherical aberration as a function of wavelength and the focal curve, as well as to observe the over-all performance at various wavelengths.

We concluded that this lens departed insignificantly from the design. The lens was placed in its telescope and pictures were taken of the sun with quite disappointing results! The detail of the solar fine structure was present on the photograph but the contrast was very poor. Tests soon convinced us that this was due to stray (or unfocused) light introduced by multiple reflections between the second and third surfaces which had the same radius of curvature.

It was felt that low-reflection coatings would not adequately reduce the reflections. The diameter of the lens is such that cementing or optical contact is not practical. We used several drops of doubly-filtered, Dow-Corning 200 centistoke silicone oil as a contacting medium. The lens elements, with the oil between them, were pressed together, using only the hands and weight of the assembler, until the gap was between 0.025 and 0.05 mm. The gap between the elements must be completely filled by the oil.

After this lens had been in use several years, it was reported in the literature that silicone oil would, in time, attack glass—at least in vacuum systems. The lens was immediately disassembled, thoroughly cleaned, and both surfaces were examined with a 50 power microscope and high-intensity, grazing illumination. *There were absolutely no signs that the oil had attacked the glass.* The lens was reassembled with the same kind of oil. After 8 more years, this lens, although exposed to an outdoor temperature range of $-25°$ to $+35°$C, shows no sign of element separation or attack. Some very light tarnish has formed, but this is only on the exposed surfaces.

This method of overcoming the image degradation, caused by unwanted reflections between closely air-spaced elements of the same curvature, should be used with caution. Nothing is known with certainty about the chemical action possibly occurring when the softer, less-stable glasses are used. Perhaps the more expensive, but no more suitable (from the optical standpoint), evaporated layers must be used. However, it has been our experience that it is safe and satisfactory for contacting B. & L. BSC_2 and DF_2 glasses.

The equatorial camera lens is an achromatic doublet of BK7 and F2 glasses purchased from Schott of Jena. The focal length is 3.55 m and the clear aperture is 197 mm (203-mm diameter blanks). This lens has a focal ratio of $f/18$ and is more nearly like the normal astronomical doublet. Thus, the design was simpler and by using simplified techniques and short-cuts,[3] we were able to arrive at a suitable design in a shorter time than with the $f/80$. Unfortunately, these methods, while yielding a well-designed objective, do not, during the course of the design, yield as much information about the expected performance of the lens as

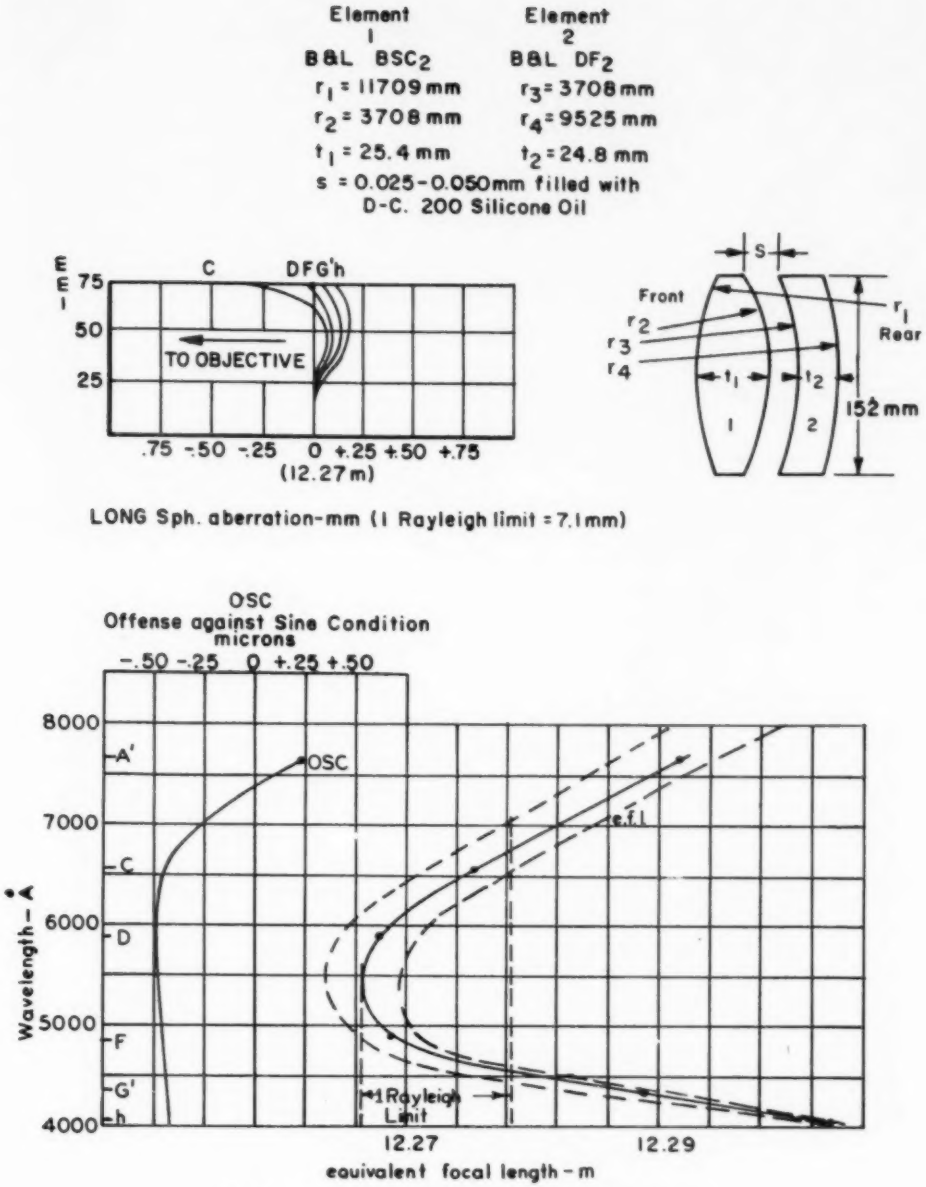

Fig. 2. 152-mm aperture, 12.27-m focal length doublet.

the more extended effort. Figure 3 gives the results of this design.

The same tolerances and techniques were used in making this lens as were described for the $f/80$ lens. The 10% difference in the radii of curvature of the inner surfaces is sufficient to insure that the stray light originating from multiple reflections does not seriously degrade the image.

Photographic and visual tests show that this instrument, as well as the $f/80$, operates to the classical diffraction limit in times of good seeing.

The camera mountings differ. The 12.27-m focal length lens is fixed with its optical axis horizontal. The lens is directly south of the photographic plate, and the sunlight producing the image is collected by a modified two-mirror coelostat. The modification is such that the orientation of the image is not fixed. However, the observer at focus has control of both right ascension and declination.

The position of the solar poles and the orientation of the sun's equator may be established by stopping the drive motor. Any point on the image will then

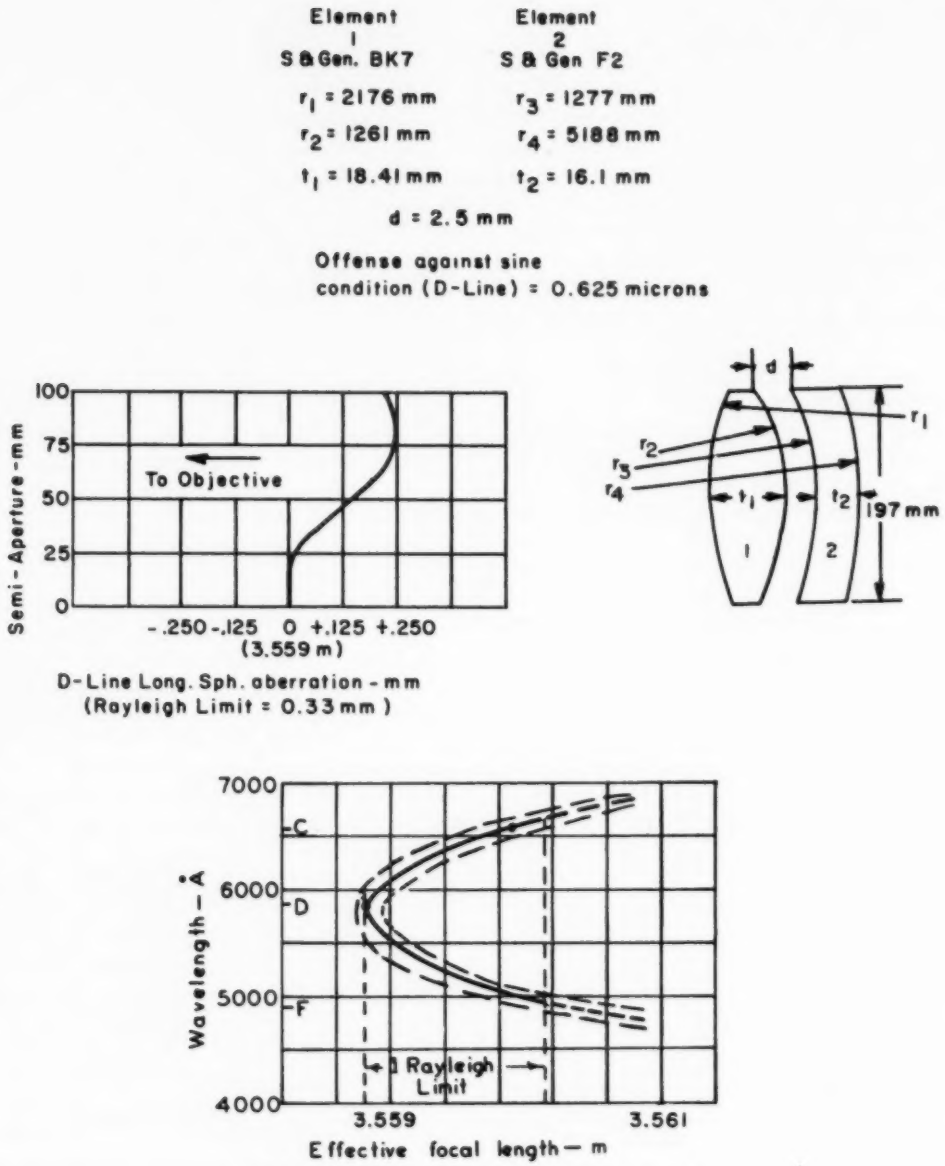

Fig. 3. 197-mm aperture, 3.55-m focal length doublet

drift parallel to the direction of motion of the earth. A knowledge of this direction allows the establishment of the North Point on the sun's limb. From the Ephemeris, one may then locate the poles of the sun on the image.

When this system was first operated it was noticed that the focal length varied nearly 147 mm during the first $^1/_2$ hr of the day. Figure 2 shows that the Rayleigh limit is about 15 mm, but we have noted that the location of the sharpest image can be found more accurately than this and a motion of the image of 7.5 mm from this position is easily detectable. After isolating the various components of the system by use of shadow screens, it was found that the primary mirror went slightly convex upon exposure to sunlight, thus increasing the over-all focal length. When this effect was discussed with O. Mohler,* he commented that the observers at Pic du Midi had found the same effect with their aluminized pyrex mirrors. Apparently, this distortion occurs because the alumi-

* McMath-Hulbert Observatory, Pontiac, Michigan.

num coats are slightly transparent to a portion of the infrared, and this allows sunlight to enter the mirror, internally heating and distorting it. Dr. Mohler also said that it was his impression that the Pic du Midi group had found that this did not occur with silver coats and that they consequently abandoned the use of evaporated aluminum and returned to the use of chemically-deposited silver coats. Such coats will have a good lifetime, there, because the air in the Pyrenees is relatively free of tarnishing agents. At Rocky Point a silver-coated front-surface mirror has a useful winter lifetime of about 3 weeks. Of course, fused quartz flats would alleviate this situation, but such a solution is quite expensive.

We were able to devise a method of producing multiple coats which solves this problem. The result is quartzlike performance at the cost of pyrex. This is so useful that we believe that it is worth considering in some detail.

In the first experiments an opaque layer of silver was deposited first, by evaporation from tantalum boats, and followed by evaporation (without breaking the vacuum) of a coat of aluminum in order to keep the silver from tarnishing. This method provides an aluminum reflector with a protected silver coat which reflects the infrared.

After 3 or 4 weeks exposure to the atmosphere, there was an accelerating separation of the silver from the glass. Small blisters would appear first, apparently accompanied with pinhole puncture of the aluminum, since each blister became a center from which oxidation and tarnish of the silver layer rapidly progressed. These mirrors lasted long enough, however, for several measurements of the focal-length change to be made. We found that, instead of a focal length change of nearly 147 mm, the focal length of the system only changed by about 12.5 mm. By allowing the mirrors to remain exposed to sunlight, while the lens was shielded from the beam, it was found that the residual change in focal length is attributable to changes in the lens. The performance proved so satisfactory that rather than abandon the multiple layer coatings, an attempt was made to develop a technique of deposition which would result in a more permanent coat.

To test the possibility that the blisters were initiated by free radicals, local impurities, etc. in the glass itself, the mirrors were next coated with three layers: an opaque layer of aluminum next to the glass, an opaque silver coat on this, and finally an outer layer of aluminum. This yielded a mirror coat of no longer life than was found in the first test. At about this time, papers appeared describing the lack of tenacity of evaporated silver and the use of such coats to provide an easy-parting plane for molding plastics. It was then felt that it might be better to find some other infrared opaque undercoat for the aluminized mirror. Rhodium and chromium were not considered because (1) they are too difficult to remove and replace, and (2) it is probable that they too are somewhat transparent to the infrared, since pyrex mirrors with rhodium–aluminum or chromium–aluminum coatings suffer distortion when illuminated with direct sunlight. Copper was then tried as an undercoat. When such mirrors are used, it was found that freshly deposited copper–aluminum mirrors produced the same focal length change as does the fresh silver–aluminum coat. These mirrors are satisfactory for about 4 to 5 months. Curiously enough, the deterioration is too subtle to be discovered by an examination of the surface. Such mirrors give evidence of their failure by a relatively sudden, unexpected return to the original focal length change. This change may be complete in as short a time as 2 or 3 weeks, while naked-eye evidence of damage will not be distinguishable for several more weeks! Defective coatings were not subjected to microscopic examination. However, the mounting was such that portions of the copper coat could be seen through the pyrex blank and at no time was there visible evidence of diffusion of the aluminum through the copper although probably some such effect occurred.

A third series of experiments was then performed using silver as the undercoat. A comment by Strong,[5] together with our experience with the deposition of hard coats of titanium metal,[6] provided the necessary clues for the successful deposition of hard coats of metallic silver. After the usual final cleaning of the mirror surface by ionic bombardment, the pressure is reduced, with bombarding voltage on, until the glow becomes intermittent. An opaque silver coat is deposited at this pressure, after removal of the bombarding voltage. Some experience is needed in order to find the correct pressure for deposition. However, this pressure is not particularly critical. This coat is as brilliant as a silver coat deposited in a hard vacuum, but it will fulfill the usual test applied to evaporated aluminum coats. (The metal will not part from the glass when Scotch tape is applied to the surface and pulled off.) After this silver coat has been deposited, the bombarding voltage is reapplied and the pressure is further reduced until the bombarding voltage is no longer sufficient to cause breakdown of the remaining gas. The potential is removed and the aluminum deposited. Such mirrors provide a system in which the thermal change of focal length is due mainly to the lens itself, and such mirrors have the same permanence as those which have been coated by aluminum alone (several years).

A final modification of the technique consists of depositing, not a heavy final coat of aluminum, but only enough aluminum to form, in time, a transparent protective coat of aluminum oxide.[5] Such mirrors

grow in brilliance for several weeks as the aluminum is converted to oxide, and we have had such mirrors with 8- to 10-month-old coats which appear to be more brilliant than freshly deposited aluminum ones.

Mirrors made by the last described method are recommended; not only have we had mirrors whose coats were usable after $2^1/_2$ years continuous exposure to the Long Island atmosphere, but also we have found another unexpected advantage to accrue from their use. While an ordinary aluminum mirror coat appears as smooth to the eye as the glass surface upon which it is deposited, there is, for layers of the required thickness, a tendency for the aluminum to form an irregular surface. These irregularities result in strong forward scattering of the sunlight. This may be demonstrated by reflecting sunlight from such a mirror, and cautiously bringing the eye close to the main beam. It will be noted that the mirror becomes unbearably bright well before the eye is in the main beam. This is likewise true of double-coated mirrors in which the aluminum layer is thick. However, silver mirrors protected with a thin coat of aluminum oxide scatter much less light—the eye can approach the main beam more closely.

Since, for solar observations, scattered light is a strong source of image degradation, this is an important benefit derived from this method of mirror coating. The performance of such stable, glass mirrors amply repays one for the effort involved, particularly if one (as we did) does one's own mirror-coating.

The mount for the 8-in. (197 mm) lens is, with minor modifications, the familiar equatorial mounting. The modifications were those required to allow the use of reversible slewing motors in declination as well as in right ascension, without interfering with the synchronous motor drive in right ascension.

Photographic Materials and Techniques

Shortly after the observing program was started, we began using the Eastman High Resolving Power emulsions exclusively. We have successfully used Eastman Types 548 and 649 emulsions with different spectral sensitizations. Their resolving power far exceeds that of the lenses, but it is reassuring to know that what one sees is due to the exposure and not to emulsion granularity even when, as we often did, one uses 50× to 100× magnification of the image. Further advantages to the use of such emulsions lie in their extreme *insensitivity* and high γ. Proper exposure and development to enhance greatly the contrast between granules and the photospheric background (a difference in intensity estimated to be about 10%) is easily achievable without using shutters of extreme speed or special processing techniques.

Spectral sensitization class "GH," which is an orthochromatic sensitizer cutting-off at about 6100 Å and with high response to about 5700 Å, was the standard for our work. Experiment showed that the position of sharpest focus for this GH emulsion was at the point of sharpest visual focus. Other classes of sensitizer were used without success until suitable filters were used.

All still photography used 12.7 × 17.8 cm glass plates with antihalation backing. Although the image diameter with the $f/80$ camera was about 11.5 cm while that of the $f/18$ was about 3.8 cm, the same size plate was used for each camera. The shutter was moved from one camera to the other. The $f/80$ camera provided one full solar image on each plate while the $f/18$ provided 2 to 4 full images. Fully 80% of all plates were calibrated by exposing a portion of the plate through a calibrated step wedge. A diffuse source and identical shutter speeds were used for this exposure.

Some attempts were made at cinephotography using a lensless 16-mm camera and film coated with 548-GH or 649-GH emulsions, also with antihalation coating. Some difficulty was experienced in getting as good contrast range with the cine-film as with the plates. This is apparently because of the difference in emulsion thickness—that on the plate is much thicker. The time available was not such that this problem could be resolved, but some rather interesting, rapidly varying sunspot features were photographed and published.[7]

In general, we have found that either the 548 or 649 emulsion is quite satisfactory for photography of the photosphere. There is a slight preference for the 649, probably because it has a higher gamma. These emulsions seem to be as near the optimum for this purpose as could be obtained.

A word of caution is required at this point. Some of the sensitizer classes mentioned below are unstable and will, in time, make the plate unusable due to chemically activated regions. This deterioration can be checked by refrigeration. The standard, GH, sensitization is not an offender in this regard, but we felt it desirable to keep all unexposed plates in refrigerated (0°F) storage regardless of the sensitizer, particularly in the summer months. Of course, development followed immediately after exposure.

We found that the best image tone (green-brown) for easy direct study and reproduction was obtained by adjusting the exposure to give complete development in 15 min, with continuous agitation, in Kodak D-76 developer at the recommended temperature. This is not the development recommended by Eastman. Development with the recommended developer yields a much blacker tone with apparently greater contrast between granule and background, but we found the D-76 image much easier to use—others may not. After development the plate was rinsed in running

water for about one minute and then fixed in Kodak Rapid Fixer. While this fixer clears the emulsion very quickly, the AH-coat on the back of the plates does not disappear as easily—10 to 15 min in the fixing bath may be required. The plates were then washed in running water for a minimum of 2 hr, rinsed in distilled water, placed in Eastman Photoflo solution for 1 min to prevent water-spotting, and dried in warm, filtered air. All solutions and the rinse water were maintained at the same temperature.

The problems encountered in using the GH emulsions for white-light photography were solved by learning how to expose and process the material. Since such photographs were rendered with exquisite detail, we soon thereafter became interested in expanding the spectral range to wavelengths beyond 5700 Å. Eastman Kodak prepared plates with other sensitizers and we quote their designations of 1953–1956, which now may well be discontinued. These ranged from the "T" (peak at 5900 Å) and "D" (6000 Å) through the "E" (6450 Å) and "F" (6550 Å) sensitizers. Also, a much less sharp, long wavelength cutoff sensitizer, "B," was used. This sensitizer has a peak at 5800 Å but does not reach zero response until nearly 7000 Å. The emulsion with no sensitization (0) was also used.

We attempted to use these plates for direct, white-light photography. Without a single exception, no photographs made with these sensitizations had the same high quality as those made with the GH-sensitized emulsions. Order of exposure and intermixing of the differentlv sensitized plates were tried repeatedly, but without success. It was not until we further considered the problem of using broad-band filters that a solution to this problem was found.

Photographing the sun by filtered light presents different aspects depending upon what information is desired. If one wishes to employ filters which will transmit only one of the lines of the solar spectrum, one must use a monochromatic filter or spectroheliograph. These are complex and expensive. Each has both advantages and disadvantages with respect to the other, and a decision, normally, must be made between them unless one is fortunate enough to afford the luxury of both.

A quartz-calcite birefringent filter[8,9] was designed for use with Hα line at 6563 Å. Its design bandwidth was 0.75 Å. This unit was about 70% complete at the time that the observatory expansion program was halted. Consequently, not much can be said about it. However, I now feel that perhaps a high-speed spectroheliograph should have been given more consideration.

Wide-band filters may vary from those simpler classes of filters such as dyed gelatin or tinted glass (bandwidth of several hundred to thousands of angstroms) to the interference filter of bandwidths of the order of 20 to 100 Å.

The most extensive analysis of the filter problem has been carried out for the $f/80$ camera in preference to the $f/18$; principally because more information is at hand concerning the optical performance of the former than of the latter. However, these problems are of the same order of magnitude with either camera, and the results of the analysis of one can be qualitatively related to the performance of the other. From Figs. 2 and 3, it will be noted that both lenses are designed so that their individual points of sharpest focus may be found visually. Also, then, the greatest possible width of the visible spectrum will be in focus if the instrument is focused by eye.

On the curves of Figs. 2 and 3 the focal curves are also shown displaced by ±Rayleigh limit/4. Experience has shown that the point of sharpest focus may be found to this accuracy. Arbitrarily, it is assumed that the instruments are in sharp focus between these limits. These curves show at a glance that the longer focal length instrument is the easier to use of the two. Were it not for its lower resolving power, the 152-mm $f/80$ camera would be superior, in every way, to the 197-mm $f/18$ camera.

These figures (2 and 3) show that when the focus is adjusted visually to maximum sharpness, the 152-mm camera will be in sharp focus from about 5300 Å to 6100 Å. Light of wavelengths just shorter than the short wavelength limit and just longer than the long wavelength limit will be partially focused and effectively increase the size of the image. This effect may be quite harmful as there is slight evidence for a true change in granule diameter as a function of the wavelength of the light in which the granule is observed. At wavelengths well outside the tolerance limits the light energy is essentially unfocused. Such light can only contribute to over-all fogging of the emulsion and masking of the detail.

The details of the various relationships between filters, emulsion sensitizers, and the focal curves will be considered for the $f/80$ camera, only. The $f/18$ camera was always used with "GH" sensitized plates and a GAB interference filter, centered at 5303 Å, and obtained from Fish-Schurman Corp.* The over-all bandwidth at one-half maximum response was about 150 Å. The position of best visual focus coincided with the best photographic focus in this case.

Estimates of the solar flux incident on the surface of the earth's atmosphere as a function of wavelength were used to find the solar flux incident, at zenith, on the primary mirror. The atmospheric transmission coefficient was adjusted for 4 to 5 cm of precipitable

* 70 Portman Road, New Rochelle, N.Y.

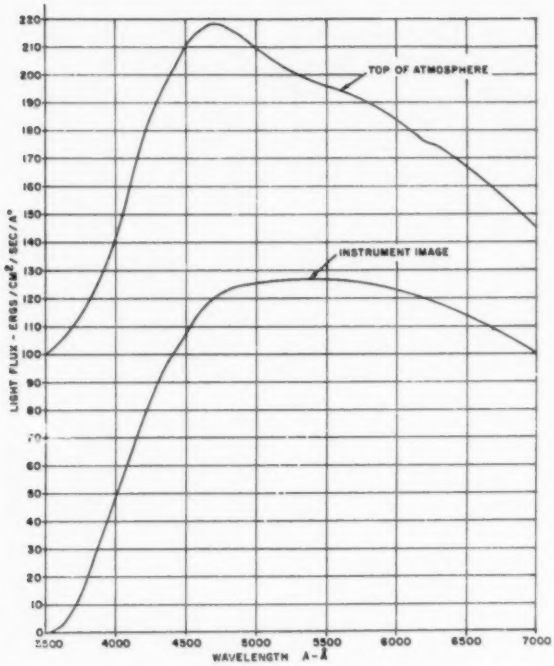

Fig. 4. Spectral distribution of light flux ($f/80$).

water (60–90% rel. hum.; 20°C to 30°C), believed to be characteristic of the summer atmosphere over Long Island. The solar flux incident on the lens was calculated by using the reflection coefficient of aluminum (we used silver undercoat and heavy aluminum-outercoat at that time) twice. The lens was assumed to cut-off at 3500 Å and be 90% transmissive at 4250 Å and to have no loss at 5250 Å and greater. The result is shown in Fig. 4, which shows both the light flux at the top of the atmosphere and at the camera image as a function of the wavelength. The next step was to find the photographic effect of this spectral distribution upon emulsions with various sensitizing treatment. The results are shown in Figs. 5 to 8, inclusive, for some of the sensitizations used. On each of these curves, the wavelength ranges for which the lens is within ±Rayleigh limit/4 and ±Rayleigh limit/2 of its sharpest visual focus are indicated. With only the exception of the GH sensitized emulsion, we have found that the portion of the response curve limited by the wavelengths of the tolerance limits has *less* integrated effect upon the photographic image than the light flux outside these limits. This simply means that for all sensitization, other than the GH type, out-of-focus light will have more effect on the photographic density than will the focused light. We believe that this is the reason that, as mentioned above, only GH emulsion produced a fine, sharp, image of the granulation. It may be argued that the focal range can be shifted, relatively to the emulsion curve, by changing the position of the plate holder, but it should be noted that this is not enough, because the greatest wavelength spread over which the focus is sharp is at the point of sharpest visual focus. A rough calculation of the focal curve for a photographic doublet (achromatized for D and G) has shown us that the above-mentioned restrictions apply to all but the "O" emulsions (no sensitizer).

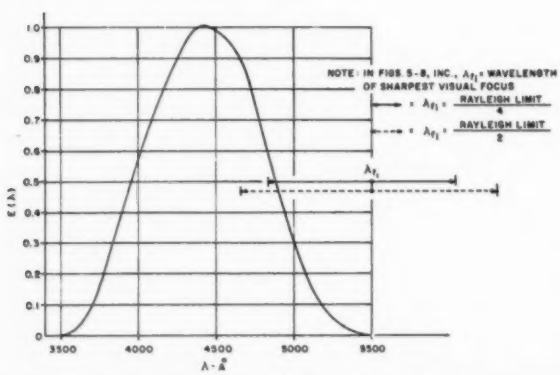

Fig. 5. Response of O sensitized emulsion in $f/80$ camera.

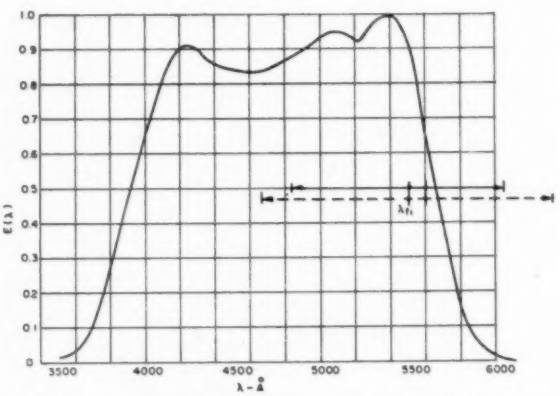

Fig. 6. Response of GH sensitized emulsion in $f/80$ camera.

Additional restrictions must be placed on the spectral energy distribution of the light incident on the emulsion. We chose to try to do this with gelatin filters, purchased from Eastman Kodak Co. Figure 9 shows the result of matching certain of these filters with either the Type 548, or Type 649 emulsions with O, GH, T, and E sensitization treatment. The focal-tolerance and wavelength of best focus is shown for each combination. The response curve of GH sensitizer, interference filter, and $f/18$ camera is shown for comparison. Note that these curves are expressed as response relative to the individual peak response so that all curves have the same height. The peak response varies considerably from one sensitizer/filter combination to another. The time available for

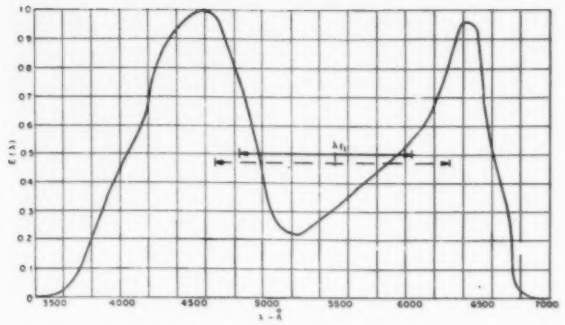

Fig. 7. Response of E sensitized emulsion in $f/80$ camera.

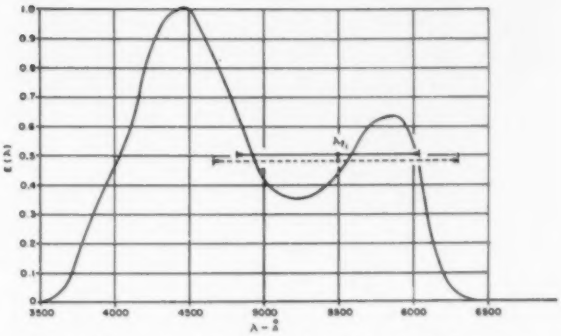

Fig. 8. Response of T sensitized emulsion in $f/80$ camera.

experimental test of the utility of these combinations was quite short, but we were able to take pictures showing solar granules with most of them.

Observational Problems

The usefulness of an observatory depends not only upon the amount of time one can see the object to be studied, but also upon how well one can see it. To those who are familiar with the weather conditions on Long Island, it may come as a surprise that both requirements are fulfilled in a quite adequate fashion, at least as far as photography of the solar photosphere is concerned.

A sampling of our plate list shows that photographs of the sun were made on 1093 days of a possible 1490 days, or there is a 73.4% utility. On 299 days of the 1093 (or 27.3%) at least one of the day's photographs showed detail to the classical limit of resolution of the lens. Figures 10 and 11 show such detail in photographs made with the $f/80$ and the $f/18$ cameras, respectively. They are not to the same scale. On 97 days of the 1093 (or 8.9%) none of the photographs was usable for analysis because all detail was obliterated. What makes this record even more remarkable is that those plates, apparently limited in detail only by the resolving power of the instrument,

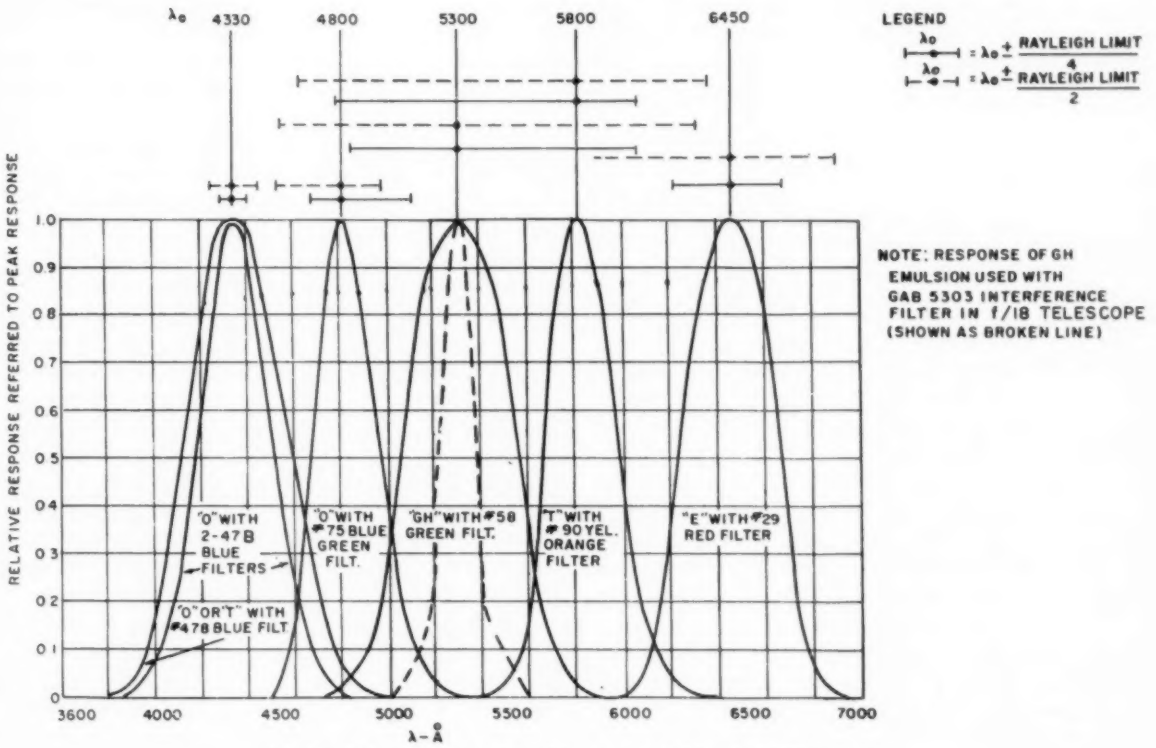
λo 4330
4800
5300
5800
6450
LEGEND
λo ± RAYLEIGH LIMIT / 4
λo ± RAYLEIGH LIMIT / 2
NOTE: RESPONSE OF GH EMULSION USED WITH GAB 5303 INTERFERENCE FILTER IN f/18 TELESCOPE (SHOWN AS BROKEN LINE)
RELATIVE RESPONSE REFERRED TO PEAK RESPONSE
"O" WITH 2-47B BLUE FILTERS
"O" OR "T" WITH #47B BLUE FILT.
"O" WITH #75 BLUE GREEN FILT.
"GH" WITH #58 GREEN FILT.
"T" WITH #90 YEL. ORANGE FILTER
"E" WITH #29 RED FILTER
λ - Å

Fig. 9. Effect of filter and emulsion on spectral band of $f/80$ camera.

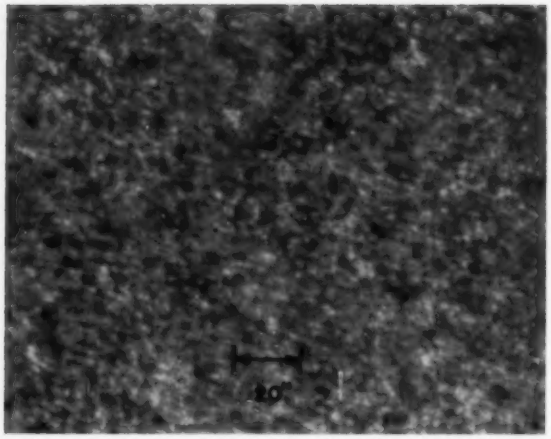

Fig. 10. Central region of solar disk (26 July 1955, 07:08 EST, $f/80$ refractor). (20" = 20 sec of arc on the sun's surface)

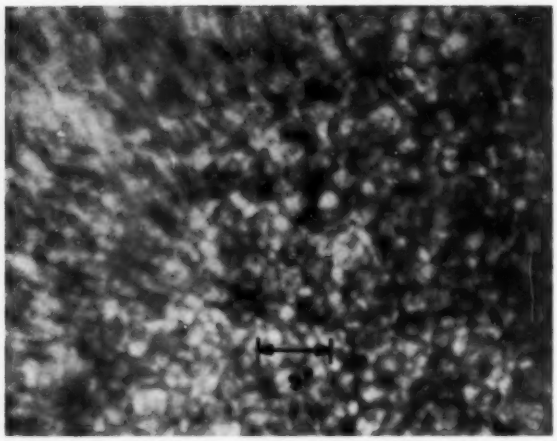

Fig. 11. Central region of solar disk (18 July 1956, 07:28 EST, $f/18$ refractor). (9" = 9 sec of arc on the sun's surface)

which were counted above (299 days) show this detail over the entire disk (except along the limb). Photographs made on at least as many *more* days show such detail in limited areas of the image. Finally, it should also be remarked that the requirements for our photographic program were satisfied by all days during which the sun was not obscured for at least half an hour during the day.

In view of the location of the observatory in a region not generally considered desirable, particularly for solar observations, several somewhat surprising conclusions may be drawn:

(i) The number of days during which the sun may be photographed is high—of the order of 75%.

(ii) The earth's atmosphere, at this location, is sufficiently stable to allow the detail shown in the photograph to be limited by the resolving power of the instrument on a large number of the days allowable for solar photography—27%.

The best seeing conditions on Long Island occur during the late spring, summer, and early fall. The worst seeing occurs during the months of December and January. During those periods in the summer when good seeing should prevail, and does not, it has been noted that the relative humidity is lower than at other times when the seeing is good. Since the relative humidity remains fairly high throughout the year on Long Island, a high humidity while necessary cannot be regarded as sufficient to produce good seeing. There is, however, a marked difference in the direction of the motion of air masses across Long Island in the winter and summer. It appears that the direction of the prevailing winter winds are such that continental air is over the Island during a large portion of the late autumn, winter, and early spring months, while during the remainder of the year the main air mass overhead is maritime. It is believed that this difference is mainly responsible for the difference in the summer and winter seeing conditions. It is not felt that continental air is inherently less desirable, but that, due to the proximity of Long Island to the large land mass of the continent, the main turbulences generated by shear, etc. have not been damped out to the degree that they are during the movement of oceanic air across the relatively uniform surface of the ocean. At any rate, it has been noted that winds from the north, northwest, etc., to the southwest, as occur often, particularly the more northerly directions, in the winter are accompanied by serious disturbances of the seeing regardless of the humidity. Also, wind directions which occur more often in the summer, i.e., from the southwest, south, etc. and east are more apt than not to produce excellent seeing conditions. These wind directions do have accompanying high humidity conditions over Long Island during the summer. The land mass of Long Island, itself, is not sufficiently large to produce deep convection cells which, when well defined, will degrade the seeing. Some of the best pictures have been taken during times when large fields of fair-weather cumulus (cumulus humilis) were present. While each such cloud may act as a cap at the top of its own convective cell, the slanted path of the sunlight will cause the rays to pass through one or more such cells. Therefore, convection, unless it is strongly developed, as in an area with strong cumulo-nimbus, does not cause great deterioration of the seeing conditions.

The following description of a course of meteorological events typical of Long Island summertime (observed at ground level), together with the seeing conditions found to accompany them, may aid in an understanding of the situation. Assume that a cold-front thunder squall has just passed over the area.

The clouds disappear rapidly, the ground wind is from the north to northwest, the air is clear and cool, the sky is deep blue (Polaris is very brilliant as seen with a 114-mm telescope, during the entire day), the relative humidity is low (compared to its value just before the squall), and the seeing is atrocious. (This also seems to be the condition of the atmosphere over Long Island during much of the winter.) Such conditions prevail for several days until the wind resumes its southwesterly direction. When this wind shift occurs the air temperature and humidity increase, and the seeing conditions improve rapidly. As long as the wind remains from southwest to southeast both temperature and relative humidity increase, and the seeing is excellent. Atmospheric haze soon builds up to the point where Polaris may be seen only rarely, during the daytime, with a 114-mm telescope. However, this haze, as yet, has no detrimental effect upon the definition of the image. The approach of another cold front is accompanied by a rapid thickening of the atmospheric haze until the sun will no longer cast a shadow. During the approach of this heavy haze condition the seeing remains excellent. Some plates which show detail limited by instrumental resolving power have been exposed when the shadow cast by the sun was extremely weak. Within a day or two the cold-front thunder squall occurs and the events described above are repeated. The period between squalls is variable, but the behavior outlined is typical.

The duration of times of excellent seeing is variable. During the summer months, some days have occurred where excellent seeing conditions lasted for 6 to 8 hr. During the late spring and early fall days the periods are much shorter and occur, with very few exceptions, during the early morning hours. The length of time, during the day, when good seeing prevails is very short at the onset of such conditions, and gradually lengthens until the end of June or mid-July, at which time the period will normally last 4 to 5 hr. This time remains fairly constant until the middle or end of August, at which time the reliable daily time of good seeing gradually shrinks until by the end of October or mid-November good seeing occurs only rarely.

There is some evidence that the equatorial camera is slightly less affected by the seeing conditions than is the horizontal one. Further investigation must be made before this can be accepted as true and not accidental.

Conclusions

Perhaps the most important conclusion to which we came during the program was that the atmospheric conditions, during the summertime, on Long Island were superb for extended study of the solar photosphere. Unfortunately, the amount of haze present at these times of good seeing would probably preclude the possibility of similarly detailed study of the chromosphere and the corona.

In striving to make the instrumentation as nearly perfect as possible, we have demonstrated the necessity for extremely narrow tolerances on the optical surfaces and the utility of silicone oil as a contacting medium.

It is hoped that the details pertaining to the improvement of the performance of the mirror system by the use of carefully deposited multilayers of metal will encourage others to try this technique. The results will repay the effort required.

The problem of matching instrumental focal curve, filter, and emulsion sensitivity is an old one. The technique described has been shown, by experiment, to provide a satisfactory solution to this problem.

It is a pleasure to acknowledge the support of RCA Laboratories, and particularly that of Irving Wolff, H. H. Beverage, C. W. Hansell, and J. L. Callahan, without whose active interest this work could not have been undertaken. It is also a privilege to thank A. B. Moulton for his assistance with a portion of the optical and mechanical design, and R. E. Franklin for his unending patience and care in making the lenses and mirrors.

References

1. M. Born and E. Wolf, *Optics* (Pergamon Press, London, 1959).
2. K. Schwarzschild, Gesellschaft der Wissenschaften zu Göttingen Math-Physik Klasse, Neue Folge, Bd. IV, 1905 (translated by W. A. Miller, RCA Laboratories Engr. Memorandum 62-51, Feb. 9, 1954).
3. A. E. Conrady, *Applied Optics and Optical Design* (Oxford Univ. Press, 1929), Vol. 1 (Reprinted by Dover, New York, 1957.)
4. H. Dennis Taylor, *Telescope Objectives, 4th ed.* (Sir Howard Grubb Parsons, London, 1946).
5. John Strong, *Procedures in Experimental Physics* (Prentice-Hall, Englewood Cliffs, New Jersey, 1938), pp. 176–177, 187.
6. W. A. Miller, U.S. Patent No. 2,539,149.
7. W. A. Miller, Nature **175,** 557 (1955).
8. B. Lyot, Ann. Astrophys. **7,** 31 (1944).
9. J. W. Evans, J. Opt. Soc. Am. **39,** 229 (1949).

Have you ordered your copy of the
OPTICAL MASERS SUPPLEMENT?

See page 104 for details

continued from page 92

point a fixed distance from the optics elements. This condition, superposition of the middle of the X and I, defines coincidence of the X and I.

Suppose the optics, mounted on a slide, were positioned such that coincidence occurs on the surface of a bare metal. If the metal is now coated by an opaque material of thickness t, then the coating's outer surface intercepts the projected reticle before coincidence, and the I is observed to the left of the X. To achieve coincidence, the optics, or slide, must be retracted a distance t equal to the coating thickness.

Since the slide's position can easily be indicated to ± 0.001 in. ($\pm 25\ \mu$), as in Fig. 2, it is clear that the gauge can nondestructively measure the thickness of wet coatings to a comparable accuracy. Tests have shown that the gauge is accurate to ± 0.002 in. ($\pm 50\ \mu$) or better.

In practice, the instrument may be quickly removed from and relocated in any one of N stations in a rigid frame. The gauge of Fig. 2 is currently being used to measure the thickness of wet sprayed plastic on large nonrotating cylinders, and the thickness of flame sprayed ceramics.

To measure the thickness of coatings on eccentric rotating drums, without contact, synchronous illumination of the reticle (or synchronous interruption of the light beam) reduces the dynamic problem to the static case solved above. A simpler problem is the monitoring of diameters of rotating *concentric* right circular cylinders or cones, such as those commonly turned on a lathe. In effect, this is also a static problem by virtue of concentricity.

With regard to process control of wet coatings, as distinct from inspection, it has been suggested[3] that by setting coincidence of images a fixed distance from the substrate, a photoelectric system could detect coincidence, and thereby provide a signal to control the coating process.

It is concluded that a number of industrial metrology problems involving dimensional accuracies of a few thousandths of an inch (a few hundredths of a mm) may be economically solved by a simple application of the optics of a projected reticle.

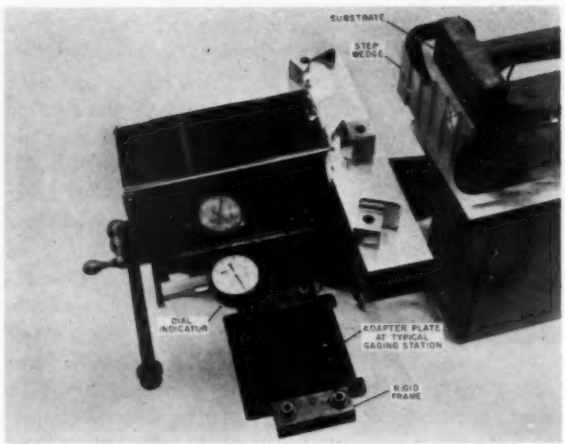

Fig. 2. Prototype instrument measures thickness to two mils (50 μ) without contact.

A. G. Hanson of the Avco RAD physics department contributed his optics experience in the design and testing of this gauge, and his assistance is gratefully acknowledged. This work was supported in part by the U.S. Air Force Ballistic Systems Division, contract AF 04 (694)-16.

References

1. R. C. McMaster (ed.), *Nondestructive Testing Handbook* (Ronald Press, New York, 1959), Vol. I, Section 18 (X-ray and isotope gauging).
2. R. C. McMaster (ed.), *Nondestructive Testing Handbook* (Ronald Press, New York, 1959), Vol. II, Section 46 (Ultrasonic immersion tests).
3. F. Brech, personal communication (June 18, 1962).

SUPPLEMENT ON OPTICAL MASERS

published December 1962

In the APPLIED OPTICS Supplement on Optical Masers, published in December 1962, concepts basic to the understanding of optical masers are discussed in a 15,000-word paper by **O. S. Heavens,** Royal Holloway College, which in addition reviews the progress in this new field. Work on solid-state systems is summarized, and applications in the areas of fundamental experiments, communications, instrumentation, and surgery discussed. Gas systems are dealt with in a comprehensive review by **W. R. Bennett, Jr.,** Yale, comprising some 20,000 words. Selected papers from the publications of the Optical Society of America and of other societies are reprinted in this comprehensive volume and suggestions for further reading are given. The editorial to this APPLIED OPTICS First Supplement is written by **Charles H. Townes,** MIT.

This valuable reference work is sold for $5.00 per copy

ORDER NOW—YOU WILL FIND A REPLY PAID ORDER CARD OPPOSITE PAGE 22

Simulating the Solar Spectrum with a Filtered High-Pressure Xenon Lamp

E. A. Boettner and L. J. Miedler

The spectral irradiance of a 1000-watt xenon lamp was determined prior to modifying its radiant output to simulate the solar spectrum. A survey of filter glasses was made and the transmission characteristics of two types found useful for this problem are described. The spectral irradiance of the xenon lamp after passing the radiation through UV-6 and KG-2 filter glasses was measured and compared with noonday solar radiation at Ann Arbor, Michigan, in 1960 and 1961 (42° N latitude). The spectral distribution of the lamp filter combination agrees closely with the solar spectrum although the rate of change in the ultraviolet region is greater than that for solar radiation.

Introduction

The spectral distribution of solar irradiance as measured at a particular point on the surface of the earth is subject to wide variations dependent on a number of factors: e.g., fluctuations in the solar radiance, variations in the distance from sun to earth, differences in atmospheric scattering by air molecules, water vapor, and dust, and differences in absorption by the atmospheric gases. However, even under selected solar and atmospheric conditions, any attempt to produce a radiation source having a spectral irradiance identical to "natural sunlight" will be an approximation because of limitations in sources and filter materials.

The spectral distribution of solar radiance and the influence of atmospheric attenuation have been under investigation for more than 80 years. A review of much of this original work is given in a summary by Sanderson and Hulburt.[1] Also, recent publications by Buttolph,[2] Nagy,[3] and Hirt *et al.*[4] provide data on many high- and low-pressure mercury arcs, carbon arcs, xenon arcs, and fluorescent lamps for simulating various portions of the solar spectrum.

The aim of this program is to develop a light source that can be modified to approximate the quartz transmitting region of the solar spectrum under diverse conditions. For this purpose, a xenon high-pressure lamp first described by Schulz[5] and further studied by others[6–8] affords a good basic source of radiation. The lamp has a high continuous spectral radiance with an apparent color temperature of approximately 6300°K. Moreover, because of the compactness of the arc, the spectral radiance can be varied with commercially available filters. This paper will describe the source and the results obtained by modifying the lamp's spectral output to approximate the solar irradiance under specific conditions for the region from 200 to 2800 mμ.

Unfiltered Lamp

The assembled unit consists of a high-pressure xenon lamp, a power supply, and glass filters. The radiation source is an XBO 1001 (1000 watts dc) xenon lamp manufactured by Osram in Germany.* The lamp (see Fig. 1), which is enclosed in a quartz envelope, has an internal pressure of 8 atm when cold, and 25 atm at operating temperature; hence care must be taken to mount the lamp within a protective case.

The lamps are made for dc operation and require a current of 30 to 45 amp. A ballast resistance must be connected in series both to limit and to control the operating current through the lamp. Since the ballast consumes considerable power, the total power used in the operation of the 1000-watt lamp at maximum current is about 3200 watts. The lamp is started by a special ignition device which applies a 33-kV high-frequency pulse across the lamp for a tenth of a second.

The authors are at the Institute of Industrial Health and Department of Dermatology, The University of Michigan, Ann Arbor, Michigan.

Received 12 December 1961.

* Distributed in this country by Macbeth Sales Corporation, Newburgh, New York. Similar lamps are made in the United States by Hanovia.

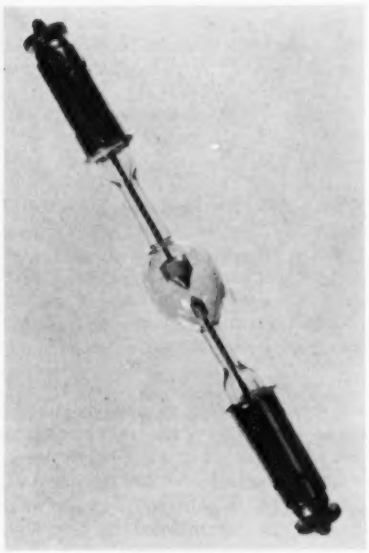

Fig. 1. Osram 1000-watt high-pressure xenon lamp.

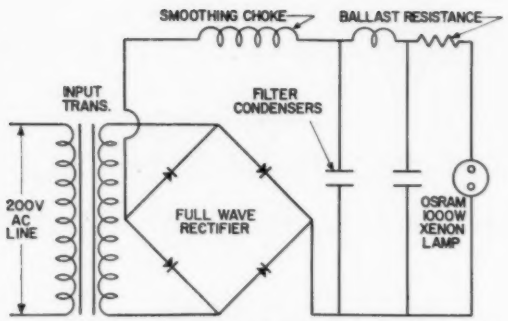

Fig. 2. Circuit diagram of power supply for 1000-watt lamp

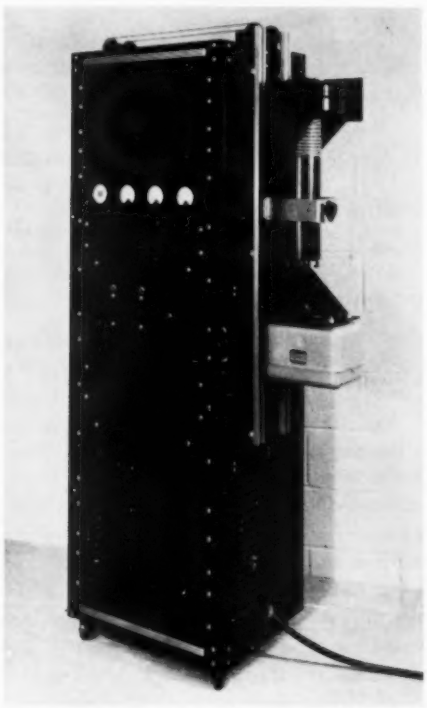

Fig. 3. Lamp and power supply.

Figure 2 is a schematic diagram of the circuitry. The lamp source and its power supply is pictured in Fig. 3. The lamp is contained in the cylindrical housing mounted on a vertical track on the side of the rack cabinet, so that its height can be adjusted. Figure 4 shows the lamp housing and its accessories. Below the lamp is the starter, and above is a blower which draws cool air past the lamp. Additional forced-air cooling is provided inside the power supply to remove the heat generated by the rectifier and ballast.

The spectral distribution of the xenon lamp was measured with a Beckman DK-1 Recording Spectrophotometer, the spectral sensitivity of the spectrophotometer having been ascertained previously, using calibrated tungsten filament lamps having known spectral distributions. The total energy output of the lamp was measured with a calibrated vacuum thermocouple* after first calibrating the thermocouple with blackbody standards.

The spectral distribution of the Osram XBO 1001 xenon lamp when operated at 43 amp is shown in Figs. 5(a) and 5(b). The total energy incident on a surface at 27 cm is 0.1 watt per square centimeter. All measurements were made utilizing the radiant flux from the entire arc gap and the hot electrodes. A single experiment to determine the degree to which the infrared radiation could be reduced by masking the electrodes demonstrated a reduction of only 10% in the amount of irradiance beyond 900 mμ. Two lamps have been measured thus far, and their spectral distribution has been the same to within 5%. Furthermore, no measurable change in spectral distribution in either lamp has been detected following 200 hr of operation

Filtered Lamp

After the spectral characteristics of the 1000-watt xenon lamp had been determined, repeated measurements of the solar spectral irradiance were made at noon on clear days in Ann Arbor, Michigan (42°N latitude), during the month of June in 1960 and 1961. The calibrated spectrophotometer and vacuum thermocouple used for these measurements were the same as used to measure the xenon source. The data obtained were found to be in close agreement with the standard solar radiation curves of Moon[9] for similar conditions of latitude and air mass. The resulting average solar irradiance curve established for the stated conditions

* Furnished by the Charles M. Reeder Company, 173 Victor Avenue, Detroit 3, Michigan.

is shown in Figs. 6(a) and 6(b). The xenon source was then modified to approach as nearly as possible the solar irradiance depicted in Figs. 6(a) and 6(b).

The spectral distribution of the xenon source with its color temperature of approximately 6300°K is similar to that of the sun with the exception of an excess of energy in the ultraviolet and near infrared portions (0.8–1.0μ) of the spectrum. To remove this excess energy by filtration, a survey was made of glass filters. Several glasses made by Corning, Tiffen, and Schott were found to have cutoff characteristics in the region of interest in the ultraviolet. Likewise, one Schott glass had transmission characteristics in the infrared so that it removed much of the xenon line radiation in the 800- to 1000-mμ region and a majority of the remaining excess infrared radiation.

Figures 7(a) and 7(b) show the transmittance of the two glasses. The Schott KG-2 glass was selected to absorb in the infrared and the Tiffen UV-6 to absorb that part of the excess ultraviolet radiation not removed by the KG-2 glass. The KG-2 glass was adjusted to absorb about 2% in excess in the region from 800 to 1800 mμ to balance the excess of radiation transmitted from 1800 to 2800 mμ. This required a 2.1-mm thickness of the particular production lot of KG-2 glass used. The UV-6 glass was then adjusted in thickness to remove the excess ultraviolet irradiance. A

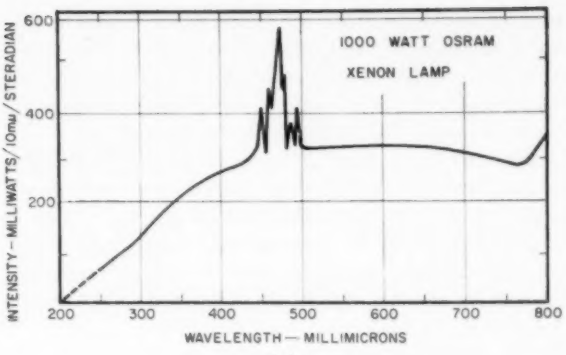

(a)

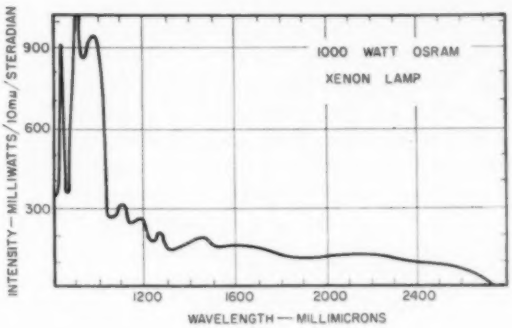

(b)

Figs. 5(a) and (b). Spectral radiant intensity of an Osram XBO 1001 lamp when operated at 43 amp.

Fig. 4. Lamp housing with starter and blower.

24-mm thickness of one particular lot of UV-6 glass was required for this purpose. It would be possible to use about 2 mm of either Tiffen UV-5 or Schott WG-5 glass for the same purpose. The great thickness of UV-6 was selected so that the source-filter combination would approach the gradual increase in the solar irradiance from 300 to 400 mμ.

Concerning the use of the KG-2 filter glass, a previous report by the authors[10] emphasized that the transmission of this glass will change rapidly when exposed to the direct radiation of the xenon lamp. However, by using the suggested filter combination with the UV-6 glass interposed between the KG-2 glass and the lamp, the rapid solarization is eliminated. Periodic transmission measurements of all the glasses in the filter combination have not revealed any solarization effects after 30 hr of use.

Figures 6(a) and 6(b) compare the spectral output of the lamp and filter combination at 16 cm with that of the Ann Arbor noonday sun in June. The total quantity of energy under these conditions for both sources of radiation was 0.10 watt per square centimeter.

Discussion

It should be emphasized that the thicknesses of glasses cited pertain to specific production lots. Be-

cause glass varies from lot to lot, despite careful production control, it is necessary to measure the transmittance of each new glass and, on the basis of the transmittance curve, adjust the glass thickness to produce the desired amount of filtration.

The spectral output of the source can be modified to simulate solar radiation at other latitudes and elevations by changing the thickness of the two types of filters. However, because of the transmission characteristics of the quartz envelope housing the lamp, it is possible only to match the radiation in the quartz transmitting region.

The spectral distribution of the modified 1000-watt xenon lamp agrees closely with the solar spectrum which it was designed to simulate, although the rate of change in spectral irradiance of the source and filter combination in the ultraviolet region [Fig. 6(a)] is still excessive. The portion of the excess of energy below 310 mμ necessitated limiting the lower transmission of the glasses to 302 mμ. This value is slightly higher than that of solar radiation under the conditions of Fig. 6(a). As a result, the total amount of energy emitted by the source and filter combination between 290 and 310 mμ is approximately the same as that of solar

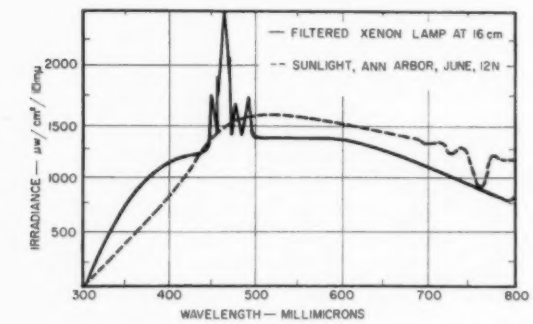

(a)

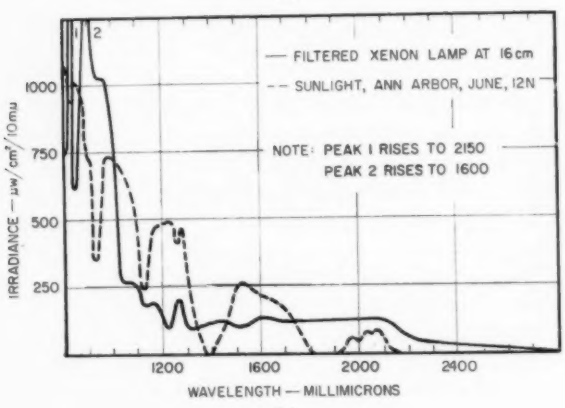

(b)

Figs. 6(a) and (b). Spectral irradiance of the xenon lamp filtered with UV-6 glass (24 mm) and KG-2 glass (2.1 mm), compared with the solar spectral irradiance.

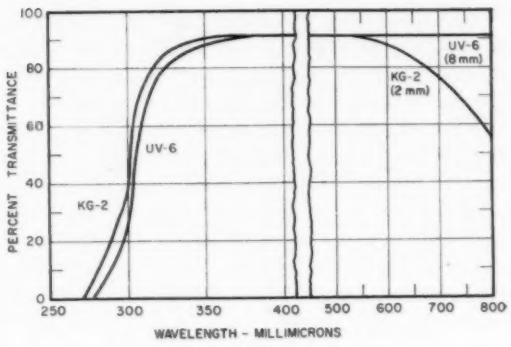

(a)

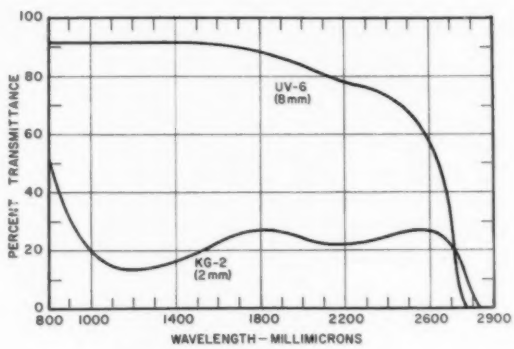

(b)

Figs. 7(a) and (b). Spectral transmittances of Tiffen UV-6 and Schott KG-2 glasses.

radiation under the conditions specified, about 70 mW per square centimeter. In the region from 310 to 380 mμ, the filtered source irradiance is about 1.9 times that of the sun.

Obtaining a better spectral conformity through the ultraviolet, while still maintaining the desired transmittance in the visible and infrared, will require a filter glass or material whose transmittance change is more gradual through this region. A search for filter materials having such characteristics is continuing.

References

1. J. A. Sanderson and E. D. Hulburt, in *Radiation Biology*, A. Hollaender, ed. (McGraw-Hill, New York, 1955), Vol. II, p. 95.
2. L. J. Buttolph, in *Radiation Biology*, A. Hollaender, ed. (McGraw-Hill, New York, 1955), Vol. II, p. 41.
3. R. Nagy, Supplement to Invest. Dermatol. **32,** 175 (1959).
4. R. C. Hirt, R. G. Schmitt, N. D. Searle, and A. P. Sullivan, J. Opt. Soc. Am. **50,** 706 (1960).
5. P. Schulz, Ann. Physik **1,** 95 (1947).
6. W. A. Baum and L. Dunkelman, J. Opt. Soc. Am. **40,** 782 (1950).
7. W. T. Anderson, Jr., J. Opt. Soc. Am. **41,** 385 (1951).
8. H. G. Frühling, W. Münch, and M. Richter, Farbe **5,** 41 (1956).
9. P. Moon, J. Franklin Inst. **230,** 583 (1940).
10. E. A. Boettner and L. J. Miedler, J. Opt. Soc. Am. **51,** 1310 (1961).

Selected Ordinates for Solar Absorptivity Calculations

O. H. Olson

This paper presents selected ordinates for the determination of solar absorptivity values from reflectance curves in the spectral range of approximately 0.3 to 3.0 μ.

Selected ordinates have been employed extensively in the field of colorimetry for the determination of tristimulus values of radiant energy.[1,2]

Solar absorptivity has assumed a new and important role with the advent of the space age. Temperature control of space vehicles is attained to a large extent by designing surfaces to have appropriate absorbing and radiating properties for radiant energy.[3] Solar absorptivity may be determined by evaluation of the expression:

$$\alpha_s = \frac{\int_{\lambda_1}^{\lambda_2} E_\lambda \cdot (1 - R_\lambda) d\lambda}{\int_{\lambda_1}^{\lambda_2} E_\lambda \cdot d\lambda} = 1 - \frac{\int_{\lambda_1}^{\lambda_2} E_\lambda \cdot R_\lambda \cdot d\lambda}{\int_{\lambda_1}^{\lambda_2} E_\lambda \cdot d\lambda}, \quad (1)$$

where

E_λ = solar spectral energy distribution,
R_λ = spectral reflectance of the test surface on an absolute basis ($R = I/I_0$),
λ_1, λ_2 = limits of integration which, theoretically, are zero and infinity, but practically, are about 0.3 and 3.0 μ because the solar energy is largely confined to this region.

To evaluate α_s strictly requires continuous multiplication of factors, plotting these products against wavelength, and measurement of areas under the curves. Most reflectance curves do not require continuous integration, however, and weighted ordinates or selected ordinates yield sufficiently accurate results.

In the weighted ordinate method the spectrum is divided into a finite number of equal intervals and the evaluation indicated in Eq. (1) becomes,

$$\alpha = 1 - \frac{\sum_{\lambda_1}^{\lambda_2} (E_\lambda \cdot R_\lambda \cdot \Delta\lambda)}{\sum_{\lambda_1}^{\lambda_2} (E_\lambda \cdot \Delta\lambda)}. \quad (2)$$

The author is at the Armour Research Foundation, Physics Division, 10 West 35th St., Chicago, Ill.

Received 19 February 1962.

The details of this computation are tedious and time consuming if carried out manually since each E_λ must be multiplied by the corresponding R_λ for every wavelength interval. Over 50 such products must be determined if $\Delta\lambda$ is taken as 0.05 μ for the effective solar range. The author[4] has used an electronic card program computer with considerable saving of time but, obviously, this is not justified unless many determinations must be made.

In the Selected Ordinate Method the spectrum is also divided into a finite number of intervals. However, instead of equal intervals as employed in the weighted ordinate method, intervals of the spectrum are selected that correspond to uniform increments of solar energy. In other words, wavelength increments $\Delta\lambda_1$, $\Delta\lambda_2$, and so forth are chosen so that: $E_\lambda(\Delta\lambda_1) = E_\lambda(\Delta\lambda_2) = E_\lambda(\Delta\lambda_3) = \ldots$. The spectral reflectance, R_λ, of the specimen is thus weighted equally in each such interval and no further weighting is necessary. The computation of the numerator in Eq. (2) consequently degenerates into simply adding together a finite number of selected ordinates of the reflectance curve, while the denominator becomes simply the number of such ordinates employed.

Several sets of selected ordinates for solar absorptivity determinations are included with this paper. Table I presents "30 selected ordinates" for solar spectral distribution above the earth's atmosphere. By taking every third ordinate in Table I (second, fifth, eighth, etc.) as marked, the "30 selected ordinates" may be abridged to ten. Table II lists "20 selected ordinates" for upper atmosphere solar energy and Table III lists "10 and 20 selected ordinates" for sea level solar energy distribution. The details of computation are not included but follow the plan outlined by Hardy.[1] The solar energy distributions used in the calculations are from the *Smithsonian Physical Tables*.[5]

Table I. Ten and Thirty Selected Ordinates for Evaluation of Solar Absorptivity Above Earth's Atmosphere

No.	λ(μ)	No.	λ(μ)
1	0.325	16	0.739
2[a]	0.373	17[a]	0.775
3	0.408	18	0.815
4	0.436	19	0.859
5[a]	0.457	20[a]	0.908
6	0.479	21	0.963
7	0.501	22	1.025
8[a]	0.522	23[a]	1.095
9	0.544	24	1.174
10	0.569	25	1.269
11[a]	0.594	26[a]	1.387
12	0.619	27	1.546
13	0.646	28	1.775
14[a]	0.674	29[a]	2.166
15	0.706	30	3.215

[a] For 10 selected ordinate evaluation use only these 10 ordinates.

Table II. Twenty Selected Ordinates for Evaluation of Solar Absorptivity Above Earth's Atmosphere

No.	λ(μ)	No.	λ(μ)
1	0.337	11	0.748
2	0.399	12	0.805
3	0.441	13	0.871
4	0.474	14	0.949
5	0.506	15	1.042
6	0.540	16	1.153
7	0.575	17	1.296
8	0.613	18	1.501
9	0.653	19	1.851
10	0.698	20	2.789

Discussion

A convenient technique for applying the method of selected ordinates is the use of templates. The selected ordinates are drawn on a sheet of tracing paper as a family of parallel lines which extend the full length of the reflectance scale. Another line is drawn parallel to the selected ordinates at some convenient wavelength to serve as a reference line for registration. This template may be laid over a reflectance curve and reflectances read off at points where the curve crosses the ordinate lines.

Integration with "20 selected ordinates" has been compared with 50 weighted ordinate integration and found to agree within 1% in all cases tested. It is believed that such agreement will always be obtained unless the reflectance curve has some unusual features such as abrupt absorption bands. The employment of more than 20 selected ordinates for the determination of solar absorptivity at sea level is probably not justified because of the wide variation in solar spectral distribution caused by water vapor and carbon dioxide absorption and scattering by atmospheric dust.

Table III. Ten and Twenty Selected Ordinates for Evaluation of Solar Absorptivity at Sea Level

No.	λ(μ)	No.	λ(μ)
1	0.390	1	0.425
2	0.444	2	0.496
3	0.481	3	0.558
4	0.551	4	0.621
5	0.543	5	0.686
6	0.574	6	0.765
7	0.606	7	0.825
8	0.639	8	1.043
9	0.669	9	1.176
10	0.705	10	1.580
11	0.745	16	1.026
12	0.786	17	1.105
13	0.831	18	1.228
14	0.877	19	1.497
15	0.959	20	1.722

Conclusion

Selected ordinate determination of solar absorptivity offers the advantage of simplicity and minimum equipment requirements. All that is necessary is to standardize on graph paper and to make up a set of suitable templates. It is particularly suited to those who are occasionally faced with the problem but do not have the volume of work to justify a more sophisticated approach.

References

1. A. C. Hardy, *Handbook of Colorimetry* (Technology Press, Cambridge, Mass., 1936), Chap. VI.
2. D. B. Judd, *Color in Business, Science and Industry* (Wiley, New York, 1952), pp. 113–120.
3. F. J. Clauss, *First Symposium Surface Effects on Spacecraft Materials* (Wiley, New York, 1960), pp. 3–87.
4. O. H. Olson and J. C. Morris, Jr., J. Opt. Soc. Am. **47**, 1048 (TC66) (1957).
5. *Smithsonian Physical Tables*, prepared by W. E. Forsythe (Smithsonian Institution, Washington, D.C., 1954), 9th ed., pp. 721–723.

ANNUAL SUBSCRIPTIONS

OSA members	$ 6.00
Other AIP societies' members	$ 8.00
Non-members and libraries	$10.00
Single copies	$ 2.00

Subscriptions should be addressed to APPLIED OPTICS Subscription Handling, American Institute of Physics, 335 East 45th Street, New York, New York.

ADVERTISING

Advertising Agent | ALFRED P. OPPENHEIM
Assistant | RUTH STEGER

Advertising inquiries, orders, plates, and correspondence should bo addressed to the APPLIED OPTICS Advertising Office, 55 West 16th Street, New York 11, New York. CHELSEA 2-1311

KODAK IRTRAN 3 Material

There are 2 new "IRTRAN" materials for infrared optics

One transmits from 0.4μ to 11μ and you can see through it well enough to line up your system

No secret that this is calcium fluoride. Our art is in making it in polycrystalline form. No cleavage planes. Therefore it can stand mechanical and thermal shock much better than either natural or man-made CaF_2 crystals (but still not as well as IRTRAN 1 and 2, both of which it beats in standing steady high temperature without forming oxide films). Index at 0.656μ, 1.4324; at 8.25μ, 1.3444. Maximum size at present: 5" diameter x ½" thick.

The other transmits all the way from 1μ to 21μ

without the fragility and extraordinarily high index of the principal alternative for this spectral span and without the cold flow of the other alternative.

Another uniquely polycrystalline triumph—this in zinc selenide. Similar to IRTRAN 2 material in strength, ability to survive high temperature and shock, and techniques for easy grinding and polishing. Just that it transmits farther into the far infrared. Index descends from 2.503 at 1.0μ. Maximum size: 2" diameter x ¼" thick for the present.

KODAK IRTRAN 4 Material

For the full facts on all four KODAK IRTRAN Optics and Optical Materials, write or call

EASTMAN KODAK COMPANY,
Apparatus and Optical Division,
Rochester 4, N.Y.

Area Code 716, LOcust 2-6000, Extension 5166

Producers of
KODAK EKTRON Detectors
KODAK Interference Filters
} for the infrared

OSA Group Flight to Europe

JULY 1963

The revised schedule for the OSA 1963 Group Flight will enable members to attend some of the following July meetings in Europe. This schedule has had to be revised because, under the new charter agreements, no group flights may take place during the period 24th June/7th July:

8–13 Ionization Phenomena in Gases Symposium, Orsay, France
10–17 IUPAC Congress, London, England
22–26 Physics of Electronic and Atomic Collisions, London, England
22–27 7th European Congress on Molecular Spectroscopy, Budapest, Hungary

The probable flight schedule is as follows:

New York—Geneva 9 July
Geneva—London 10 July
London—Budapest 20 July
Budapest—Zurich 28 July
Zurich—New York 29 July

Because there is no same day connection Budapest—Zurich—New York, Swissair will absorb hotel and meal expenses for one day.

Such a round-trip group fare would cost $416 + $4 handling charge, **i.e., $420,** assuming a minimum of 25 participants. This fare includes internal European travel only if the members travel as a group, i.e., the ticket cannot be used for other planes. Forty seats have been tentatively reserved, and we need your deposit ($50 per seat) as soon as possible; the balance of the fare ($360) must be paid by 30th April.

THIS GROUP FLIGHT WILL BE ON A SWISSAIR REGULARLY SCHEDULED JET AIRCRAFT. TIMES WILL BE ANNOUNCED LATER.

There are three other meetings in Europe in 1963 of particular interest to opticists:

11–15 February 3rd Quantum Electronics Conference, Paris, France
May 2nd Hungarian Optical Conference, Budapest, Hungary
late September (tentative) ICO Symposium on Thin Films, Marseille, France

If sufficient members (minimum of 25 per meeting) are interested, the Assistant Secretary will endeavor to arrange group transportation for these too.

Assistant Secretary, OSA, Room 101,
1155 Sixteenth Street, N.W.
Washington 6, D.C.

REPLY

( ) I wish to reserve .... seats on the OSA GROUP FLIGHT N.Y.-Geneva-London-Budapest-N.Y. 9 July through 29 July.
( ) I enclose my check for a deposit of $ ... (.... seats)
( ) I am an OSA Member and will be accompanied by .... my wife
.... children (how many?)
( ) I am interested in principle in attending the February ☐ May ☐ September ☐ meeting and wish to hear whether group transportation can be arranged.

ONLY OSA MEMBERS THEIR WIVES AND THEIR CHILDREN MAY PARTICIPATE IN THE GROUP FLIGHT

Name.....OSA Membership No.....

Address.....

.....

THE NAME TO REMEMBER FOR PRECISION ANGULAR MEASUREMENTS

is

DAVIDSON

Specialists in Optical and Electro-Optical Instrumentation

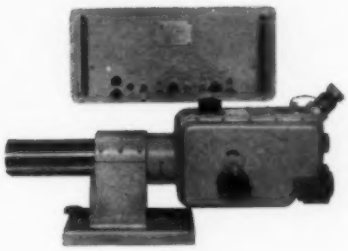

SINGLE AND TWO-AXIS AUTOMATIC AUTOCOLLIMATORS AND THEODOLITES

Since first pioneering autocollimator automation, Davidson has become the largest producer of these instruments. Sensitivity to angular change is available from ±0.01 second of arc to ±1 minute of arc; measuring range of ±6 seconds of arc to ±10 minutes of arc. A wide selection of automatic readouts are also available for measuring reflector deviations in both single and two orthogonal planes.

MANUAL AUTOCOLLIMATORS

Davidson's manual autocollimators are adaptable to most optical alignment situations that arise in the standard and calibration laboratories. Aligning laser optics, calibration of polygons and turn tables, placement of optical elements in optical systems, and making precision angular measurements are but a few applications. According to model, measuring ranges are available from 2 minutes to 20 minutes; direct readings from 0.1 second to 15 seconds; and both single and two axis readout.

OIL BEARING GYRO TEST STANDS

These stands are a new line of instrumentation developed by our company for balancing inertial guidance platforms and guidance packages, performing scale factor tests, and determining a gyro's rate of progression. The bearings are both stable and nearly frictionless, requiring less than 5 gm. cm. breakaway torque. Some models allow the rotating axis of the bearing to be positioned in any attitude between horizontal and vertical.

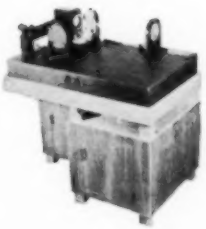

INTERFEROMETERS

Davidson interferometers will check flatness of any surface smooth and flat enough to reflect light, or check optical quality of elements such as, windows, wedges, prisms or plane mirrors. These elements can be placed in a train with the integral of errors presented in the eyepiece in the form of fringes. Correction can then be made on any one or more of the elements.

POLYGONS

REFERENCE MIRRORS

WEDGES

OPTICAL CUBES

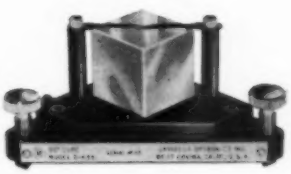

For complete data, contact your nearest D.O.I. representative or write:

DAVIDSON OPTRONICS, INC.

2223 Ramona Boulevard
West Covina, California

EDER ASSOCIATES, 2603 N. DOWNER AVE., MILWAUKEE, WISC.
HOLCO, 122 WEST CHESTER PIKE, HAVERTOWN, PA.
PRODUCTION TOOLS, INC., 959 SOUTH 3RD. WEST, SALT LAKE CITY, UTAH
YALE ASSOCIATES, 14 EVERETT PAINE BLVD., MARBLEHEAD, MASS.
J. K. TRIPLETT, BOX 3286 RIDGEWAY STATION, STAMFORD, CONN.
BUD WATTS MACHINERY CO., P.O. BOX 5435, MEMPHIS 16, TENN.
SCIENTIFIC SALES CO., 3603 LEMMON AVE., DALLAS, TEXAS
H. R. BEAL, 7547 RANCHO VISTA DR., SCOTTSDALE, ARIZONA
L. VAN VALKENBURG, 2730 S. HACIENDA BLVD., LA PUENTE, CALIF.

Crystals of all types and sizes, guaranteed to laser!

In stock, hundreds of single crystals. All configurations (plain flat and parallel ends, TIR configuration, Brewster's angle). Optically corrected for lowest threshold, narrowest beam divergence. Extra slow grown and annealed for minimum strain. **Guaranteed to laser!**

- NEW glass crystals w/neodymium^{3+} 2.0% — finest quality, no bubbles, straie, strains.
- New NPS1 super-uniform ruby crystals.
- Ruby rods up to 12″
- Calcium tungstate crystals w/neodymium^{3+} 0.5% up to 5″ long.
- Strontium fluoride crystals w/samarium^{2+} 0.1%, neodymium^{3+} 0.5%.
- Barium fluoride crystals w/neodymium^{3+} 0.5%, uranium^{3+} 0.1%.
- Calcium fluoride crystals w/neodymium^{3+} 0.5%, samarium^{2+} 0.1% dysprosium^{2+} .05%, or uranium^{3+} 0.1%.

For full specifications and prices, write or call Adolf Meller Company, Box 6001, Providence 1, R. I. Telephone: DExter 1-3717 (Area Code 401).

MELLER SAPPHIRE PRODUCTS

Synthetic Sapphires • Ruby Lasers & Masers
Alumina Powder

An equal opportunity employer.

laser physicists

Hughes' broad experimental program in the development of new LASER techniques, components and systems is being enlarged. With the unusually varied and significant applications of LASERS, the opportunities created through this expansion will be professionally rewarding and exciting and of long range promise. Three of the several openings are indicated below. We invite your inquiry.

1 PHYSICISTS
A background in experimental techniques (optical spectroscopy, flash photometry, etc.) involving phenomenon at optical frequencies, an advanced degree or compensating experience and demonstrated ability will be preferred. We will also consider Physical Chemists with strong backgrounds in optical physical techniques.

2 ELECTRONIC ENGINEERS or PHYSICISTS
Pulse circuit techniques experience is required.

3 SYSTEMS ENGINEER
About five years of experience, preferably in radar systems, and a physical, as opposed to a mathematical, orientation are required.

Airmail your resume to:
MR. ROBERT A. MARTIN
Head of Employment
Hughes Aerospace Divisions
11940 W. Jefferson Blvd.
Culver City 2, California

CREATING A NEW WORLD WITH ELECTRONICS

HUGHES

HUGHES AIRCRAFT COMPANY
AEROSPACE DIVISIONS

WE PROMISE YOU A REPLY WITHIN ONE WEEK

K-37 Camera

with 12″ f.1. f/2.5 Kodak Aero-Ektar Lens. This camera lens has long been a favorite for astronomical photography. The first Sputnik pictures were taken with the 12″ f/2.5 lens. Shutter speeds 1/25, 1/50, 1/100 second. Less magazine, with instruction manual..... **$145.00**

B-1 Cut film back for above. Uses standard 8x10 cut film holders..... **$37.50**

A-5 Roll film back. May be used to take rapid sequence photography with K-37 motor drive (supplied with camera) picture size 9″x9″. Uses $9^1/_2$″ strip film rolls..... **$45.00**

LA-12 Image-Motion-Compensation Back. For above or any 9x9 camera such as K-3, K-17, K-19, K-22, K-29. By properly orienting this back and setting the movement correctly, the motion of a moving object such as a satellite may be compensated for, and long exposures may be taken with the camera stationary. Range of movement speeds is 0.15 to 15″ per second in the focal plane. This back is an unusual piece of machinery and cost the government almost $3000..... **$95.00**

28 Volt D.C. Supply. Works from standard 115 v. 60 cycle line. To supply power to run camera drive for rapid sequence work..... **$16.00**

Modification of camera to focusing mount. Will focus from infinity to 13′ (delivery 2–4 weeks)..... **$75.00**

Focalscope for accurate focusing of K-37 camera..... **$45.00**

Fiberglass carrying case for K-37 camera..... **$17.50** extra

48″ f/6.3 Kodak Lens. This surplus lens has been successfully used for accurate determination of satellite position by moving the plate or chopping the satellite image. We imagine this lens would have many other applications in astrophotography. Original cost to the government was $9,000.00. Cover 9x18 plate. Focuses from 1000′ to infinity. Rear element clear aperture $9^1/_2$″. Front element clear aperture $8^1/_2$″..... **$240.00**

Other Lenses available:

6″ f/4.5 B and H Eyemax (Tel.)
6″ f/6.3 B & L Metrogon (W.A.)
6″ f/3.5 B and H Miltar (L.F.)
7″ f/2.5 Kodak Aero-Ektar
12″ f/6.3 B & L Metrogon (W.A.)
12″ f/4.0 Perkin-Elmer Type II
12″ f/2.5 Kodak Aero-Ektar
14″ f/3.5 Kodak Aero-Ektar
24″ f/6.0 Kodak, B & L Tessar
36″ f/8.0 B and H or P.-E. Telephoto

Thermoelectric Devices has a complete modern electronics and machine shop. We can adapt your specific needs at a fraction of the cost of doing it in your own machine shop. Let us quote you on your specific requirements.

T.E.D., Inc. | Surplus Sales Division of Thermoelectric Devices, Inc.

302–304 Massachusetts Avenue, Cambridge 39, Massachusetts

MULTI-LAYER INTERFERENCE FILMS

for dichroic and achromatic beam splitters and filters. High efficiency. Relatively wide band.

MULTI-LAYER HEAT DEFLECTORS

XUR-96. Reflects substantial portion of infrared spectrum while transmitting nearly all of the visible radiation.

#6143. Colorless, non-absorbing filter. Completely removes the ultra-violet and reflects the infrared. Transmits about 90% from 425 to 700 mμ reflecting longer wavelengths. Half transmission points at 412 mμ and 725 mμ.

Cold Mirror IRT-211. To reflect visible radiation from 400 to 700 mμ and transmit from 725 to 1200 mμ and longer.

COATINGS FOR LASERS and MASERS

For Ruby: #3132-N. 99.5% reflectivity from 694 to 760 mμ.

For Glass: #3117. 99.5% reflectivity from 1,000 to 1,200 mμ.

Other coatings available with peak reflectivity at any desired wavelength.

LOW REFLECTING COATING

Double and triple layer with minimum reflection of less than .1% on glass of low index.

Coatings also available to increase transmission to 9 micron on Germanium and Silicon.

SCHOTT Narrow Band Interference Filters

Made by JENAer Glaswerk Schott & Gen. WEST GERMANY

For the spectral region from 300 to 2,000 mμ.

Transmission up to 60%. Half-value width down to 5 mμ. Tolerance at peak wave length: ±1% for regular quality. ±0.5% for precision quality.

AVAILABLE AS

Line Filters • Line Double Filters • Band Filters
Band Double Filters • Wedge Filters • Broad Band Filters

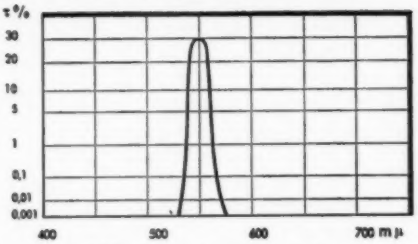

Double Band Filter

Tmax about 30%.
Half width about 16 mμ.
Ratios: Tenth width to half width 1.5, Hundredth width to half width 2, Thousandth width to half width 3.5.

SCHOTT Colored Optical Filter Glass • Available in about 100 types for ultraviolet, visible and infrared spectral regions, including absorption filters containing neodymium for use in lasers and masers.

FISH-SCHURMAN CORPORATION, 90 Portman Road, New Rochelle, N. Y.

ROCKETDYNE

in Southern California is seeking

PHYSICISTS

Strong in education and/or experience in optics, spectroscopy, radiometry, infra-red technology, cryogenics and high vacuum, solid state physics and microwaves for work in the experimental and theoretical study of rocket exhaust radiation and laser applications. Position also offers possibility of basic research in area of individual choice.

Those interested in placement with a progressive research activity are invited to send resume or inquiry to:

Mr. Z. L. Mayborn
Professional Employment Office
6633 Canoga Avenue
Canoga Park, California

All qualified applicants will receive consideration for employment without regard to race, creed, color or national origin.

ROCKETDYNE
Division North American Aviation

APPLIED OPTICS

Subscription Order

☐ 1 year, at OSA member rate of $6.00

☐ 1 year, at special rate, to other AIP Societies members, of $8.00

☐ 1 year, at non-member rate of $10.00

☐ Please send OSA membership information

Membership No.....

Name.....

Address.....

.....

.....

OPTICAL CRYSTALS

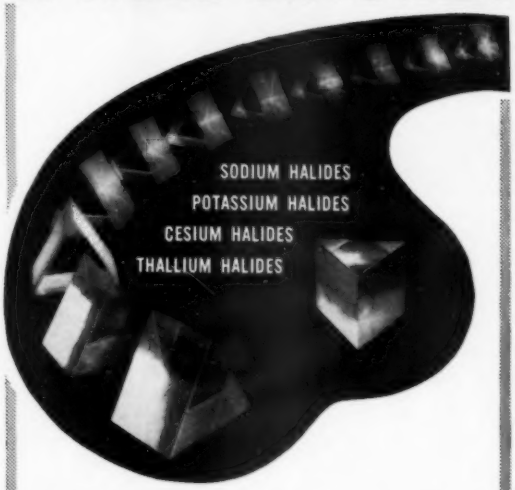

Special crystals grown to order, optical blanks cut to specifications, finish polishing as required.

123 WOODLAND AVENUE
WESTWOOD
NEW JERSEY

CRYSTALS DIVISION
ISOTOPES, INC.

IF YOU USE GLASS BEAM SPLITTERS
MIRRORS • FILTERS • PRISMS

in apparatus you are designing, manufacturing or using

THIS FREE BOOKLET IS FOR YOU.

Thin film pellicles introduce neither refractive error nor ghost images, can be had flat to $1/20$ wave, and offer full coating selection including dichroics. This booklet tells you how and when to specify thin film pellicles.

NATIONAL PHOTOCOLOR CORP.
225 EAST 44TH STREET NEW YORK 17, NEW YORK

Ask for "*Application and Specification of Pellicles*"

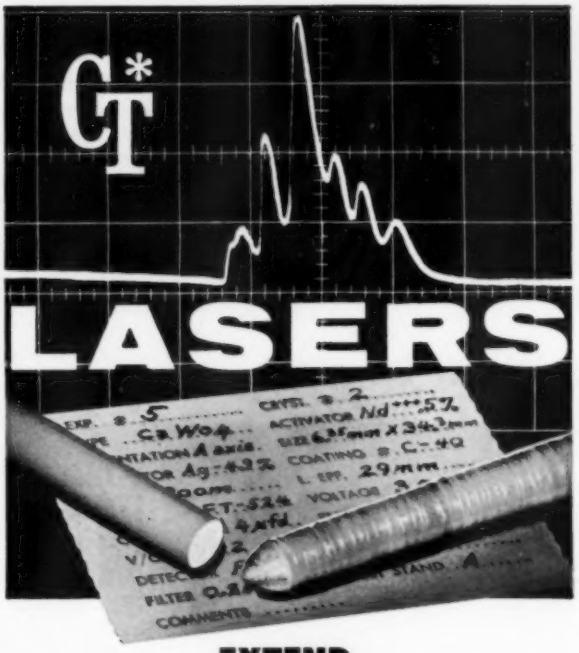

EXTEND YOUR LASER INVESTIGATION CAPABILITIES

ISOMET has the nation's most extensive facilities for high quality Laser Crystal growth, fabrication, finishing, and quantity production.

TESTED LOW THRESHOLD

✱ ***Certified Threshold*** Each ISOMET laser rod is accompanied by an actual oscilloscope photograph of its output performance at threshold and complete data on the experimental conditions of the test.

BOULES OR FABRICATED RODS ends polished optically flat and parallel, confocal, spherical or faceted to meet your requirements.

STOCKED FOR IMMEDIATE DELIVERY

$CaWO_4$, $SrMoO_4$, $PbMoO_4$ doped with Nd^{3+}
Chromium doped Ruby, 0° or 90° orientation
Nd^{3+} doped glass
CaF_2 and BaF_2 doped with Sm^{2+}, U^{3+}, Nd^{3+}

GROWN TO ORDER

$CaWO_4$, $SrMoO_4$, $PbMoO_4$, CaF_2, CdF_2, BaF_2 or other hosts doped with any of the rare earths or transition elements.

REFLECTIVE SURFACES Evaporated metallic or multiple dielectric coatings.

NEW LARGE SIZE LASERS

ISOMET has perfected a method of growing Calcium Tungstate doped crystals in sizes never before possible. As a result, we stock $CaWO_4$ boules capable of being fabricated into laser rods up to ¼" diameter x 5" long and ½" x 4" long. On special order, we can supply ¼" rods up to 10" long, ½" rods up to 6".

Write for new technical bulletin AO1000

ISOMET
CORPORATION
PALISADES PARK, NEW JERSEY

NEW! Matched remote control lenses for VIDIKON and other systems
—a complete line of lenses with uniform diaphragm and focus controls. Single, remote, or ganged lenses can be driven from central control units. Temperature stabilization from 65 to —20° centigrade—vibration proofed to 8 "G"s. Coverage 9.6 mm x 12.8 mm.

QUALITY OPTICS

for these and all other applications!

- MISSILE TRACKING
- CLOUD CHAMBER OPTICS
- SCHLIEREN CAMERAS
- AERIAL IMAGE TRANSFER
- OPTICAL COMPARATORS
- SCOPE READING
- INSTRUMENT RECORDING
- COPYING CAMERAS
- MICRO-FILM CAMERAS
- READERS, PRINTERS

SYMMAR
— infinity designed 6 element lenses with excellent resolution for camera use. Used for missile tracking, satellite cameras and other industrial and scientific camera applications.

SUPER-ANGULON
— with extremely wide angle of 100°, ideal for instrument readers and cloud chamber work, etc. Highest quality 6 element construction.

COMPONON
— designed for 1 to 10 conjugates, with flat field and excellent color correction. For a wide range of industrial applications.

For *any* lens requirement...simple or complex... check first with Schneider, world's leader in precision optics. For even your special need may be a stock item in the extensive Schneider line which includes over *300 different lens types.* Correspondence on technical lens problems invited. Literature available on request.

Schneider **LENSES...**
Classics of Optical Precision

BURLEIGH BROOKS, Inc. • 420 Grand Ave., Englewood, N. J.
ATLANTA • CHICAGO • DALLAS • HOLLYWOOD

QUICKLY...

THINK OF A PRODUCT

Slide rules . . . Transits . . . Tracing paper? Correct . . . but to round out the picture, please enter K&E in your file for these highly advanced space-age instruments . . .

Space and Missiles Systems

Solar and Star Simulators
•
Cine and Special Theodolites
•
Antenna Contour Checking Instruments
•
Contour Probing Instruments
•
Polaris Guidance and Fire Control Instruments
•
Collimation Test Instruments
•
Deviators
•
Borescopes—Electronic and Visual

R&D and Laboratory Instruments

Auto-Collimators—Electronic and Visual
•
Electronic Levels
•
Gravity Reference Instrument
•
Jig Theodolite
•
Angle Index Tables and Readout Devices
•
Gratings
•
Targets and Special Scales

Instruments for Manufacturing, Inspection, Quality Control

A complete line of alignment instruments and accessories

Want specific product information?

Write K&E today.
Our O&M Division can assist you with R&D.

KEUFFEL & ESSER CO.

3993

HOBOKEN, NEW JERSEY

HIGH RESOLVING POWER APPARATUS

HILGER & WATTS

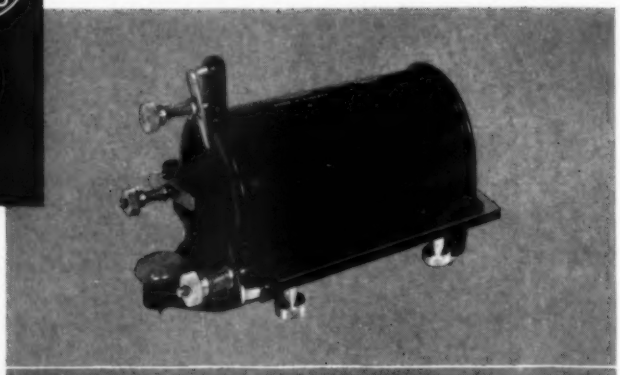

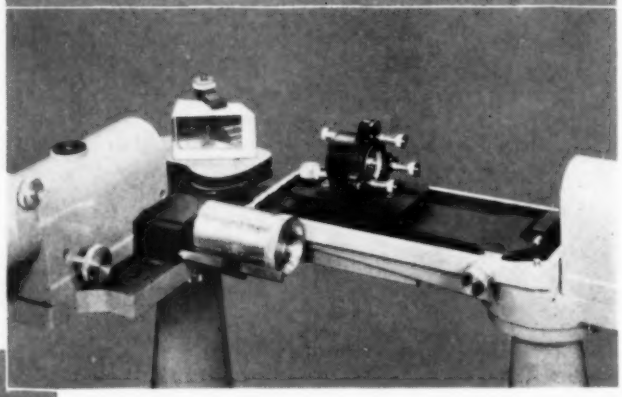

The development of the maser and laser has substantially broadened the use of high resolving power apparatus. Hilger & Watts now provide a comprehensive selection of equipment to meet the increased requirements.

Among the more important are etalon and interferometer plates — ranging from 20 mm. aperture to 100 mm. aperture; with flatnesses to 1/200 of a wavelength. Mounts for these plates, as well as wave length spectrometers designed to accommodate etalons within the instrument, are standard stock items.

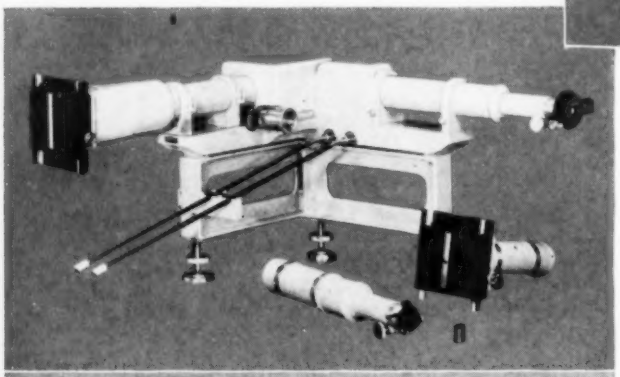

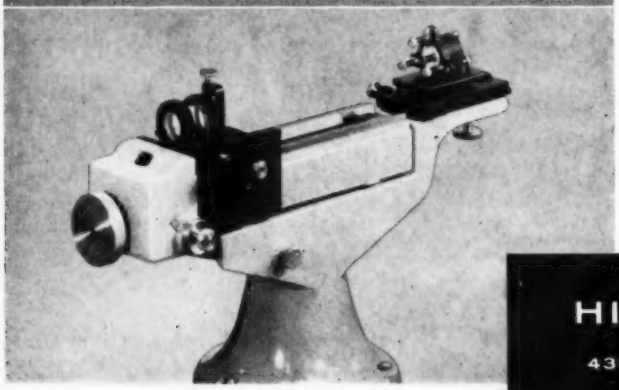

Other new developments include: motor driven Fabry-Perot and Michelson interferometers with fringe counting and amplitude measuring equipment; dielectric coatings for all plates. Lummer-Gehrcke plates and transmission echelon gratings are also available.

Illustrated Top Right—
B345 100 mm. Aperture Etalon

Illustrated Center Right—
D186 Spectrometer with Etalon mounted

Illustrated Center Left—
D260 Large Aperture Spectrometer with Etalon

Illustrated Bottom Left—
N34 Interferometer with Etalon

• *Ask for individual catalog sheets and for complete instrument listing.*

HILGER & WATTS, INC.

431 SOUTH DEARBORN ST. CHICAGO 5, ILL.

Sales, Service, Parts by

ENGIS EQUIPMENT COMPANY

CHICAGO 5, ILL.